N71-32369

NASA CONTRACTOR REPORT

NASA CR-1783

NASA CR-1783

FULL-SCALE WIND TUNNEL TESTS OF A LOW-WING, SINGLE-ENGINE, LIGHT PLANE WITH POSITIVE AND NEGATIVE PROPELLER THRUST AND UP AND DOWN FLAP DEFLECTION

by Edward Seckel and James J. Morris

Prepared by
PRINCETON UNIVERSITY
Princeton, N. J.
for Langley Research Center

NATIONAL AERONAUTICS AND SPACE ADMINISTRATION • WASHINGTON, D. C. • AUGUST 1971

1. Report No. NASA CR-1783	2. Government Accession No.	3. Recipient's Catalog No.
4. Title and Subtitle FULL-SCALE WIND TUNNEL TESTS OF A LOW-WING, SINGLE-ENGINE, LIGHT PLANE WITH POSITIVE AND NEGATIVE PROPELLER THRUST AND UP AND DOWN FLAP DEFLECTION		5. Report Date August 1971
		6. Performing Organization Code
7. Author(s) E. Seckel and J. J. Morris		8. Performing Organization Report No. Princeton U. Report No. 922
9. Performing Organization Name and Address Princeton University Princeton, New Jersey		10. Work Unit No. 736-01-10-01-00
		11. Contract or Grant No. NAS1-9443
12. Sponsoring Agency Name and Address National Aeronautics and Space Administration Washington, D. C. 20546		13. Type of Report and Period Covered Contractor Report
		14. Sponsoring Agency Code
15. Supplementary Notes		

16. Abstract

Full-scale wind-tunnel data for a low-wing single-engine light airplane, with up and down flap deflections and a range of negative through positive propeller thrust, are presented. The data are analyzed to determine the effects of flap deflection, propeller thrust and angle-of-attack on the aerodynamic characteristics of the airplane. Longitudinal and lateral-directional static stability, control, and trim characteristics are considered in some detail.

17. Key Words (Suggested by Author(s))		18. Distribution Statement	
Low-wing light plane Forward and reverse thrust Up and down flap deflection Full-scale tunnel tests		Unclassified Unlimited	
19. Security Classif. (of this report) Unclassified	20. Security Classif. (of this page) Unclassified	21. No. of Pages 154	22. Price* $3.00

*For sale by the National Technical Information Service, Springfield, Virginia 22151

FOREWORD

The authors wish to acknowledge with thanks and admiration the part in this project of the wind-tunnel staff at Langley Research Center, NASA. Messrs. Marion O. McKinney, Jack Paulson, and Marvin P. Fink produced the needed data in the wind-tunnel tests; and by their interest, patience, and guidance, helped educate the participating group of Princeton students.

The Princeton Department of Aerospace and Mechanical Sciences students who assisted the Langley staff in the wind-tunnel test program were C. W. Staley, P. W. Howard, and R. C. Hubenet, graduate students; and H. W. Davis, P. S. Basile, and W. K. Woodrow, seniors.

The analysis of the aerodynamic data has been largely done as Independent Work by two groups of seniors: P. S. Basile, G. F. Kline, S. F. Gripper; and H. W. Davis, J. J. Morris, P. E. Griffin. The authors greatly appreciate and freely acknowledge the importance and advantage of all this student participation.

The wind-tunnel test project, including analysis of the test data, is Phase I of a larger project involving extensive automatic control installations and other modifications to another aircraft of the same type, and ultimately flight tests on flying qualities for landing. The whole program is supported at Princeton University by Langley Research Center under Contract No. NAS 1-9443. The technical monitor for LRC is Mr. Harold Crane.

SUMMARY

Full-scale wind-tunnel data for a low-wing, single-engine, light plane, with up and down flap deflections and negative through positive propeller thrust, are presented. These data are analyzed to determine the effects of flap deflection, thrust and angle-of-attack on the longitudinal and lateral-directional static stability, control effectiveness, and trim characteristics.

Although the interacting effects of these variables are strong and sometimes irregular, the factors limiting the use of large negative thrust are probably loss of elevator effectiveness for longitudinal characteristics and rudder effectiveness for directional characteristics.

TABLE OF CONTENTS

LIST OF SYMBOLS

C_D	Drag coefficient
C_L	Lift coefficient
C_ℓ	Rolling moment coefficient
C_{ℓ_ψ}	Directional stability; $\partial C_\ell / \partial \psi$; per degree
$C_{\ell_{\delta a}}$	Aileron effectiveness; $\partial C_\ell / \partial \delta a$; per degree
C_m	Pitching moment coefficient
C_{m_α}	Static stability derivative; $\frac{\partial C_m}{\partial \alpha}$; per degree
C_{m_δ}	Elevator effectiveness; $\frac{\partial C_m}{\partial \delta}$; per degree
$C_{m_{i_t}}$	Tail effectiveness; $\frac{\partial C_m}{\partial i_t}$; per degree
dC_m / dC_L	Static stability derivative
C_n	Yawing moment coefficient
C_{n_ψ}	Directional stability; $\frac{\partial C_n}{\partial \psi}$; per degree
$C_{n_{\delta r}}$	Rudder effectiveness; $\frac{\partial C_n}{\partial \delta r}$; per degree
T_c'	Thrust coefficient; $\frac{T}{qS}$
δ_a	Aileron deflection angle; degrees
δ_e	Elevator deflection angle; degrees
δ_f	Flap deflection angle; degrees
δ_r	Rudder deflection angle; degrees
i_t	Tail incidence angle; degrees

α	Angle of attack; degrees
ψ	Angle of yaw; degrees
β	Angle of sideslip; degrees
ϵ	Downwash angle; degrees
$d\epsilon / d\alpha$	Downwash factor
T.O.	Horizontal tail off
L/D	Lift to drag ratio
η_t	Tail efficiency
S	Wing area or propeller disk area; ft^2
D	Propeller diameter
τ_e	Elevator effectiveness; $C_{m_\delta} / C_{m_{i_t}}$
Γ	Dihedral angle; degrees
c.g.	Center of gravity position
N_m	Maneuver point
$\bar{x}_{cg}$	Position of center of gravity on mean aerodynamic chord
u	Airplane density factor; $\frac{m}{\rho S \bar{c}}$
ℓ_t	Distance from c.g. to horizontal tail; ft
$\bar{c}$	Mean aerodynamic chord; MAC; ft

FULL-SCALE WIND TUNNEL TESTS OF A LOW-WING, SINGLE-ENGINE, LIGHT PLANE WITH POSITIVE AND NEGATIVE PROPELLER THRUST AND UP AND DOWN FLAP DEFLECTION

By Edward Seckel and James J. Morris
Princeton University

INTRODUCTION

Early in 1969, it was proposed by Princeton University to equip a light single-engine aircraft for variable stability with separate control of lift and drag by a modified lift-flap and a blade pitch control propeller.

The special flap would be the standard flap unit, but with the hinge position altered, and provision for up as well as down deflections. In contour and shape, the flap being the same as the aileron, the new hinge position was chosen for convenience to be in line with the aileron hinge (see Figure 2). This expedient detail would greatly simplify the detail design of hinge brackets, attachments, and the installation.

The blade pitch propeller was to be used for automatic control of thrust to simulate arbitrary drag properties, including large drag, low L/D vehicles. This would involve large amounts of negative thrust, and rapid changes of thrust due to automatic command of the propeller pitch angle.

It was anticipated that both the up-and-down flap and the negative thrust propeller would cause complicated and unpredictable aerodynamic effects which would interfere with their proper use in simulation unless at least major interference phenomena could be identified quantitatively by wind-tunnel test data. Accordingly, it was agreed with Langley Research Center of NASA that the airframe, with the modified flap and propeller, would be tested in the Full-Scale Tunnel to furnish the required data. An electric motor was to be installed by the wind-tunnel staff to facilitate power control in the tunnel, and simplify general operating procedures.

The wind-tunnel program was done in August and September of 1969, with a group of graduate and undergraduate Princeton students assisting the wind-tunnel staff. A very complete and definitive set of aerodynamic data data was obtained, as would be required ultimately in the flight program. The Princeton students, of course, benefitted tremendously by the experience and contact with research operations and personnel at LRC.

During the academic year 1969-70, a group of students at Princeton extensively analyzed the wind-tunnel data to find basic aerodynamic parameters of the airplane and the various special controls. This data reduction is scarcely complete - in fact, it will probably continue for special effects through the life of several flight projects - but the substantial results so far achieved are presented in this report.

The Light Single-Engine Airplane

The dimensional and typical inertial properties of the aircraft are shown in Figure 1 and Table 1. Details of the modified flap are shown in the accompanying large-scale drawing of the outboard flap section.

The Wind-Tunnel Program

The wind-tunnel tests involved some 365 runs - each "run" consisting of readings over a complete range of angle of attack from -4 to 22 degrees. Among the 365 runs, there were variations in tail incidence (i_t), including tail-off; elevator angle (δ_e); flap deflection (δ_f); thrust coefficient (T_c'), including propeller-off; aileron deflection (δ_a); rudder angle (δ_r); and sideslip angle (β).

A table of runs is given in Table 2 for detail reference. The scope and shape of the tests conditions can better be appreciated, however, by a short description of the test program.

The sets of conditions for the longitudinal parameters can best be described in two parts. For a flap angle of zero degrees, 66 runs were made using all combinations of 6 values of T_c' (nominally .215, .095, 0, -.05, -.13, -.175), 2 values of i_t ($\pm 5^\circ$), tail-off, and 5 values of δ_e (17.9°, 0°, -10°, -17°, -23° for i_t -5° and 11.3°, 0°, -10°, -20°, -30° for $i_t = +5^\circ$). For flap angles of $\pm 20^\circ$, $\pm 30^\circ$, 132 runs were made using all combinations of 3 values of T_c' (nominally .215, 0, -.175), 5 values of δ_e (17.9°, 0°, -10°, -17°, -23°), 2 values of i_t ($\pm 5^\circ$), and tail-off.

For aileron characteristics runs (α from -4 to 22 degrees) were made for five values of δ_a (24.4°, 12.2°, 0°, -8.8°, -18.8°) at $\delta_e = \delta_r = \delta_f = \psi = T_c' = 0$, and $i_t = -5^\circ$. Runs were also made for three values of δ_a (24.4°, 12.2°, 0°), at 2 values of δ_f ($\pm 30^\circ$) for $i_t = -5^\circ$, $\delta_e = \delta_r = \psi = T_c' = 0$.

The scope of the wind tunnel runs to determine the effect of yaw angle and rudder inputs is more complex than that for the longitudinal or aileron runs. The combinations are shown in the matrix below using three symbols to indicate combinations of ψ and δ_r for different T_c' and δ_f. The X represents runs for 3 values of T_c' (nominally .215, 0, -.175) for $\delta_f = 0$. The + represents runs for 4 values of T_c' (nominally .095, -.05, -.09, -.13), also for $\delta_f = 0$. Finally, the O represents runs for 3 values of T_c' (nominally .215, 0, -.175) and 4 values of δ_f ($\pm 20^\circ$, $\pm 30^\circ$). In all of these, $i_t = -5^\circ$, $\delta_e = \delta_a = 0^\circ$.

		δ_r (deg)				
		13.2	7	0	-9	-17.5
	15	X		X		X
	10		X	X+O	X	
	5			X		
ψ (deg)	0	X	X+O		X+O	X
	- 5			X		
	-10		X	X+O	X	
	-15	X		X		X

In the actual tests the remote control of propeller blade pitch angle was rather inaccurate and inconsistent - so that between runs at the same nominal T_c' there were considerable variations of actual T_c'. The true values of T_c' were deduced in the data reduction by subtracting the overall effective C_D (with propeller operating) from a corresponding $C_{D_{prop\ off}}$ read in runs with the propeller removed. The variations of T_c' within runs greatly complicated certain aspects of the data reduction, as explained in the next section.

Wind-Tunnel Data Reduction and Aerodynamic Parameters

The reduction of the basic wind-tunnel data is described and discussed in the following paragraphs. The results are presented graphically in Figures 3 through 20.

Lift curve, C_L vs α. - Lift curves, C_L vs α, for the five flap deflections tested, and for positive, negative, and zero thrust coefficients are shown in Figures 3 a, b, c. The lift increments due to flap deflection and thrust are about what might be expected. The lift for 30° up flap is practically the same as for 20° up flap, and it may be concluded that for 30° up deflection, separation occurs on the bottom surface, limiting the negative lift increment. This may be caused prematurely by the protruding nose of the flap at negative deflections. The shape is, and characteristics ought to be, like those of a typical Frise aileron.

The lift curves of Figure 3, discussed above, are derived from fairings of the test data points presented in Figures 16 (a to e). The latter are done in carpet fashion, with the independent carpet variables α and T_c'. This was to facilitate the plotting and interpolations necessitated by variations in T_c' from nominal, constant values. The magnitude of the T_c' scatter can be appreciated by observing the data points in the carpets. Some scheme like this was quite necessary in order to regularize T_c' in the final data presentation. The scheme, however, is not really feasible near $C_{L_{max}}$ and the stall, where the lift curves are quite irregular. In that area, the curves of Figure 16 are less precise and shown dotted to indicate reduced confidence.

Pitching Moment Stability, Trim and Control, C_m vs α and δ_e

The longitudinal static stability and trim of the light single-engine aircraft are presented in the various parts of Figure 4, with C_m a function of α and δ_e. The graphs are presented in carpet style, to facilitate interpolations. In the test program, the maximum elevator deflections were 23 deg up and 17.9 deg down for $i_t = -5^o$ and 30 degrees up and 11.3 degrees down for $i_t = +5^o$. There are fifteen of these carpets, for five flap deflections and three thrust coefficients.

Several important effects are visible in the various parts of this figure. Most outstanding are the effects of power on the static stability, elevator effectiveness, and linearity. The static stability, indicated by the slope of C_m vs α, is affected little in the range of forward thrust but it is reduced by rearward (negative) thrust; and for the latter case the C_m curve is quite nonlinear, corresponding to a strong variation of C_{m_α} with angle-of-attack or lift coefficient. C_{m_δ} is of course strongly affected by T_c', being reduced by negative thrust and increased by forward thrust. These effects are assumed to be more-or-less directly related to slipstream effects on the horizontal tail.

The C_m vs α and δ_e carpets of Figure 4 are derived from fairings of original data shown in Figures 17 (a to ii). The latter are carpets with α and T_c' the independent variables, done that way to facilitate the interpolations required by variations in T_c'. They would be useful in further interpolation for intermediate or uneven values of T_c'.

Stabilizer Effectiveness, C_m for two i_t, and Tail-off

Curves of C_m vs α for $i_t = \pm 5^o$, and tail-off, are presented in Figure 5. There are fifteen of these, for five flap deflections and three thrust coefficients. These curves, derived from the α, T_c' carpets of Figure 17 are used for the $C_{m_{i_t}}$ and ϵ computations as described in the next sections.

It can be seen from the tail-off curves that without the horizontal tail, the effects of power (forward thrust) are destabilizing, the wing-fuselage combination being more stable at negative thrust. This effect of thrust appears to be greatest at down-flap deflections, almost disappearing at large up-flap positions.

Elevator and Stabilizer Effectiveness as a Function of Power

C_{m_δ} and $C_{m_{i_t}}$ are shown as a function of T_c' in Figure 6. The former is derived from the α, δ_e graph of Figure 4 and the latter, of course, directly from the i_t curves of Figure 5. There are variations of both parameters with angle-of-attack and flap deflection, but they are small over the useable range of C_L and not very regular. The variations with T_c' stand out as the principal trend. The values shown in Figure 6 may be considered averages which apply approximately for all α and δ_f. Particular values, needed accurately, can be deduced readily from the source carpets as described above.

It is interesting that both C_{m_δ} and $C_{m_{i_t}}$ are strongly influenced by T_c' in the manner to be expected due to slipstream effects on tail efficiency. The effect, however, is only about 37 percent of what would be predicted by the simple momentum formula

$$\eta_t = 1 + \frac{8}{\pi} T_c = 1 + \frac{4}{\pi} \frac{S}{D^2} \cdot T_c'$$

The two parameters appear to be affected to the same extent by T_c', maintaining a constant ratio over the range of T_c'. The ratio, of course, is the <u>relative</u> elevator effectiveness

$$\tau_e = \frac{C_{m_\delta}}{C_{m_{i_t}}} = .71$$

Effective Downwash Angles

Effective downwash angles, derived basically from Figure 5 using the difference between tail-on and tail-off C_m, and the local $C_{m_{i_t}}$ are presented as functions of α and T_c' in Figure 7. There are five parts, corresponding to the various flap deflections tested. These graphs are actually derived from fairings of the calculated ϵ values which are included for reference in Figure 18.

The variations of ϵ with α, and the effects of T_c' and δ_f are interesting and worthy of further study. Superficial examination indicates, for $\delta_f = T_c' = 0$, a downwash factor $\frac{d\epsilon}{d\alpha} = .38$ at low angle-of-attack. It appears to reduce as α increases, which is somewhat unexpected since the tail is initially above the wing wake. The trend, however, is quite clear, being stronger for down-flap deflections; and weaker, or slightly reversed, for up-flap positions. The effects of forward thrust are seen to increase $\frac{d\epsilon}{d\alpha}$, and those of negative thrust to decrease it and cause a strong nonlinear variation with α. These details are well worth further study and comparison with the predictions of Silverstein and Katzoff in Reference 1.

Static Trim, C_m vs C_L

Curves of C_m vs C_L for various δ_e are shown in Figure 8. There are fifteen parts, for the five flap deflections and three thrust coefficients. They are derived from the C_m vs α, δ_e of Figure 4 and the C_L vs α of Figure 3.

This form of the stability and trim data is the most useful for calculating the allowable CG range from the point of view of stability and trim. Although these interpretations are not complete at this time, certain facts can be seen easily by inspection. Effects of thrust on stability and control effectiveness, and nonlinearity at negative thrust, are most visible. Casual inspection indicates that the principal limitations would be on trim and maneuverability at negative thrust. The reduced control effectiveness, especially at high C_L, would create some control problems in that condition, with restrictions on CG range.

Another important matter is also visible - the trim changes due to flap deflection and thrust. The trim change ΔC_m or $\Delta\delta_e$ at a constant C_L is of interest for piloting the basic single-engine aircraft; but for design of the simulation artificial stability system, the ΔC_m at constant α is of more significance. The latter, more directly visible in the C_m vs α curves (Figure 5), have not been evaluated, in detail, as yet. It is apparent, however, that they are large and important.

Maneuvering Stability, N_m

The effect of thrust on maneuvering stability is shown in Figure 9. The maneuver point is estimated by the formula

$$\bar{x}_{CG} - N_m = \frac{d\,C_M}{d\,C_L} + \frac{1}{2\mu} \cdot \frac{\ell_t}{\bar{c}} \cdot C_{m_{i_t}}$$

The formula involves, of course, the slope of the curves of Figure 8, and an estimate of the pitch damping effect represented by the second term.

The figure indicates some possible stability problems at high negative thrust. The larger difficulty for that case, however, is probably the reduced control power previously identified.

Directional Stability, C_n vs ψ

Yawing moment coefficient, C_n, versus yaw angle, ψ, and thrust coefficient, T_c', is plotted in the form of carpets for various angles of attack and flap angle, $\delta_f = 0$, in Figure 10. This form of the carpet is useful for the interpolations necessitated by the uneven values of T_c' in the test data. It also directly displays, by its slope, the directional stability, C_{n_ψ}.

For the flap deflected cases, $\delta_f = \pm 20, \pm 30$ degrees, there were data points at only three yaw angles. For T_c' interpolation, the different carpets, C_n vs α and T_c', were preferable. These are given in Figures 19a through d. In these cases the directional stability was reckoned by the difference of C_n between points for $\psi = 10$ deg and $\psi = -10$ deg.

The directional stability, C_{n_ψ}, resulting from the two sets of carpets, is shown itself in carpet form as a function of angle of attack and flap deflection in Figure 11. There are three parts for negative, zero, and positive thrust.

It is seen that C_{n_ψ} is strongly affected by all three variables: α, δ_f, T_c'. The values range from .0010 to .0030 per degree - all probably in a satisfactory range for the speed and inertia of the light single-engine aircraft. What is not shown, however, is the nonlinearity of C_n vs ψ for the high angle of attack, negative thrust cases. This can be seen in the carpets of Figure 10. In the worst cases the directional stability is actually near zero for a small range of sideslip angles. This kind of nonlinearity might be quite troublesome in simulation work with the airplane if the corresponding combinations of flight variables were to be traversed.

Rudder Effectiveness, C_n vs δ_r

The rudder effectiveness is shown in Figure 12 by the carpets of C_n vs δ_r and T_c'. There are three parts corresponding to combinations of α and δ_f for a wide spread of directional stability, C_{n_ψ}. Again, this manner of plotting facilitates the interpolations and fairing required by the variations in T_c'.

The derivative, $C_{n_{\delta_r}}$, is shown in Figure 13, based on the carpets. It is plotted against C_{n_ψ} representing different combinations of α, δ_f; and for the negative, zero, and positive thrust. It is seen that the directional stability is not a good correlating parameter, at least for differences of thrust coefficient, T_c'. At any rate, there is a general strong effect of T_c' in the expected direction, so that at large negative thrust the rudder effectiveness is very much reduced.

Dihedral Effect, C_ℓ vs ψ

The variations of rolling moment coefficient, C_ℓ, versus ψ and T_c' are shown in carpets in Figure 14, similar to those for C_n. There are three parts, for variations in α for $\delta_f = 0$. The slopes, C_{ℓ_ψ}, are of course the dihedral effect.

For the intermediate flap angles, where data were only taken at three ψ, the carpets have α and T_c' as abscissa. They are Figures 20. Here the C_{ℓ_ψ} is calculated from the points at $\psi = \pm 10$ deg.

The dihedral effect derivative, C_{ℓ_ψ}, is shown as a function of α and δ_f in Figure 11, where there are the three parts for negative, zero, and positive thrust. Only at zero thrust is C_{ℓ_ψ} more-or-less independent of angle-of-attack and flap deflection. Its value there is about .0017, corresponding in effective dihedral angle exactly to the true dihedral of $7\frac{1}{2}$ degrees! With positive or negative thrust, however, the effective Γ varies from zero to as much as 25 degrees. The trends and the effect of flap deflection are what would be expected from slipstream-flap interactions. With large thrust coefficients, the variations of C_{ℓ_ψ} with α and δ_f are strong - but they are quite regular except where wing stall or flap separation are involved.

Plots of C_ℓ vs ψ, as in Figures 14 are reasonably linear in all cases not involving stall. The regularity of the C_ℓ function is a favorable feature for simulation work, where the interactions of α, δ_f, and T_c' could be compensated quite easily by coupling in the automatic command of aileron deflection.

Roll Control, C_ℓ vs δ_a

The aileron effectiveness is shown by Figure 15, C_ℓ vs δ_a. The curve drawn is an average one for all combinations of α, δ_f, and T_c'. Short of wing stall, the effects of variations in those parameters are very small, and no attempt is made to show them separately. The general effectiveness of the ailerons is, of course, a feature favorable for variable-stability flight simulation.

CONCLUSIONS

Analysis of full-scale wind-tunnel data for a low-wing, single-engine, light plane, with both up and down flap deflection and over a full range from negative to forward propeller thrust, indicates the following:

1) The negative lift effectiveness of the flap deflected upward is limited to deflections between 20 and 30 degrees. The negative lift increment is less with negative propeller thrust, and more with positive thrust.

2) There are strong interactions between flap deflection and propeller thrust effects on pitching moments. These will affect both the static stability and trim of the airplane. At large negative thrust, the effects are large and irregular.

3) At large negative thrust the elevator effectiveness is greatly reduced, and appears to be a limiting factor for longitudinal characteristics.

4) Directional stability is strongly affected by flap deflection and propeller thrust and angle-of-attack. With large reverse thrust at high angle-of-attack, C_n vs ψ is quite nonlinear; with C_{n_ψ} very low, or negative, through zero sideslip.

5) The rudder effectiveness is strongly affected by propeller thrust. Its reduction at large negative thrust would be a limiting factor for lateral-directional characteristics.

6) The dihedral effect is strongly affected by flap deflection, propeller thrust, and angle-of-attack. Its largest variations are at negative thrust, from about zero at low α and up flap, to about three times normal at high α and down flap.

7) The aileron effectiveness is strong and relatively unaffected by flap deflection, angle-of-attack, or propeller thrust.

REFERENCE

1. Silverstein, A. and Katzoff, S.; Design Charts for Predicting Downwash Angles and Wake Characteristics Behind Plain and Flapped Wings. NACA Report 648, 1939.

TABLE 1 - AIRPLANE DIMENSIONS

Wing	
Area, S	184 ft^2
Sweep	2° 59'46"
Aspect Ratio, A	6.04
Taper Ratio, λ	.54
Mean Aerodynamic Chord, $\bar{c}$	5.7 ft
Dihedral	7.5°
Incidence Root, i_{w_r}	$+2^\circ$
Incidence tip, i_{w_t}	-1°
Airfoil tip	NACA 6410 R
root	NACA 4415 R
Horizontal Tail	
Area	43 ft^2
Sweep	6°
Aspect Ratio	4.0
Taper Ratio	.67
Airfoil	NACA 0012
Incidence	-3°
Vertical Tail	
Area (above horizontal stabilizer)	12.5 ft^2
Airfoil root	NACA 0013.2 MOD
tip	NACA 0012.04 MOD
Fin offset	2°

Power Plant

Reciprocating Engine; Model No. 10520 B

HP Rating 285 HP at take-off at 2700 RPM

Control Surfaces

Surface	Area (ft^2)	Deflection (deg)	C_f / C
Flaps (plain)	83.6	40	.24
Stabilizer	30.0	-	-
Elevator	14.1	up 30 down 20	.23
Aileron	5.4	20	.18
Rudder	6.0	15	.39 base .45 tip

Mass and Inertia Characteristics

Gross weight	2940 pounds
Center of gravity	25% MAC
I_x	1284.08 slug-ft^2
I_y	2772.86 slug-ft^2
I_z	3234.72 slug-ft^2

Propeller Characteristics

Diameter 84"

Number of blades 2

Side force factor 100

TABLE 2 - WIND TUNNEL TEST RUNS

Run	δ_f	i_t	ψ	δ_r	δ_a	δ_e	T_c' (nominal)
1	0	-5°	0	0	0	-23	.215
2						0	
3						17.9	
4						-10	
5						-17	
6						17.9	.095
7						0	
8						-10	
9						-17	
10						-23	
11						17.9	0
12						0	
13						-10	
14						-17	
15						-23	
16						17.9	-.05
17						0	
18						-10	
19				VOID			
20	0	-5°	0	0	0	-17	-.05
21						-23	
22						17.9	-.09
23						0	
24						-10	
25						-17	
26						-23	
27						17.9	-.13
28						0	

Run	δ_f	i_t	ψ	δ_r	δ_a	δ_e	T_c' (nominal)
29	0	-5^{o}	0	0	0	-10	-.13
30						-17	
31						-23	
32						17.9	-.175
33						0	
34						-10	
35						-17	
36						-23	
37				13.2		0	
38				7.0			
39				- 9.0			
40				-17.5			
41				+ 7.0			-.13
42				- 9.0			
43				+ 7.0			-.09
44				- 9.0			
45				+ 7.0			-.05
46				- 9.0			
47				+13.2			0
48				+ 7.0			
49				- 9.0			
50				-17.5			
51				+ 7.0			.095
52				- 9.0			
53				13.2			.215
54				7.0			
55				- 9.0			
56				-17.5			

Run	δ_f	i_t	ψ	δ_r	δ_a	δ_e	T_c' (nominal)
57	0	-5°	0	0	-18.8	0	0
58					- 8.8		
59					+12.2		
60					+24.4		
61			+ 5		0		
62							.215
63							-.175
64			+10				.20
65				+ 7.0			
66				- 9.0			
67				0			.095
68							0
69				+ 7.0			
70				- 9.0			
71			+10	0			-.05
72							-.09
73							-.13
74							-.175
75				+ 7			-
76				- 9			
77				VOID			
78	0	-5°	+15	13.2	0	0	.20
79				0			
80				-17.5			
81							0
82				0			
83				13.2			
84							-.175
85				0			
86				-17.5			

Run	δ_f	i_t	ψ	δ_r	δ_a	δ_e	T_c' (nominal)
87	0	-5^o	-5^o	0	0	0	-.175
88							0
89							.215
90			-10				.20
91				+ 7			
92				- 9			
93				0			.095
94				+ 7			0
95				0			
96				- 9			
97				0			-.05
98							-.09
99				VOID			
100	0	-5^o	-10	0	0	0	-.13
101							-.175
102				+ 7.0			
103				- 9.0			
104			-15	+13.2			
105				0			
106				-17.5			
107				0			0
108				13.2			
109				-17.5			
110							+.20
111				13.2			
112				0			
113	+20		0			17.9	
114						0	
115						-10	
116						-17	

Run	δ_f	i_t	ψ	δ_r	δ_a	δ_e	T_c' (nominal)
117	+20	-5°	0	0	0	-23	+.20
118				+ 7.0			
119				- 9.0			
120				0		17.9	0
121						0	
122						-10	
123						-17	
124						-23	
125				+ 7.0		0	
126	VOID						
127	+20	-5°	0	- 9.0	0	0	0
128						17.9	-.175
129						0	
130				0		-10	
131						-17	
132	VOID						
133	20	-5°	0	0	0	-23	
134				7		0	
135				0			
136						17.9	
137			10			0	.175
138							0
139							-.175
140			-10				
141							0
142							.175
143	30						0
144							.175
145							-.175

Run	δ_f	i_t	ψ	δ_r	δ_a	δ_e	T_c' (nominal)
146				VOID			
147				VOID			
148	30	-5°	0	0	0	0	0
149	↓	↓	↓	↓	↓	17.9	↓
150	↓	↓	↓	↓	↓	-10	↓
151	↓	↓	↓	↓	↓	-17	↓
152	↓	↓	↓	↓	↓	-23	↓
153	↓	↓	↓	↓	12.2	0	↓
154	↓	↓	↓	↓	24.5	↓	↓
155				VOID			
156	30	-5°	0	7	0	0	0
157	↓	↓	↓	-9	↓	↓	↓
158	↓	↓	↓	0	↓	↓	.215
159	↓	↓	↓	↓	↓	17.9	↓
160				VOID			
161	30	-5°	0	0	0	-10	.215
162	↓	↓	↓	↓	↓	-17	↓
163	↓	↓	↓	↓	↓	-23	↓
164	↓	↓	↓	7	↓	0	.205
165	↓	↓	↓	-9	↓	↓	.200
166	↓	↓	↓	0	↓	↓	-.175
167	↓	↓	↓	↓	↓	17.9	↓
168	↓	↓	↓	↓	↓	-10	↓
169	↓	↓	↓	↓	↓	-17	↓
170	↓	↓	↓	↓	↓	-23	↓
171	↓	↓	↓	7	↓	0	↓
172	↓	↓	↓	-9	↓	↓	↓
173	↓	↓	10	0	↓	↓	0
174	↓	↓	↓	↓	↓	↓	.200
175	↓	↓	↓	↓	↓	↓	-.175
176	-20	↓	0	↓	↓	↓	0
177	↓	↓	↓	↓	↓	17.9	↓

Run	δ_f	i_t	ψ	δ_r	δ_a	δ_e	T_c' (nominal)
178	-20	-5°	0	0	0	-10	0
179						-17	
180						-23	
181				7		0	
182				-9			
183							.175
184				VOID			
185	-20	-5°	0	0	0	17.9	.175
186						0	
187						-10	
188						-17	
189						-23	
190				7		0	
191				0			-.175
192						17.9	
193						-10	
194						-17	
195						-23	
196				7		0	
197				-9			
198			10	0			0
199							.175
200							-.175
201			-10				0
202							.175
203							-.175
204	-30		0				.175
205						17.9	
206						-10	
207						-17	
208						-23	
209				7		0	

Run	δ_f	i_t	ψ	δ_r	δ_a	δ_e	T_c' (nominal)
210	-30	-5°	0	-9	0	0	.175
211				0			0
212						17.9	
213						-10	
214						-17	
215						-23	
216				7		0	
217				-9			
218				0	12.2		
219					24.5		
220					0		-.175
221						17.9	
222						-10	
223						-17	
224						-23	
225				7		0	
226				-9			
227			10	0			0
228							.125
229							-.175
230			-10				0
231							.125
232							-.175
233		+5	0				0
234						11.3	
235						-10	
236						-20	
237						-30	
238						0	-.175
239						11.3	

Run	δ_f	i_t	ψ	δ_r	δ_a	δ_e	T_c' (nominal)
240	-30	+5	0	0	0	-10	-.175
241	↓	↓	↓	↓	↓	-20	↓
242						-30	
243						0	.175
244						11.3	↓
245						-10	
246						-20	.095 (max)
247						-30	↓
248	-20					0	0
249	↓					11.3	↓
250						-10	
251						-20	
252						-30	
253						0	-.175
254						11.3	↓
255						-10	
256						-20	
257						-30	
258						0	.125
259						11.3	↓
260						-10	
261						-20	
262						-30	
263	0					0	0
264	↓					11.3	↓
265						-10	
266						-20	
267						-30	
268						0	.175
269						11.3	↓

Run	δ_f	i_t	ψ	δ_r	δ_a	δ_e	T_c' (nominal)
270	0	+5	0	0	0	-20	.175
271						-10	
272						-30	
273						0	.095
274						11.3	
275						-10	
276						-20	
277						-30	
278						0	-.05
279						11.3	
280						-10	
281						-20	
282						-30	
283						0	-.09
284						11.3	
285						-10	
286						-20	
287						-30	
288						0	-.13
289						11.3	
290						-10	
291						-20	
292						-30	
293						0	-.175
294						11.3	
295						-10	
296						-20	
297						-30	
298	20					0	.175
299						11.3	

Run	δ_f	i_t	ψ	δ_r	δ_a	δ_e	T_c' (nominal)
300	20	+5	0	0	0	-10	.175
301						-20	
302						-30	
303						0	0
304						11.3	
305						-10	
306						-20	
307						-30	
308						0	-.175
309						11.3	
310						-10	
311						-20	
312						-30	
313	30					0	0
314						11.3	
315						-10	
316						-20	
317						-30	
318						0	.175
319						11.3	
320						-10	
321						-20	
322						-30	
323						0	-.175
324						11.3	
325						-10	
326						-20	
327						-30	
328-336			SLOTS OPEN				

Run		δ_f	i_t	ψ	δ_r	δ_a	δ_e	T_c' (nominal)
337		30	Off	0	0	0	Off	0
338								.175
339								-.175
340		20						0
341								.175
342								-.175
343		-20						0
344								.175
345								-.175
346		-30						0
347								.175
348								-.175
349		0						0
350								.095
351								.175
352								-.05
353								-.09
354								-.13
355								-.175
356	TP=12	0	-5	-15	0	0	0	Off
357	1			0				
358	4							
359	8							
360	12							
361				+15				
362		-30		0				
363		-20						
364		20						
365		30						

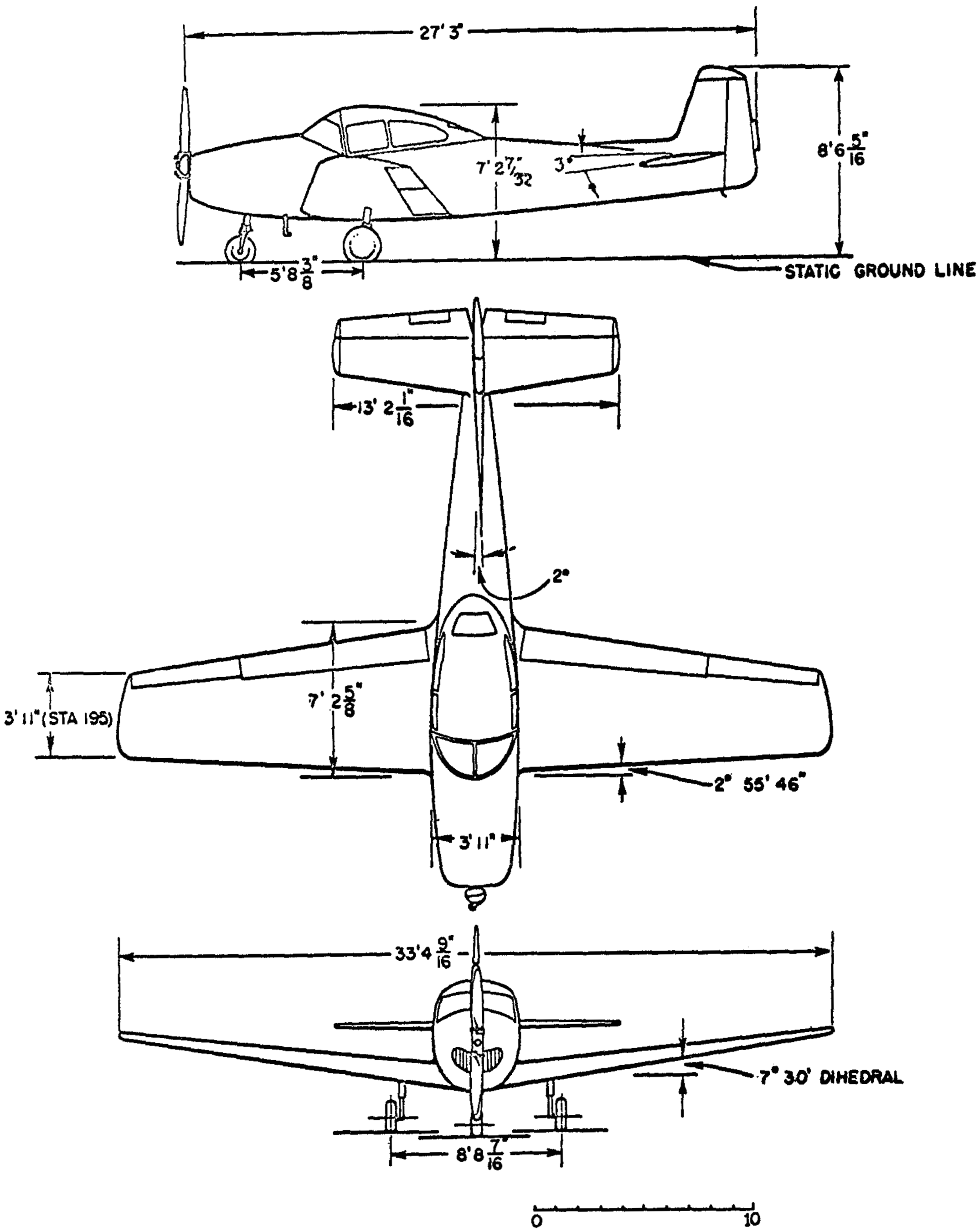

FIGURE 1. THREE VIEW DRAWING OF THE LIGHT SINGLE-ENGINE AIRPLANE

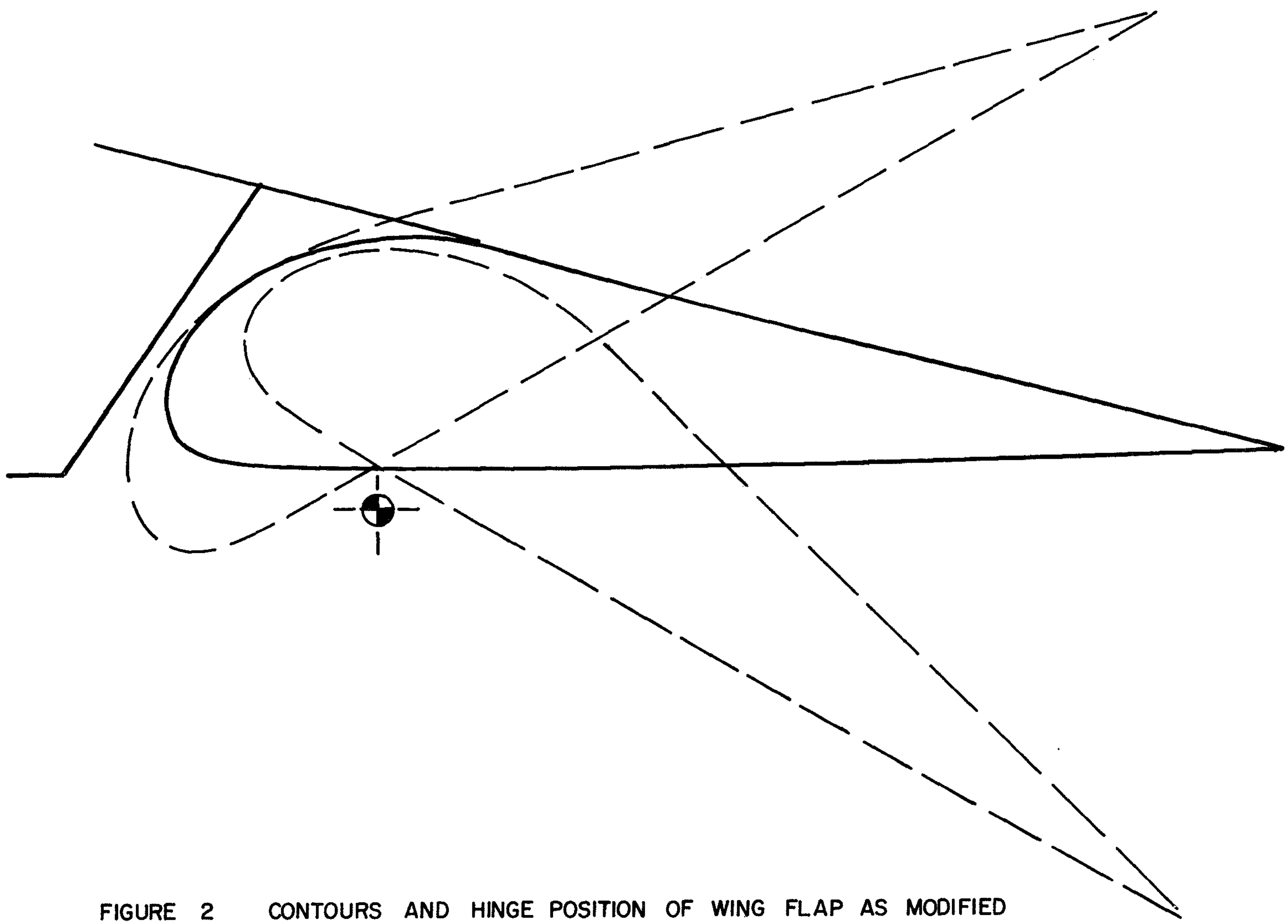

FIGURE 2 CONTOURS AND HINGE POSITION OF WING FLAP AS MODIFIED FOR UP AND DOWN DEFLECTION

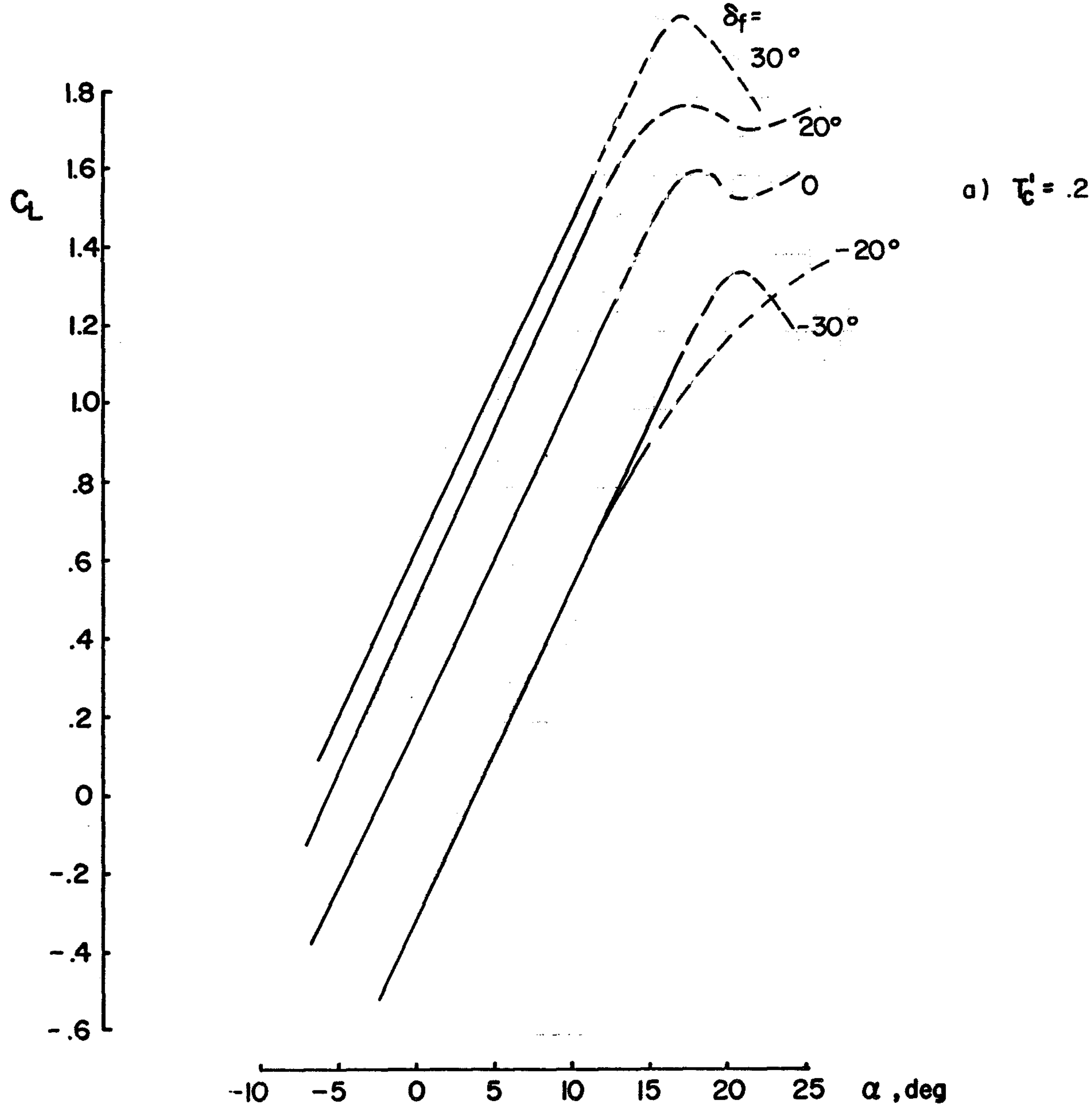

FIGURE 3 VARIATION OF LIFT COEFFICIENT WITH ANGLE OF ATTACK AND FLAP DEFLECTION FOR $i_t = -5°$, $\delta_e = 0°$

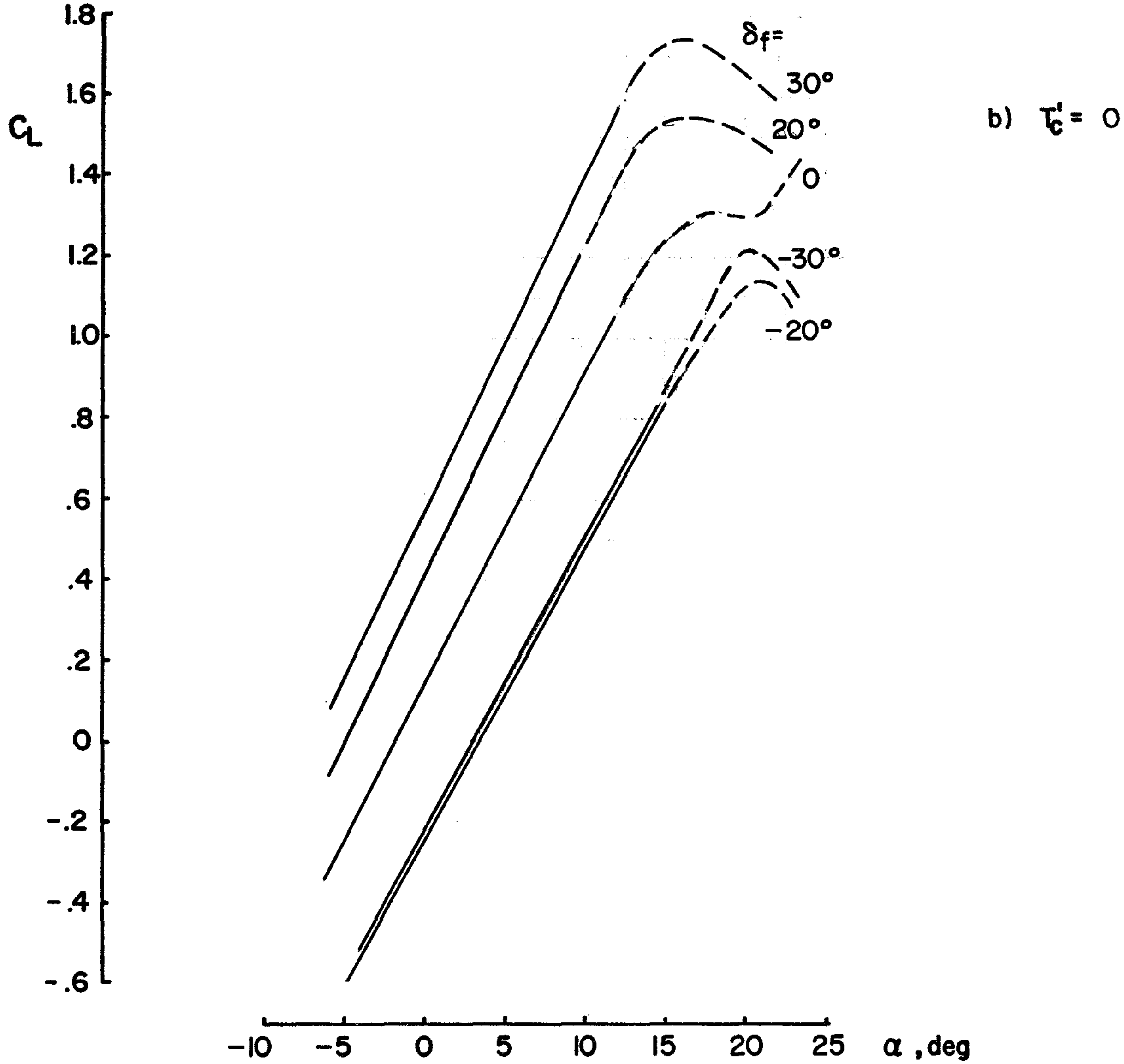

FIGURE 3 Continued

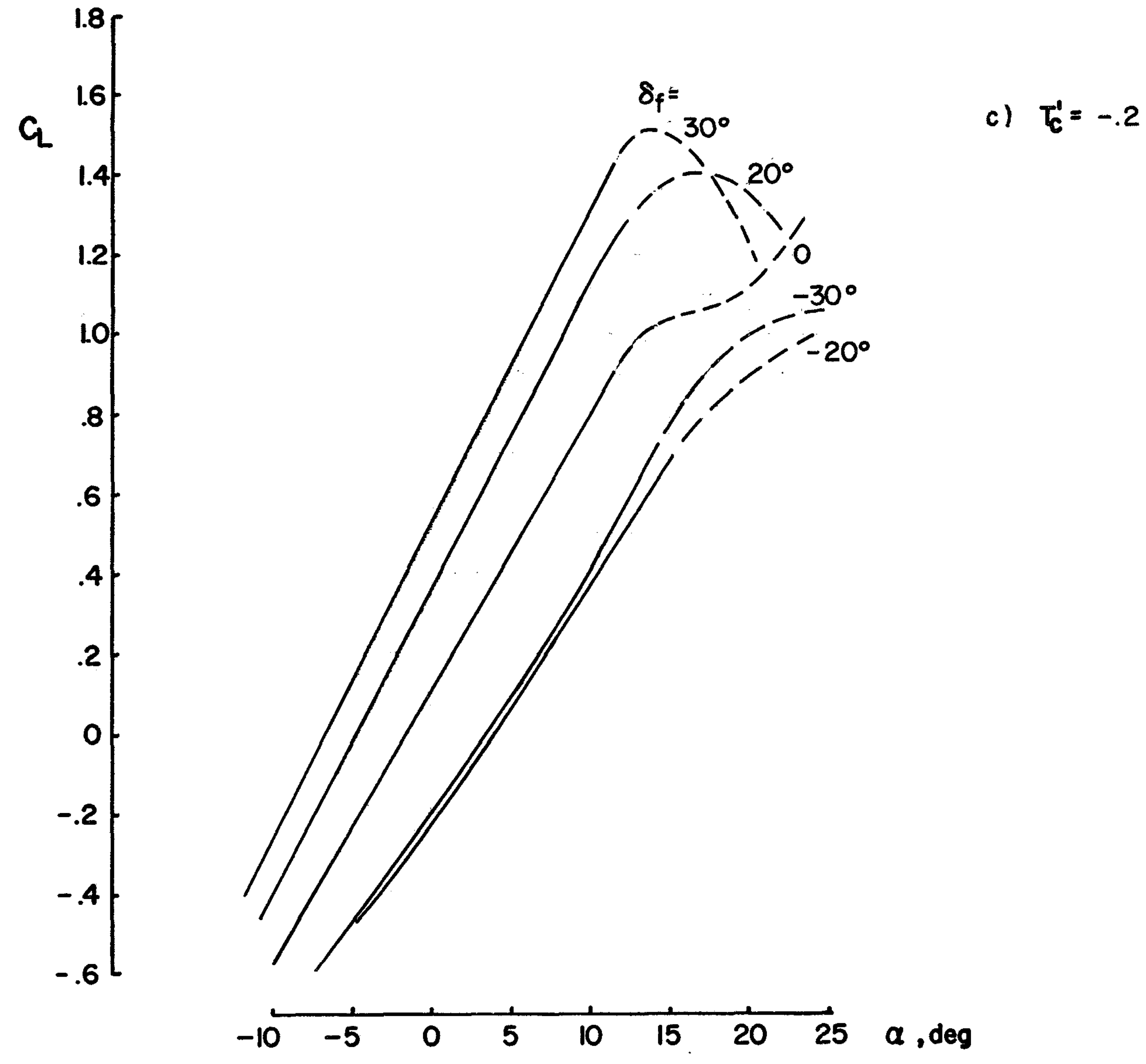

FIGURE 3 Concluded

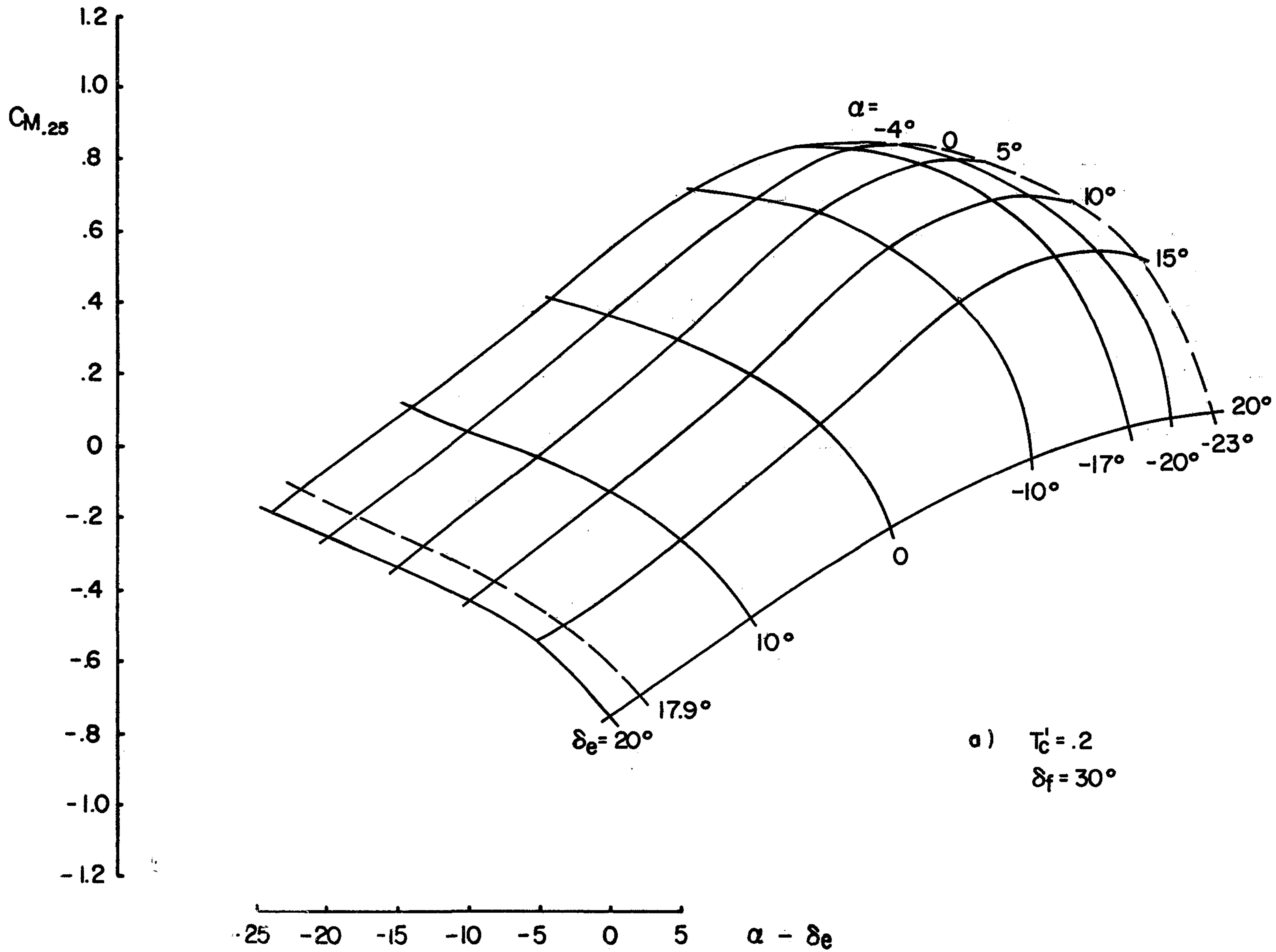

FIGURE 4 VARIATION OF PITCHING MOMENT COEFFICIENT WITH ANGLE OF ATTACK AND ELEVATOR ANGLE FOR $i_t = -5°$

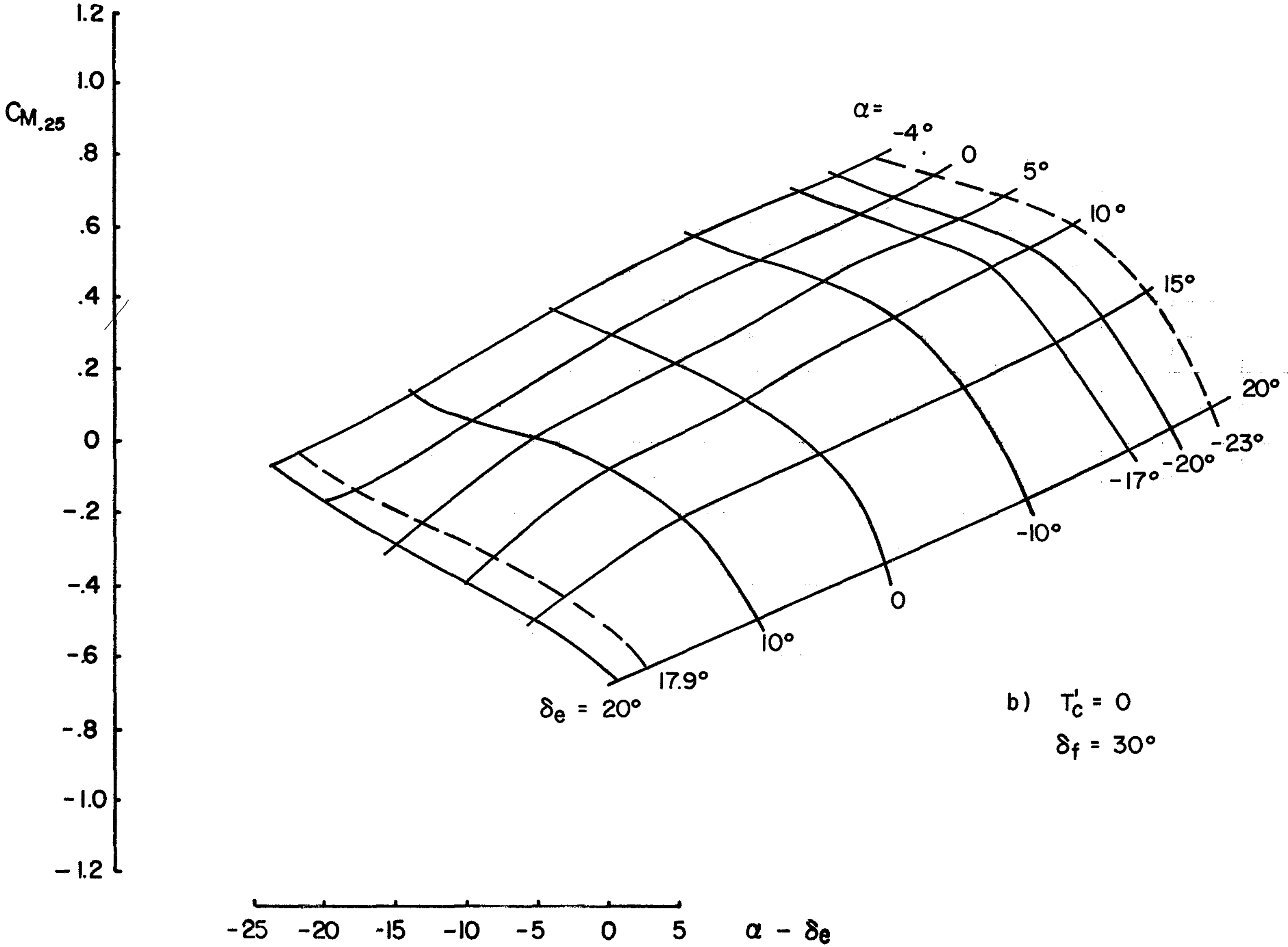

FIGURE 4 Continued

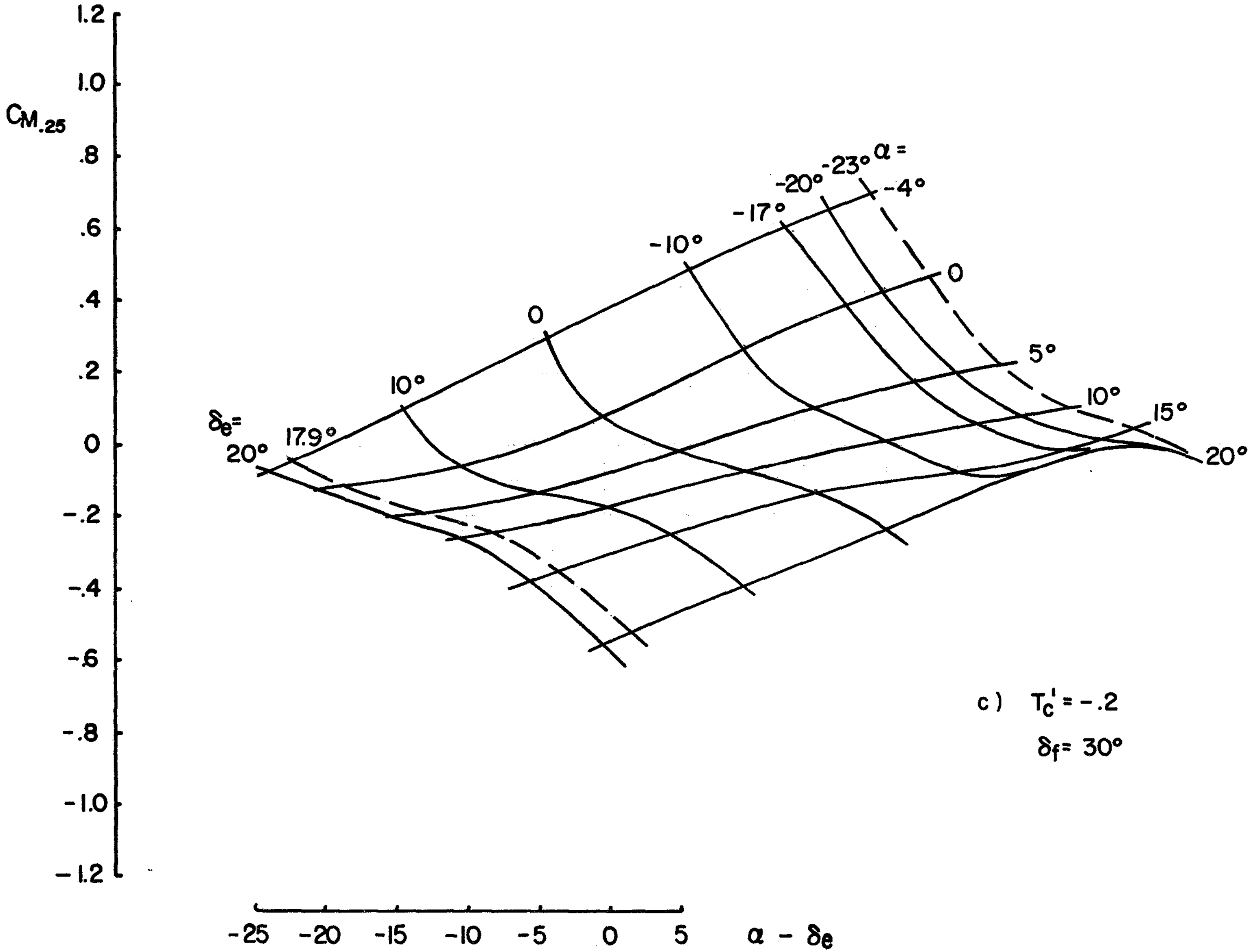

FIGURE 4 Continued

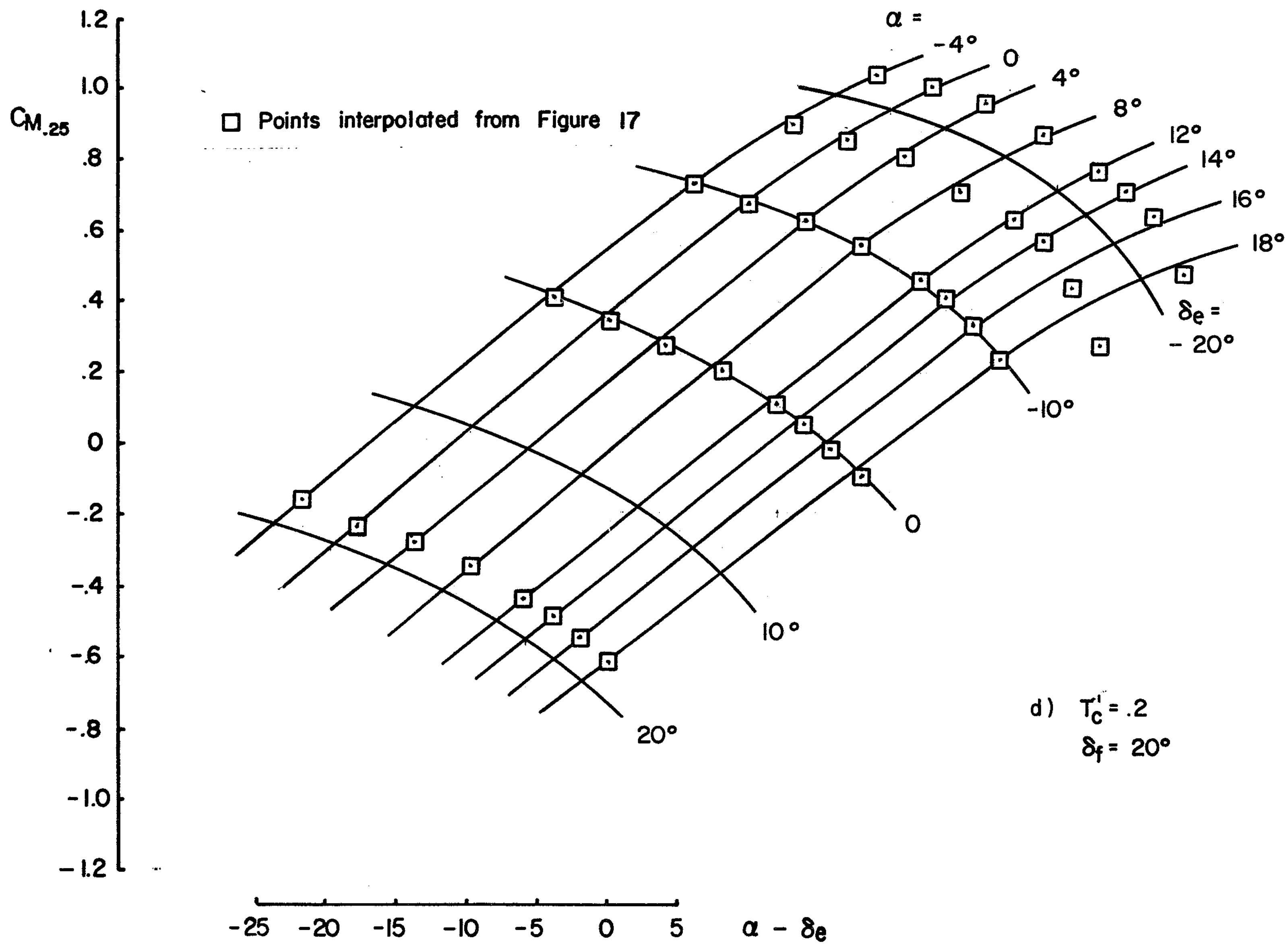

FIGURE 4 Continued

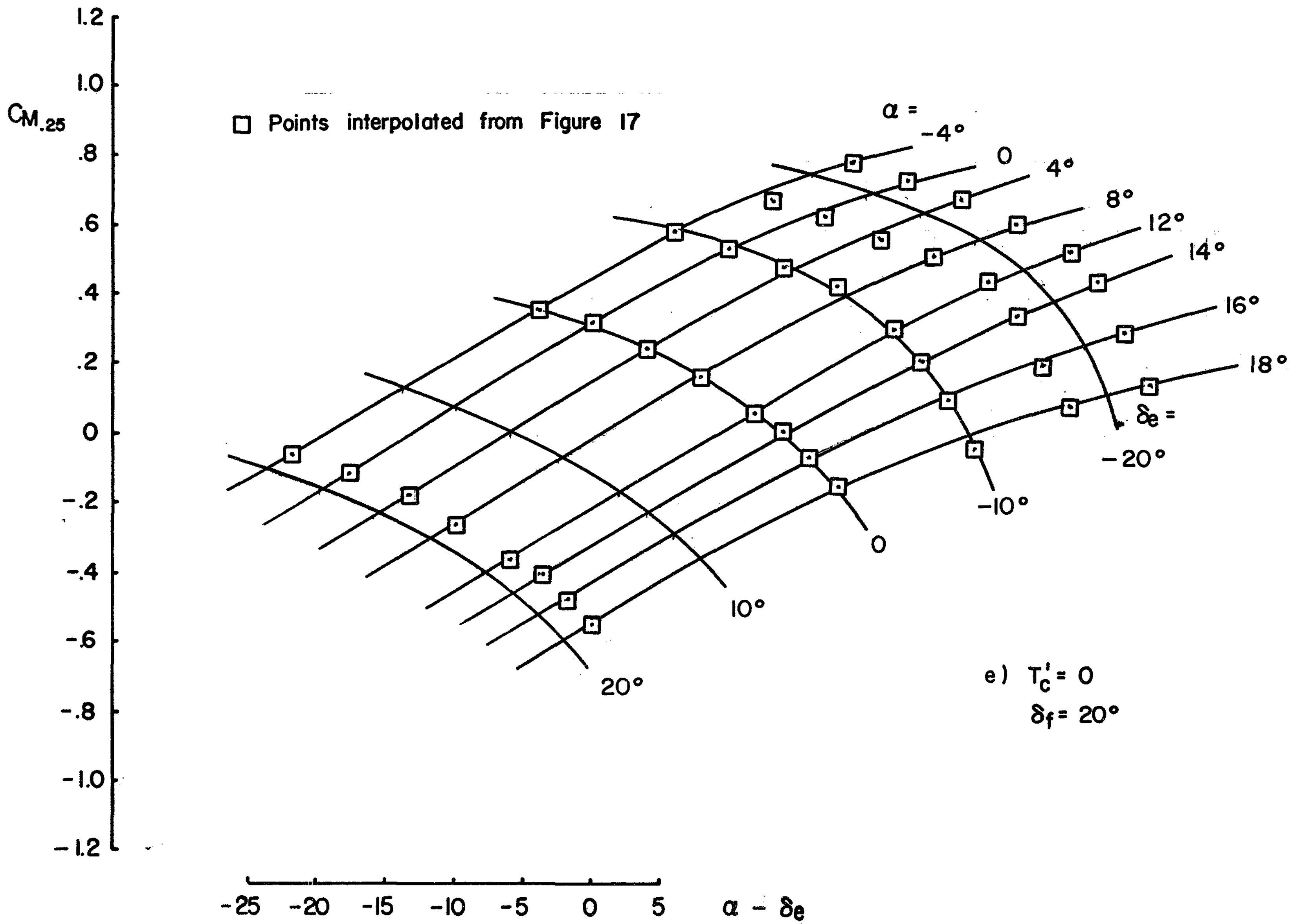

FIGURE 4 Continued

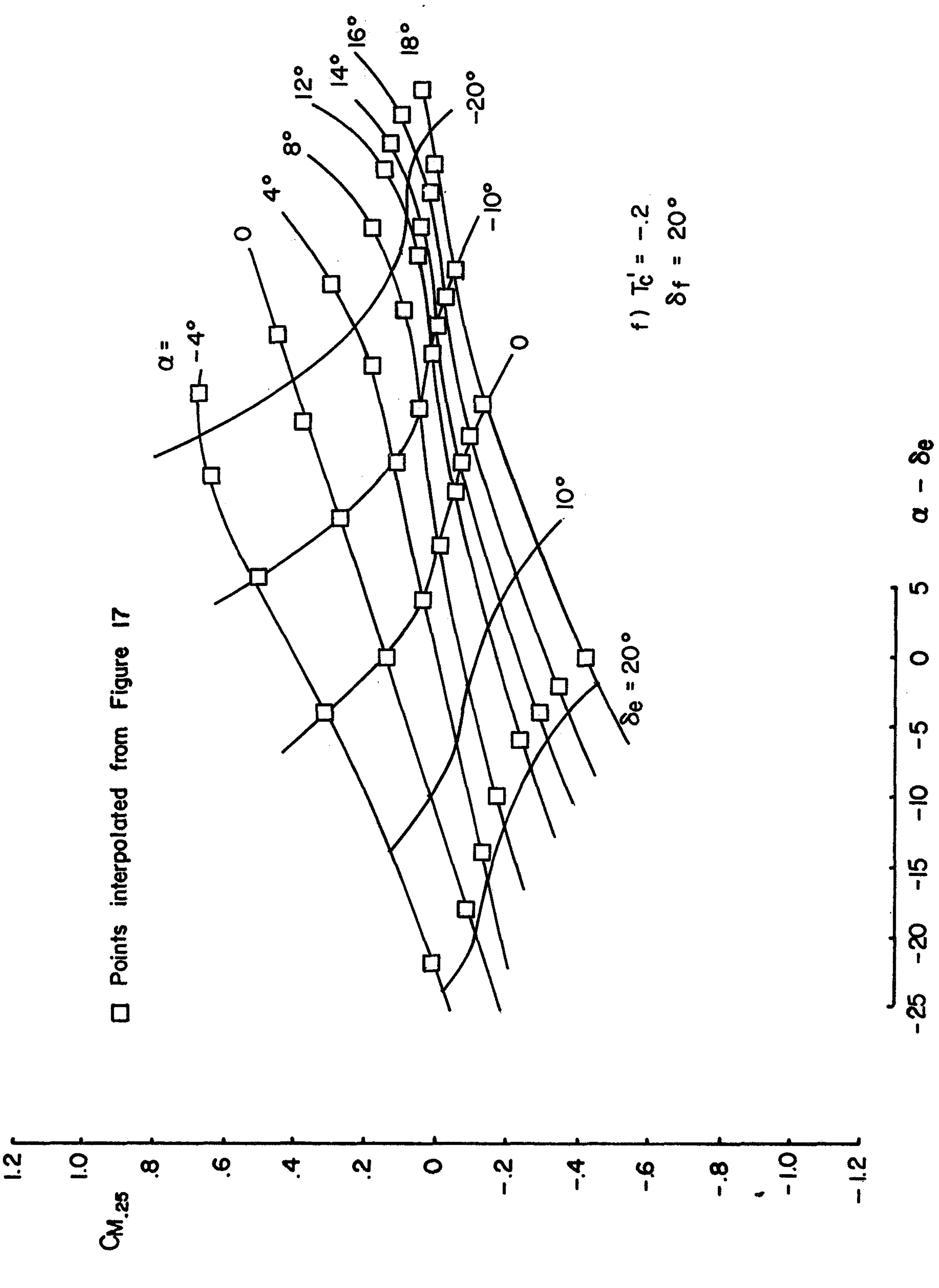

FIGURE 4 Continued

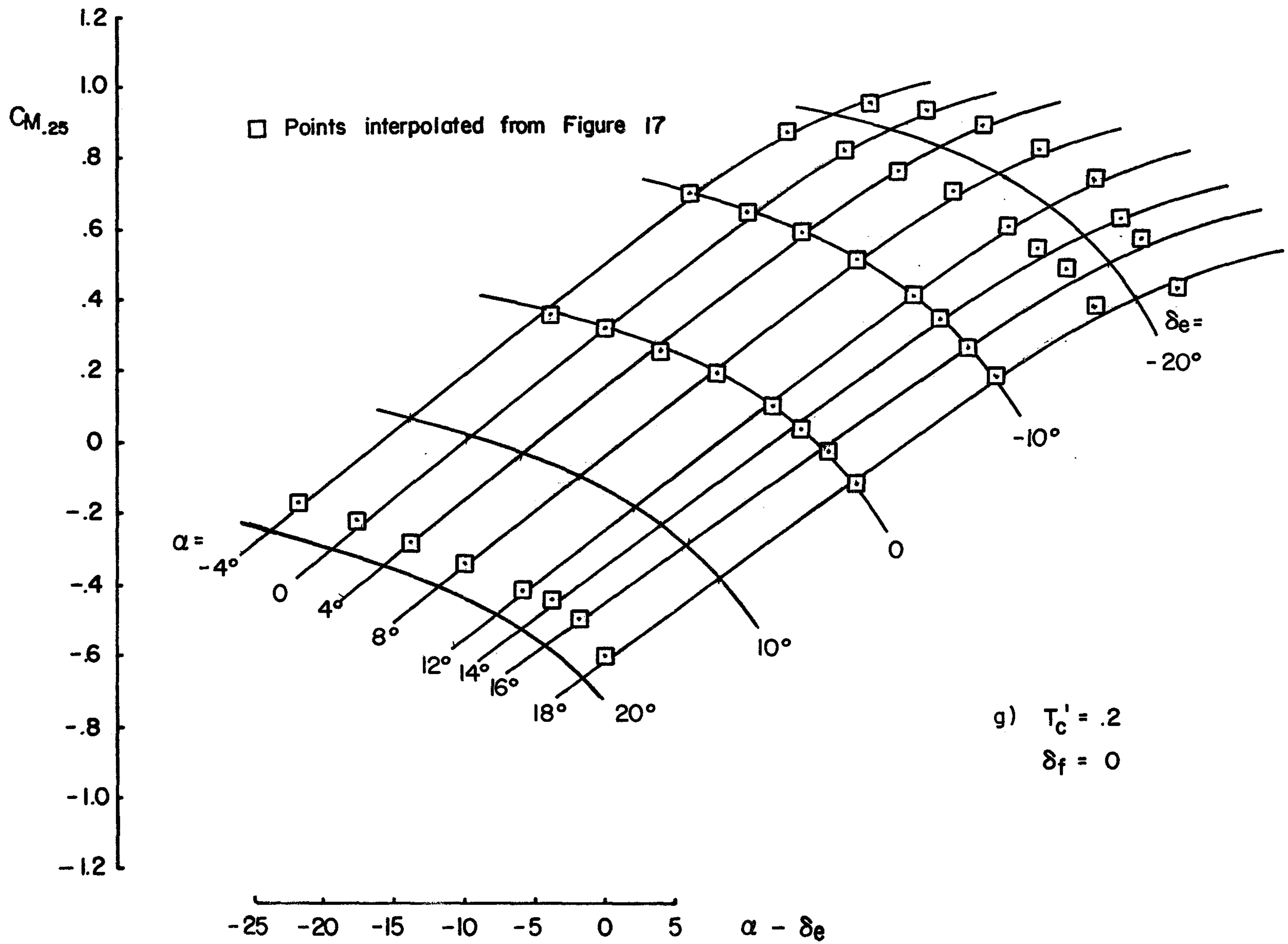

FIGURE 4 Continued

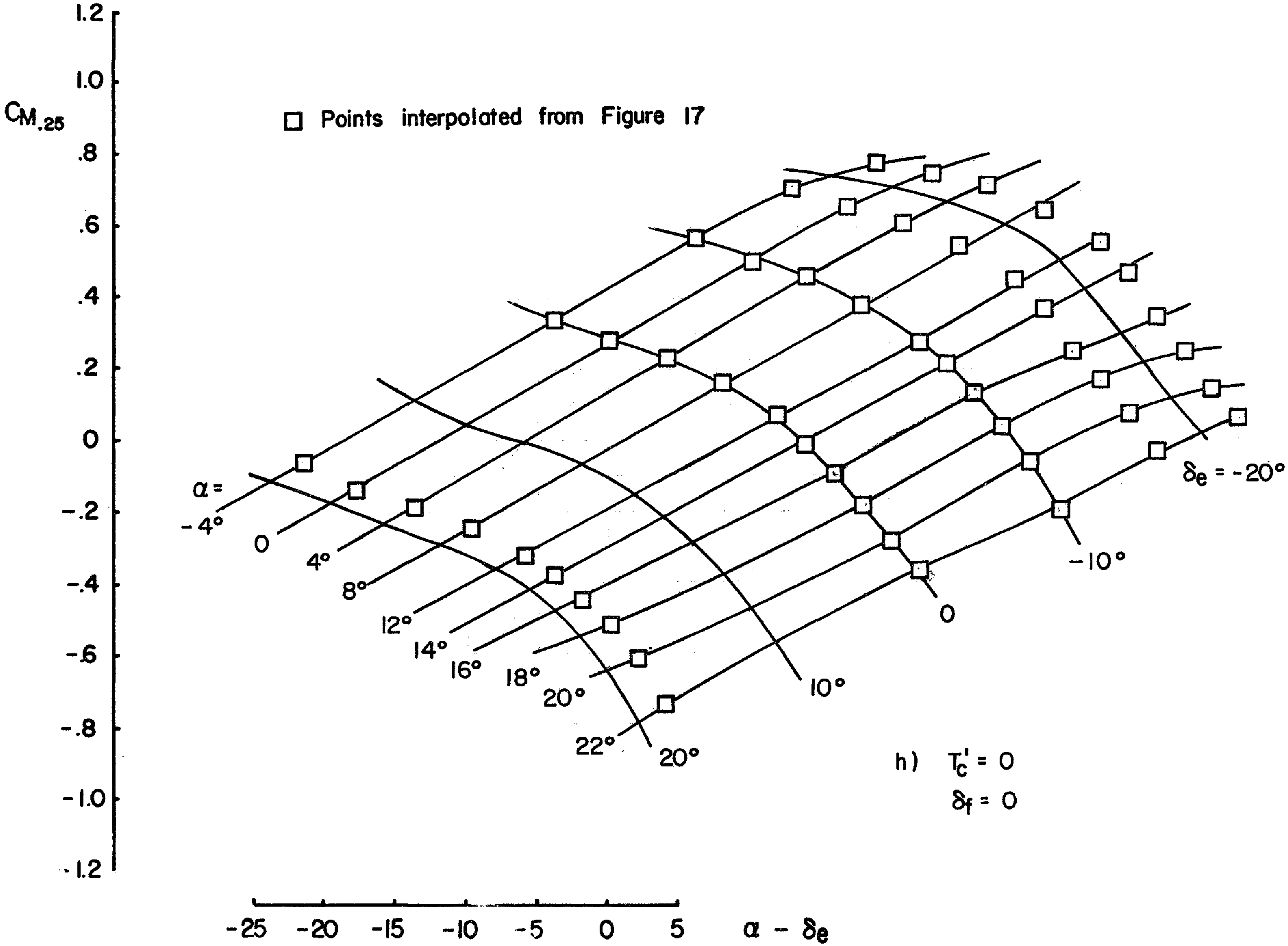

FIGURE 4 Continued

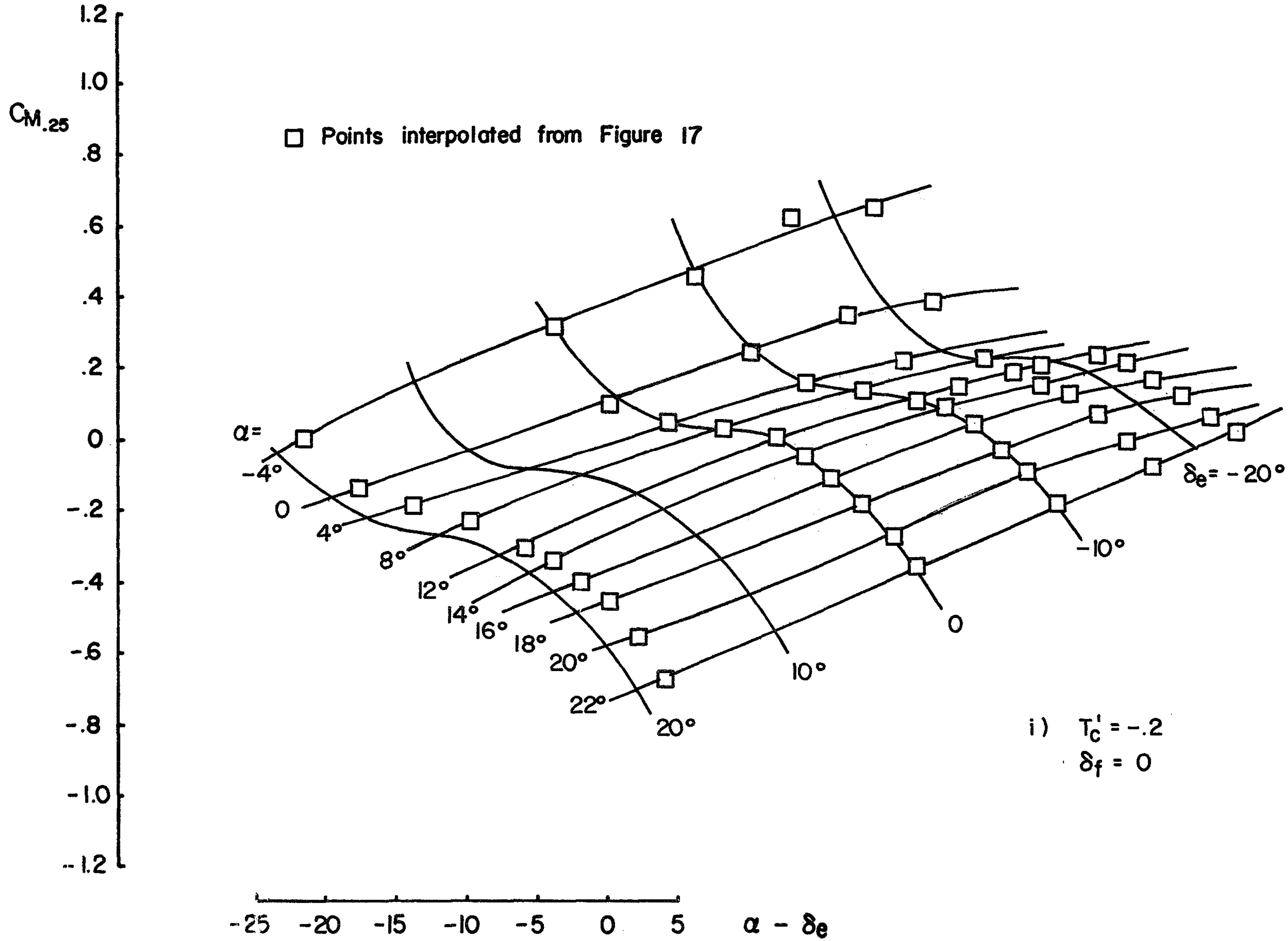

FIGURE 4 Continued

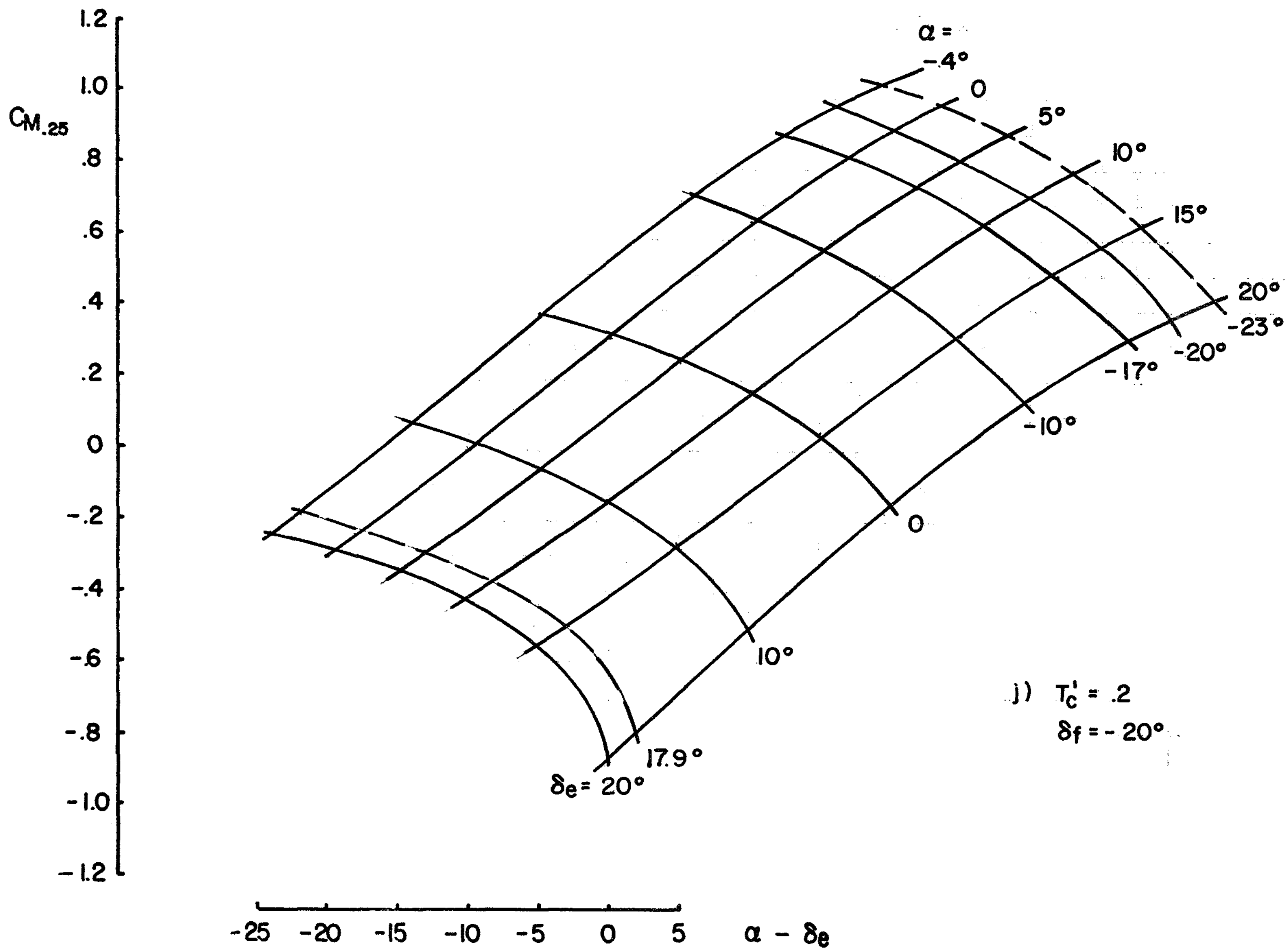

FIGURE 4 Continued

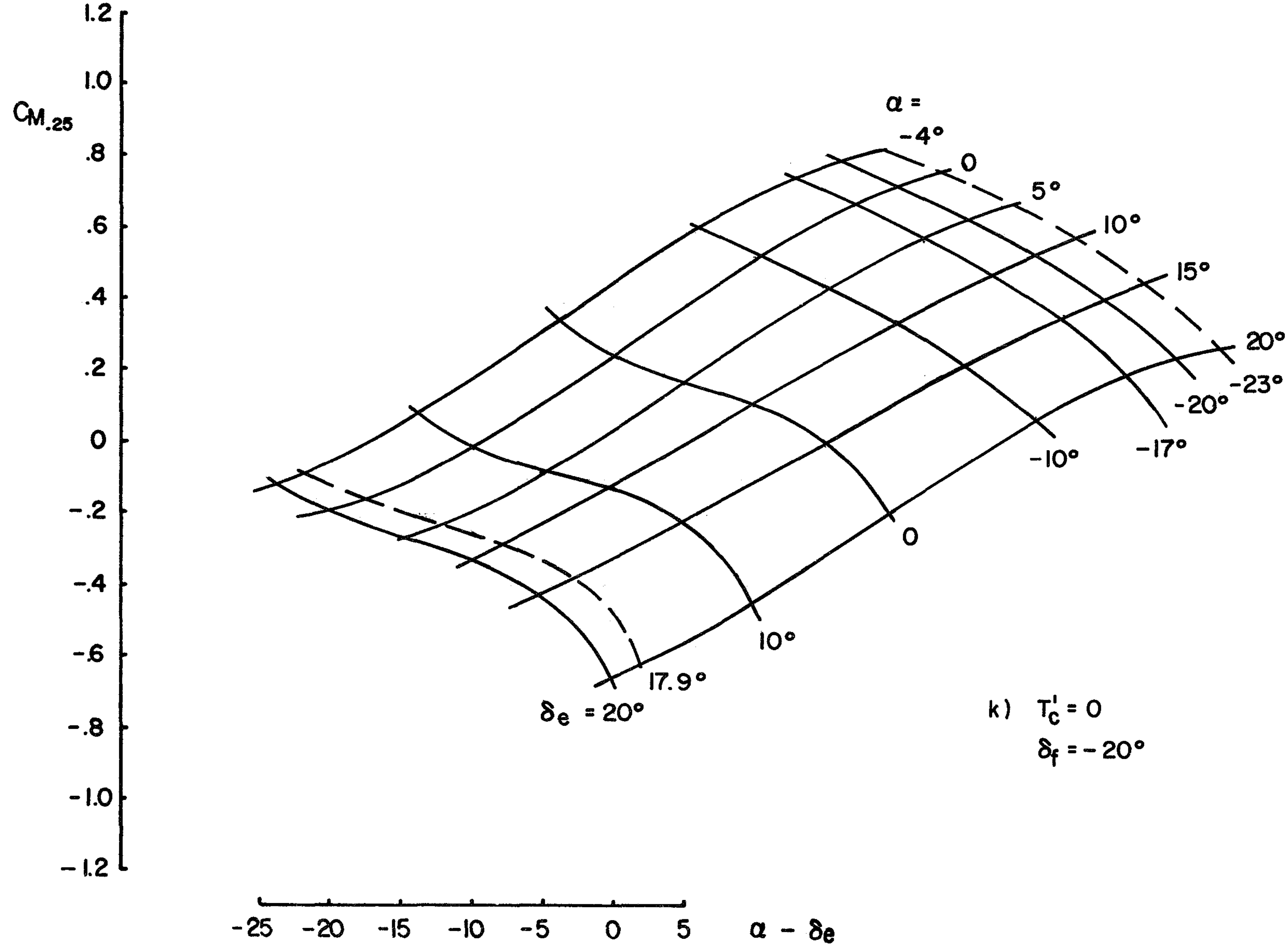

FIGURE 4 Continued

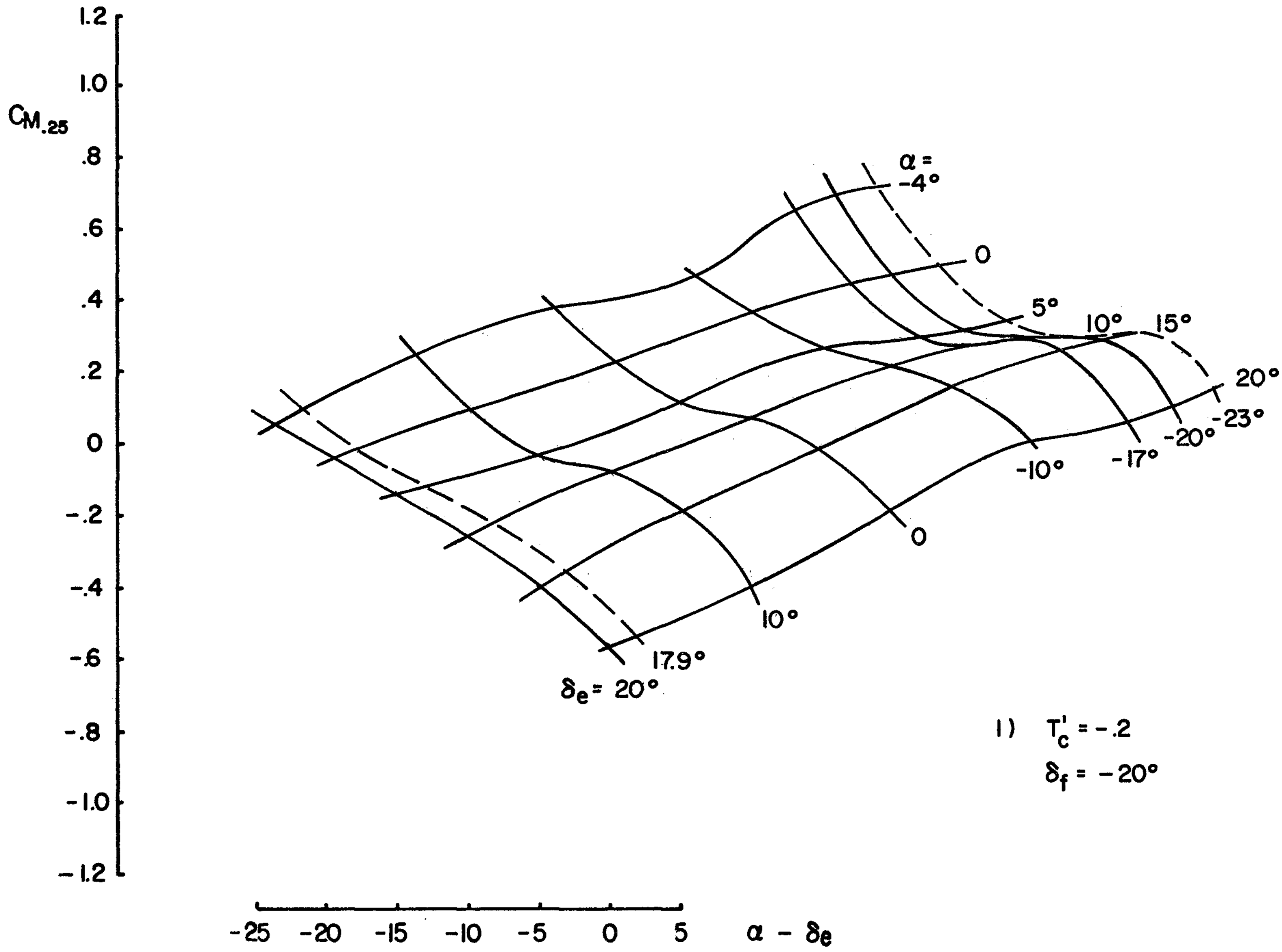

FIGURE 4 Continued

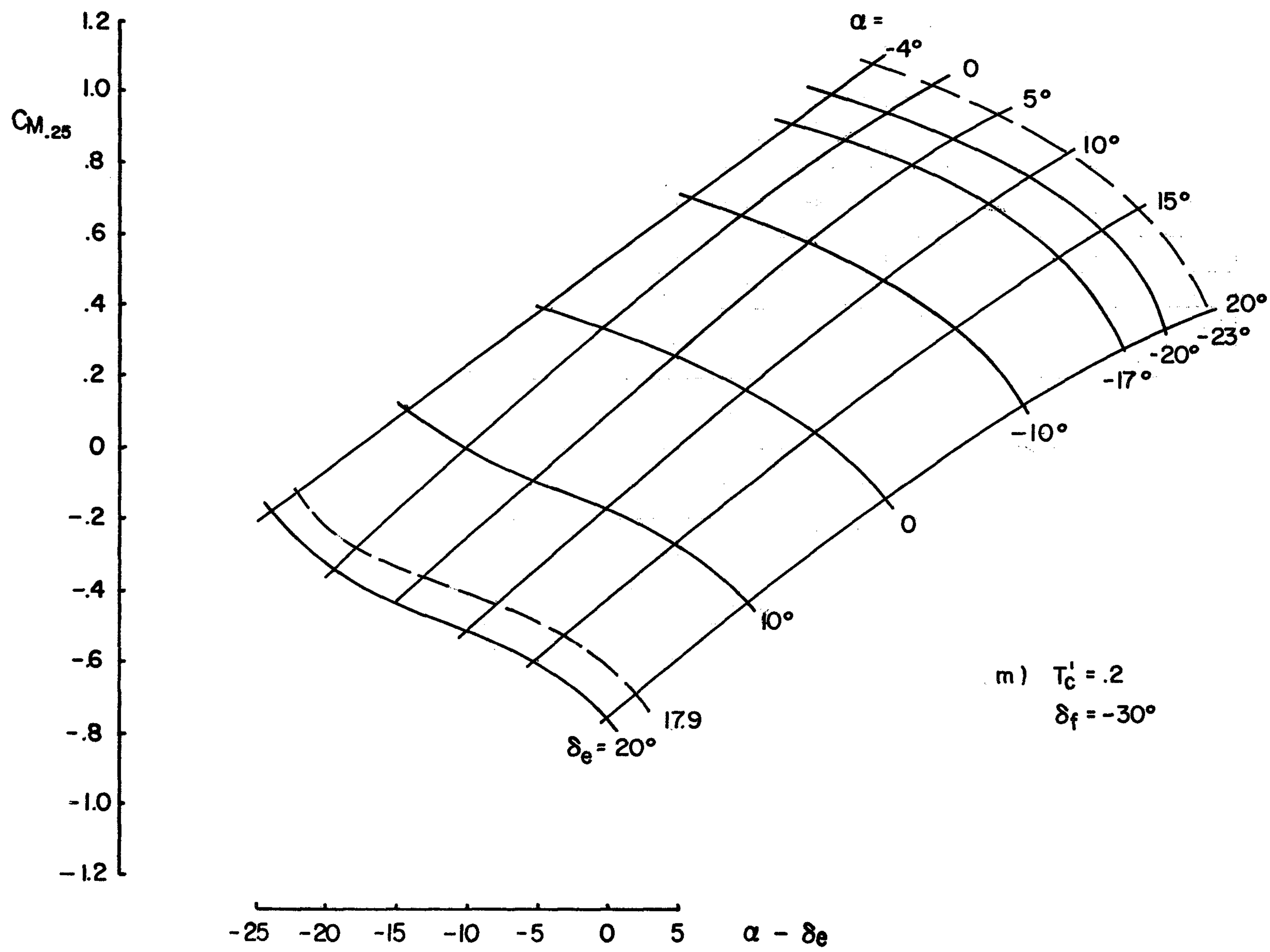

FIGURE 4 Continued

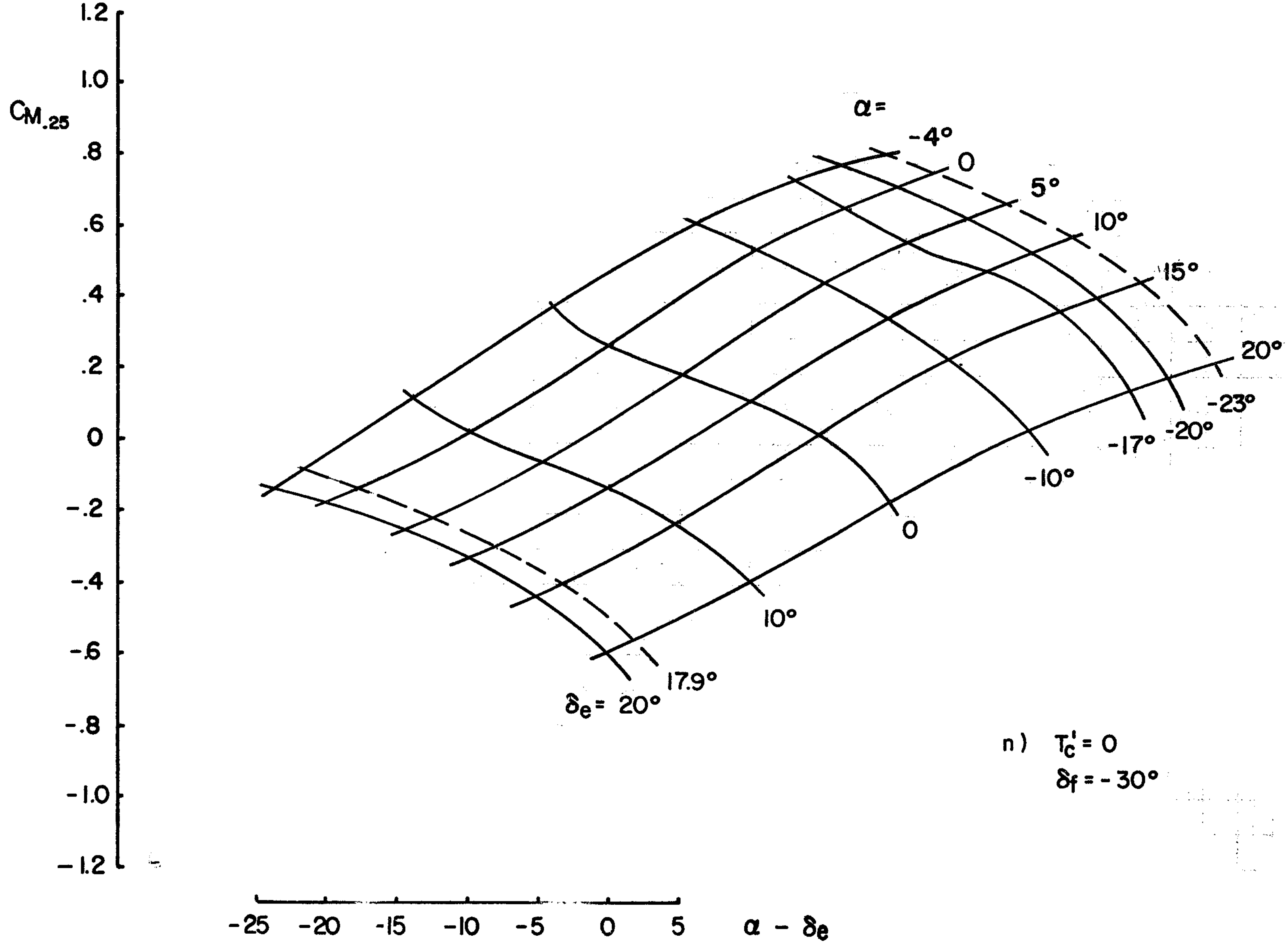

FIGURE 4 Continued

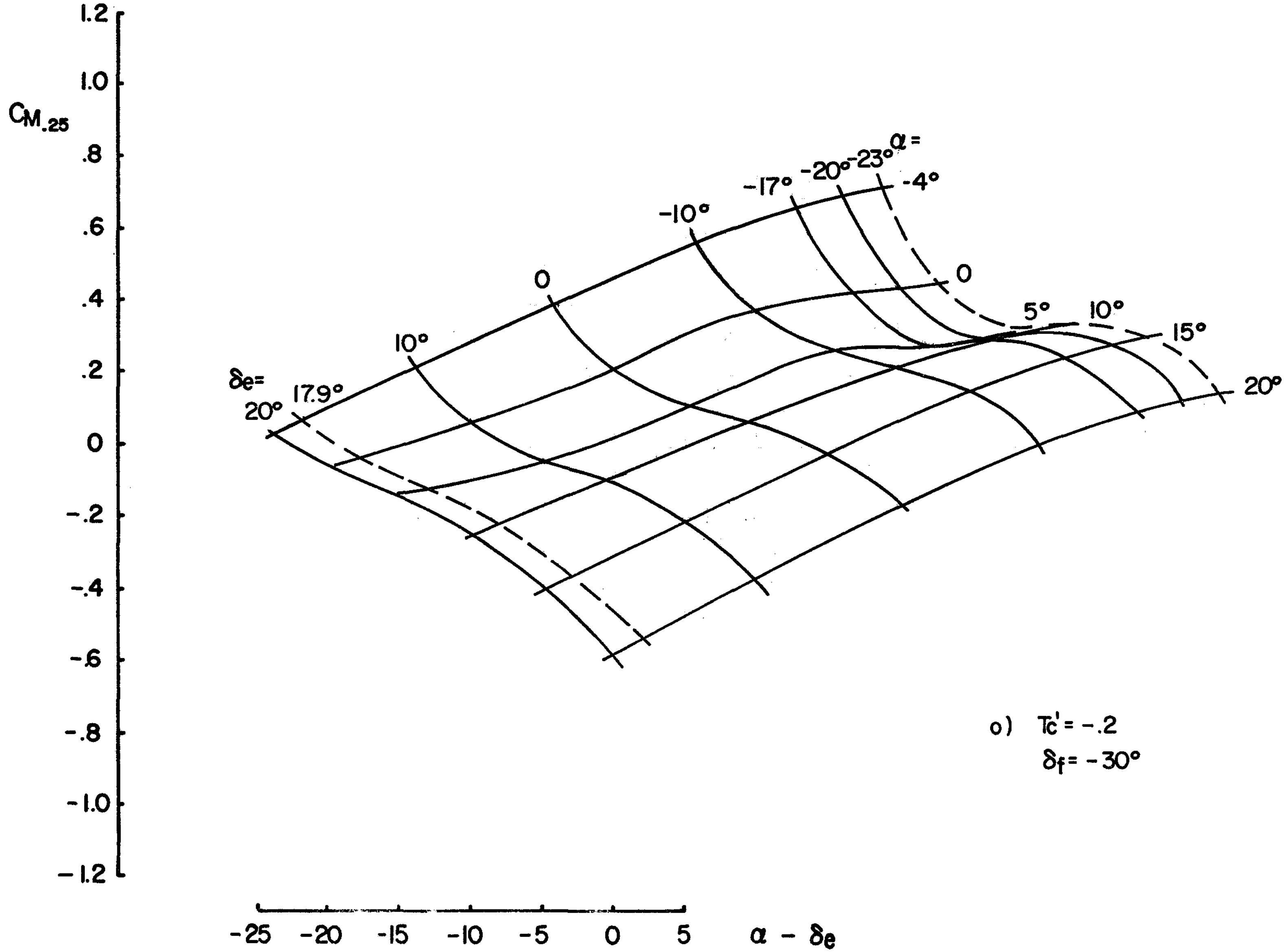

FIGURE 4 Concluded

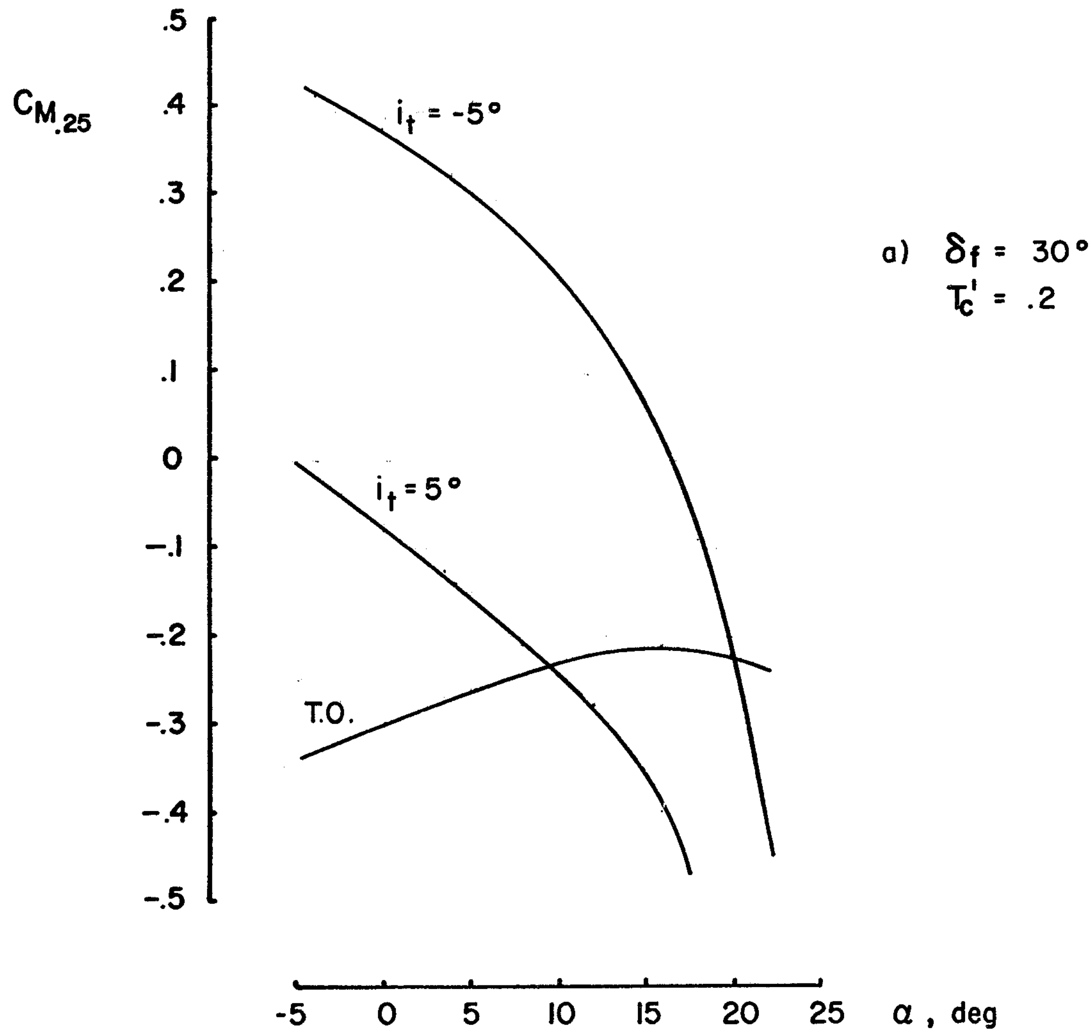

FIGURE 5 VARIATION OF PITCHING MOMENT COEFFICIENT WITH ANGLE OF ATTACK FOR $\delta_e = 0$

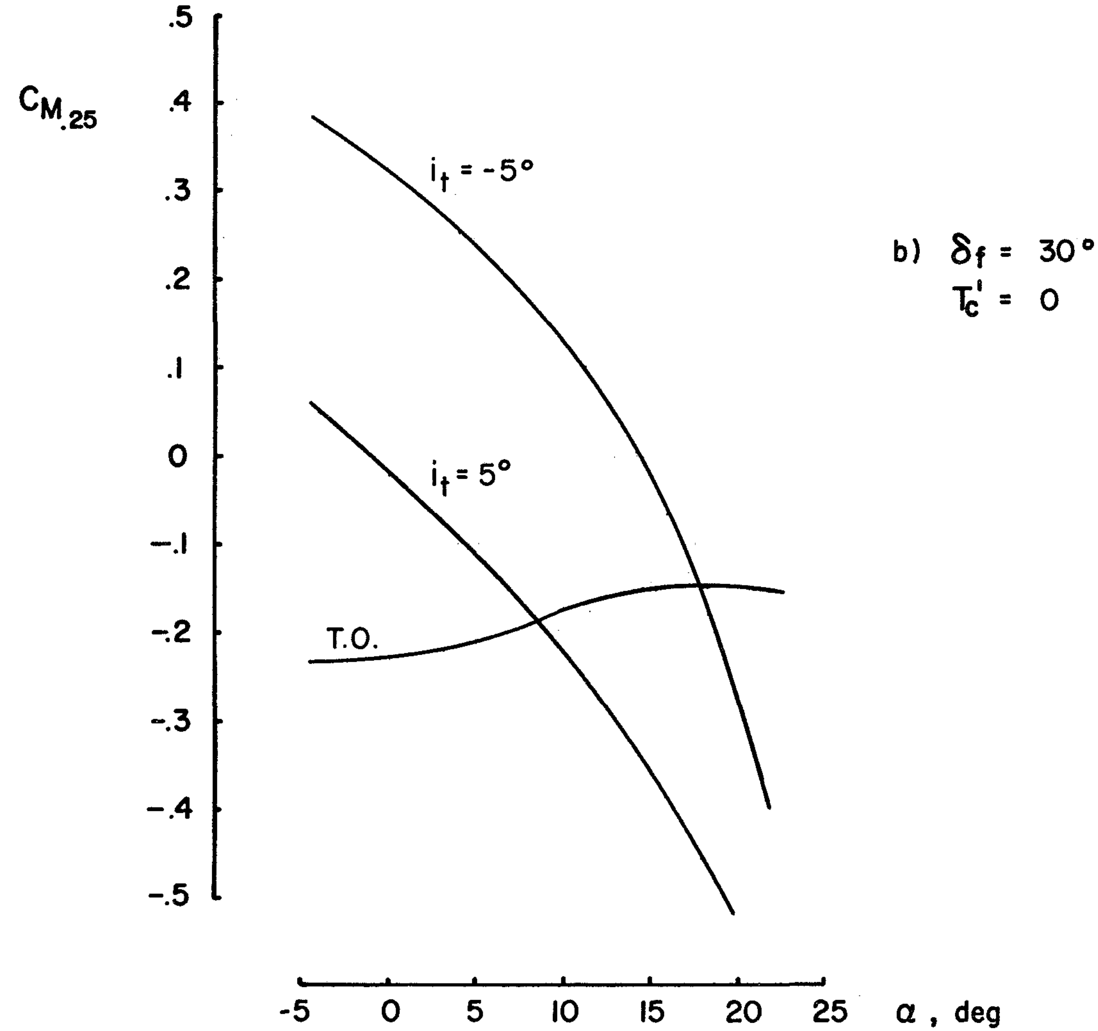

FIGURE 5 Continued

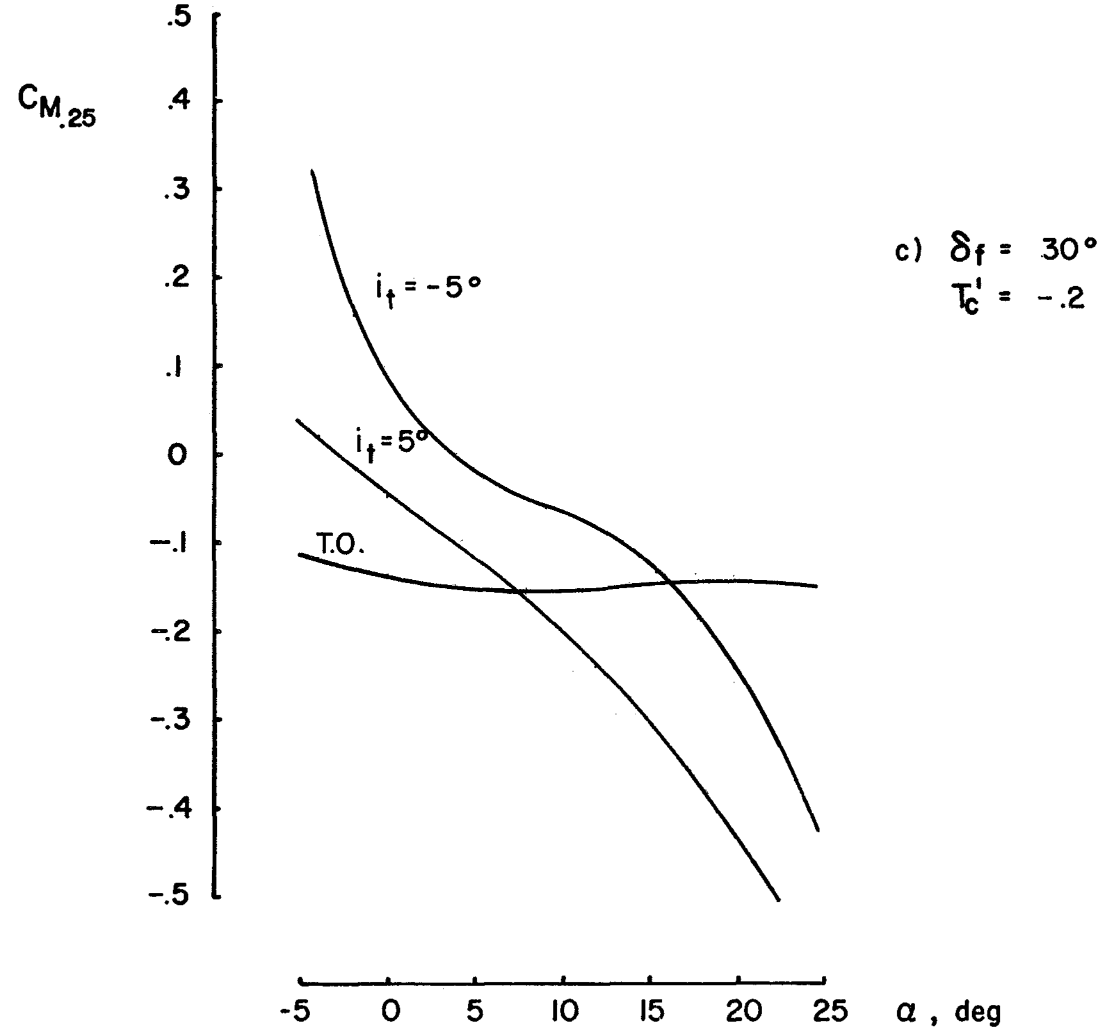

FIGURE 5 Continued

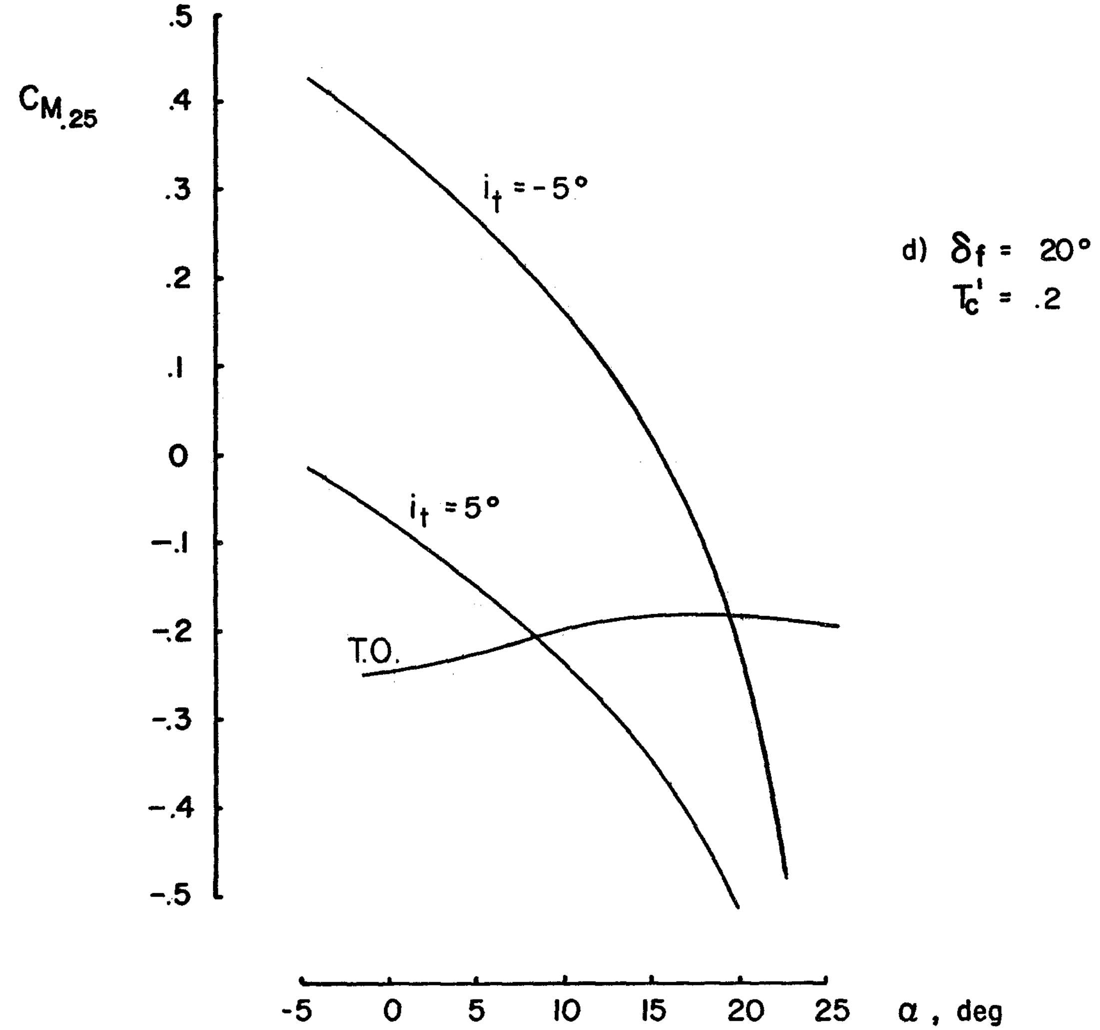

FIGURE 5 Continued

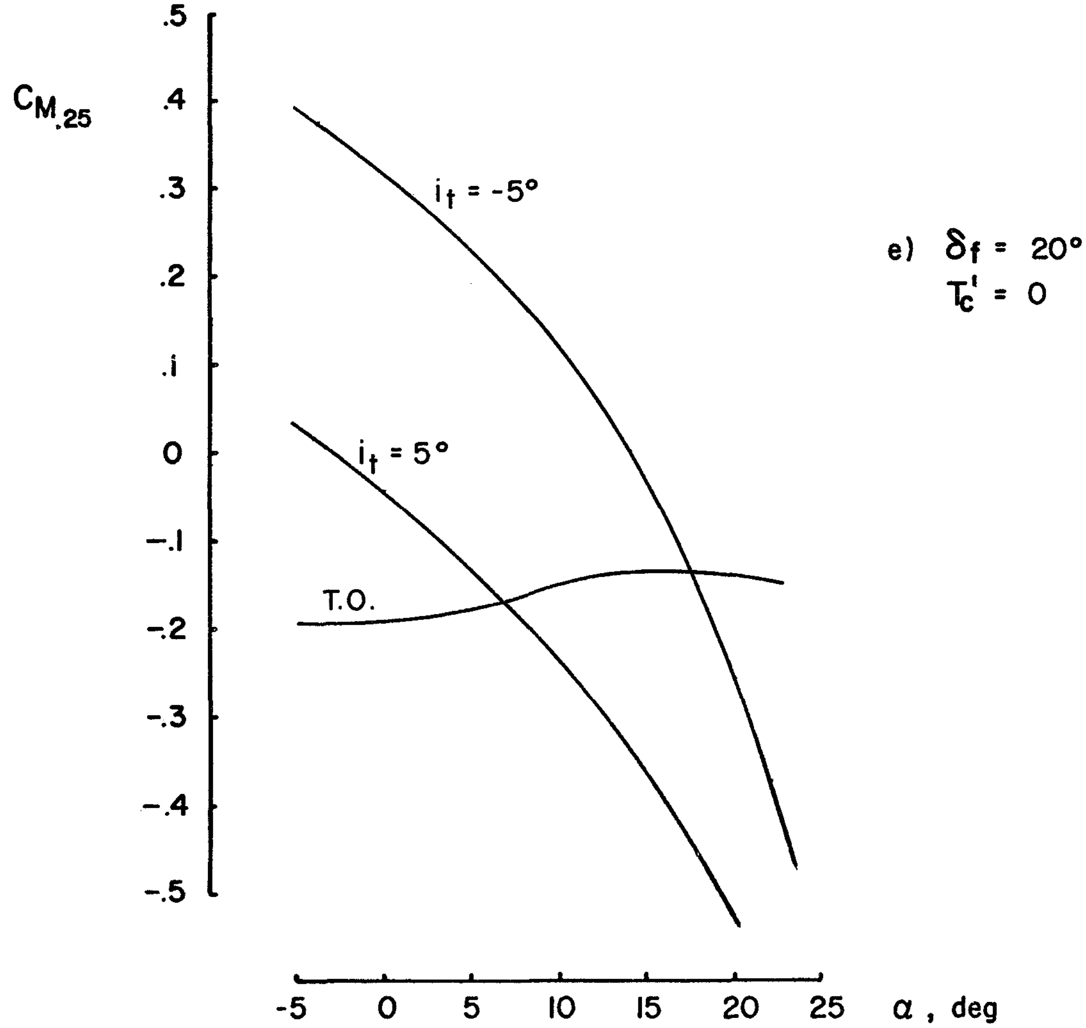

FIGURE 5 Continued

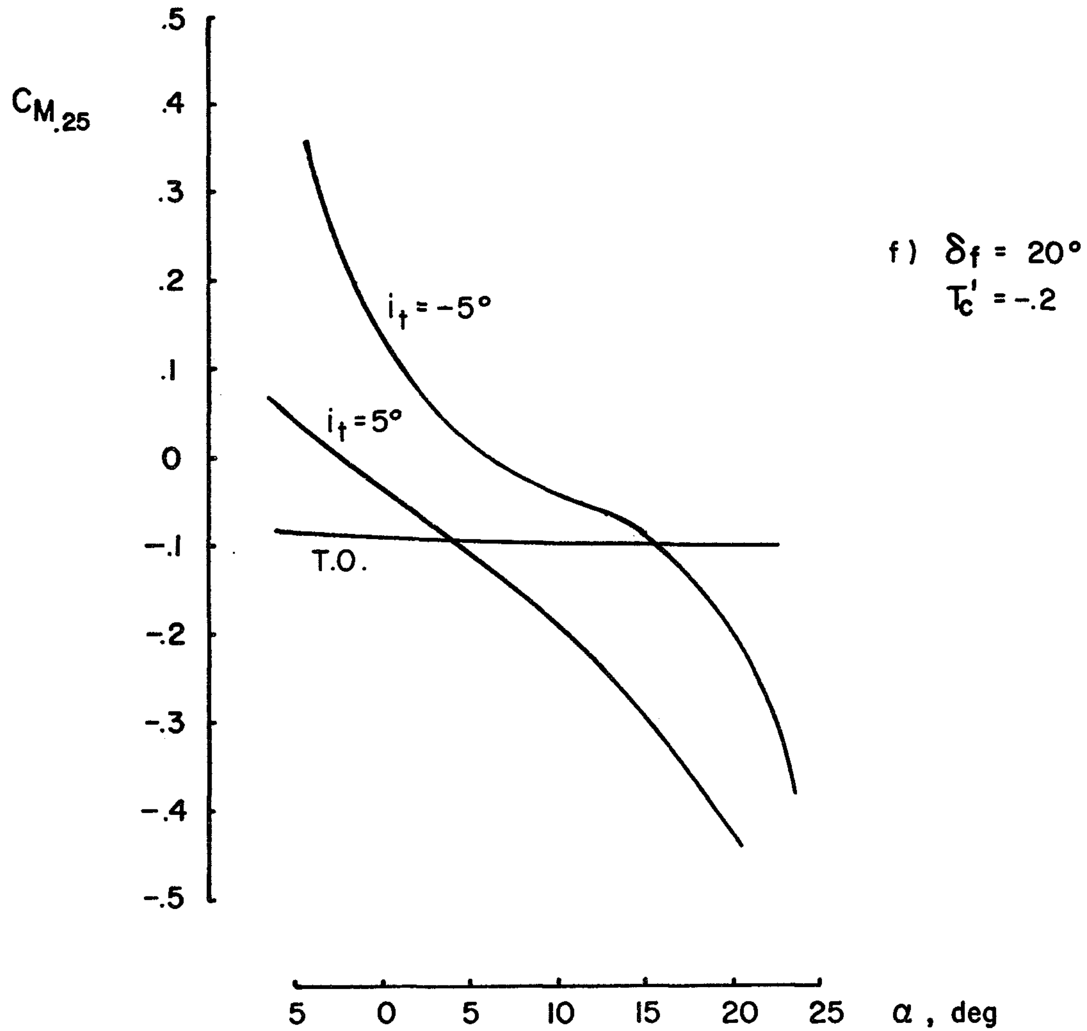

FIGURE 5 Continued

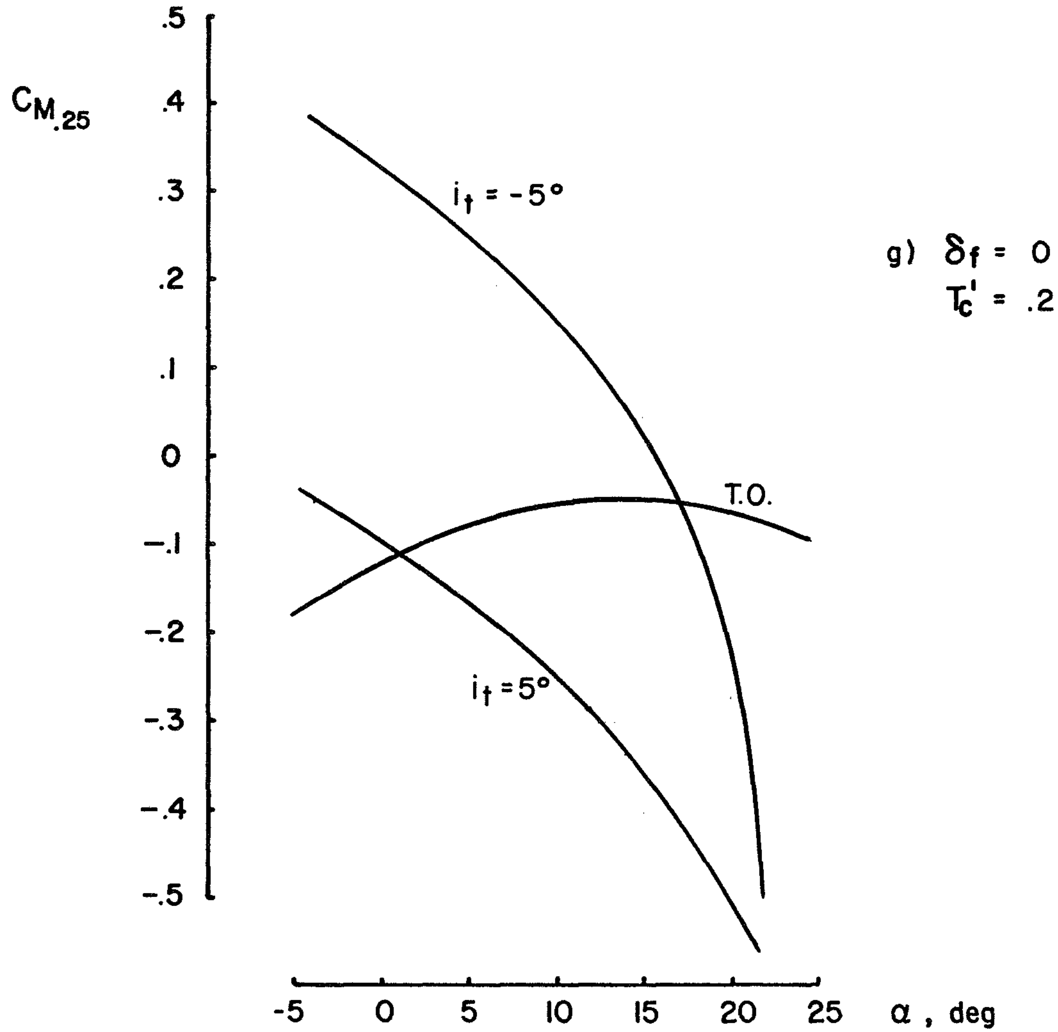

FIGURE 5 Continued

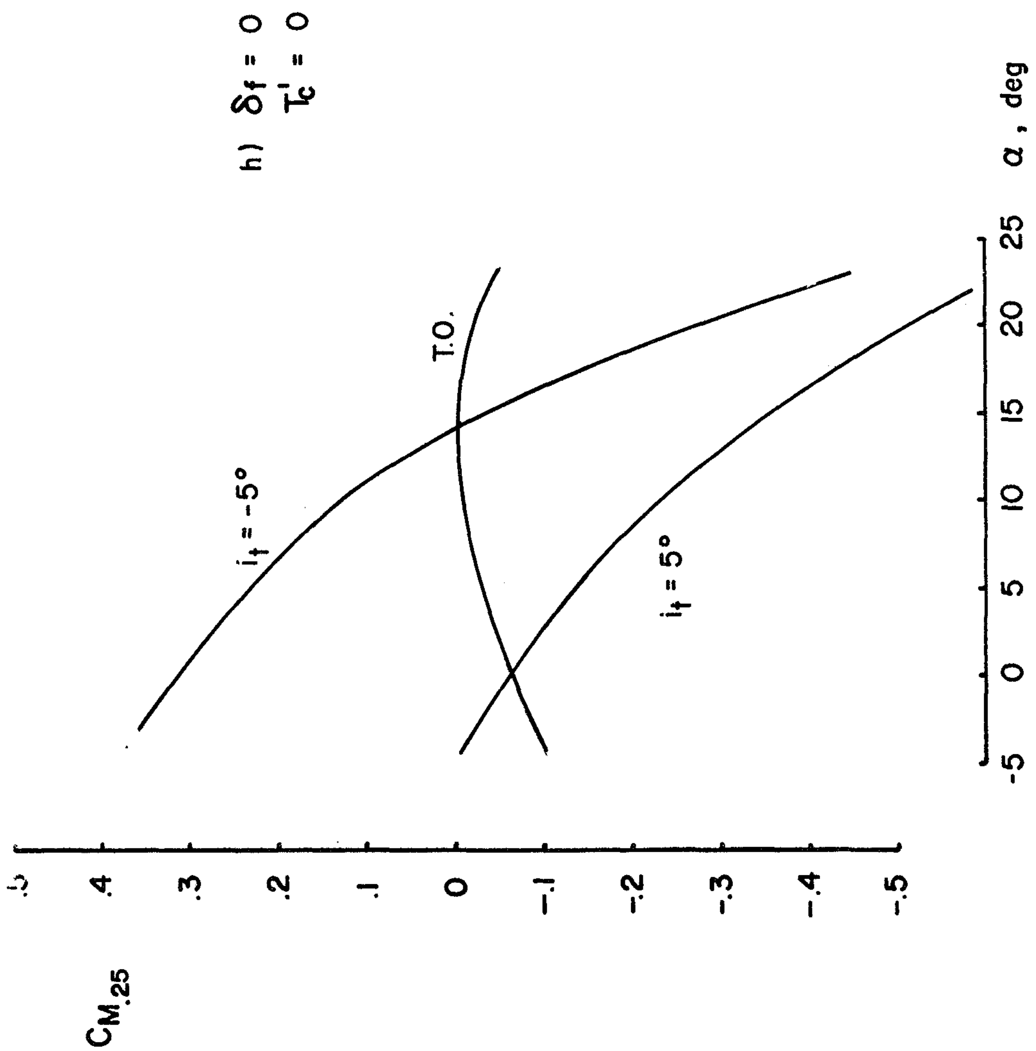

FIGURE 5 Continued

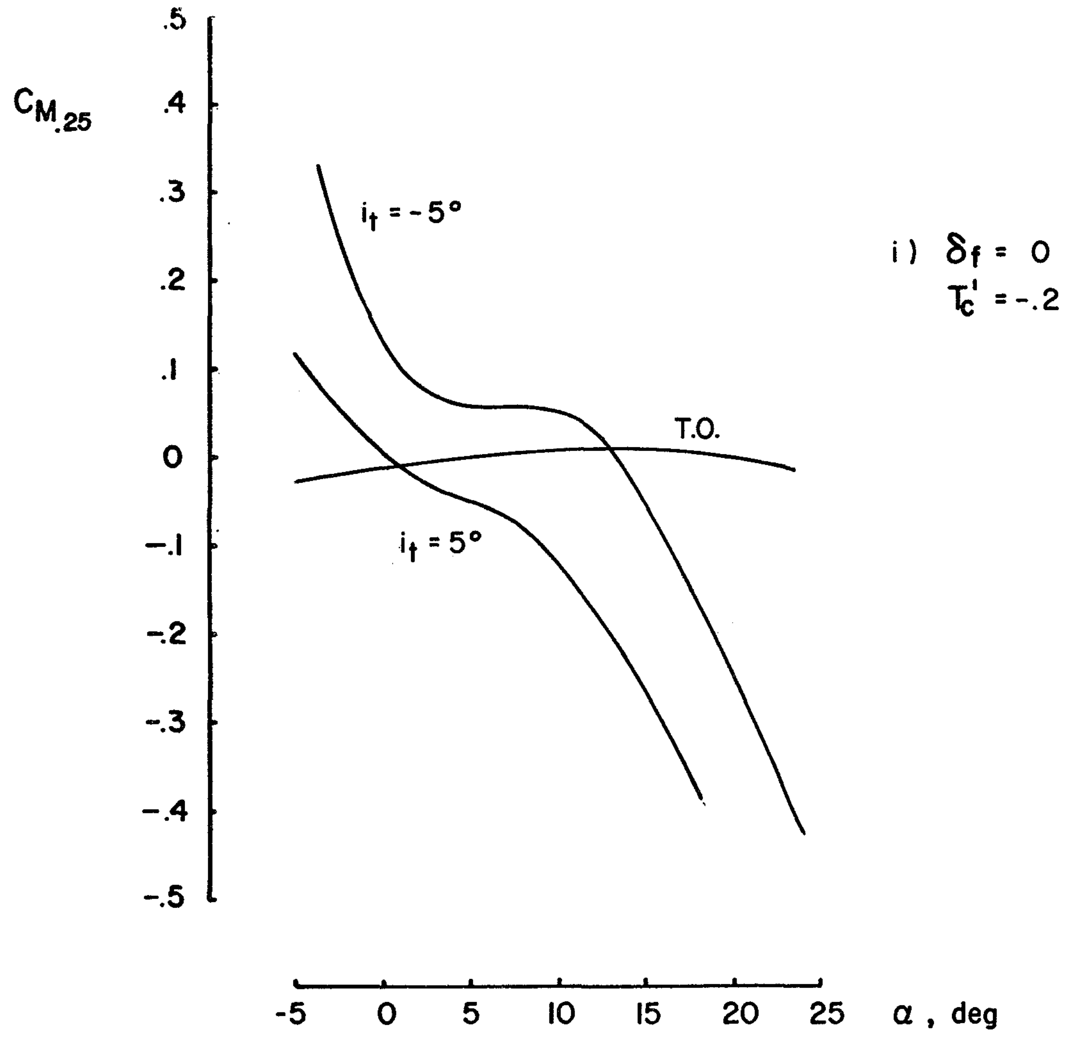

FIGURE 5 Continued

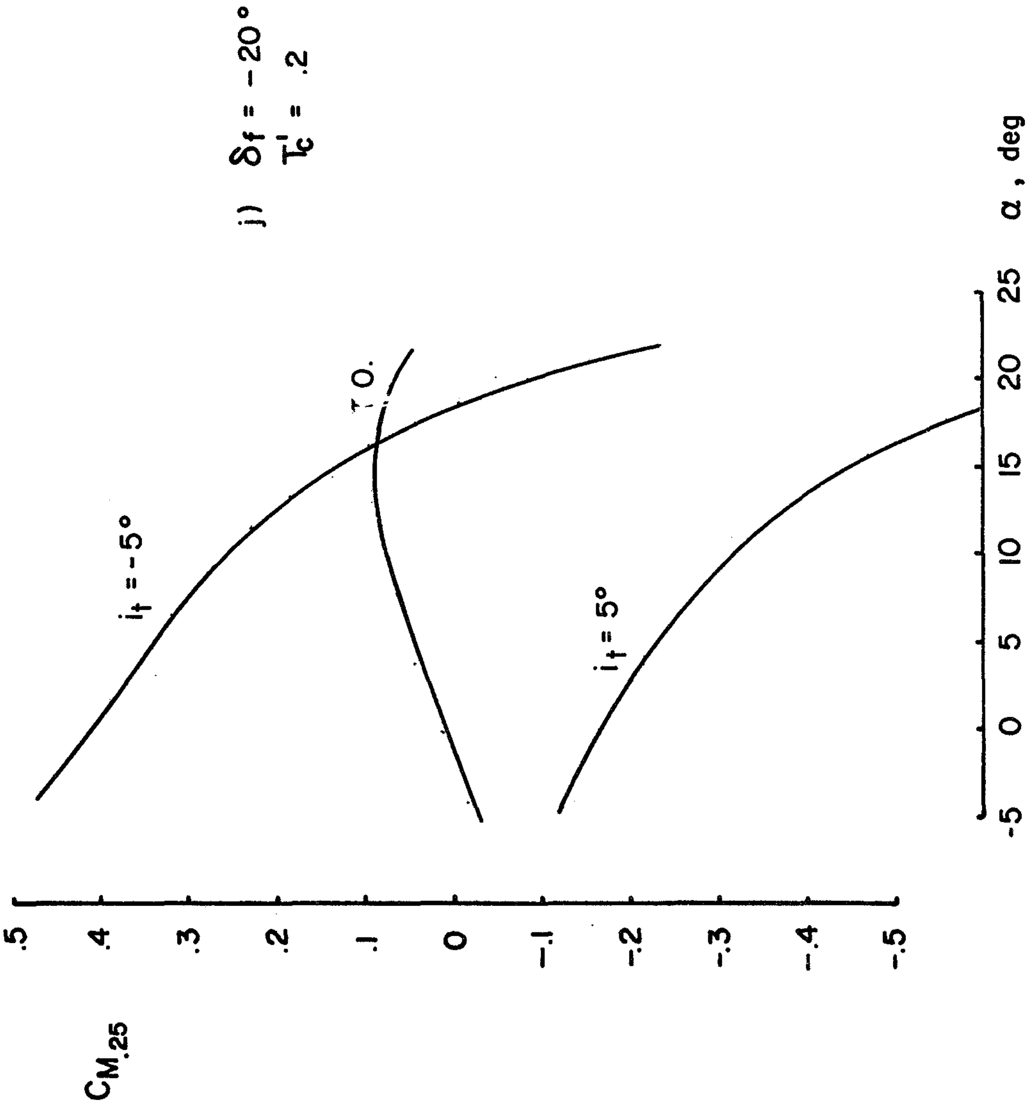

FIGURE 5 Continued

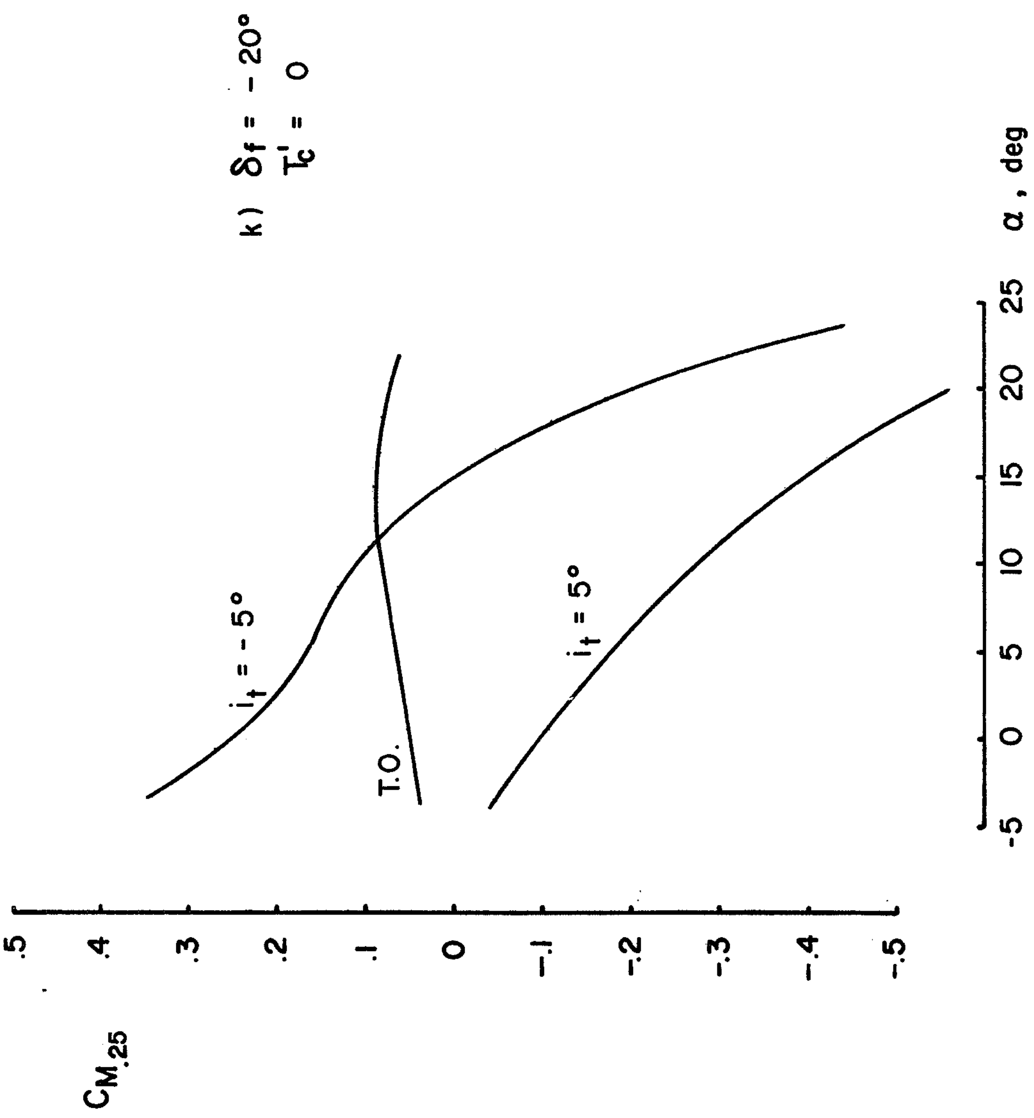

FIGURE 5 Continued

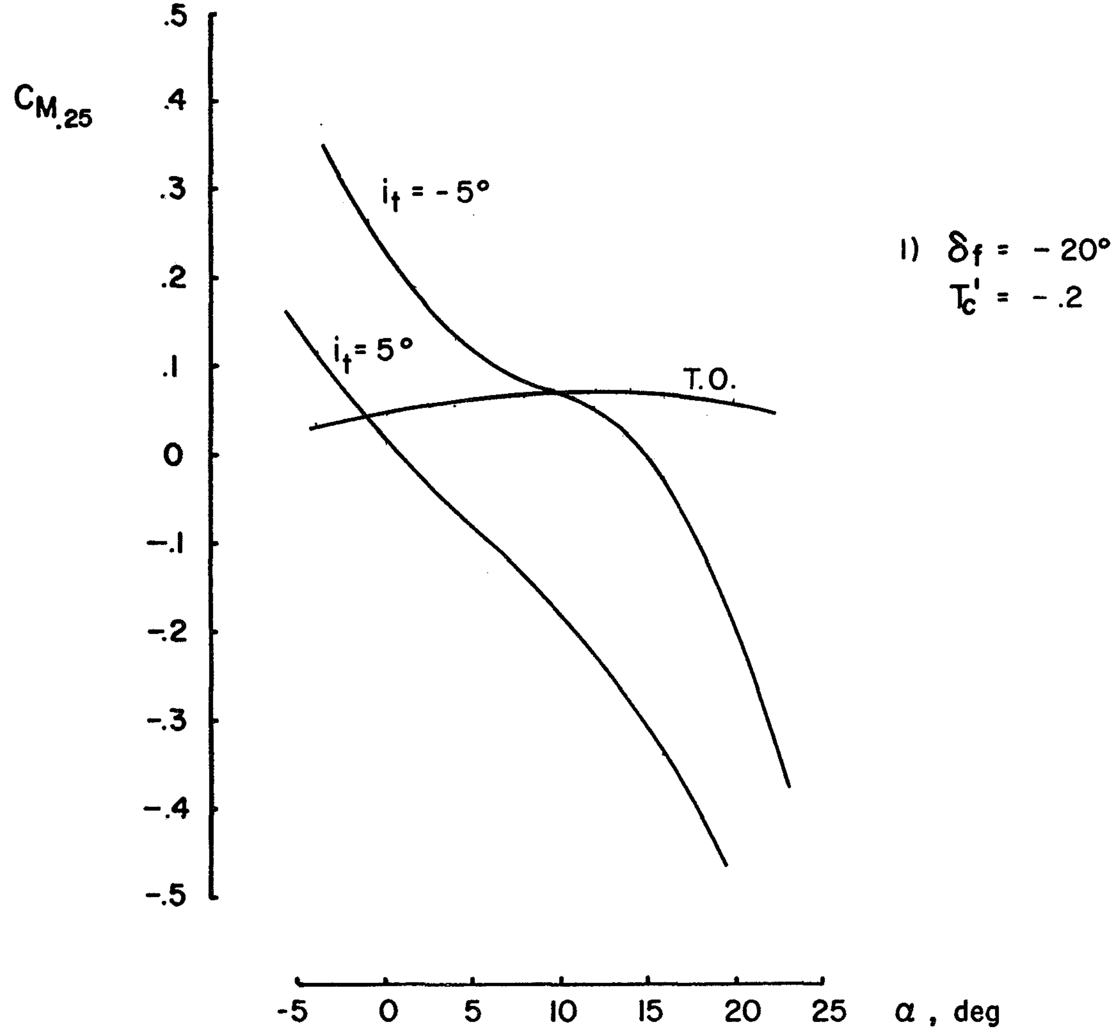

FIGURE 5 Continued

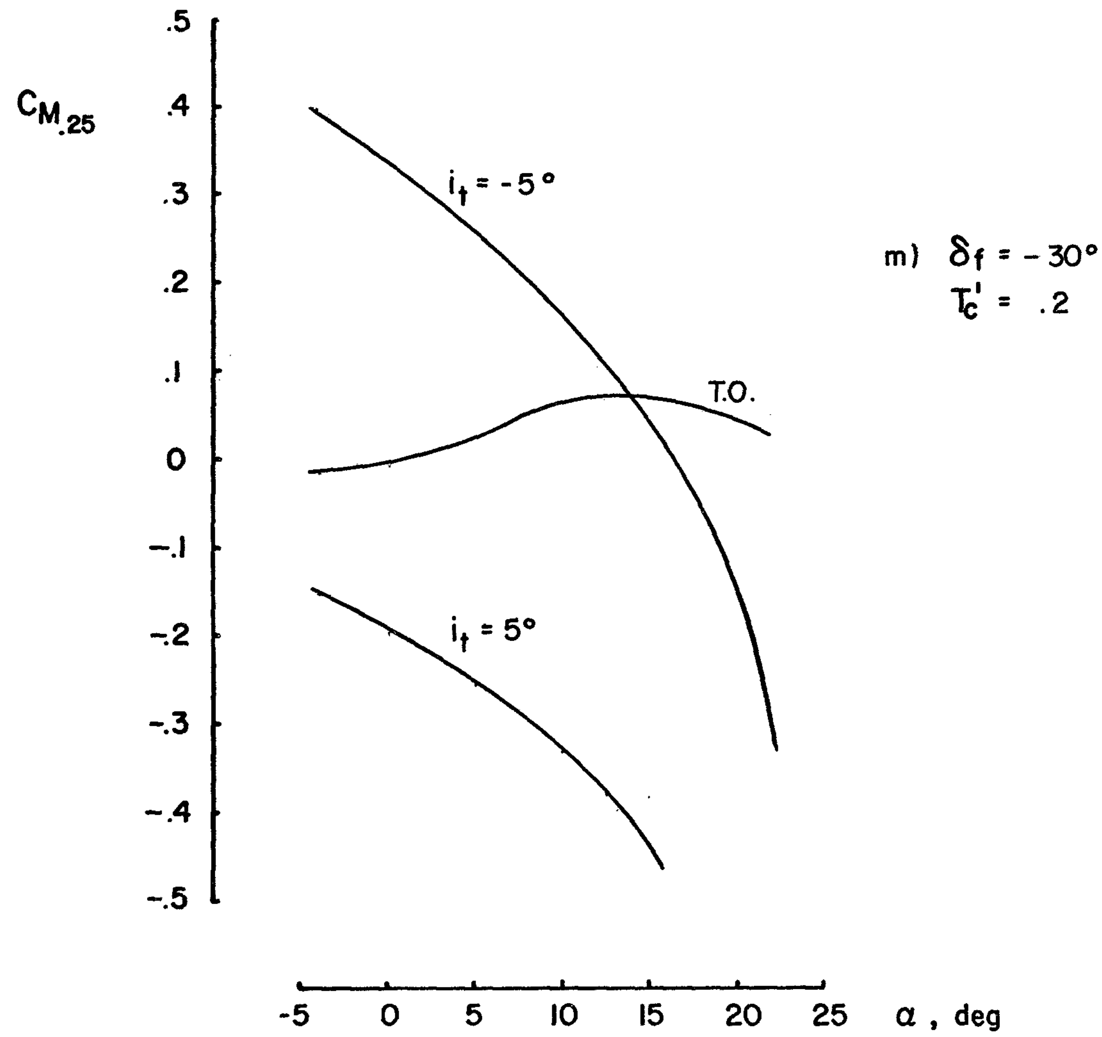

FIGURE 5 Continued

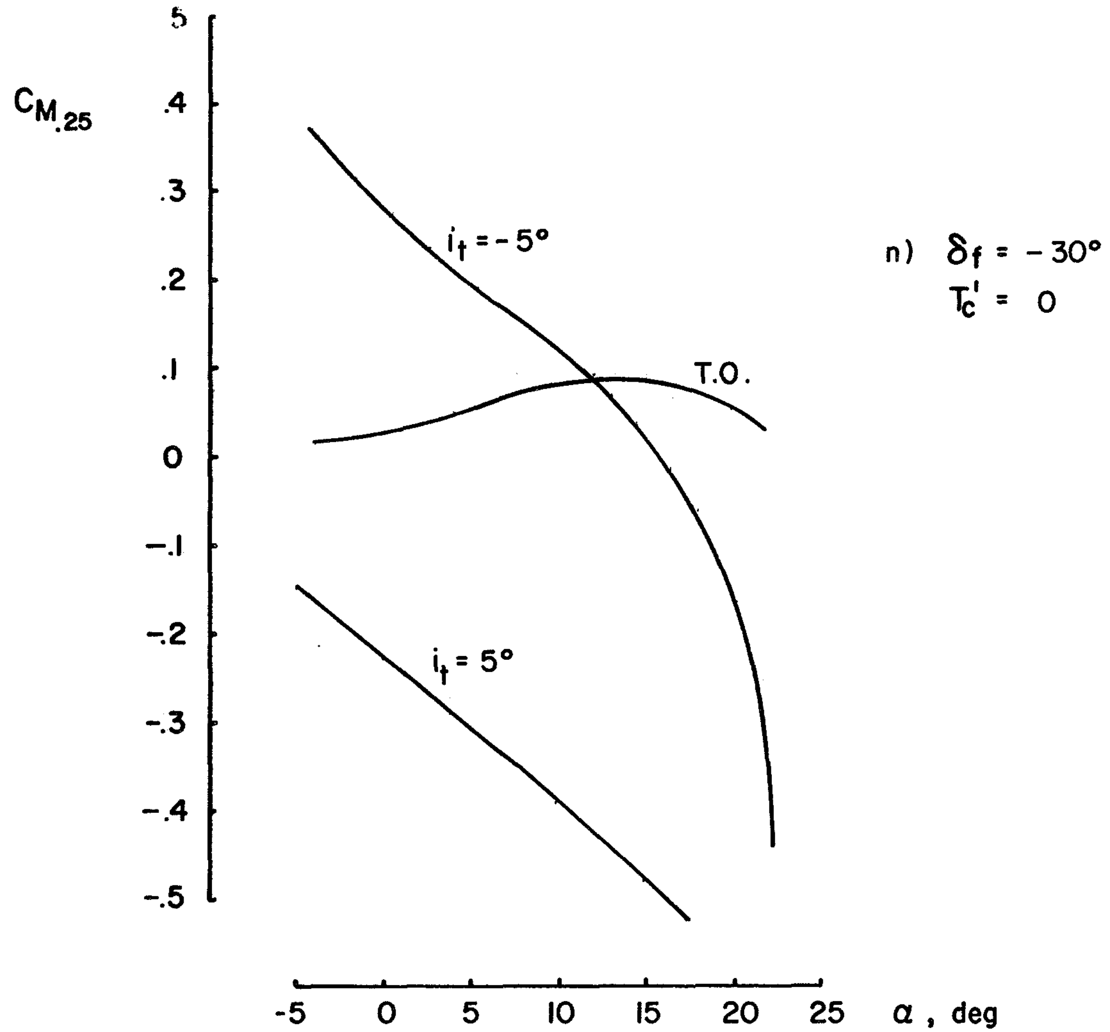

FIGURE 5 Continued

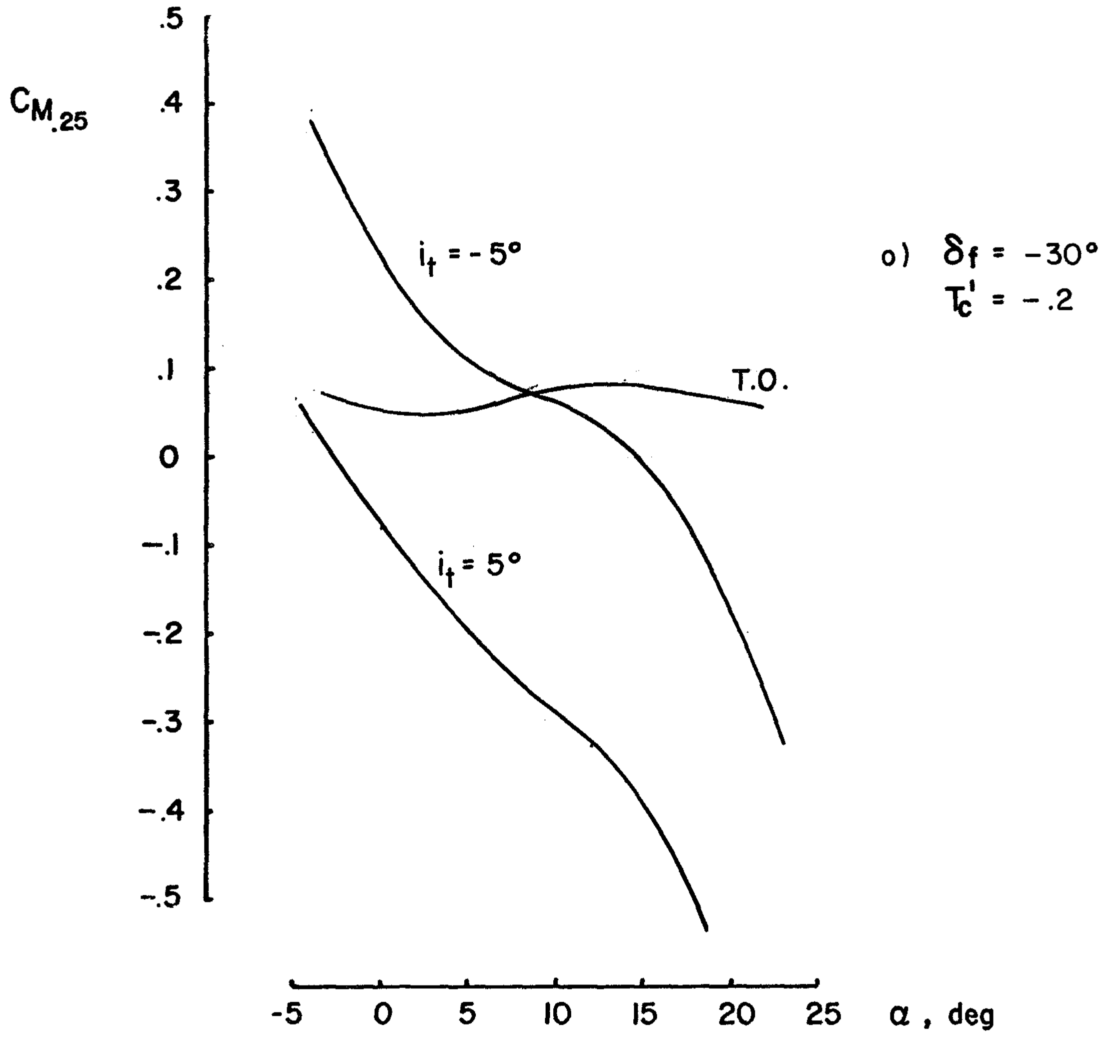

FIGURE 5 Concluded

Note

The points marked by □ are interpolated points taken from Figures 4 and 5

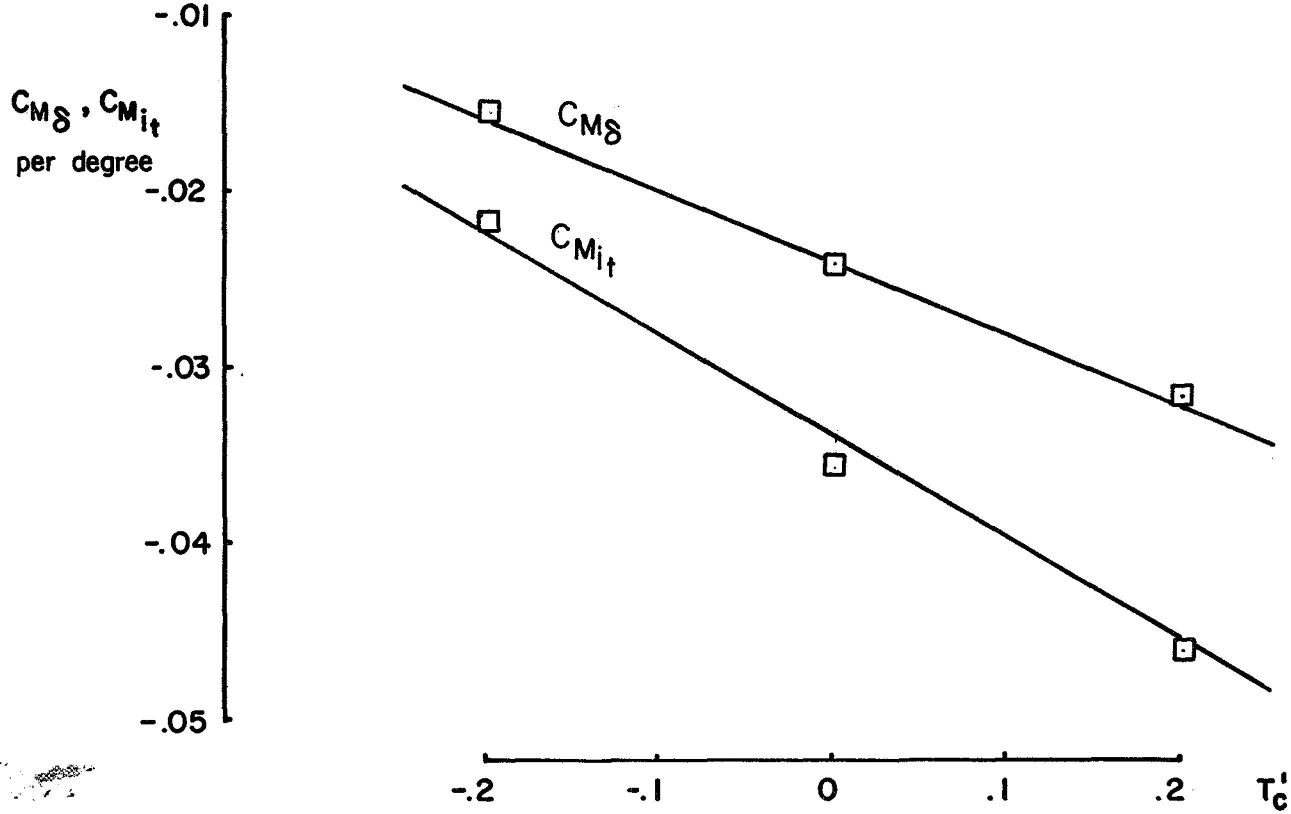

FIGURE 6 VARIATION OF STABILIZER EFFECTIVENESS AND ELEVATOR EFFECTIVENESS WITH THRUST COEFFICIENT

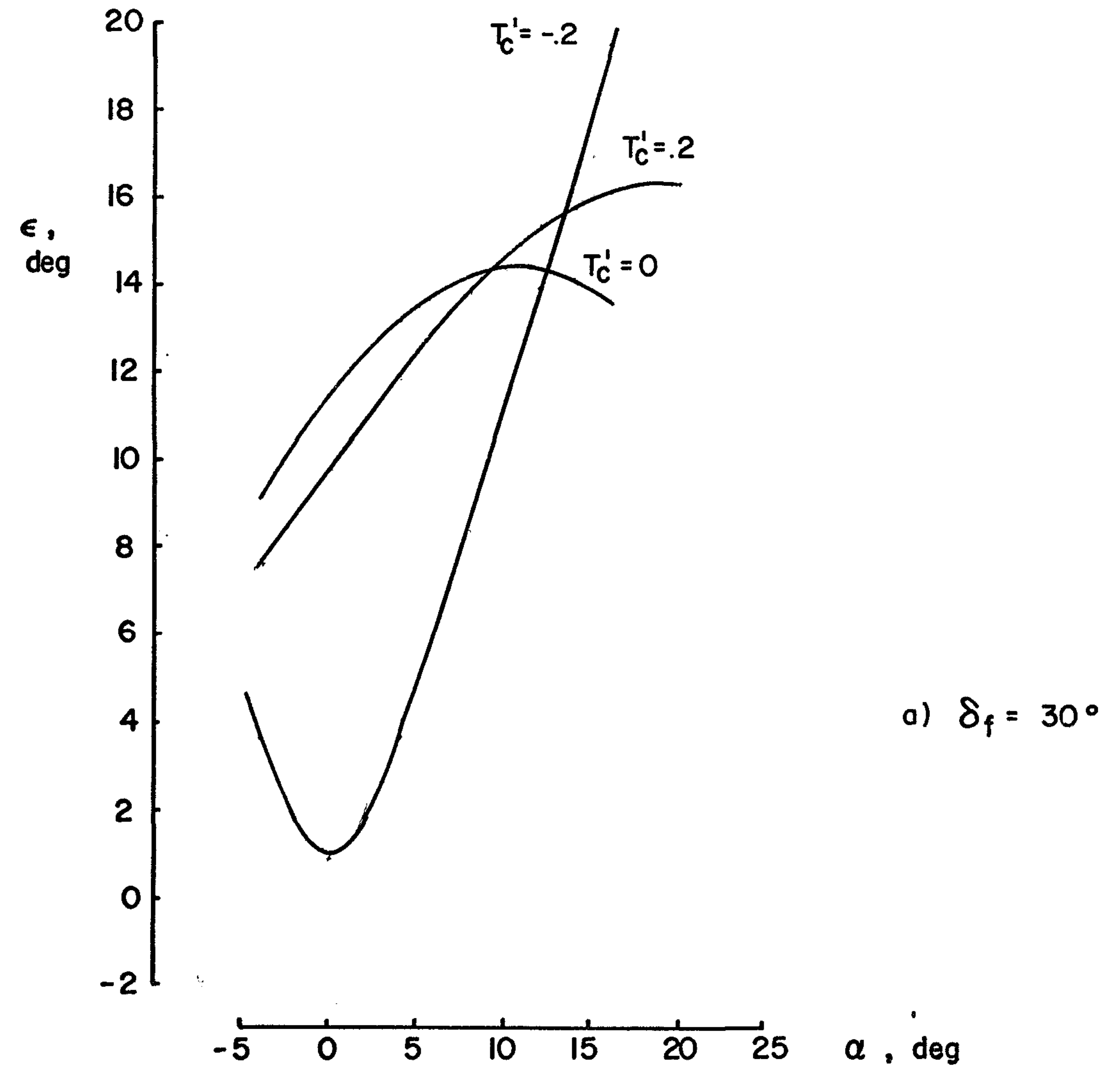

FIGURE 7 VARIATION OF DOWNWASH WITH ANGLE OF ATTACK

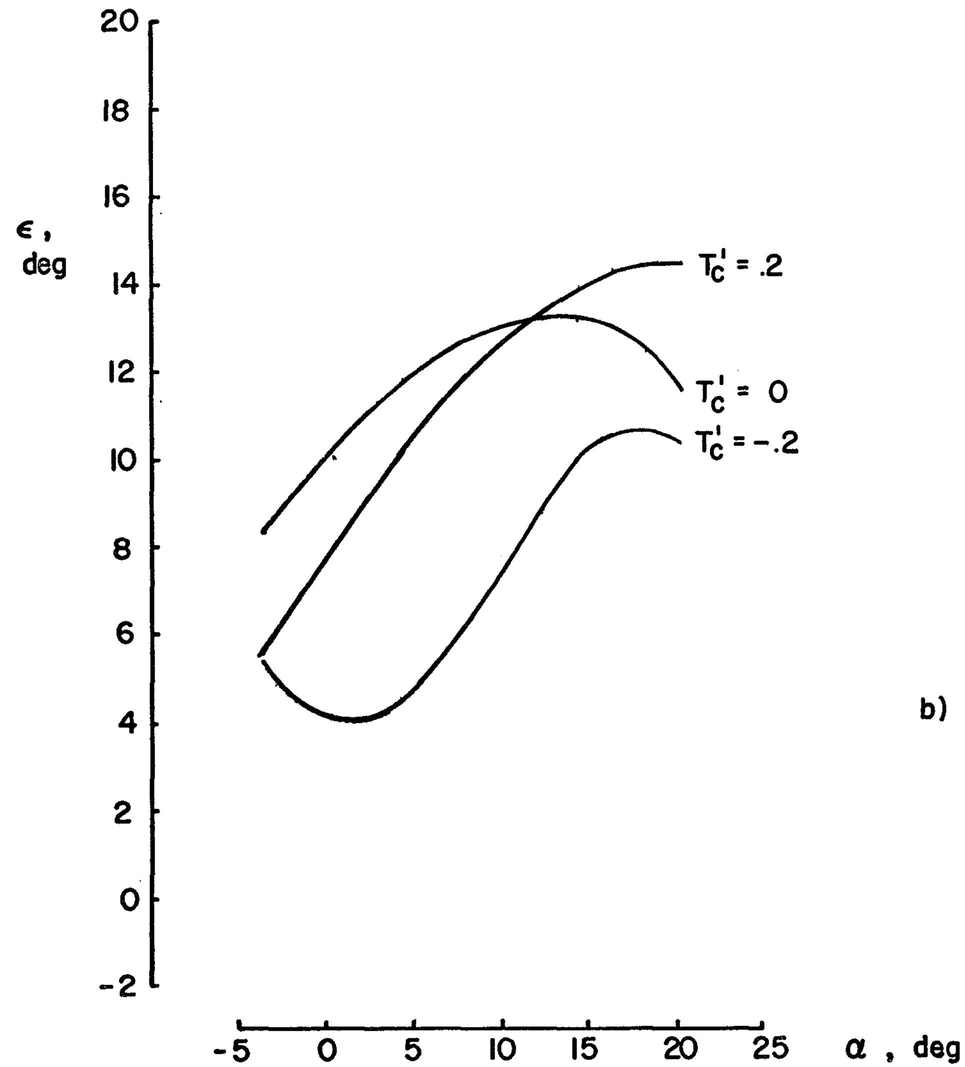

b) $\delta_f = 20°$

FIGURE 7 Continued

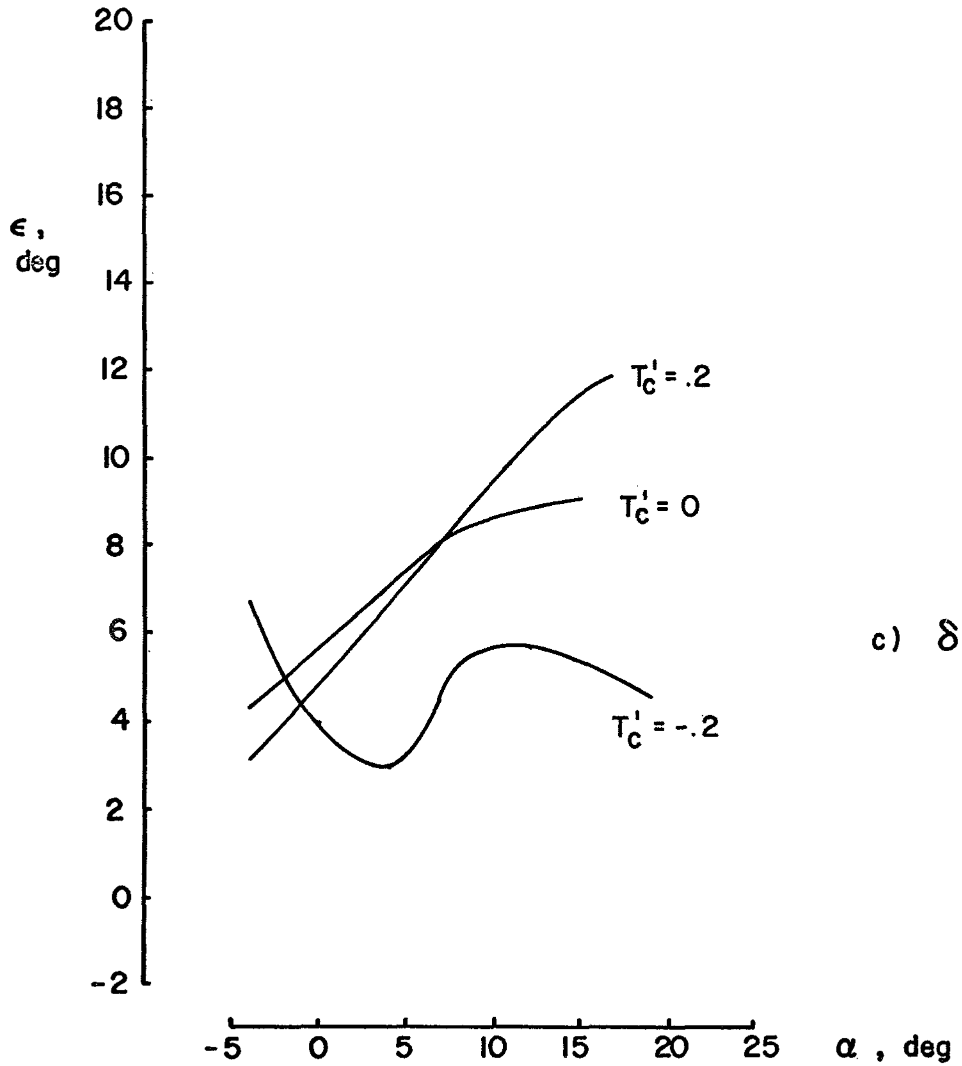

c) $\delta_f = 0°$

FIGURE 7 Continued

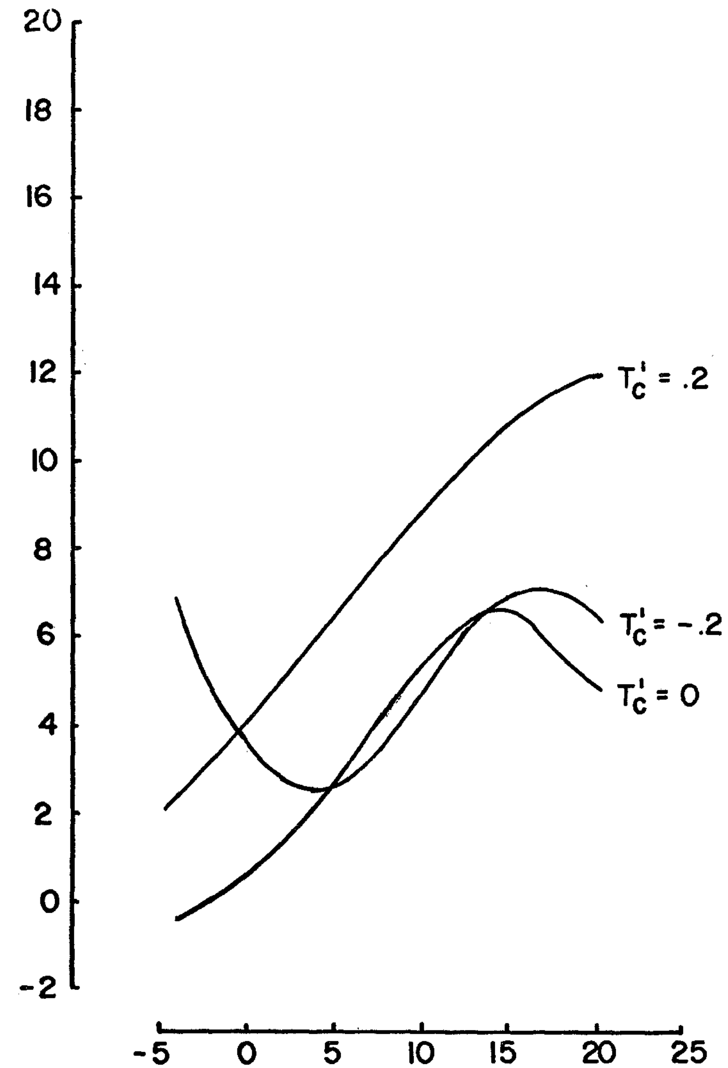

d) $\delta_f = -20°$

FIGURE 7 Continued

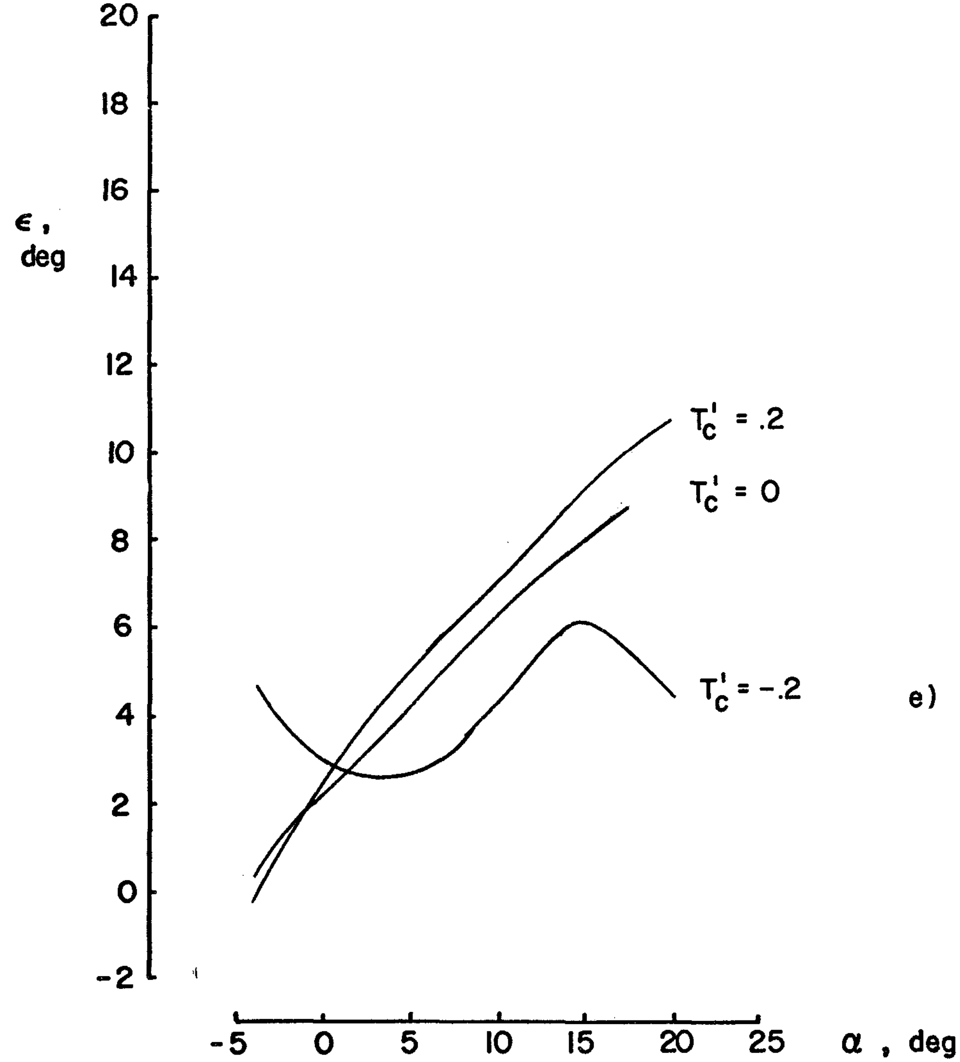

e) $\delta_f = -30°$

FIGURE 7 Concluded

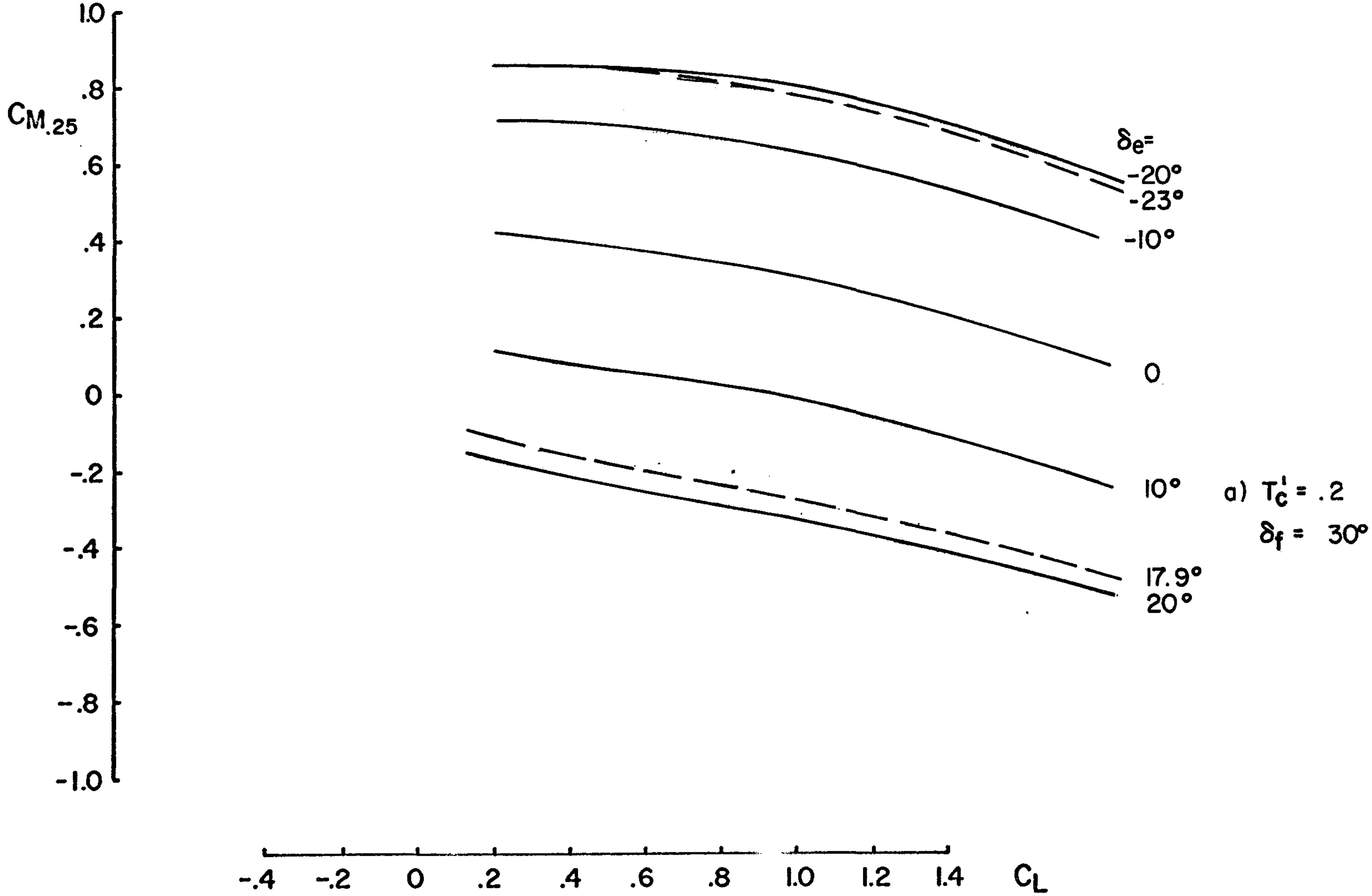

FIGURE 8 VARIATION OF PITCHING MOMENT WITH LIFT COEFFICIENT FOR $i_t = -5°$

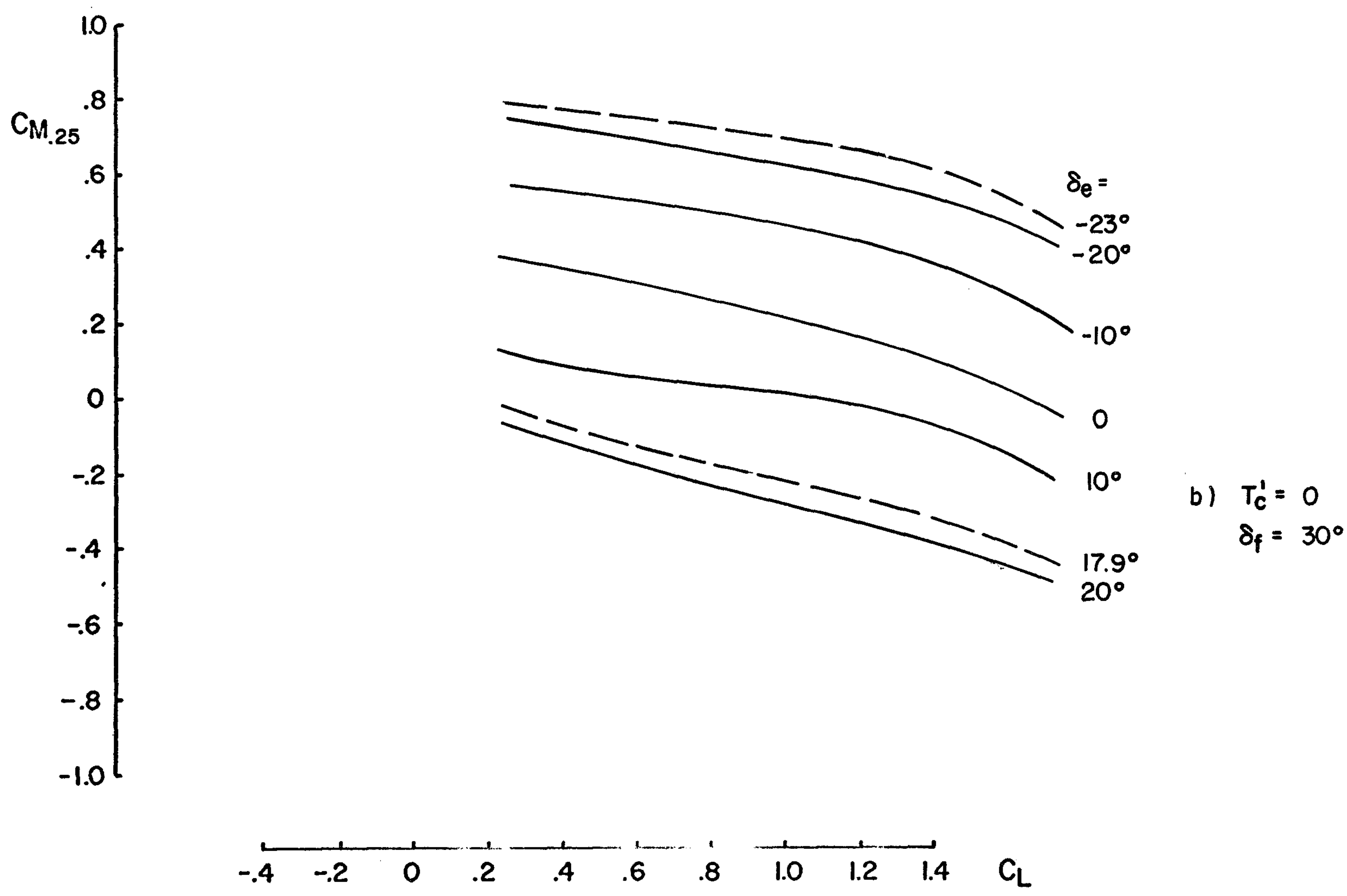

FIGURE 8 Continued

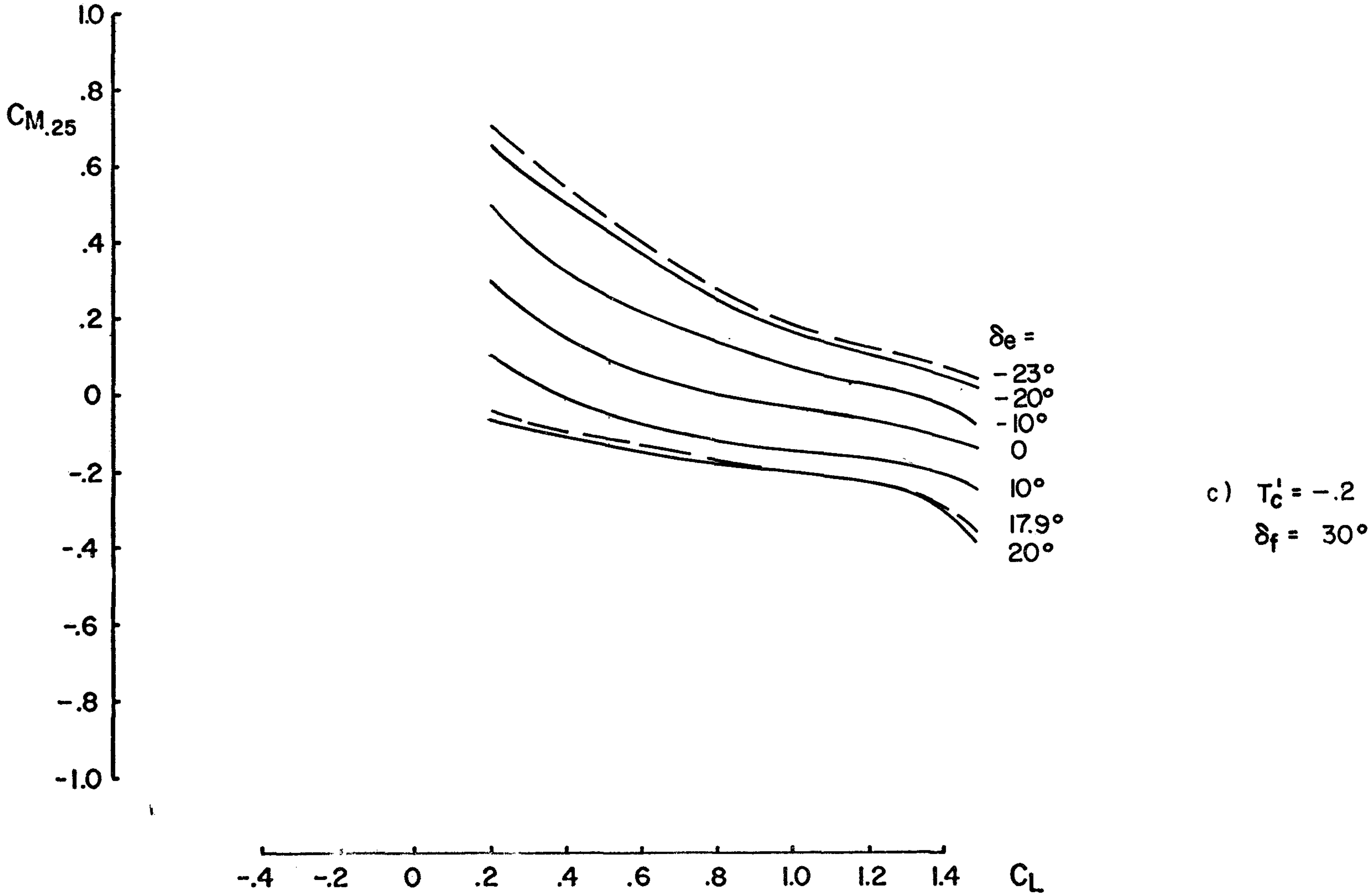

FIGURE 8 Continued

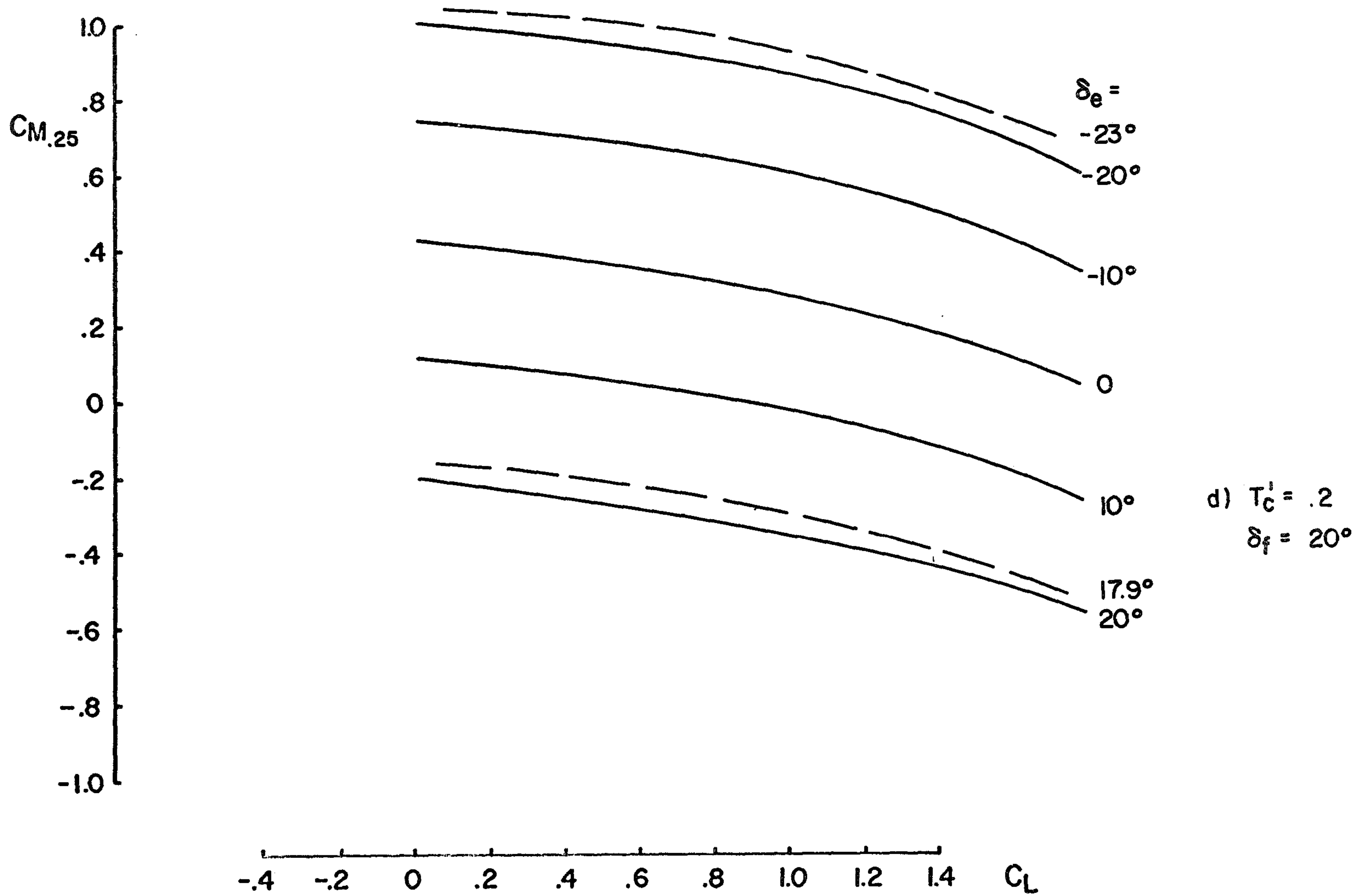

FIGURE 8 Continued

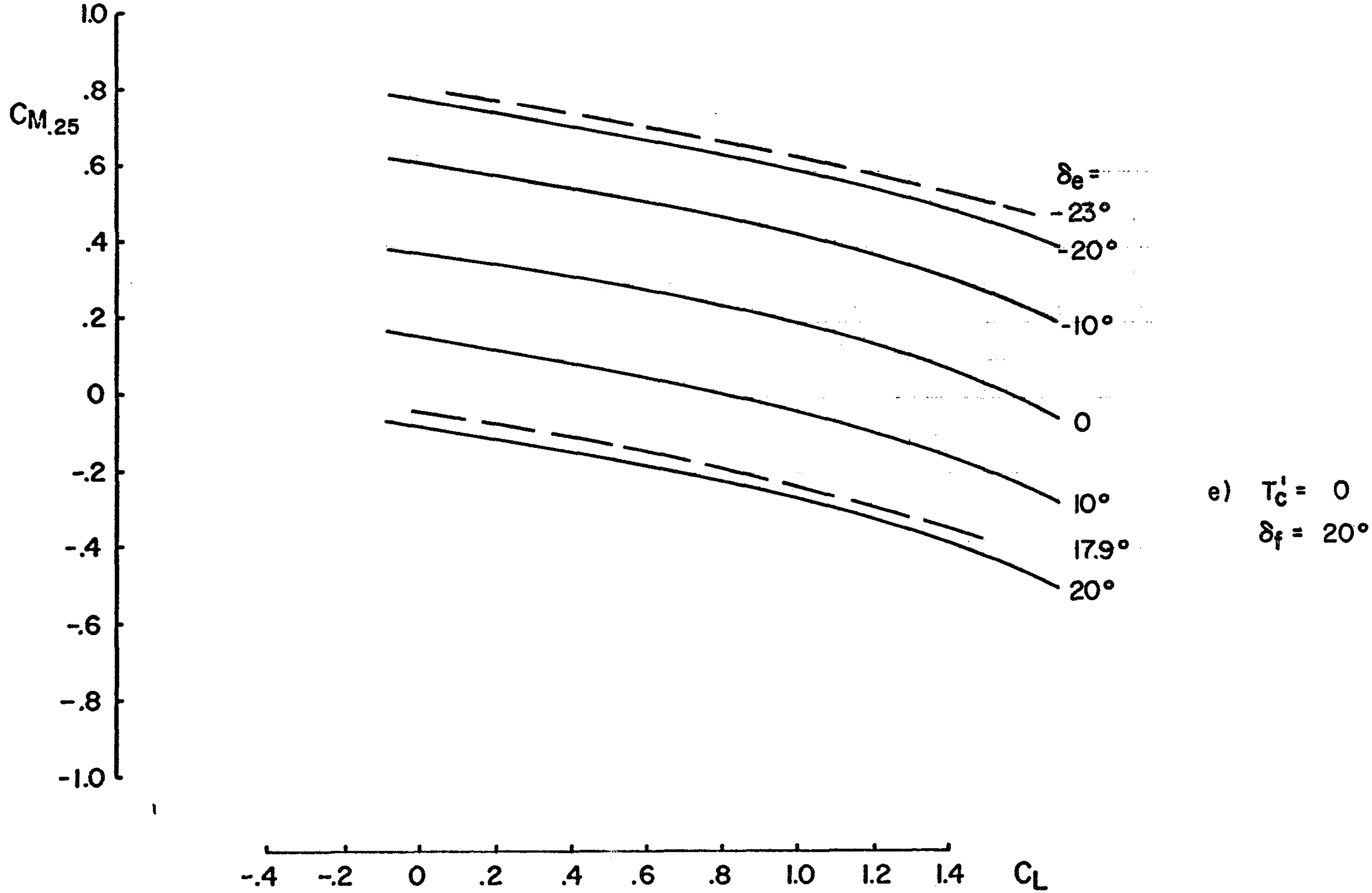

FIGURE 8 Continued

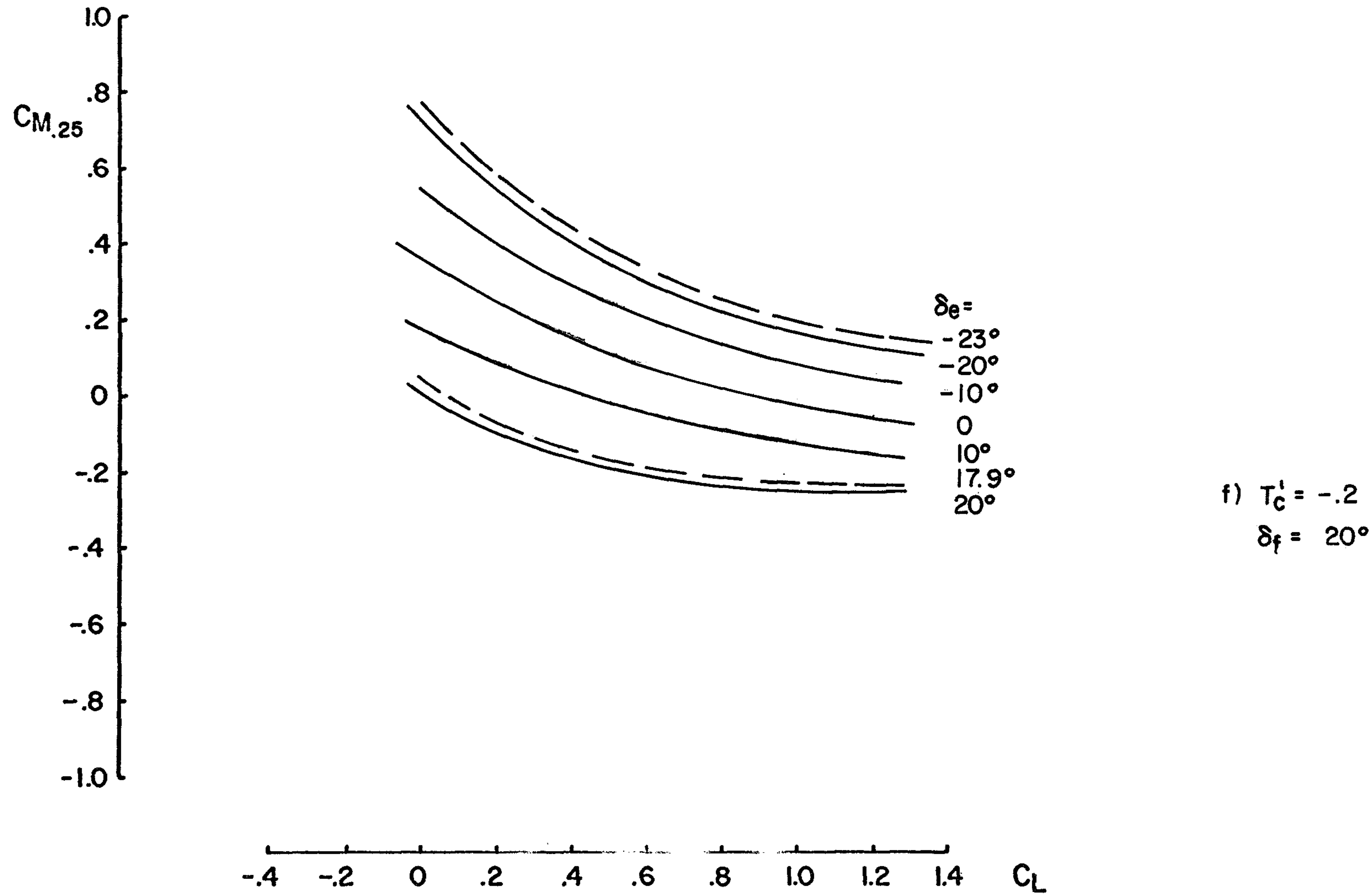

FIGURE 8 Continued

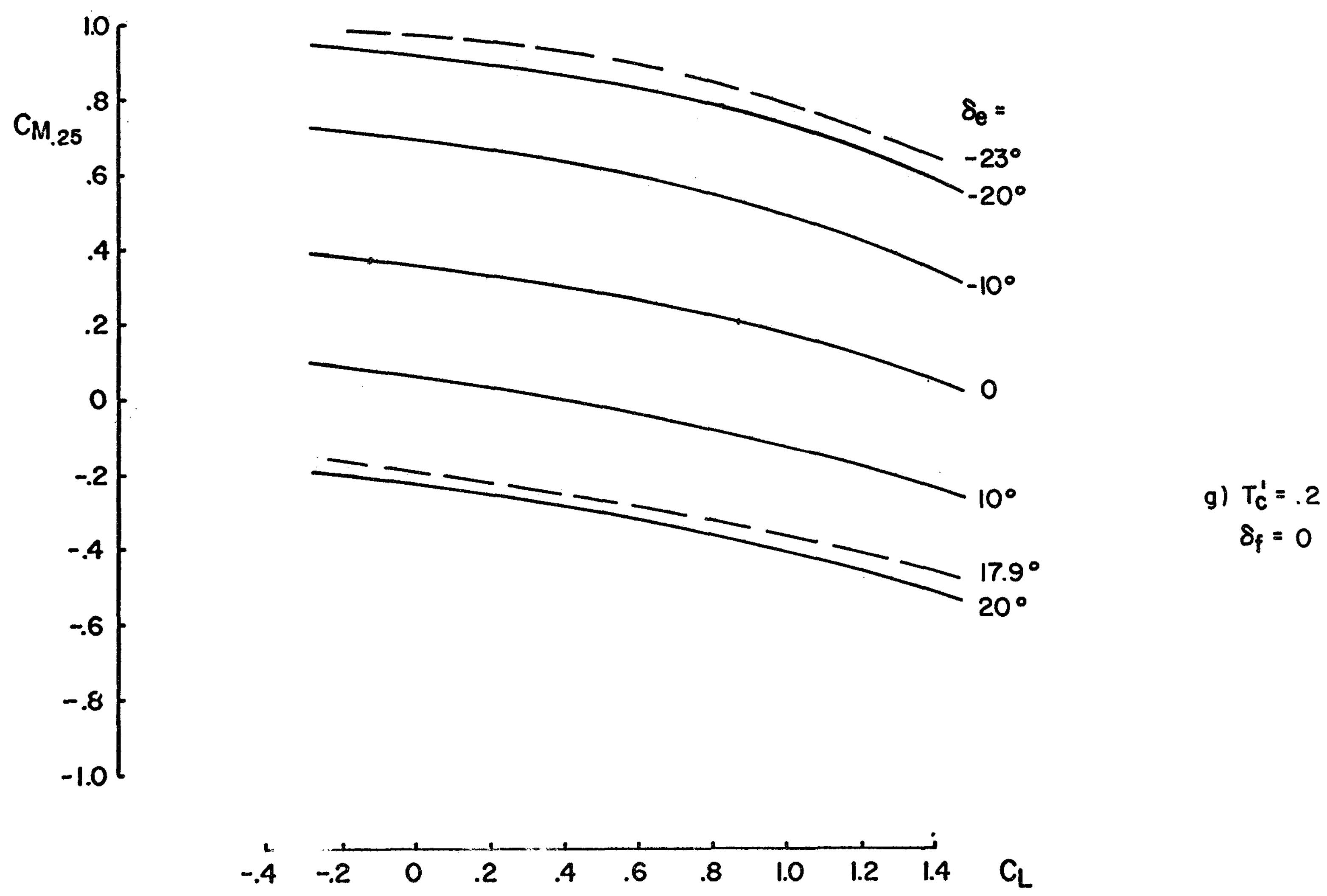

FIGURE 8 Continued

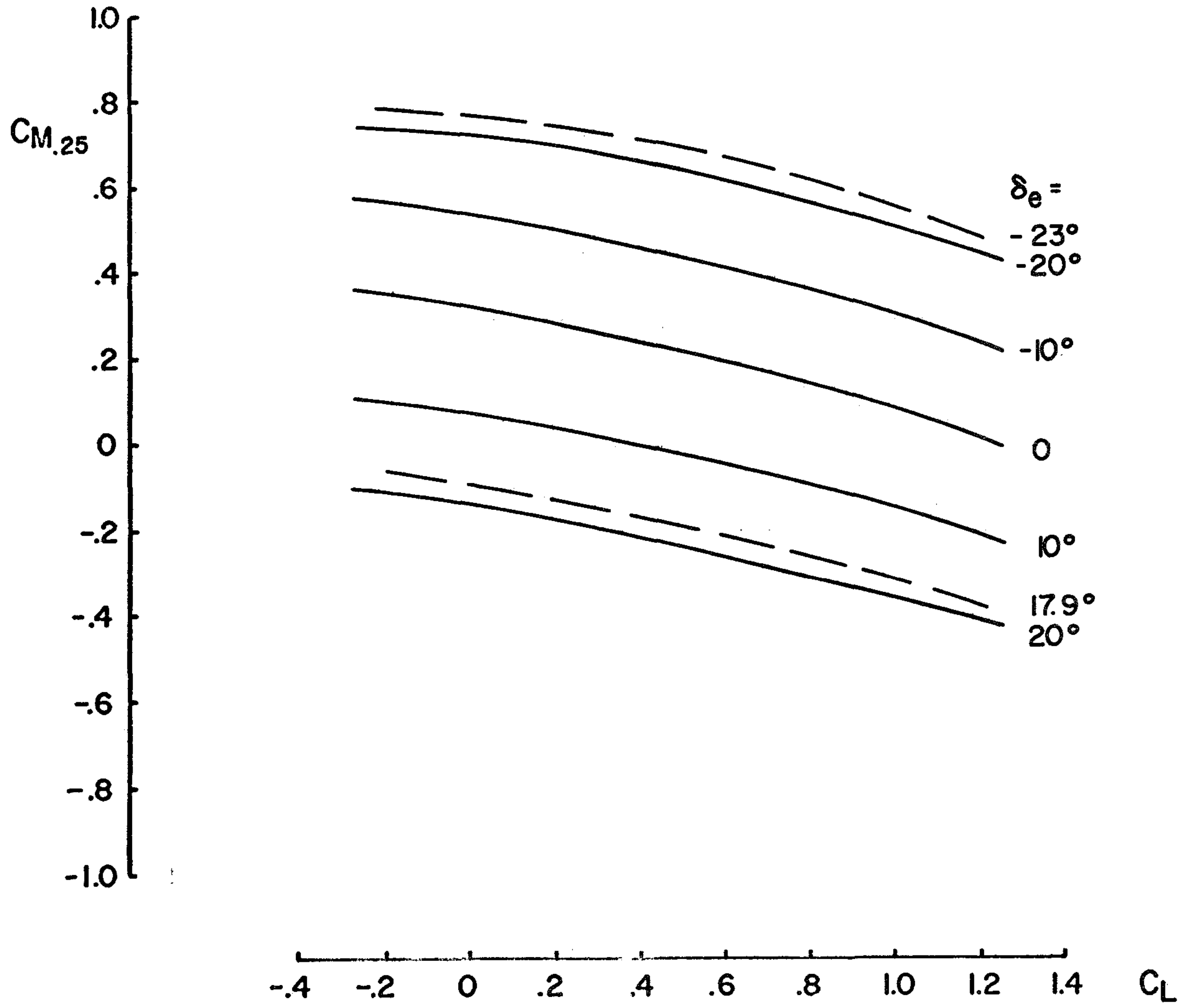

h) $T_c' = 0$
$\delta_f = 0$

FIGURE 8 Continued

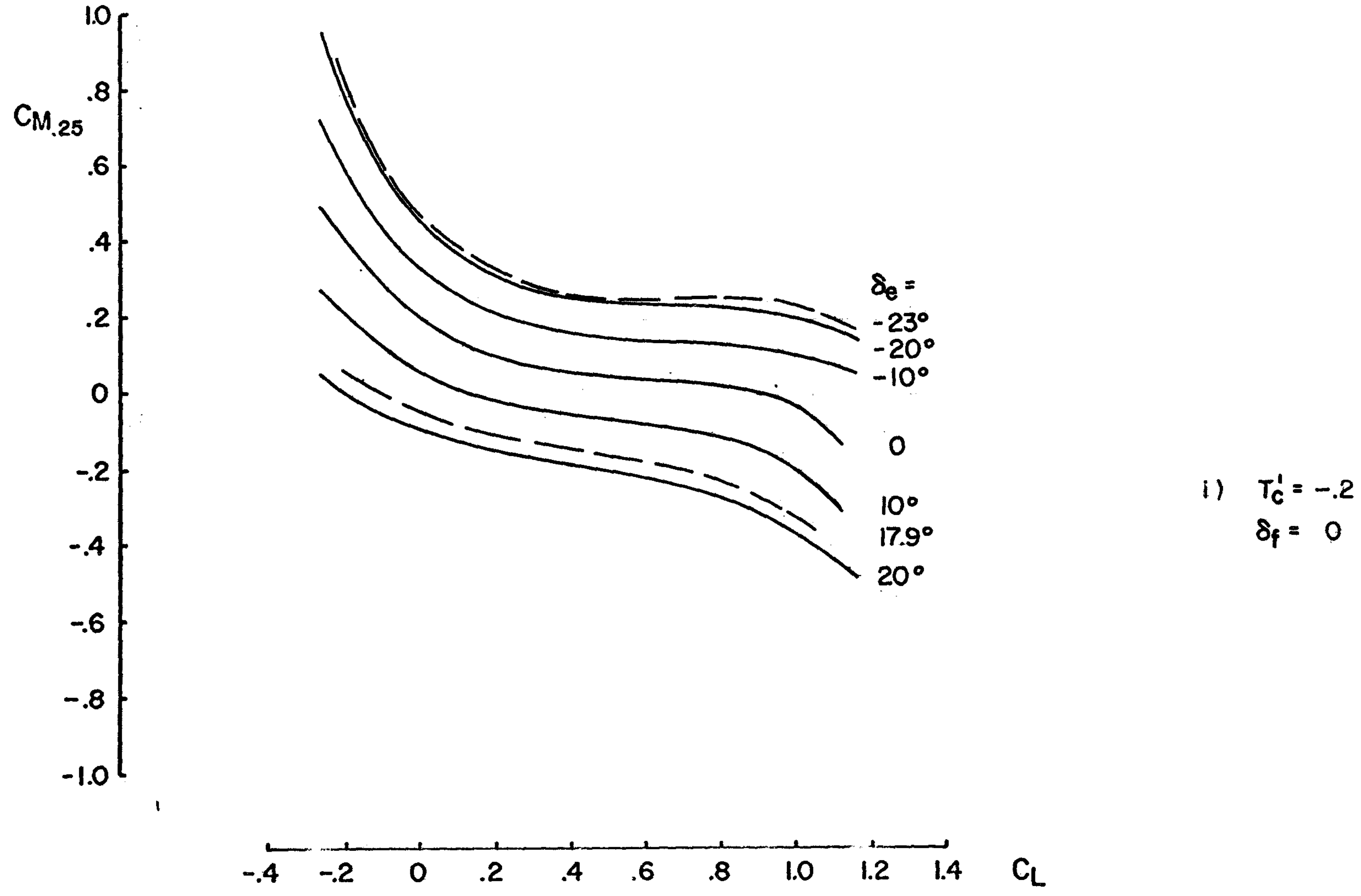

FIGURE 8 Continued

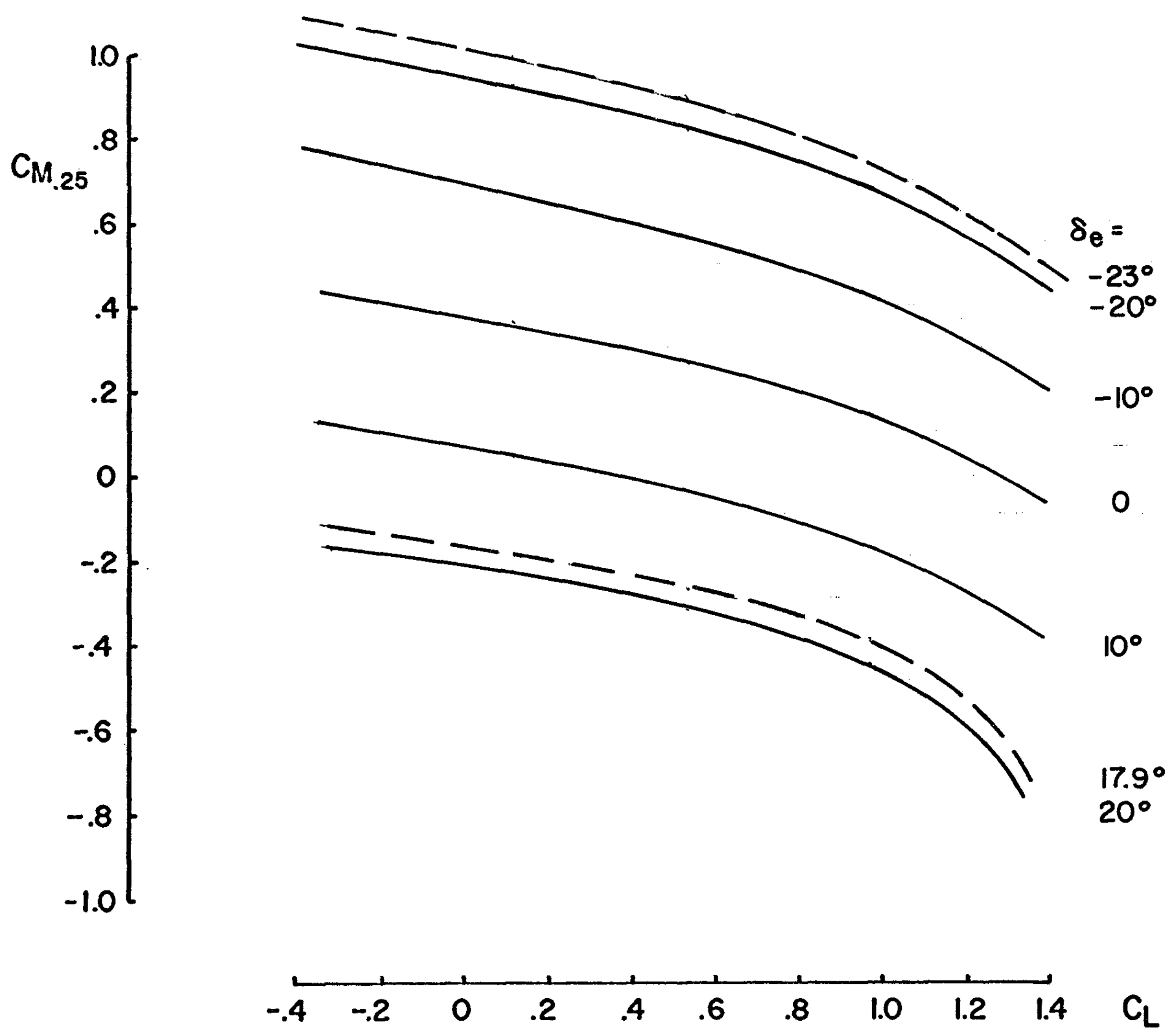

j) $T_c' = .2$
$\delta_f = -20°$

FIGURE 8 Continued

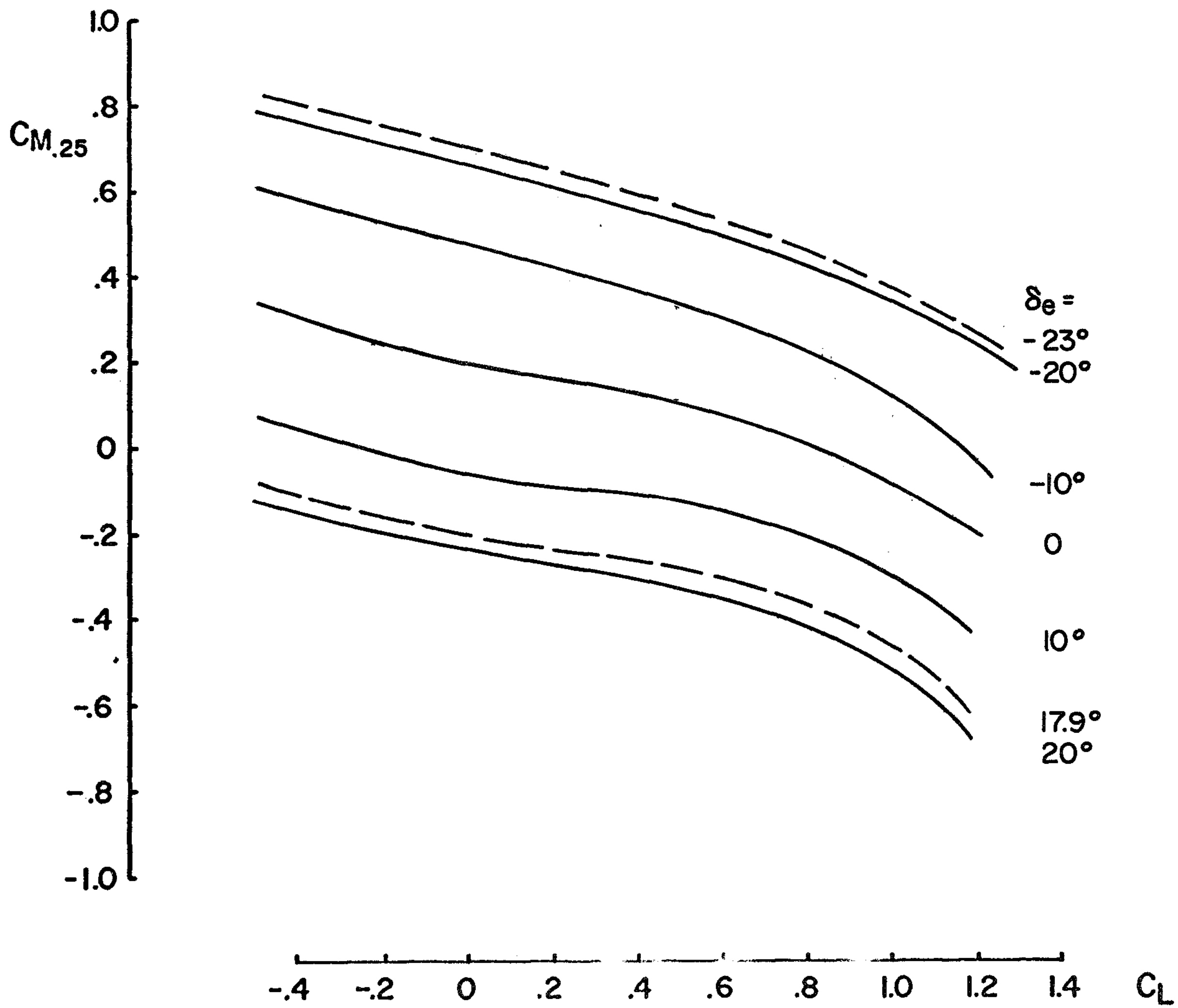

k) $T_c' = 0$
$\delta_f = -20°$

FIGURE 8 Continued

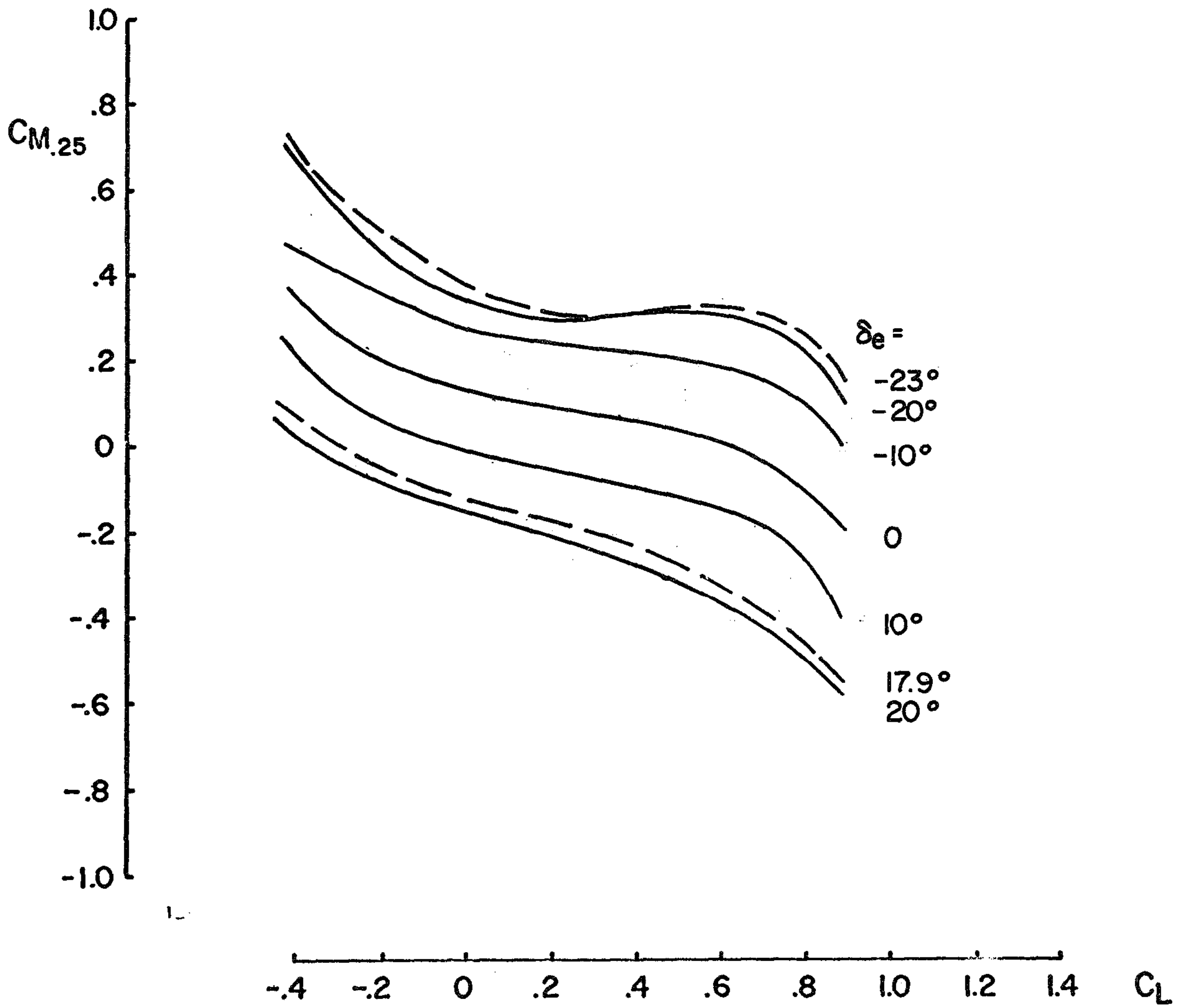

l) $T_c' = -.2$
$\delta_f = -20°$

FIGURE 8 Continued

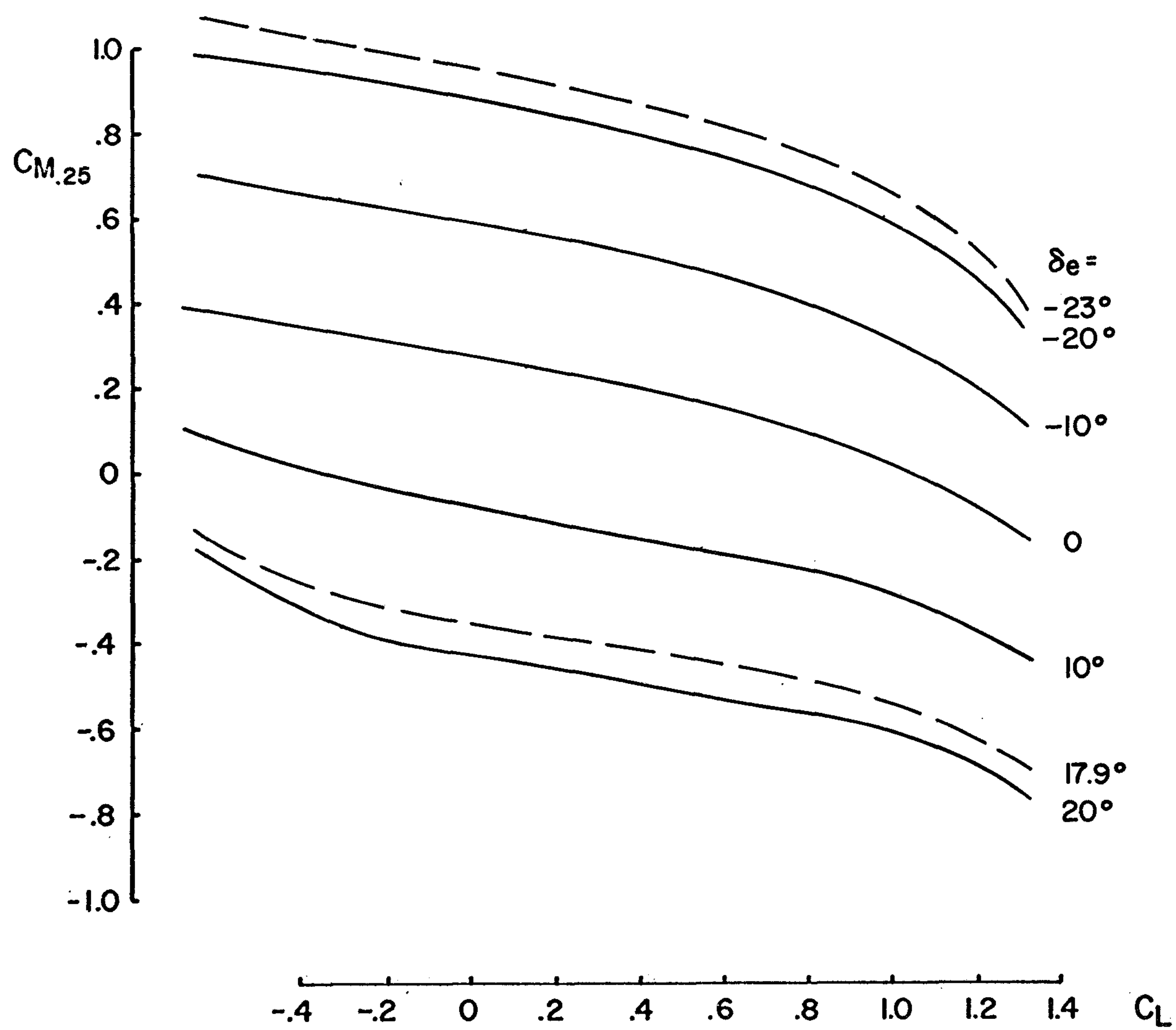

FIGURE 8 Continued

m) $T_c' = .2$
$\delta_f = -30°$

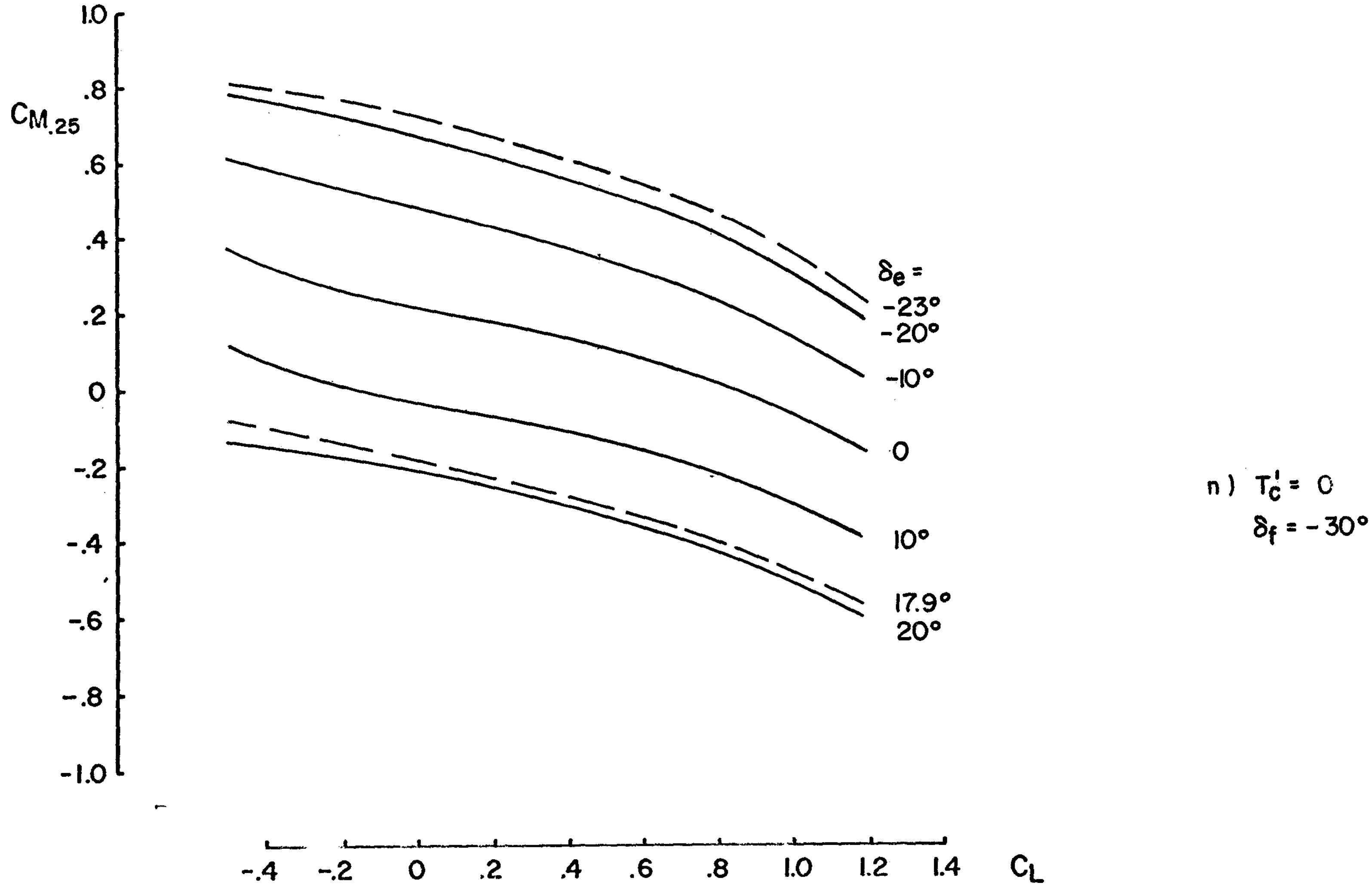

FIGURE 8 Continued

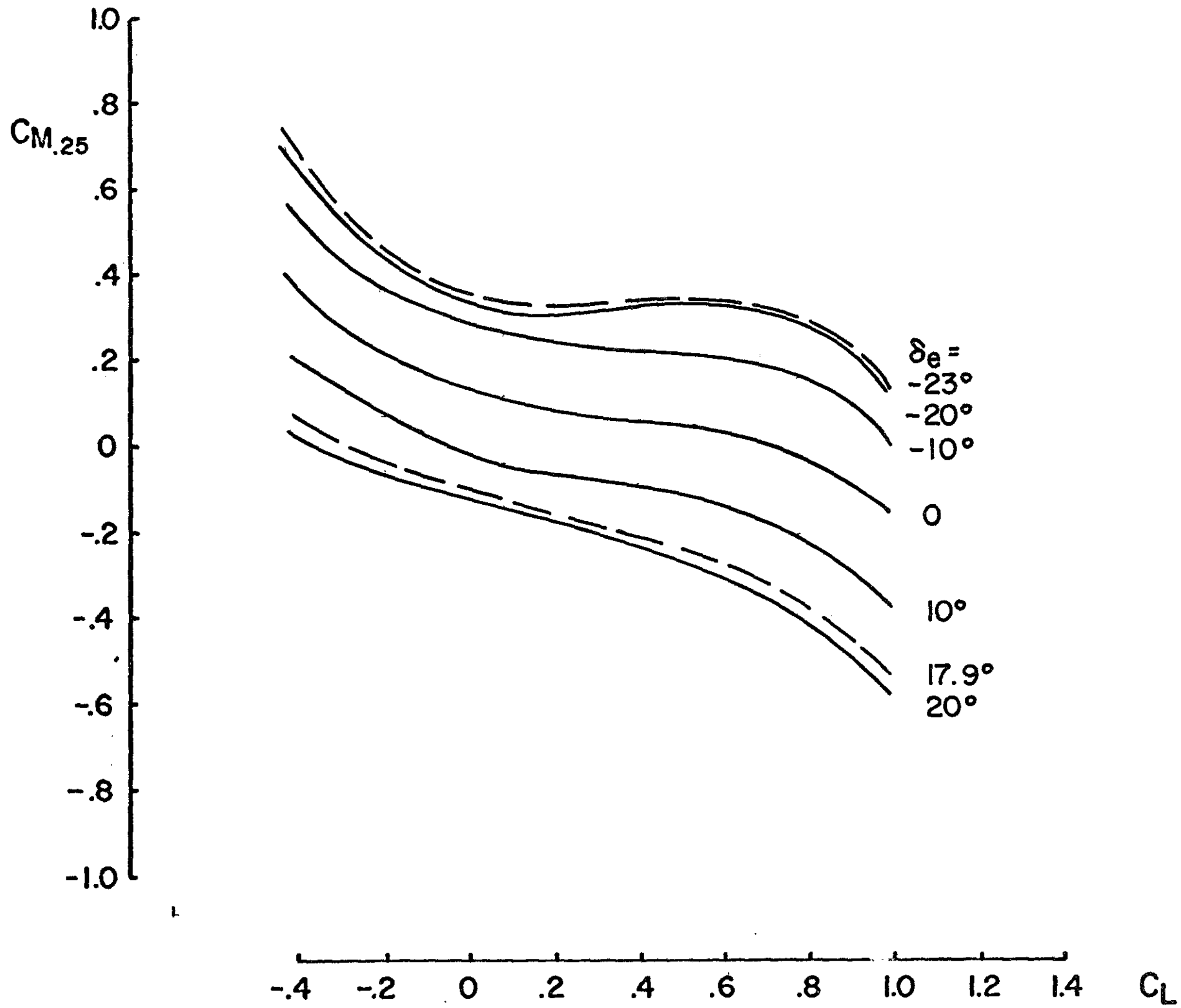

o) $T_c' = -.2$
$\delta_f = -30°$

FIGURE 8 Concluded

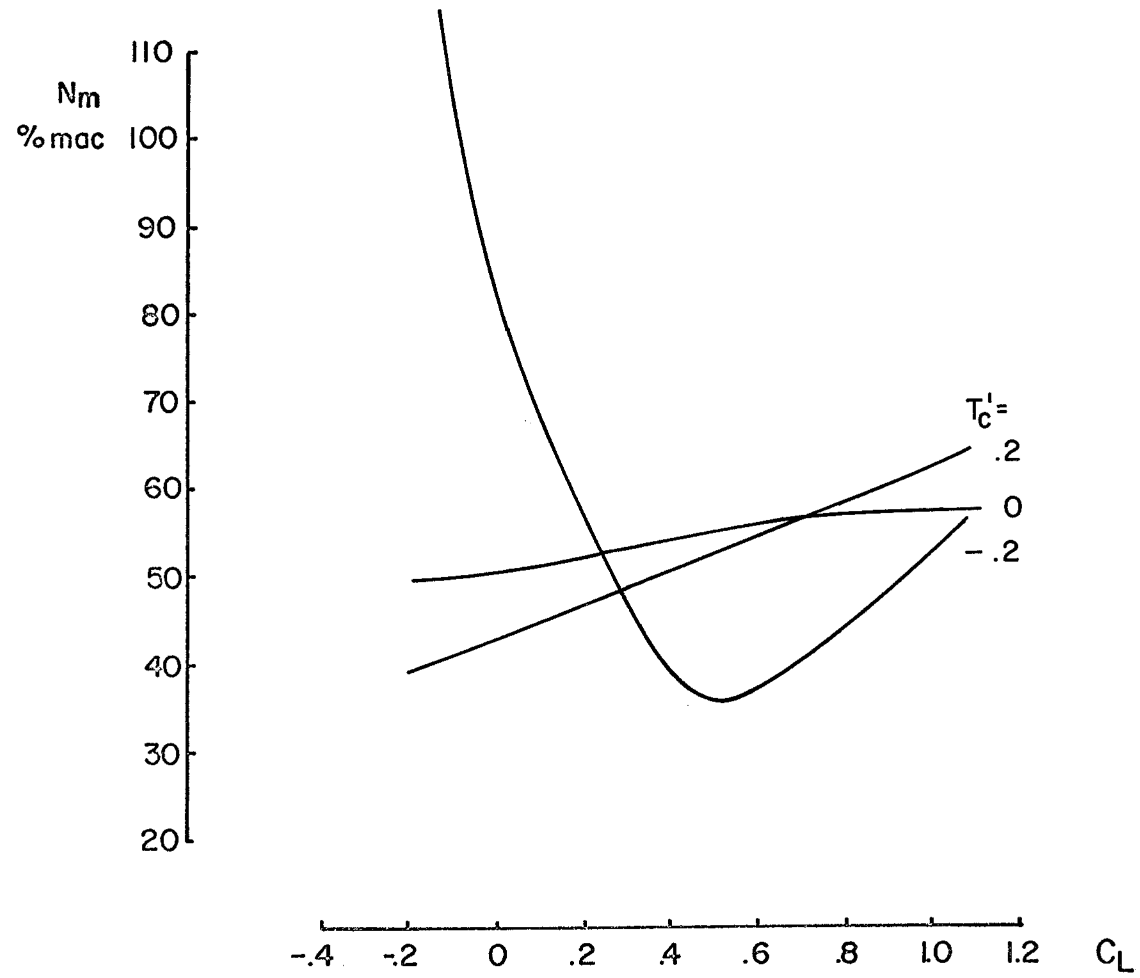

FIGURE 9 VARIATION OF MANEUVER POINT WITH LIFT COEFFICIENT

FOR $\delta_e = 0$, $\delta_f = 0$

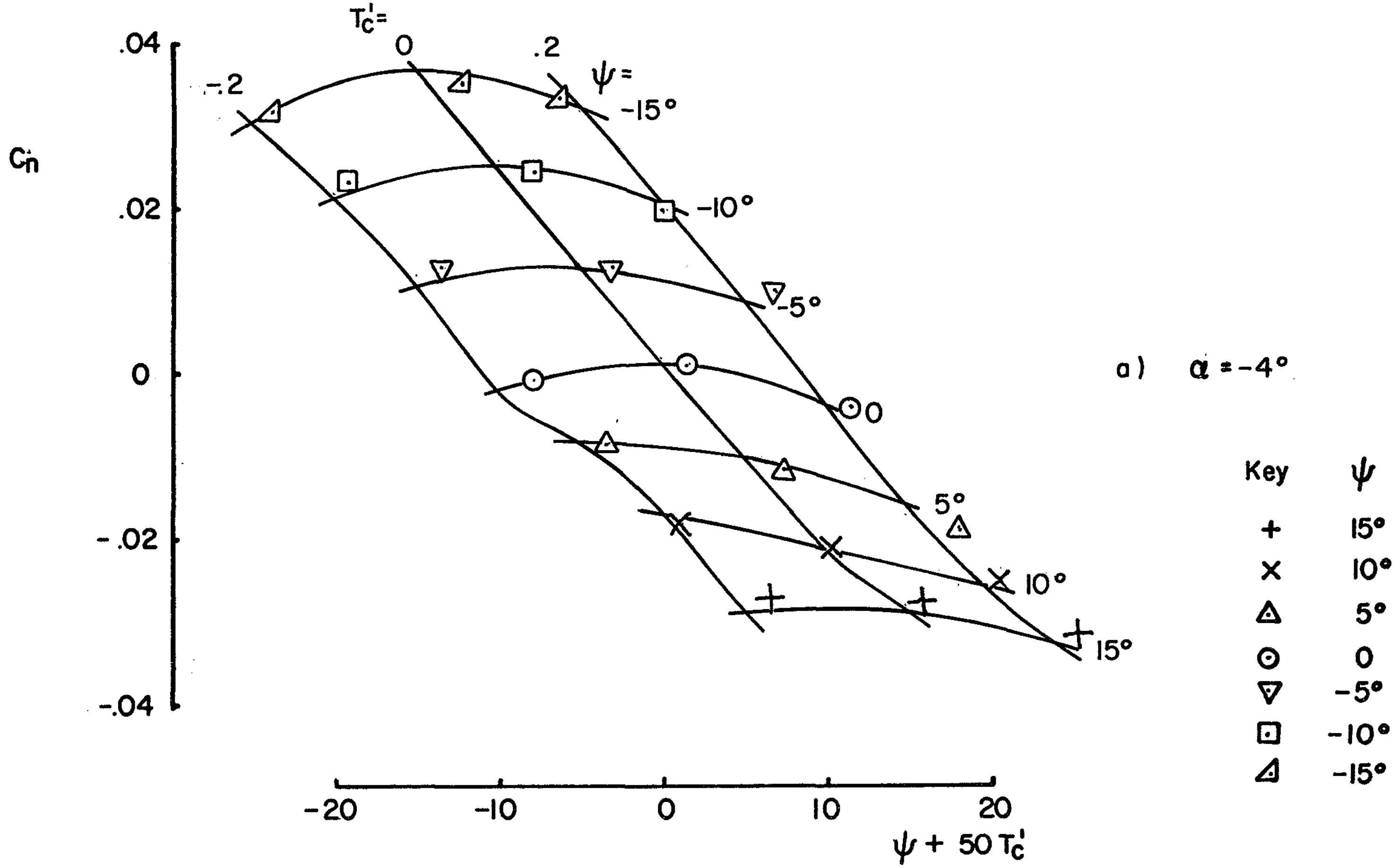

FIGURE 10 VARIATION OF YAWING MOMENT COEFFICIENT WITH YAW ANGLE AND THRUST COEFFICIENT FOR $\delta_f = 0$

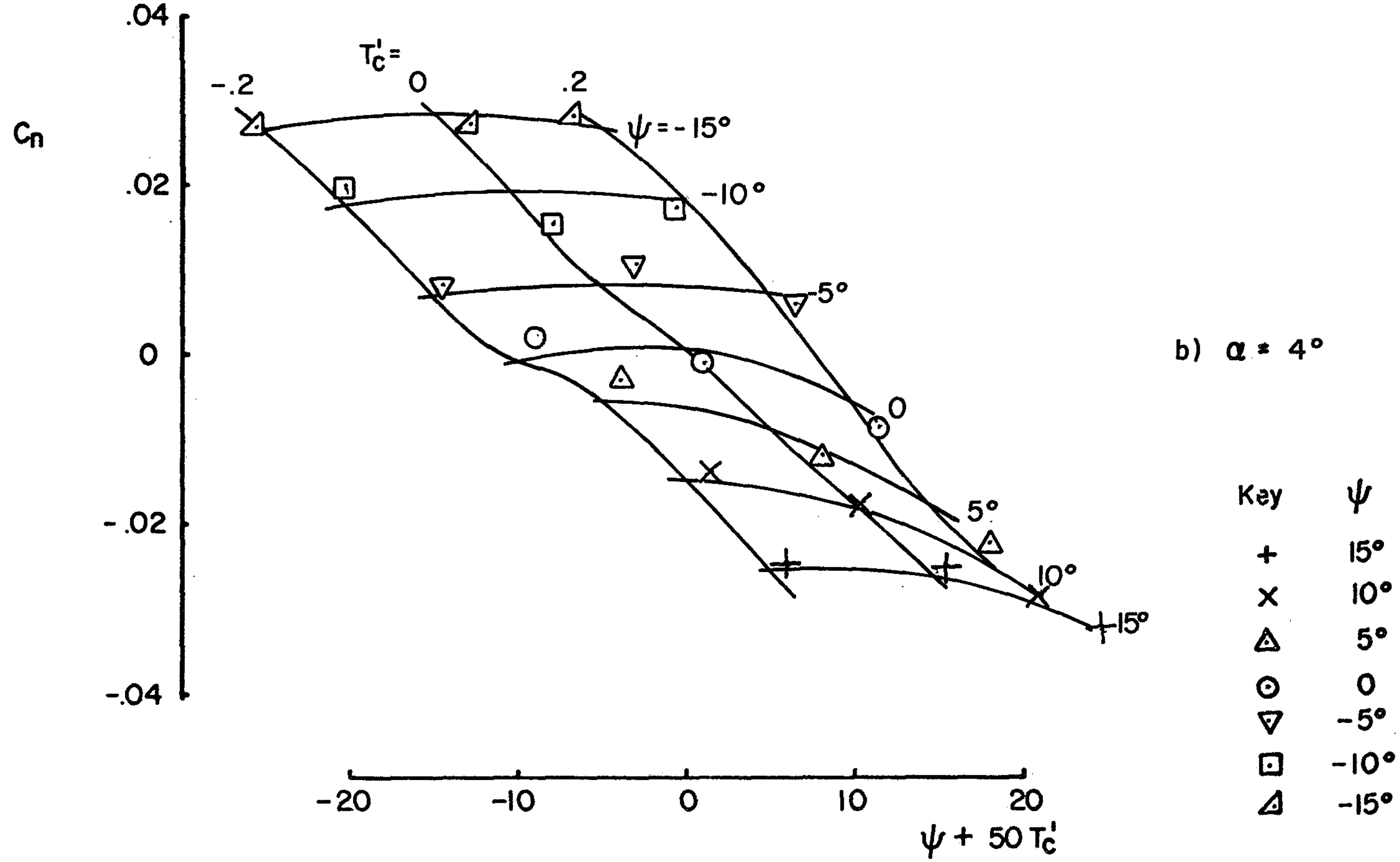

FIGURE 10 Continued

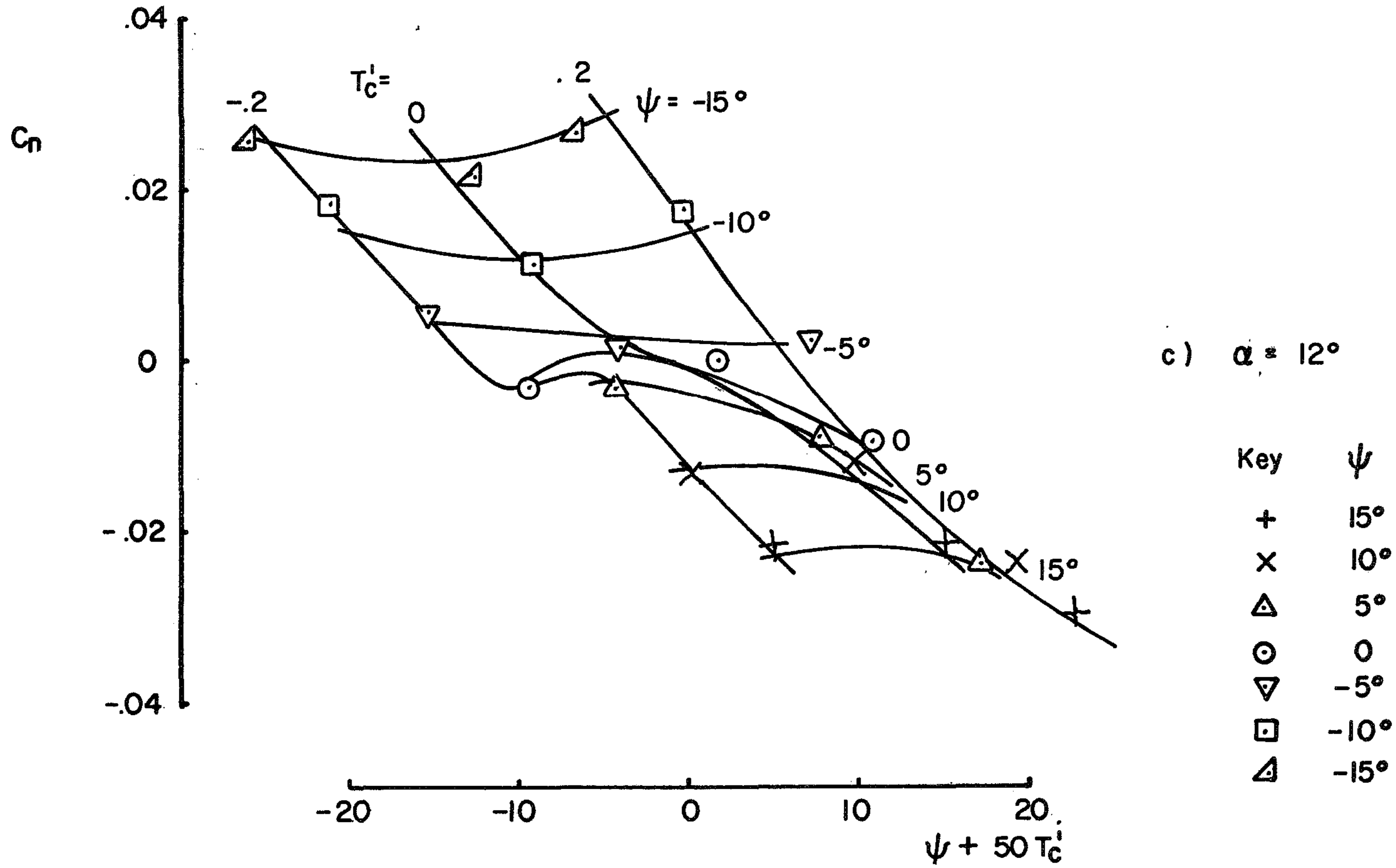

FIGURE 10 Concluded

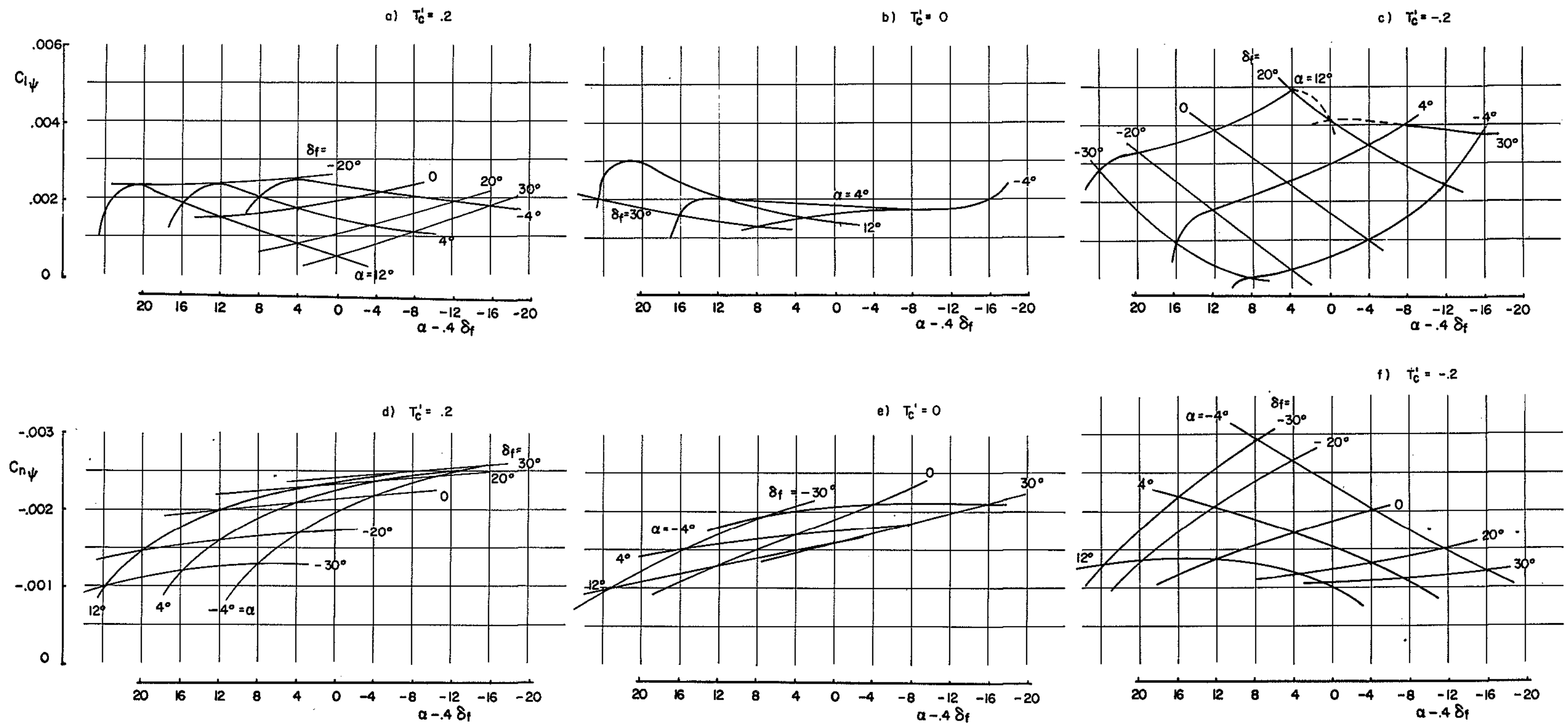

FIGURE 11 VARIATION OF DIHEDRAL EFFECT AND DIRECTIONAL STABILITY WITH ANGLE OF ATTACK AND FLAP DEFLECTION

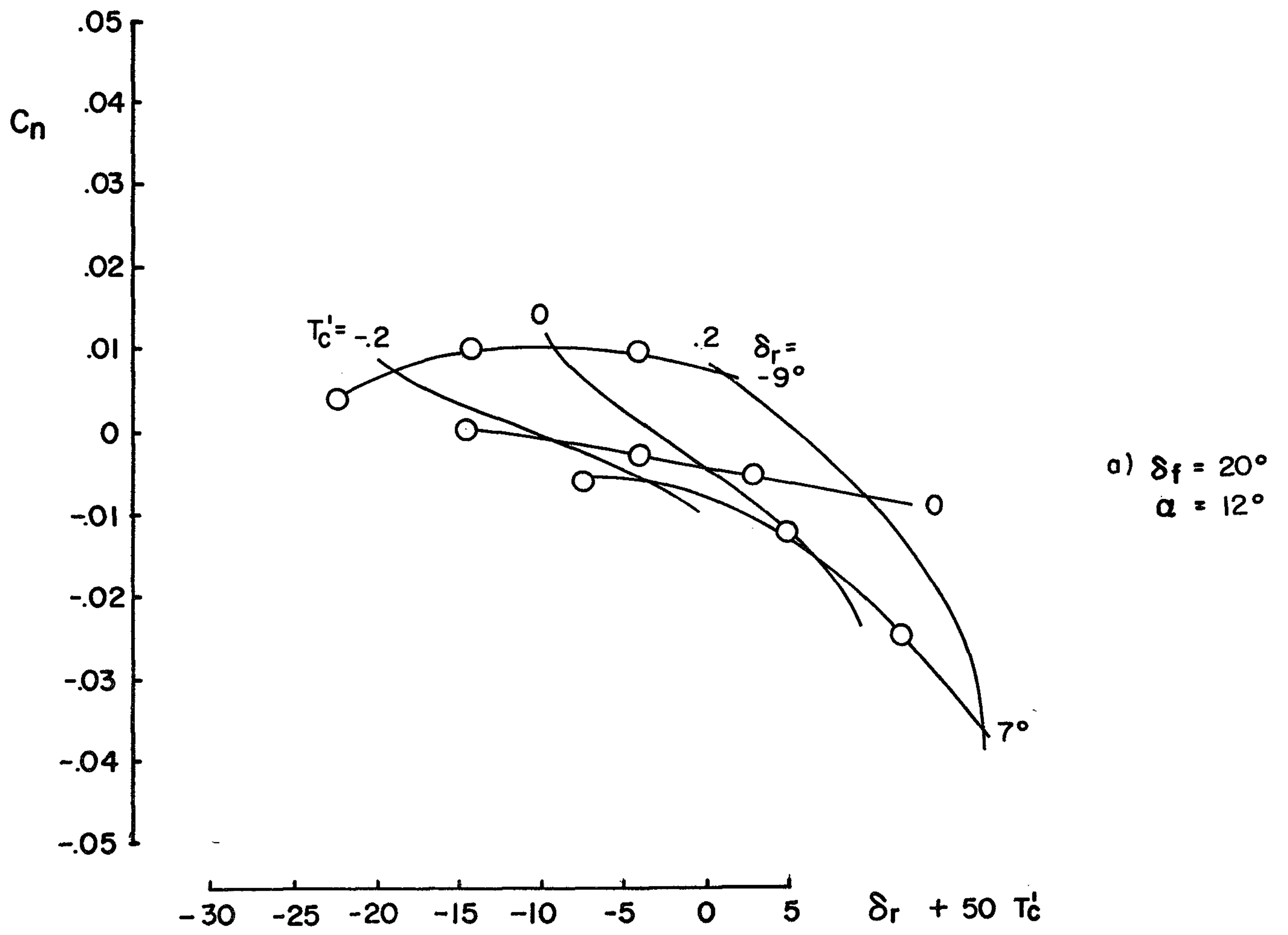

FIGURE 12 VARIATION OF YAWING MOMENT COEFFICIENT WITH THRUST COEFFICIENT AND RUDDER DEFLECTION FOR $\psi = 0$

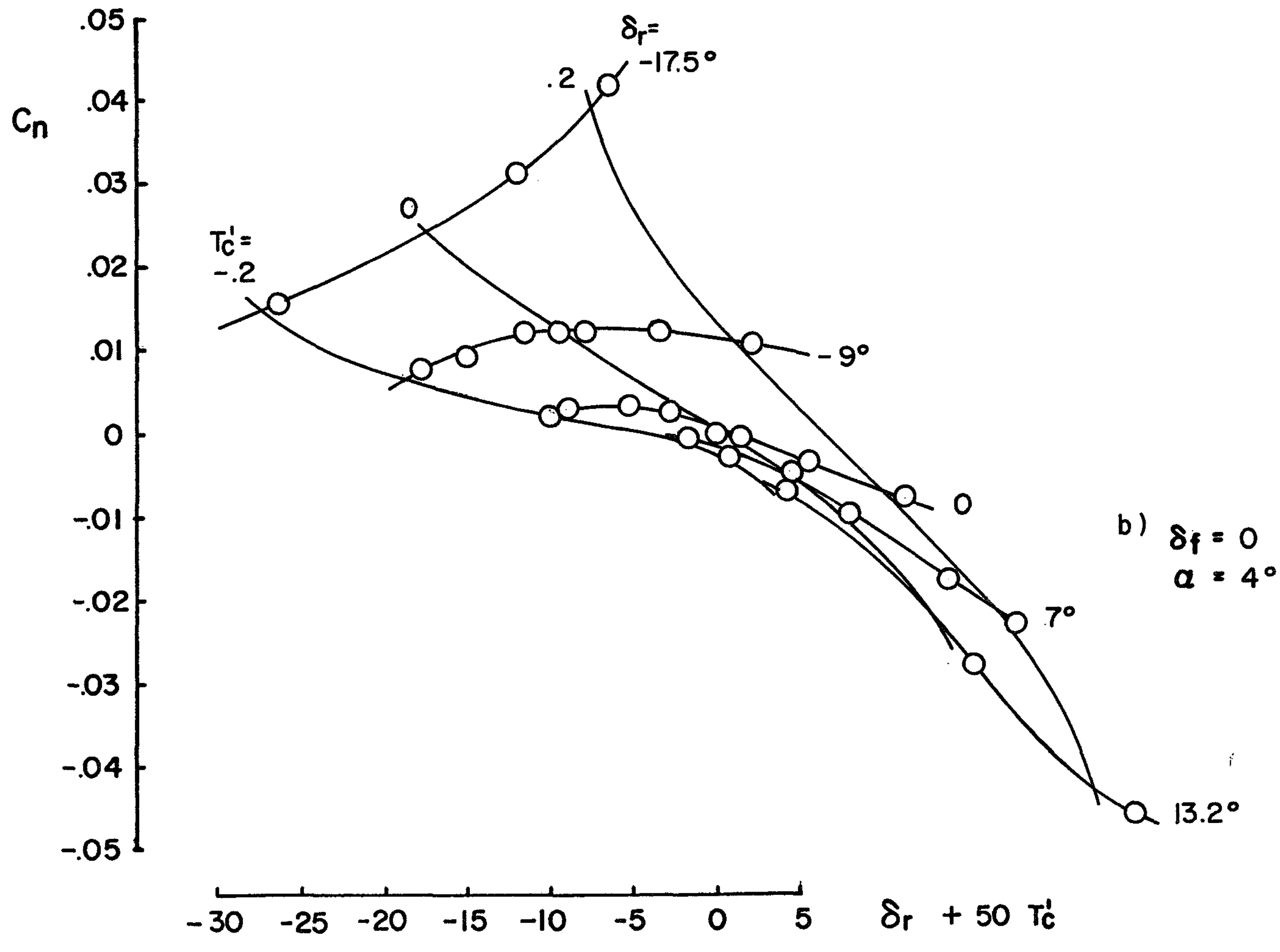

FIGURE 12 Continued

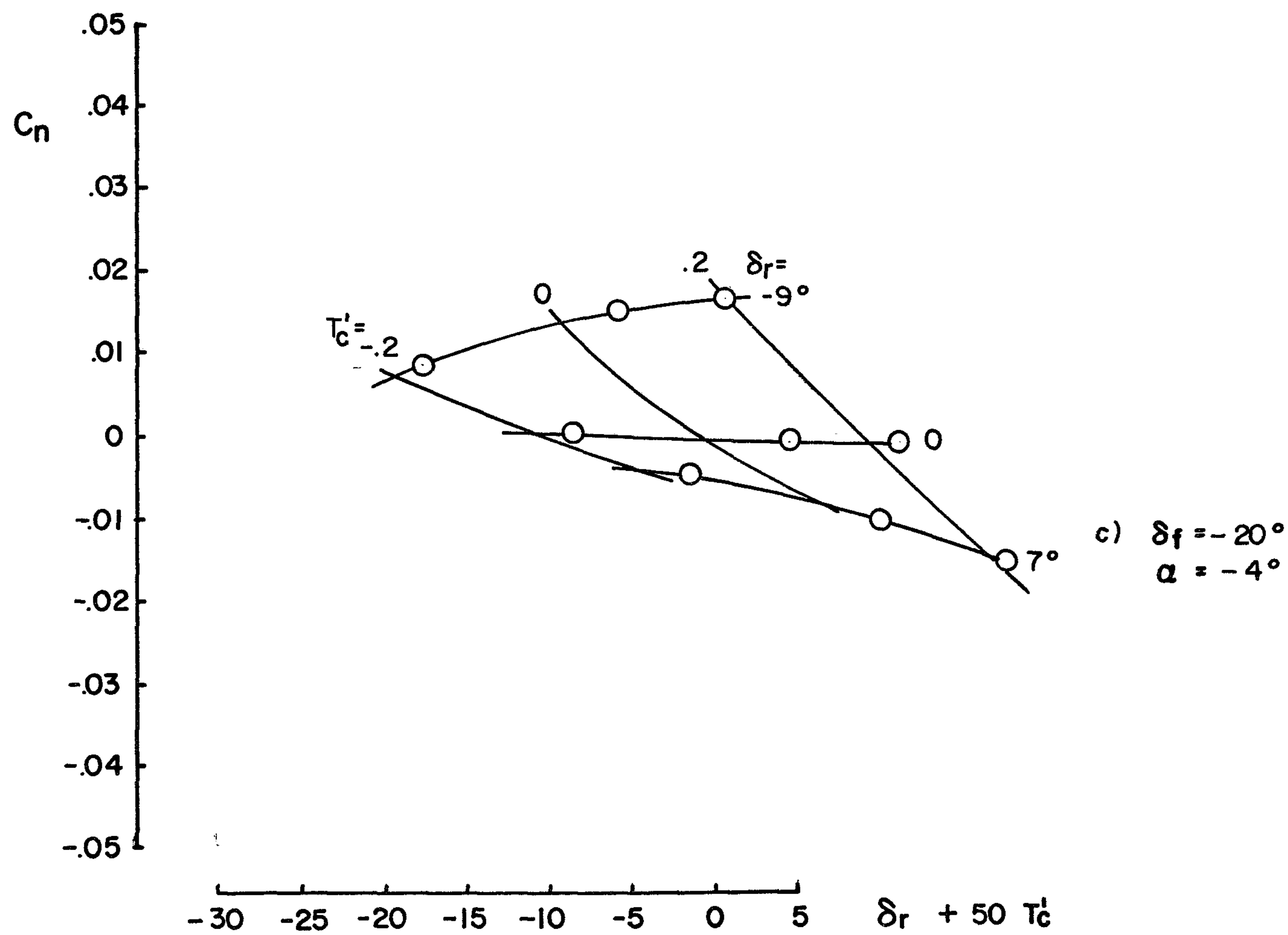

FIGURE 12 Concluded

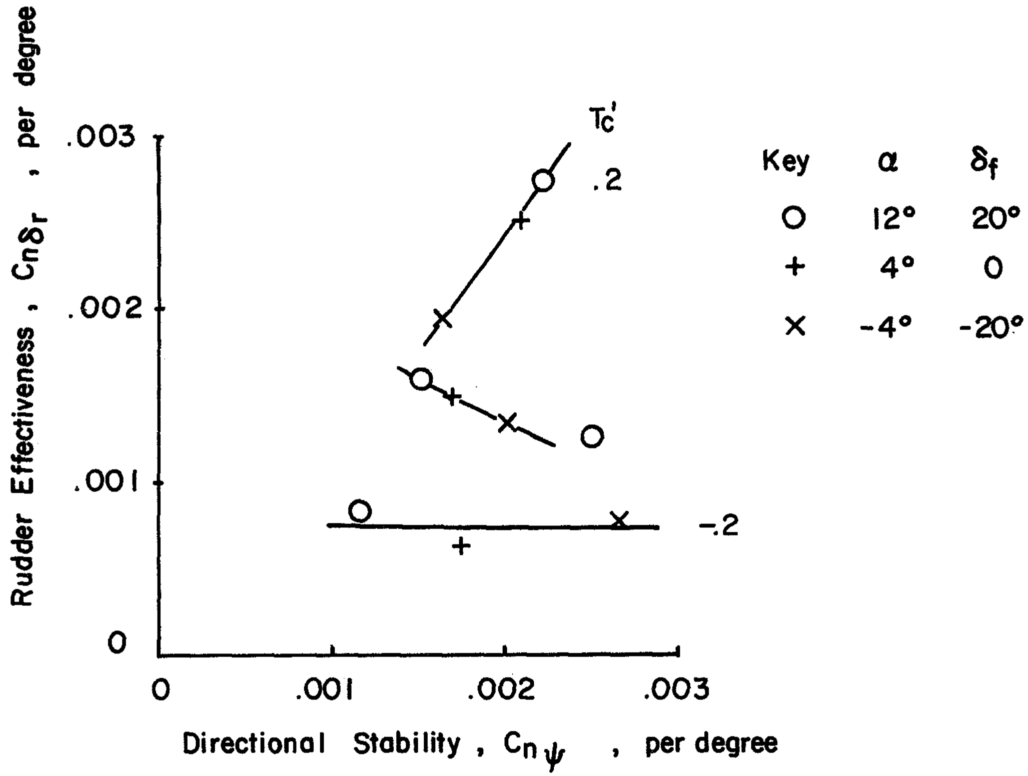

FIGURE 13 VARIATION OF RUDDER EFFECTIVENESS WITH DIRECTIONAL STABILITY

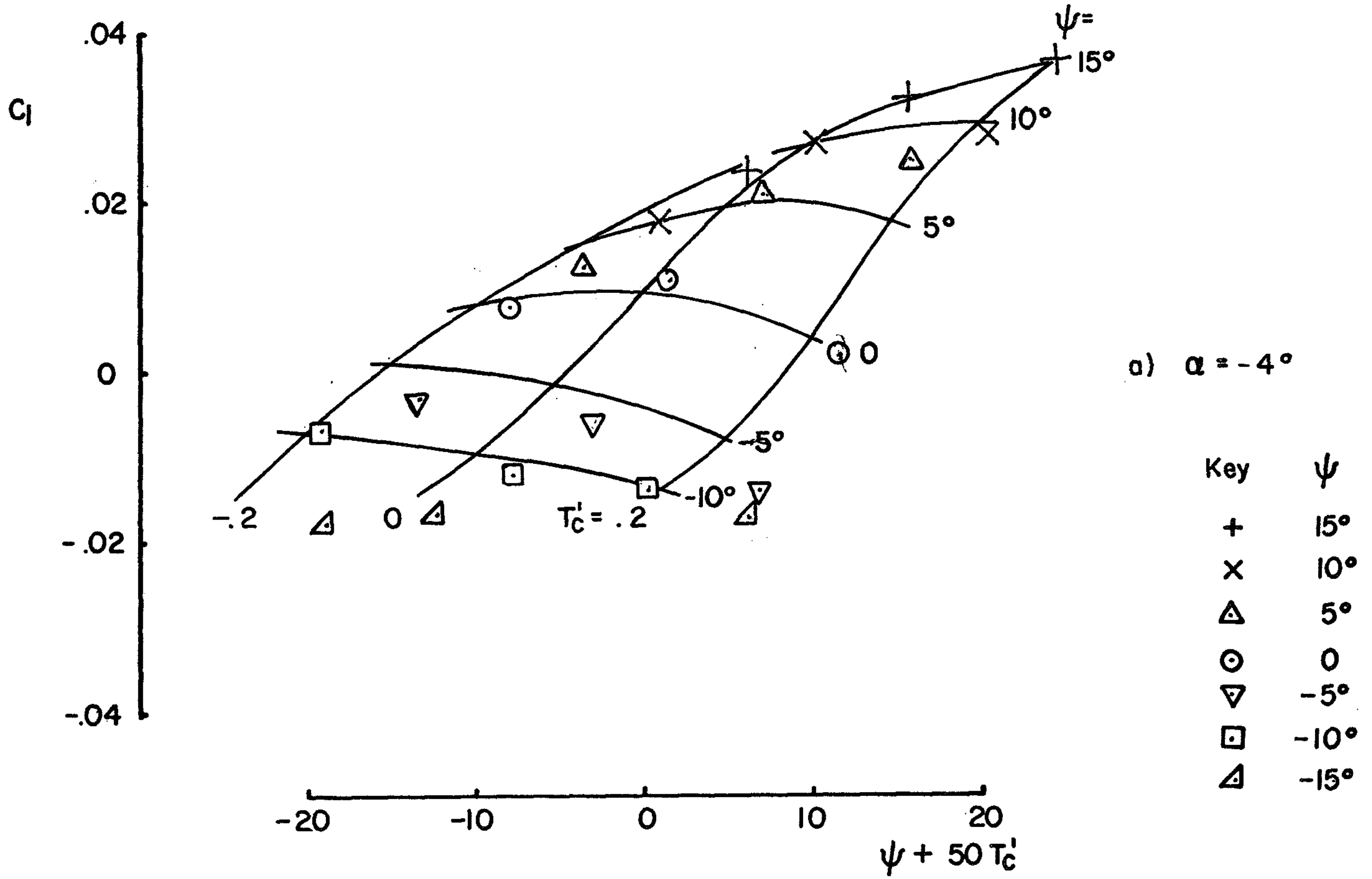

FIGURE 14 VARIATION OF ROLLING MOMENT COEFFICIENT WITH YAW ANGLE AND THRUST COEFFICIENT FOR $\delta_f = 0$

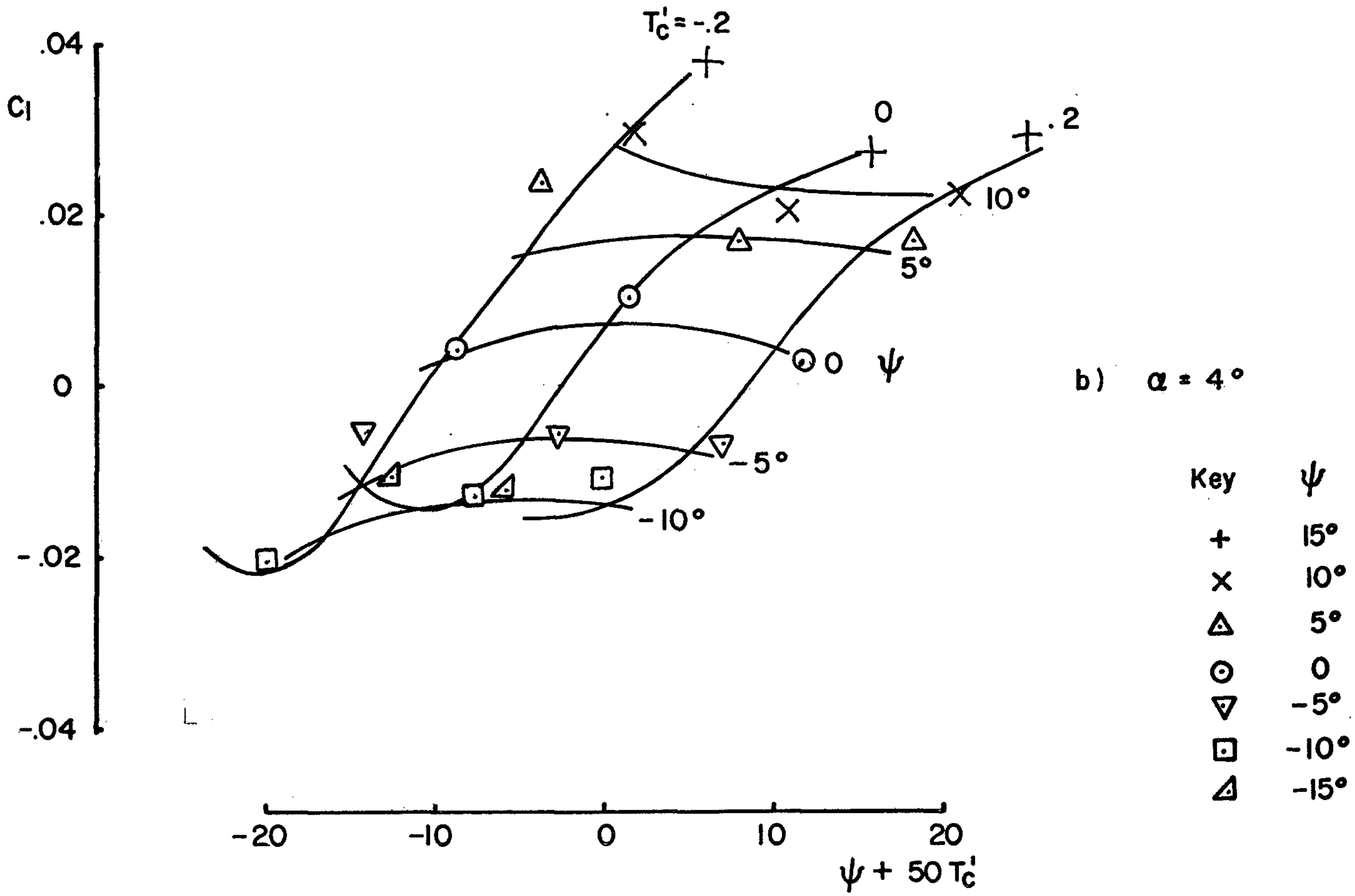

FIGURE 14 Continued

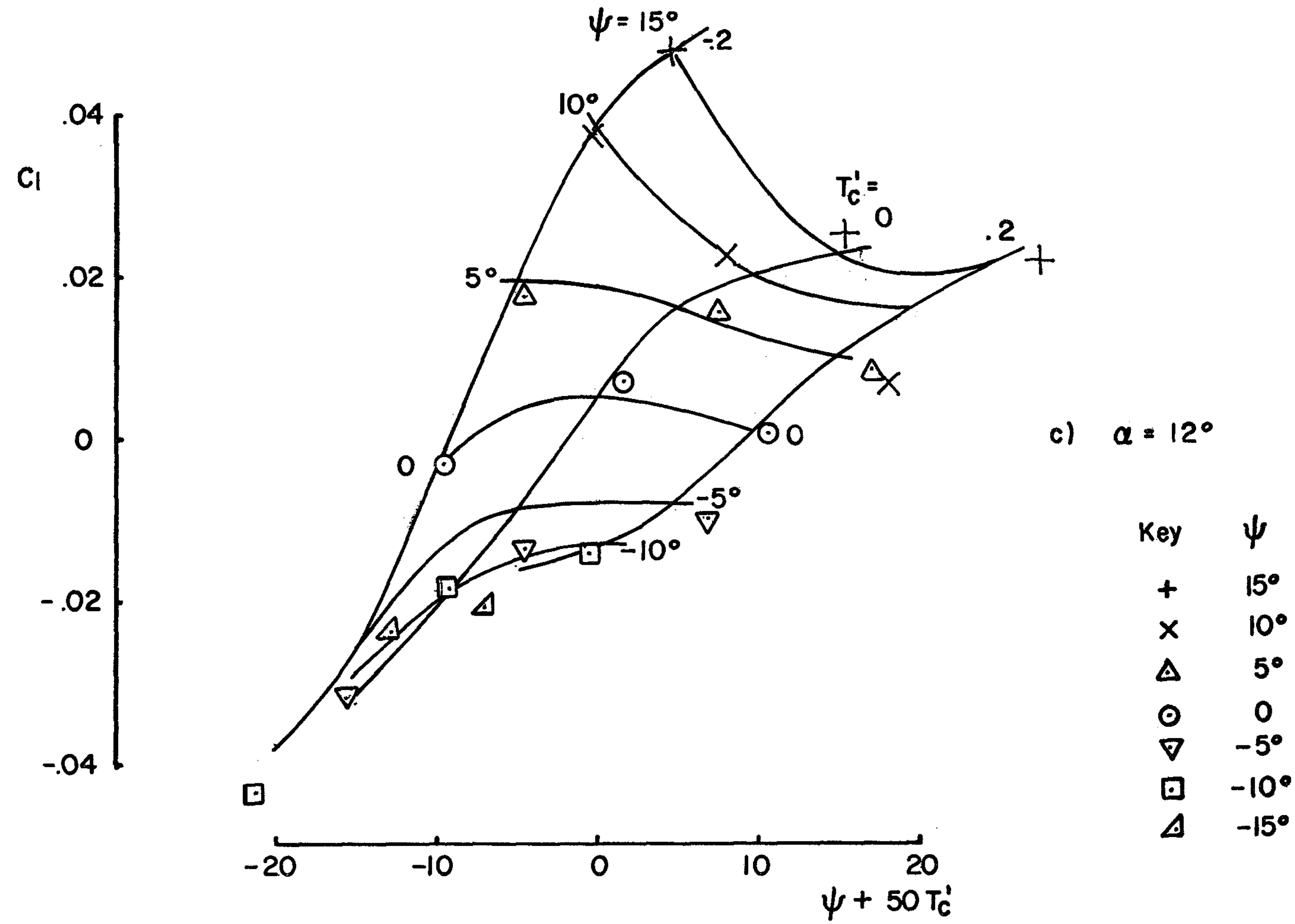

FIGURE 14 Concluded

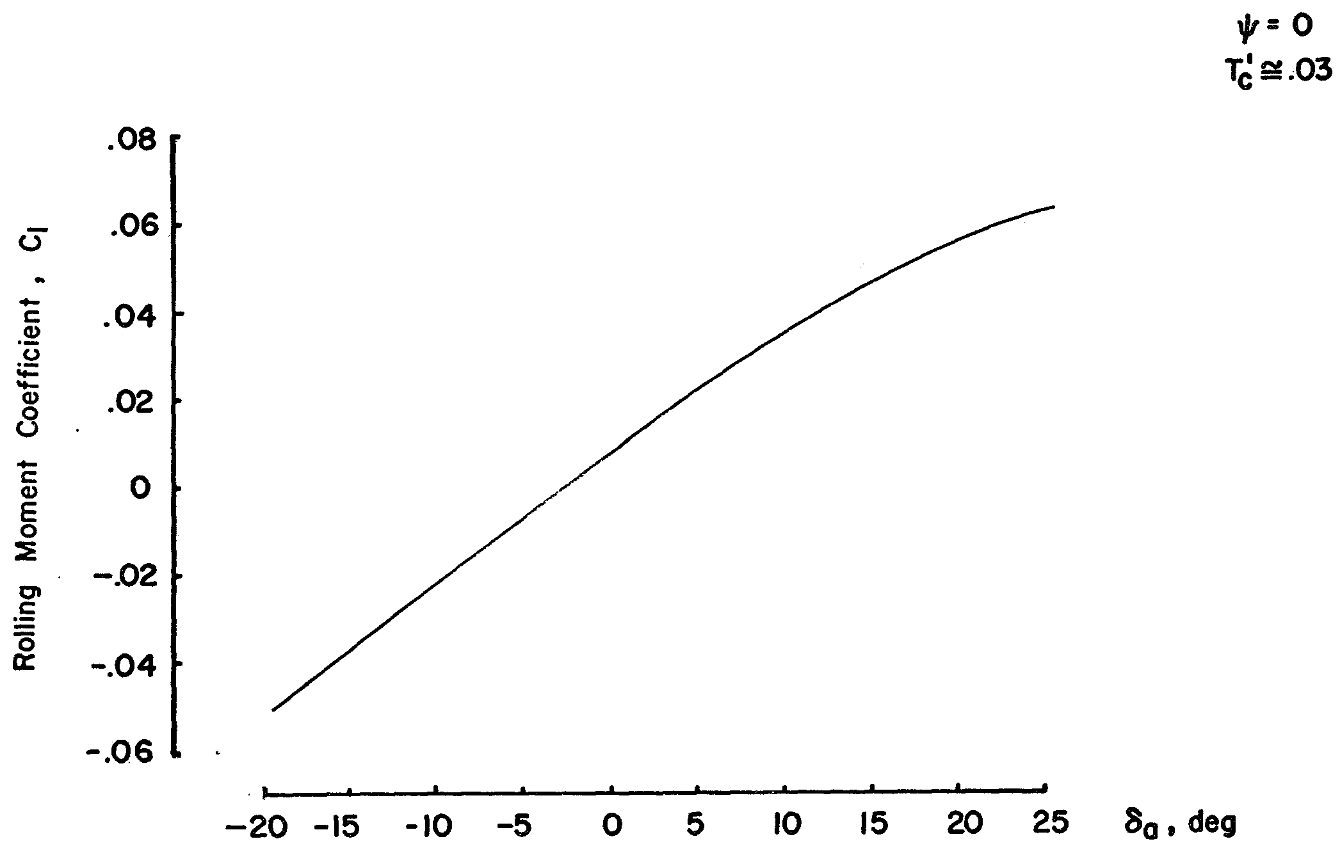

FIGURE 15 VARIATION OF ROLLING MOMENT COEFFICIENT WITH AILERON DEFLECTION FOR $\psi = 0$, $T_c' \cong .03$

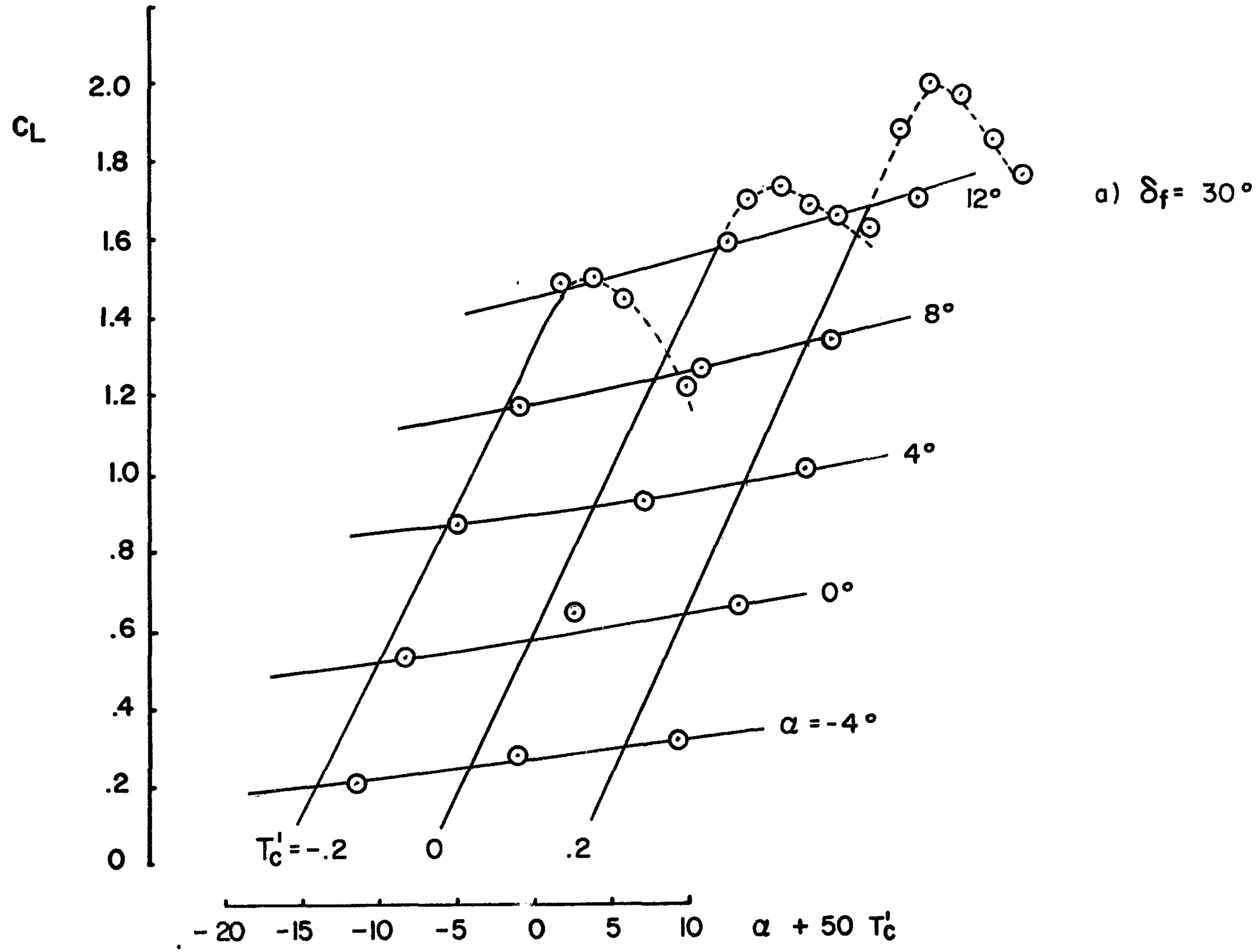

FIGURE 16 VARIATION OF LIFT COEFFICIENT WITH ANGLE OF ATTACK AND THRUST COEFFICIENT FOR $i_t = -5°$

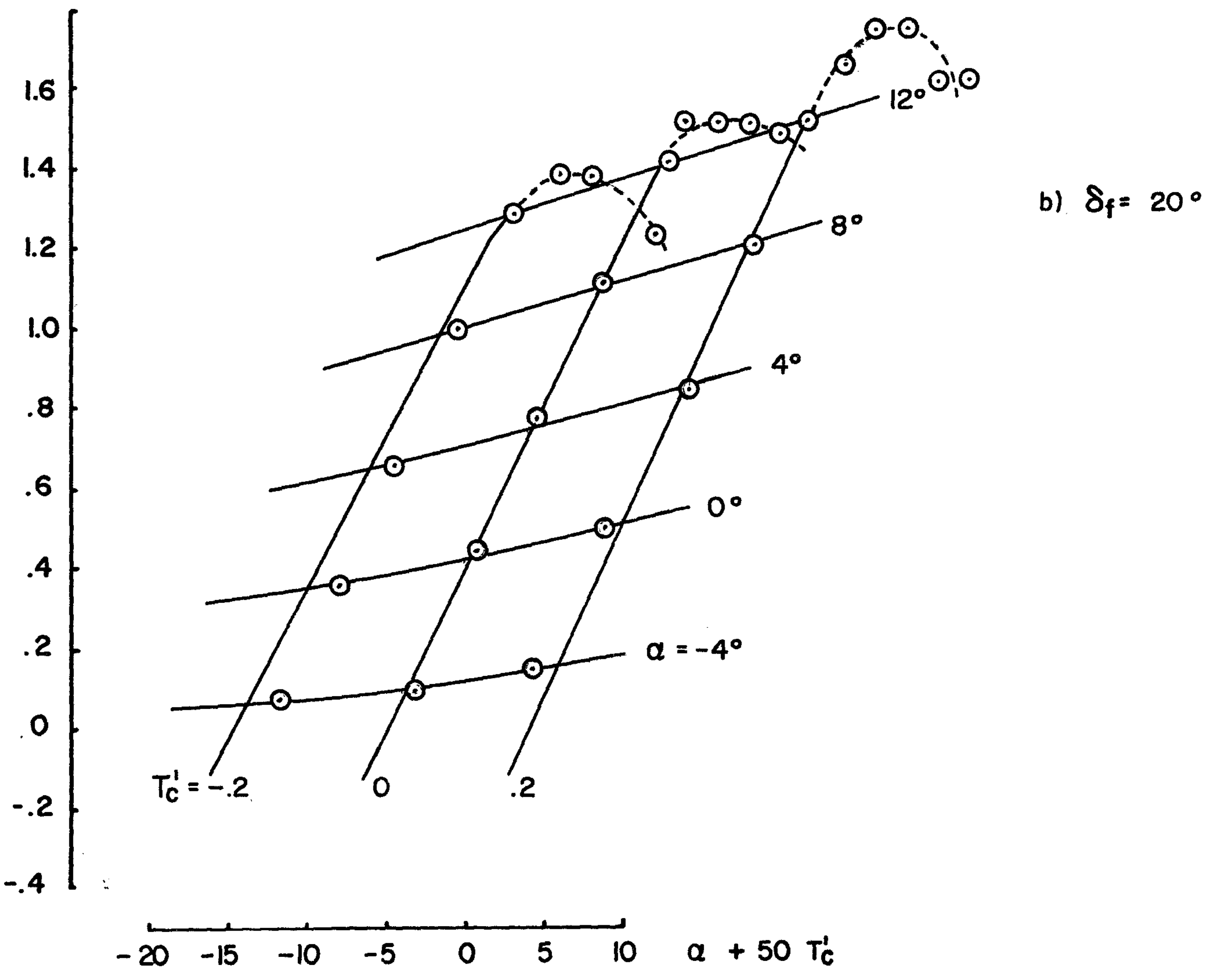

FIGURE 16 Continued

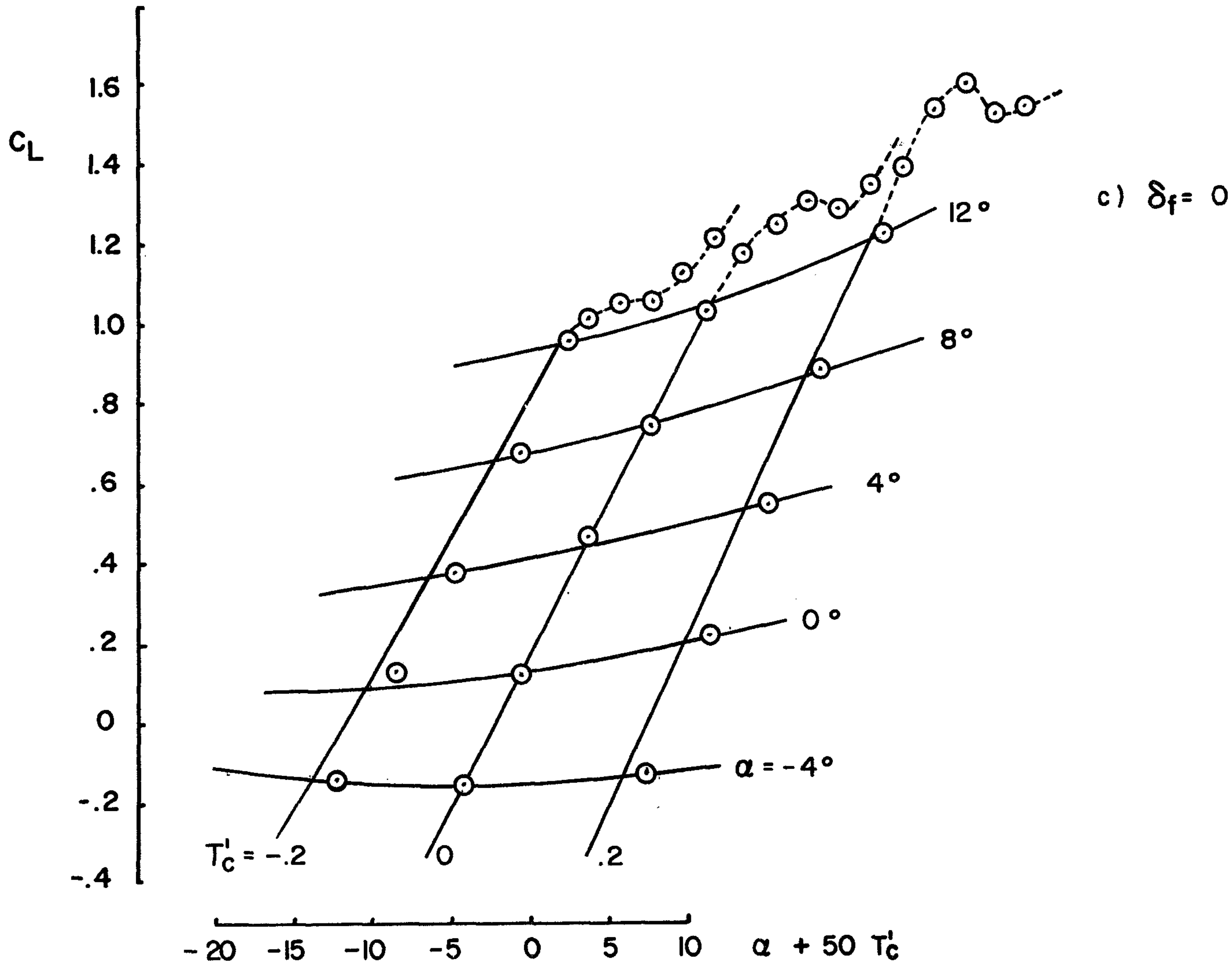

FIGURE 16 Continued

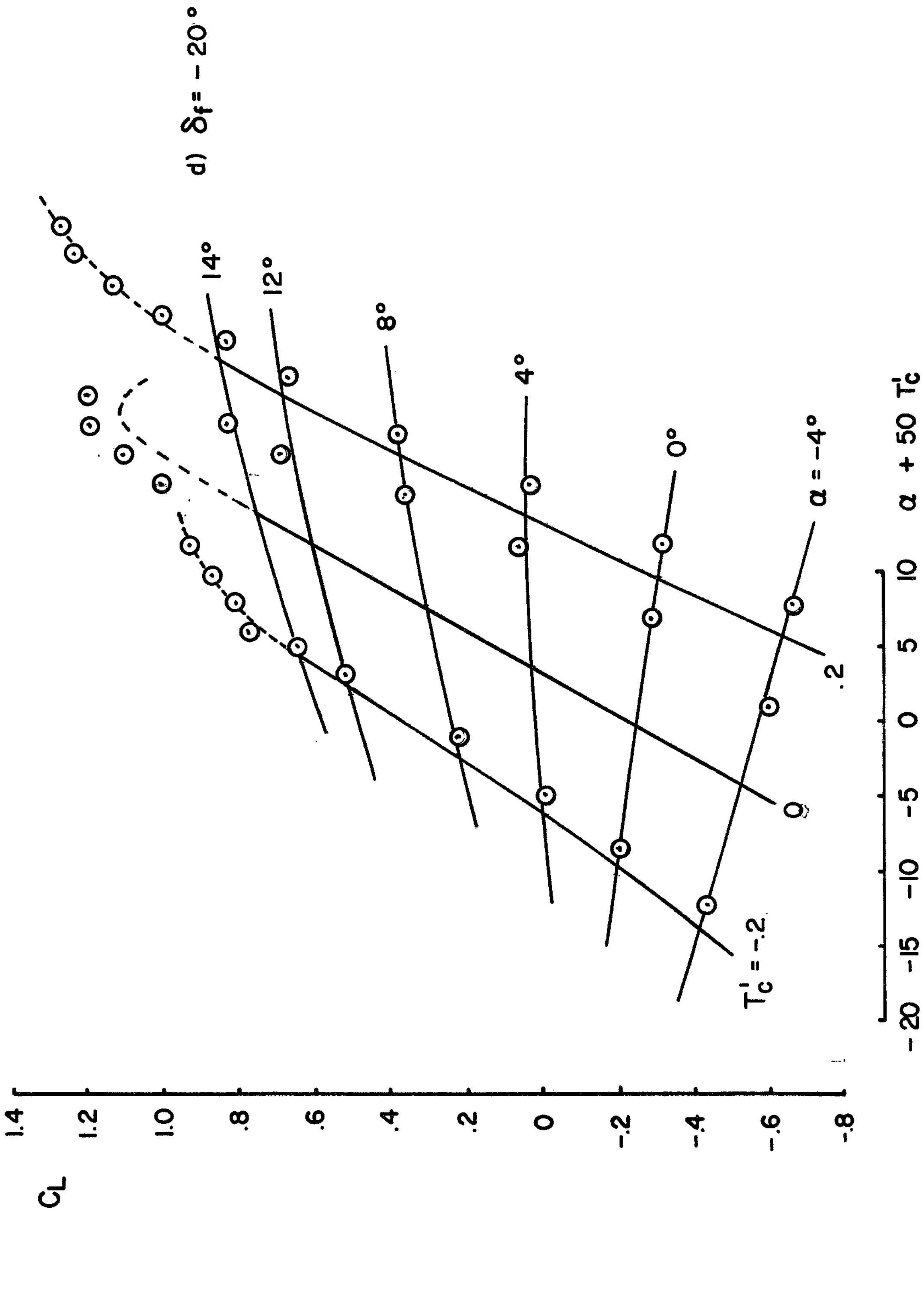

FIGURE 16 Continued

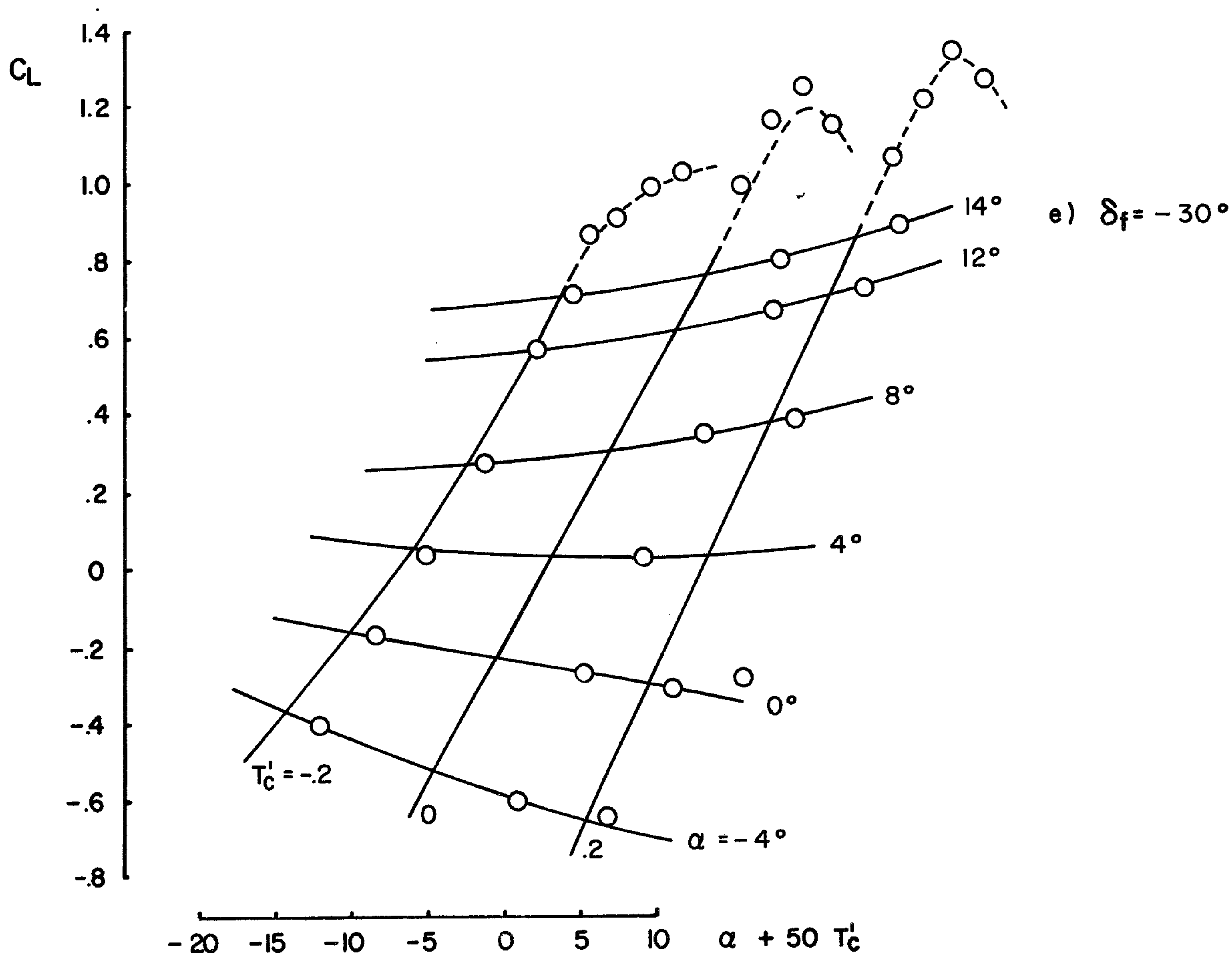

FIGURE 16 Concluded

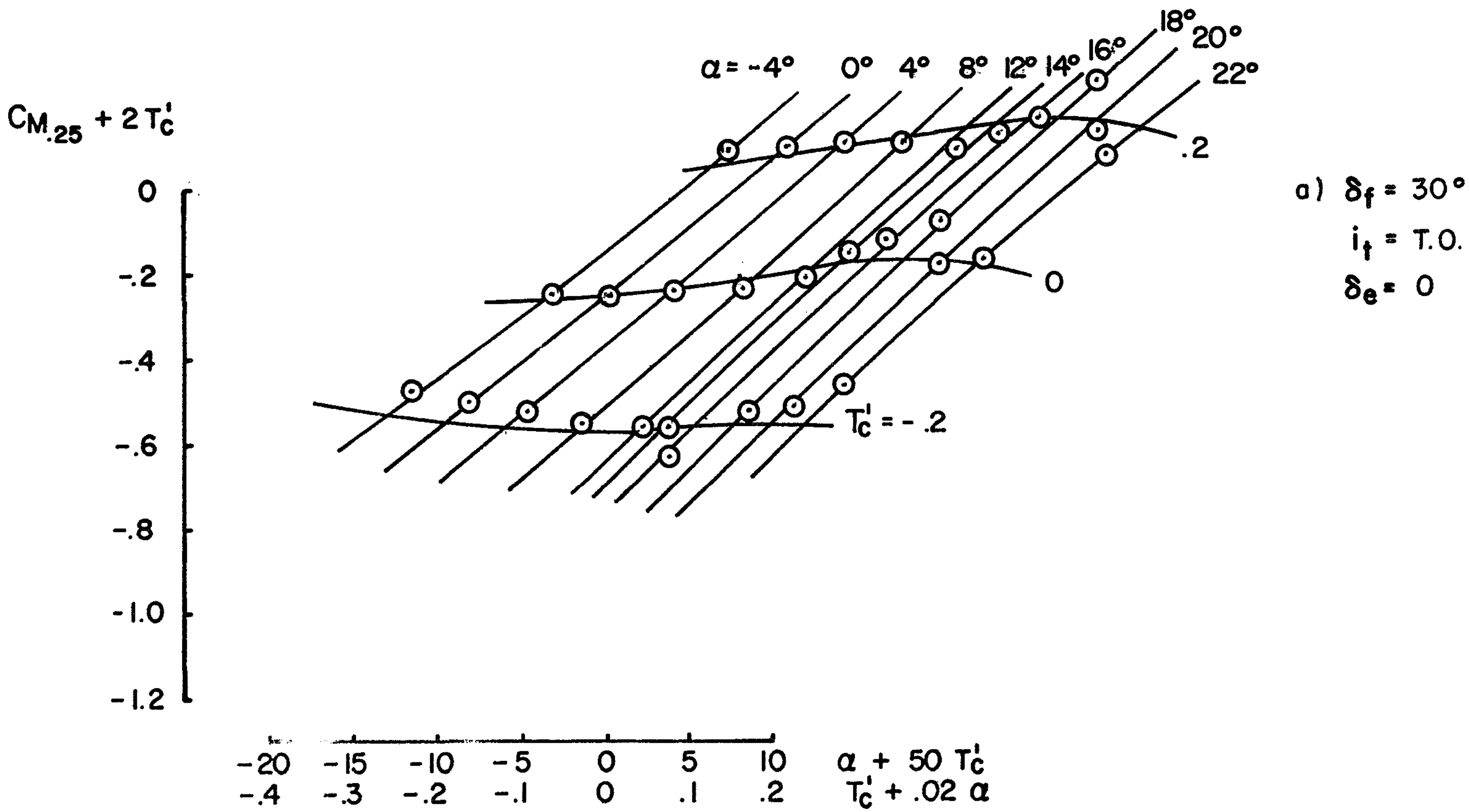

FIGURE 17 VARIATION OF PITCHING MOMENT COEFFICIENT WITH ANGLE OF ATTACK AND THRUST COEFFICIENT

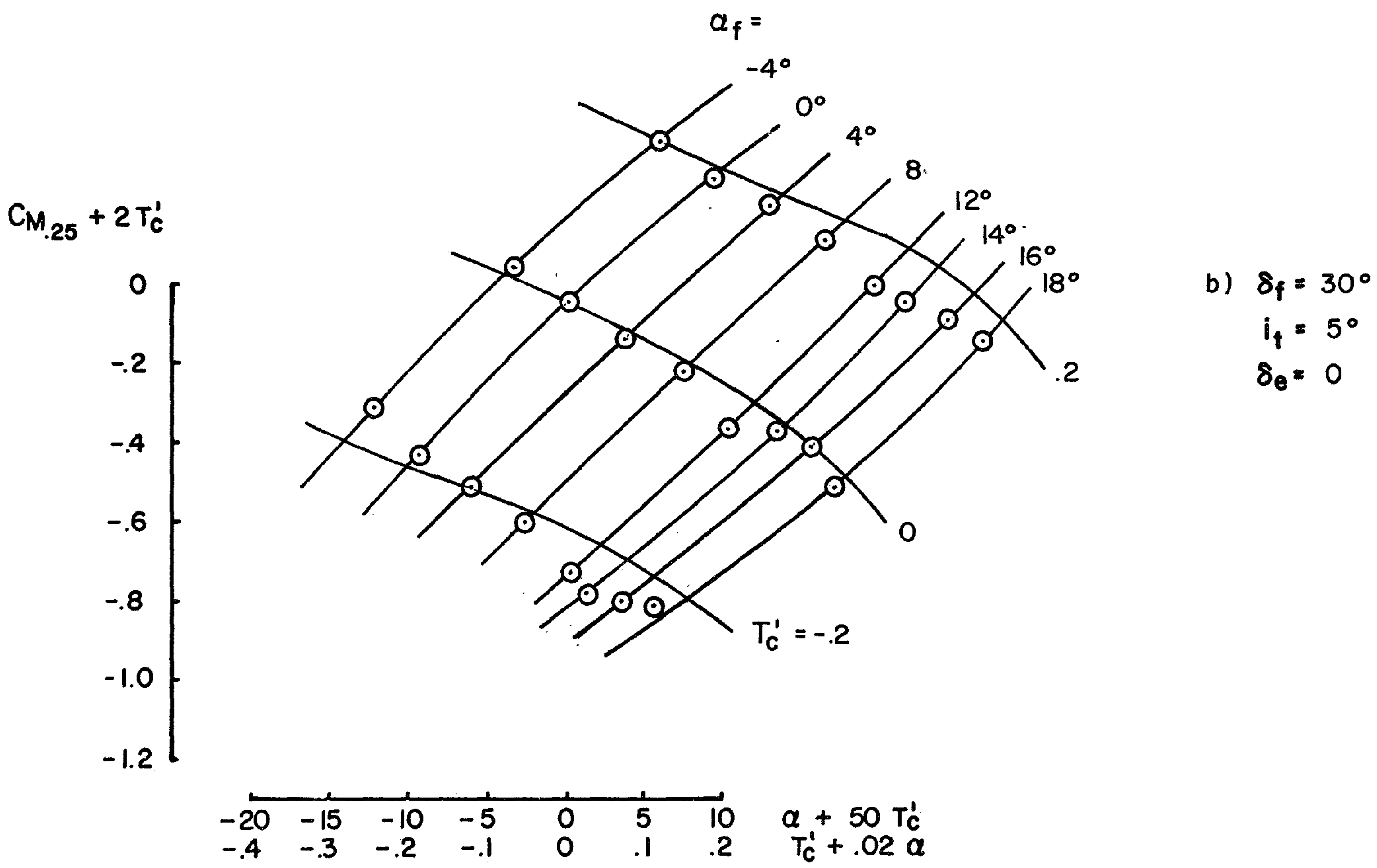

FIGURE 17 Continued

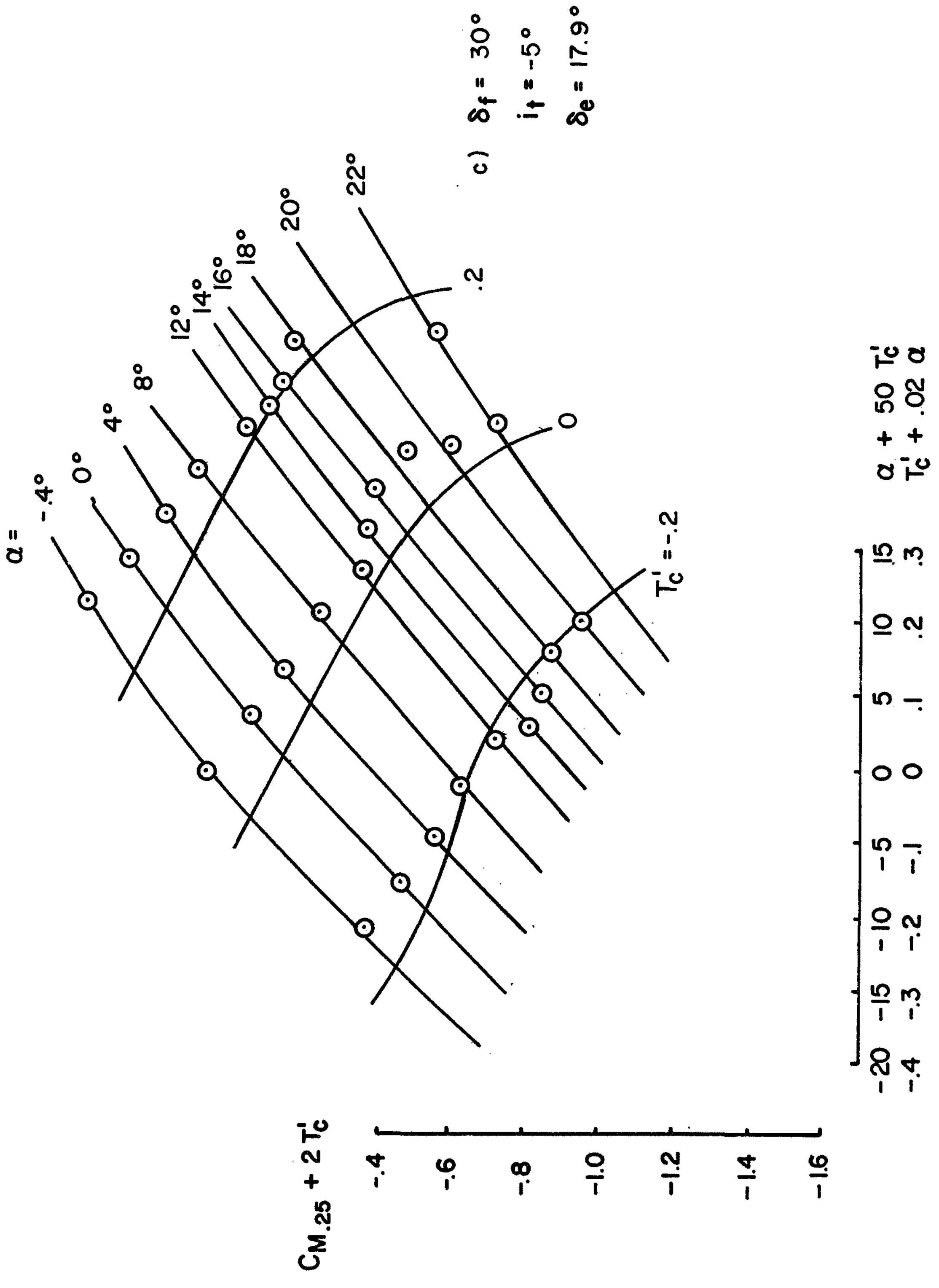

FIGURE 17 Continued

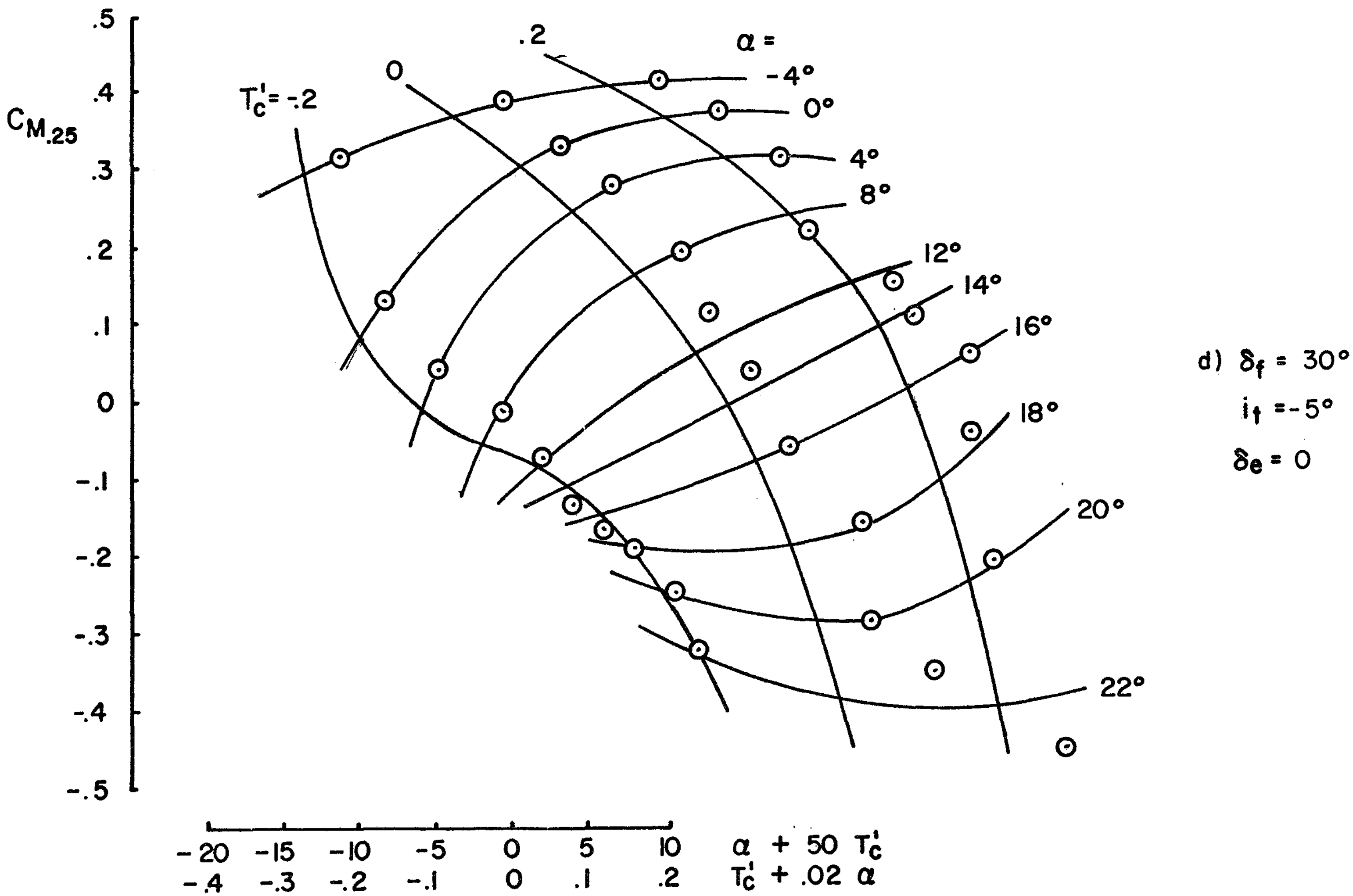

FIGURE 17 Continued

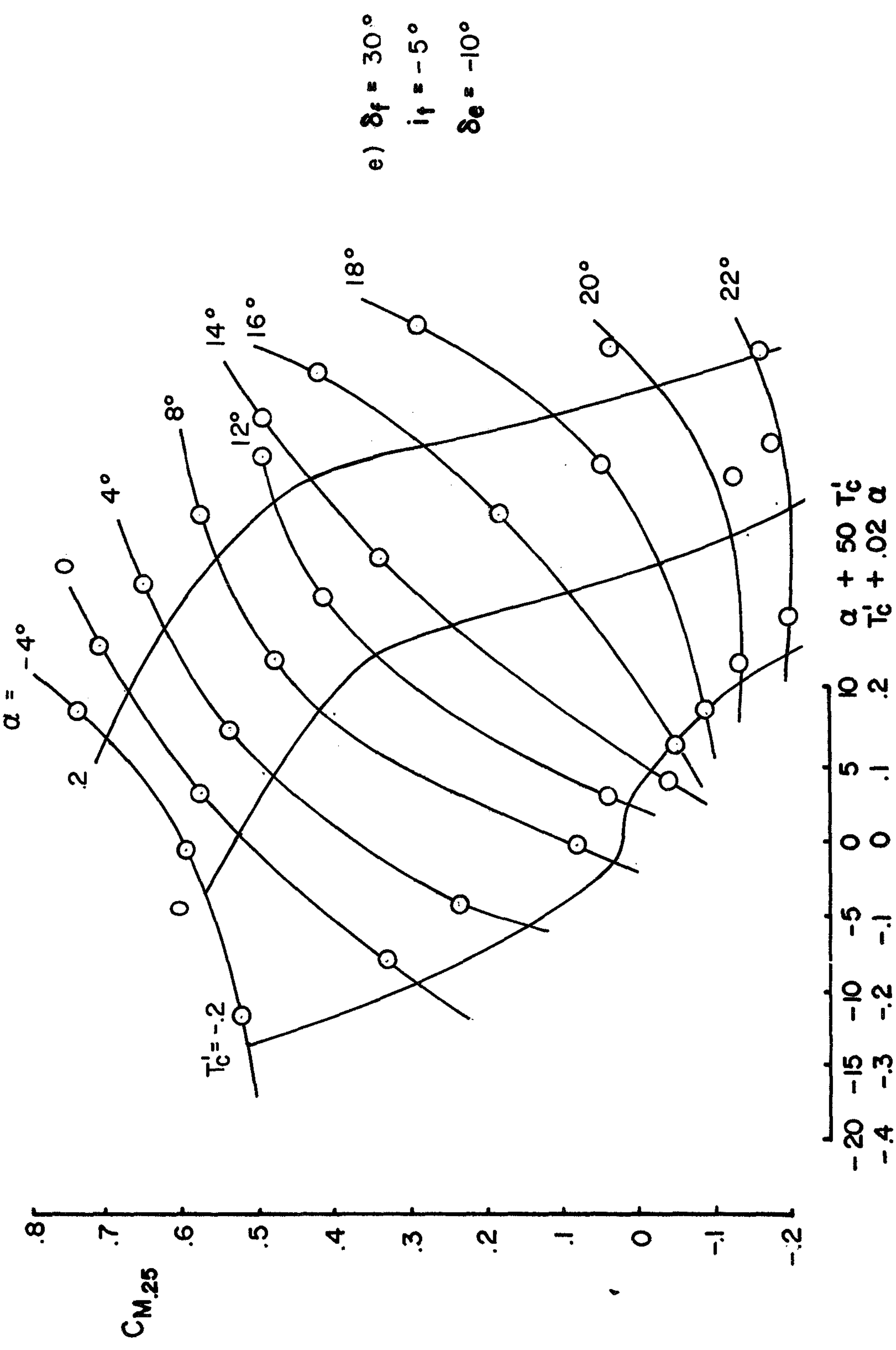

FIGURE 17 Continued

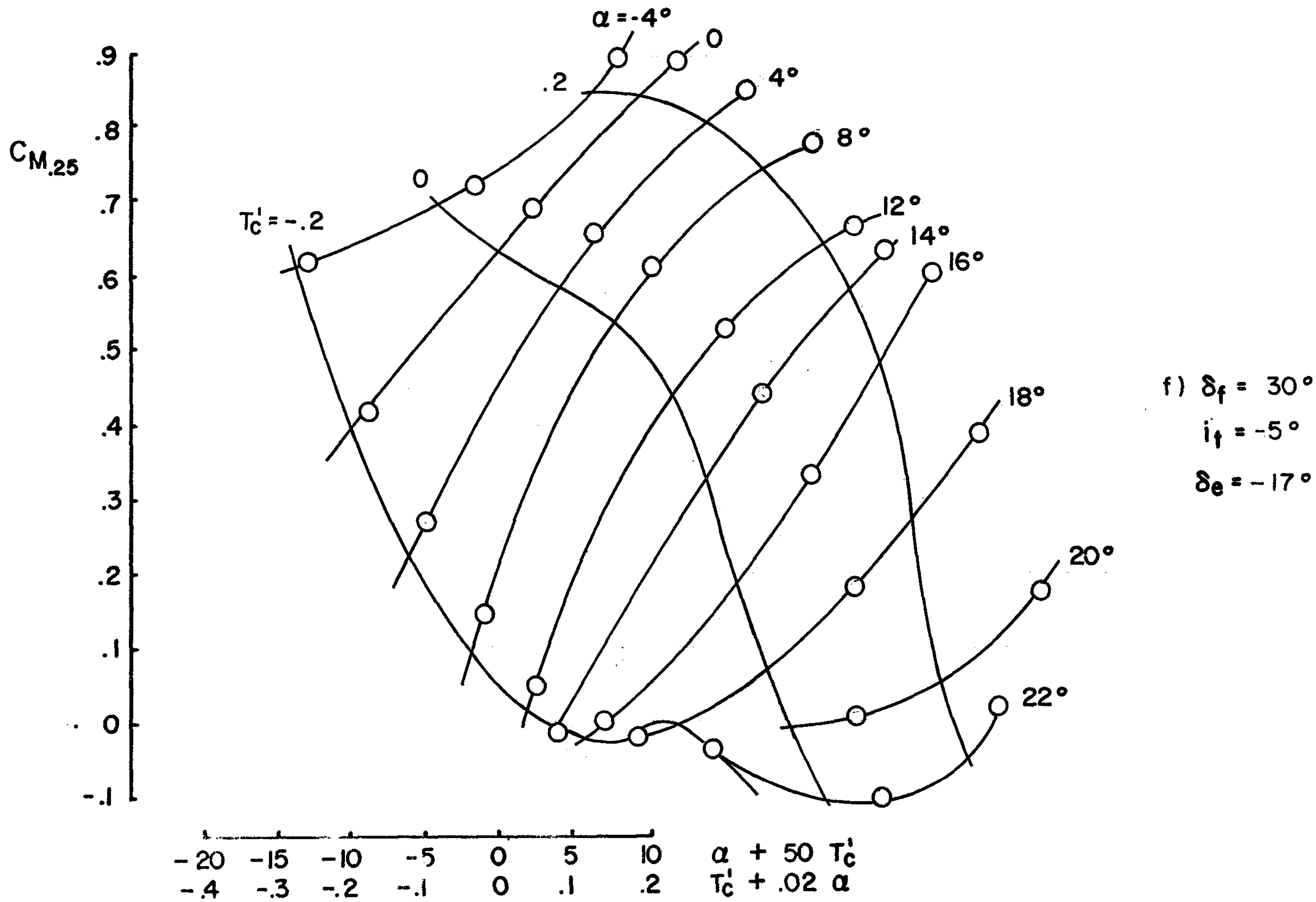

FIGURE 17 Continued

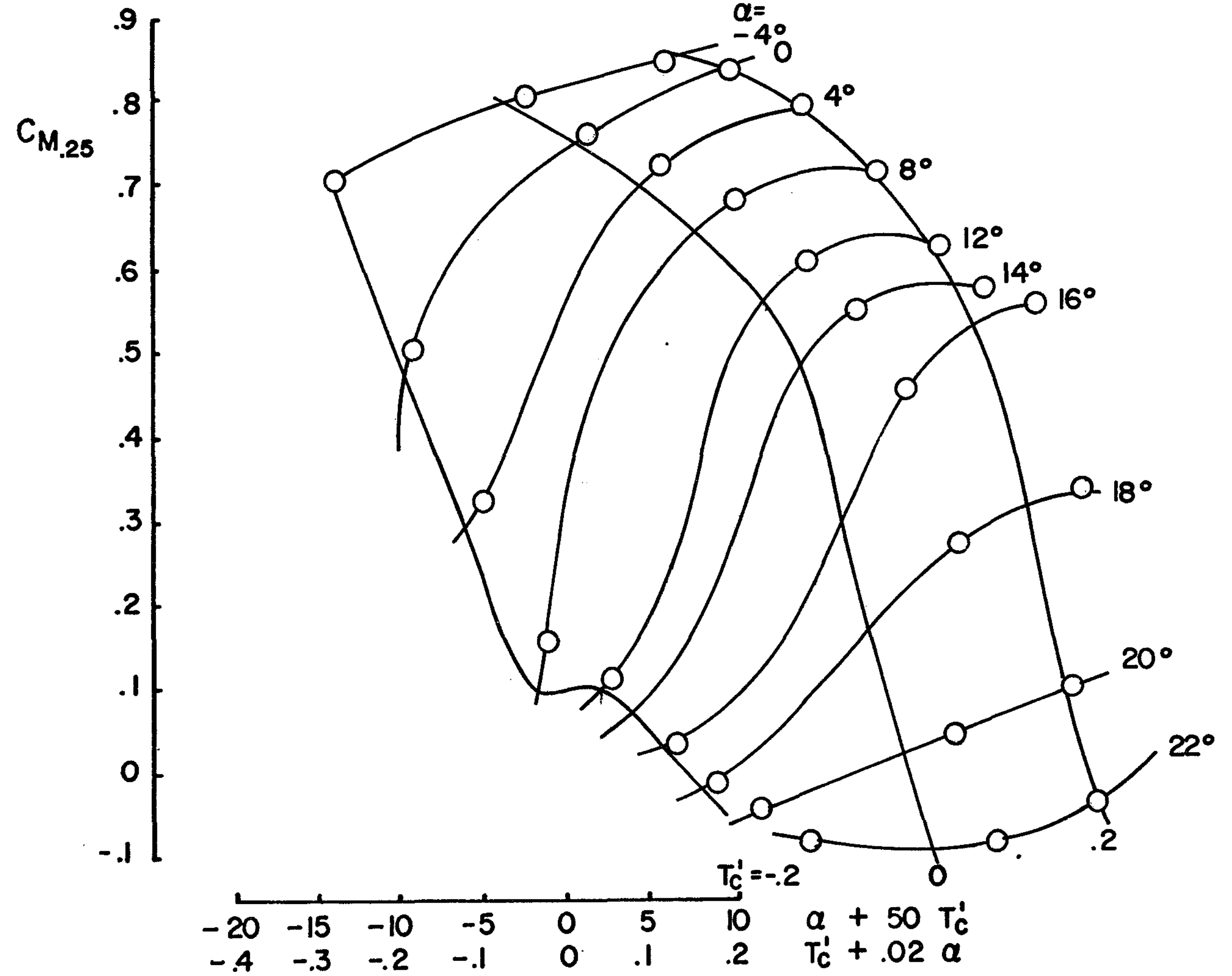

g) $\delta_f = 30°$

$i_t = -5°$

$\delta_e = -23°$

FIGURE 17 Continued

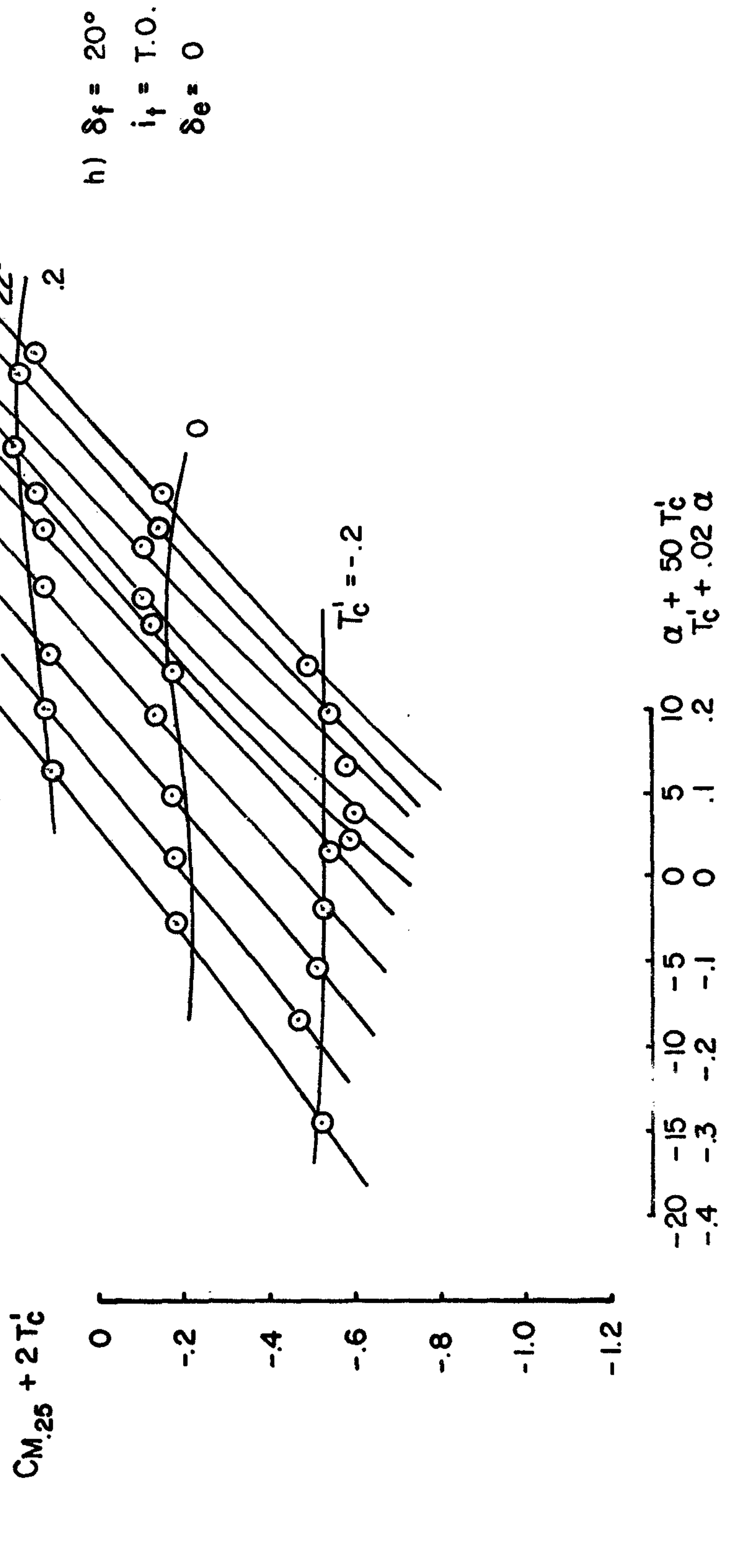

FIGURE 17 Continued

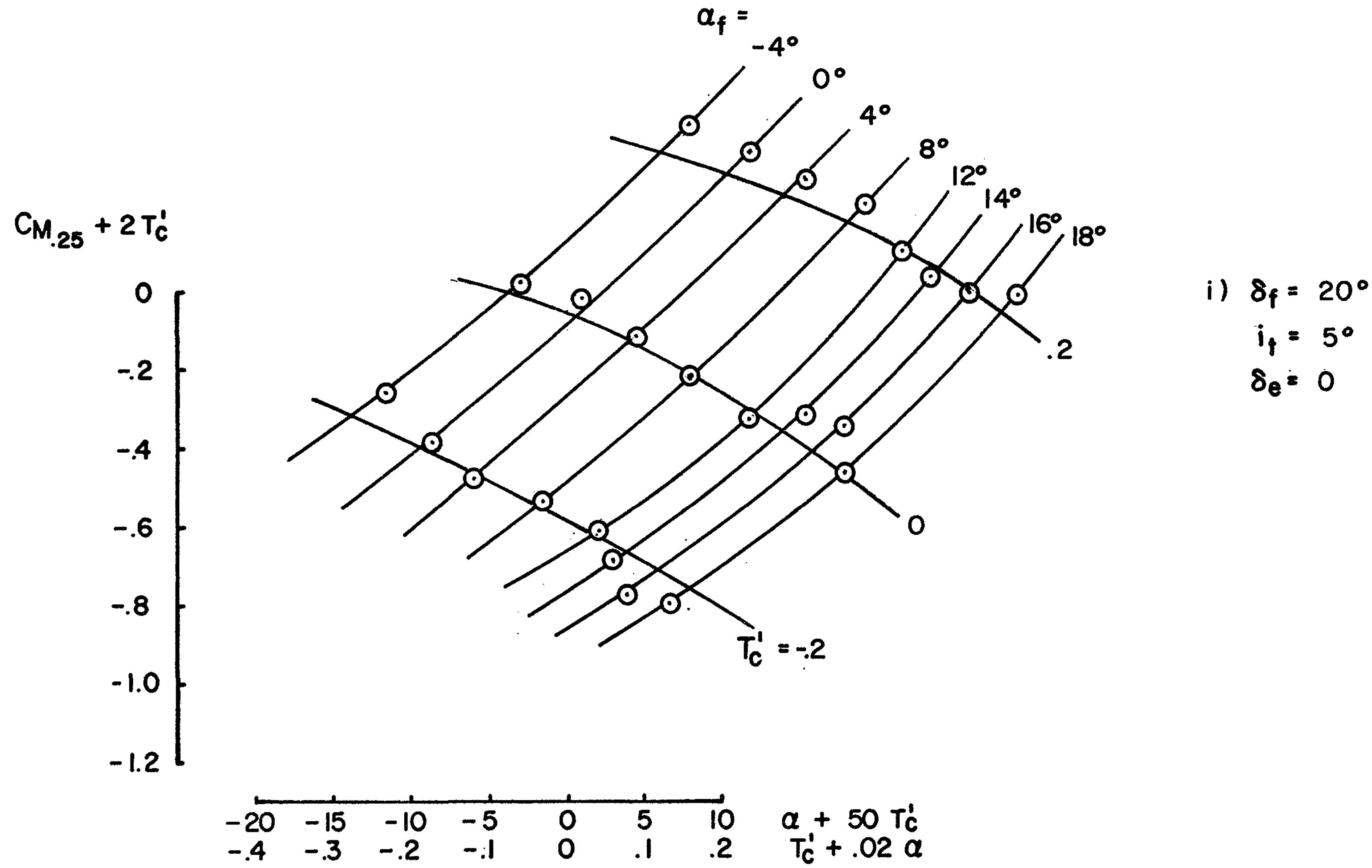

FIGURE 17 Continued

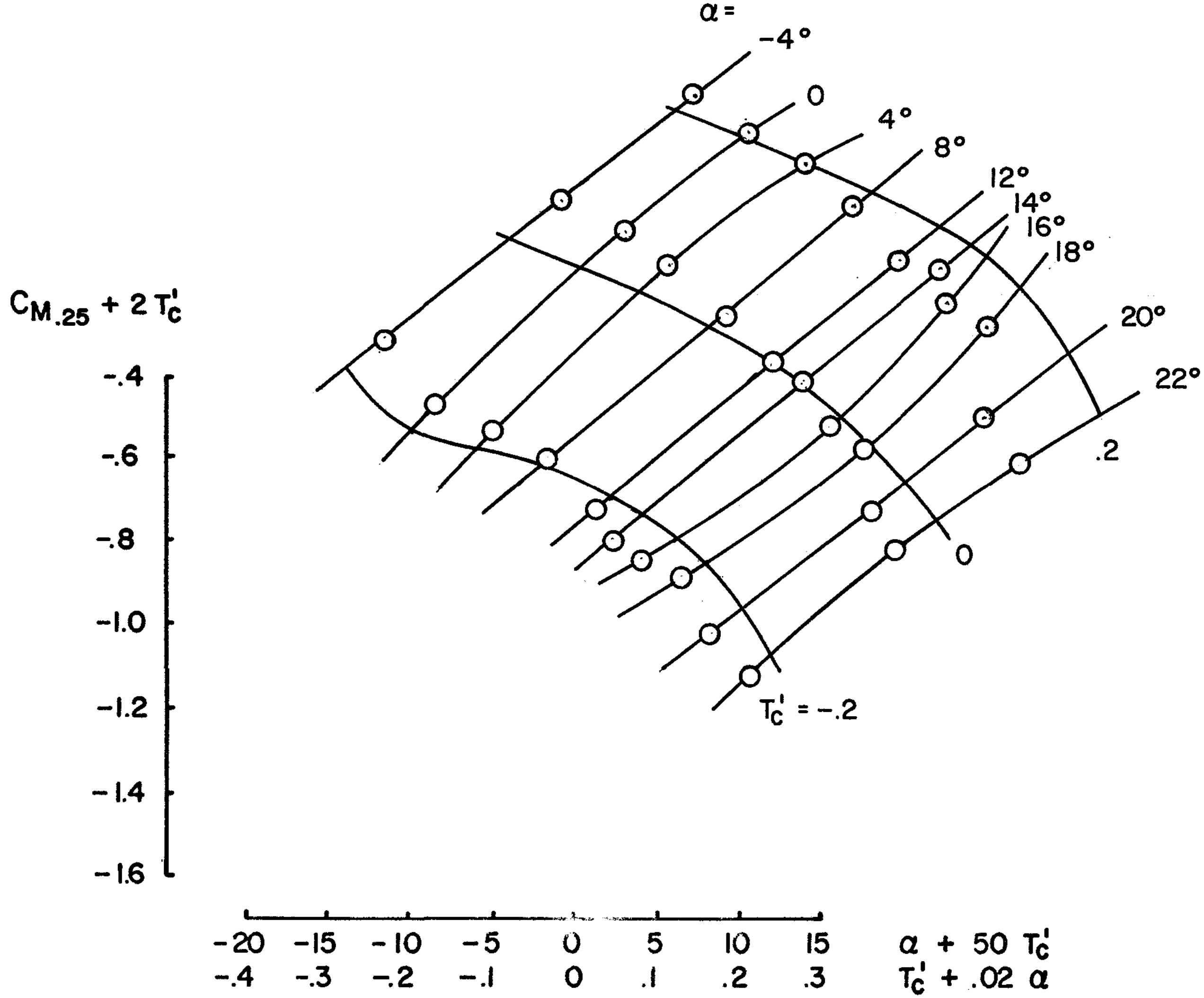

j) $\delta_f = 20°$

$i_t = -5°$

$\delta_e = 17.9°$

FIGURE 17 Continued

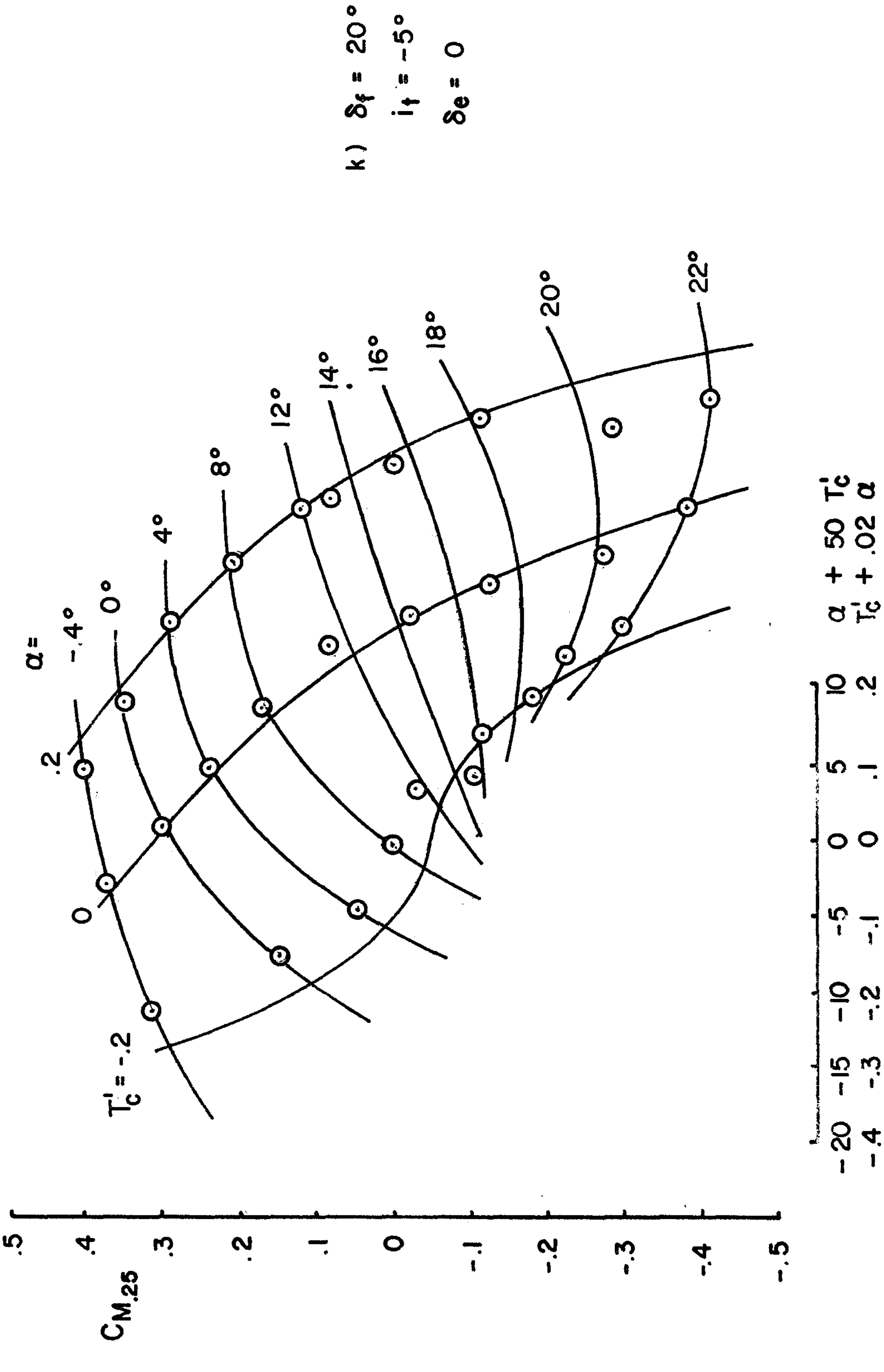

FIGURE 17 Continued

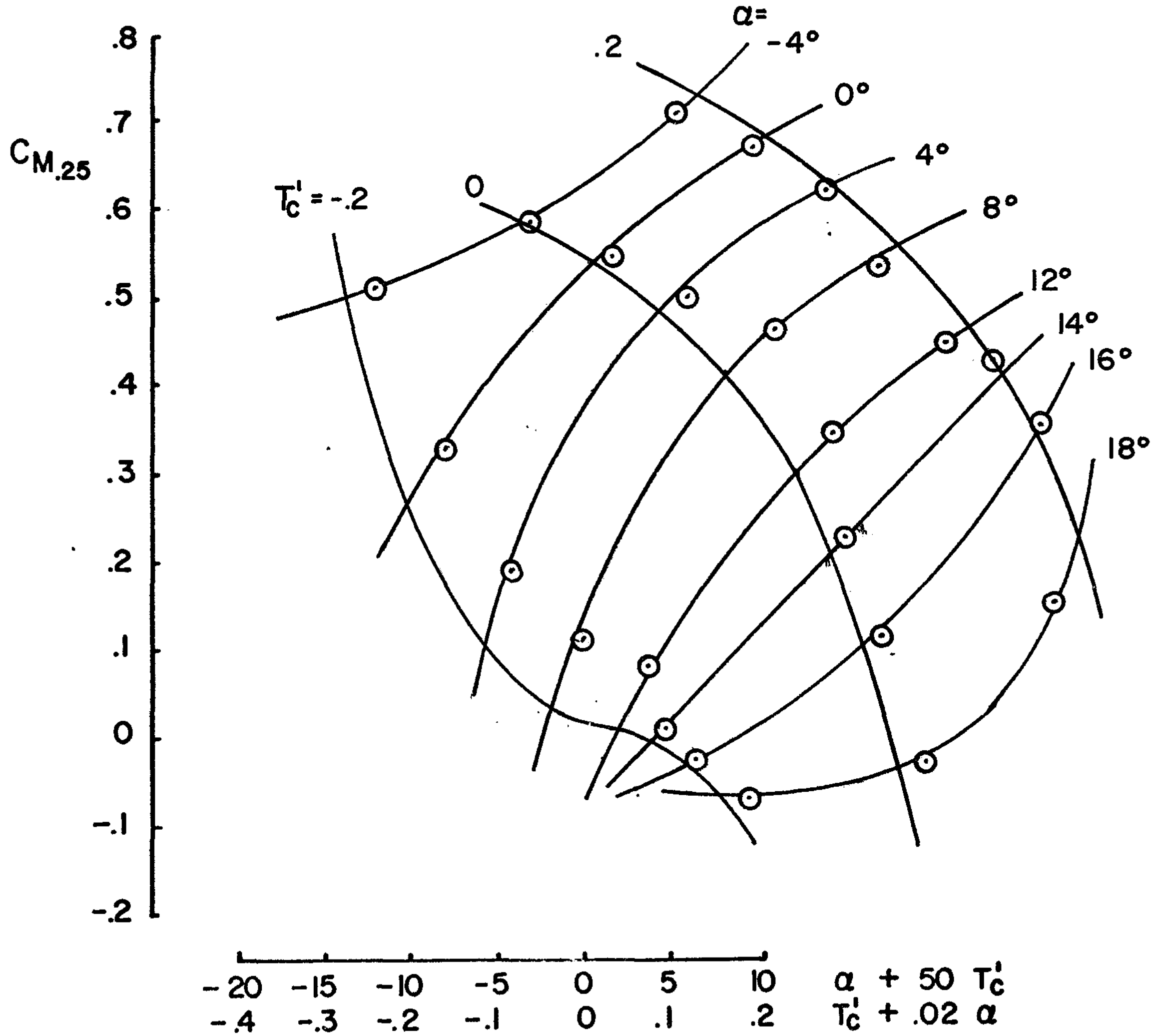

FIGURE 17 Continued

1) $\delta_f = 20°$
$i_t = -5°$
$\delta_e = -10°$

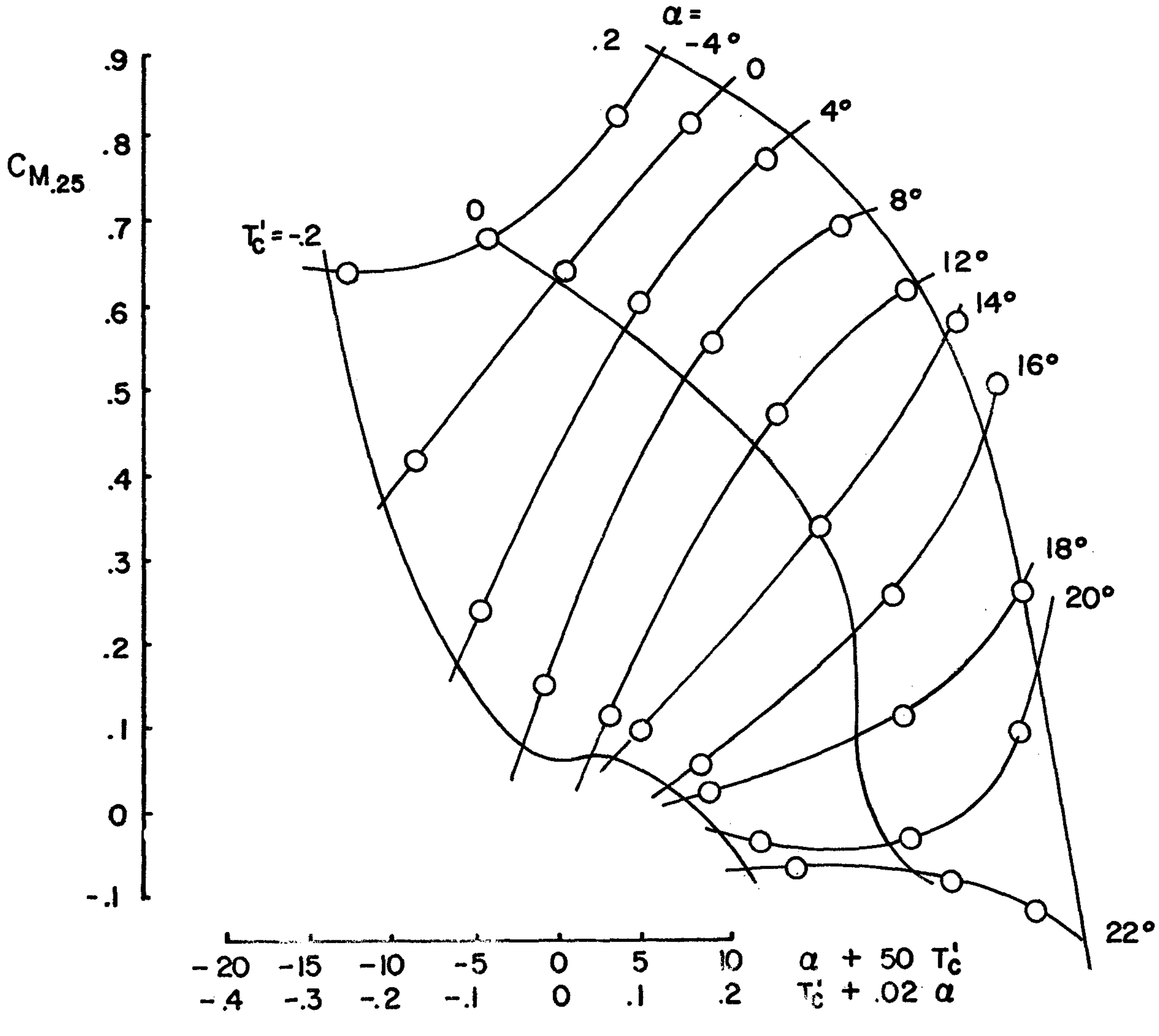

FIGURE 17 Continued

m) $\delta_f = 20°$

$i_t = -5°$

$\delta_e = -17°$

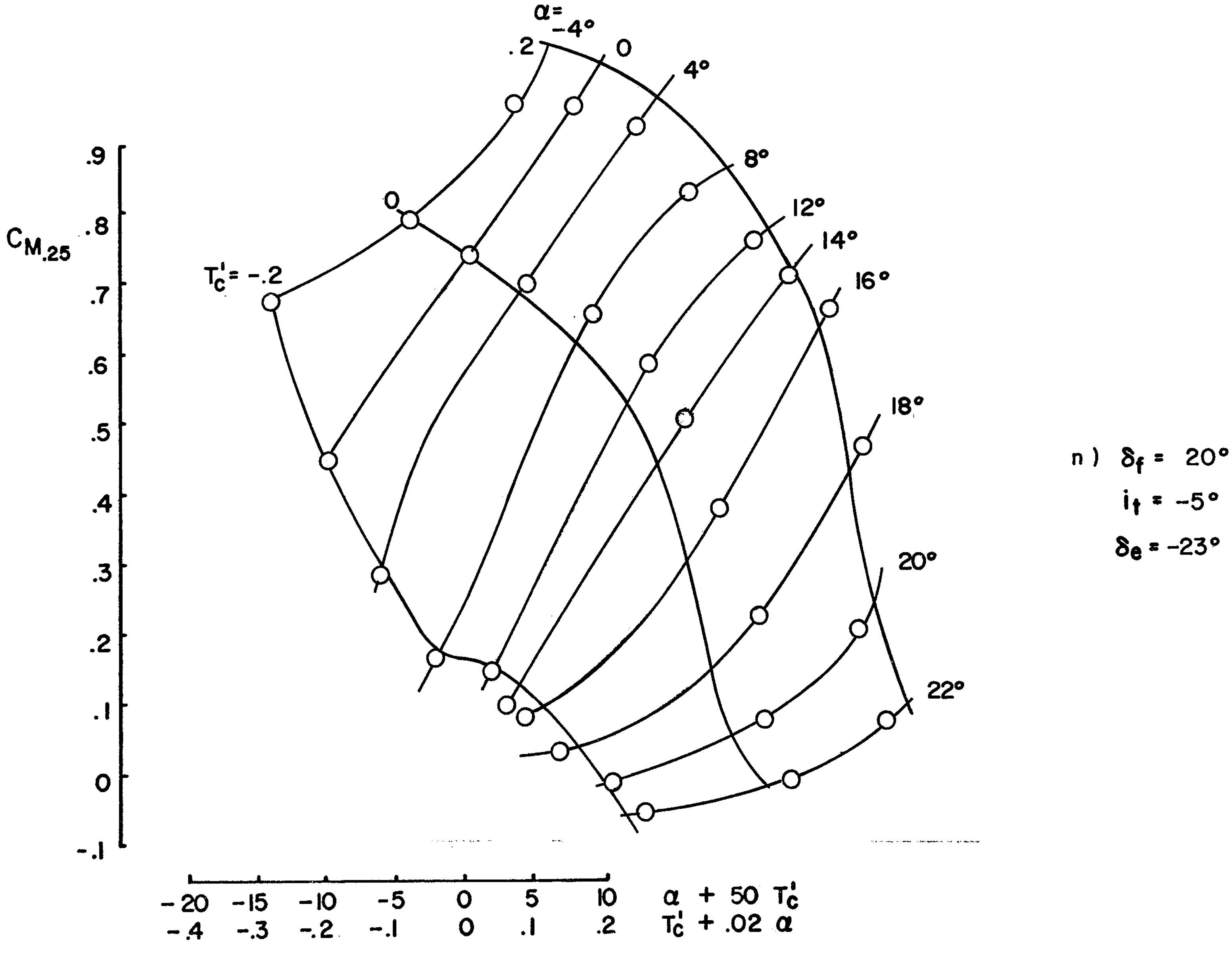

FIGURE 17 Continued

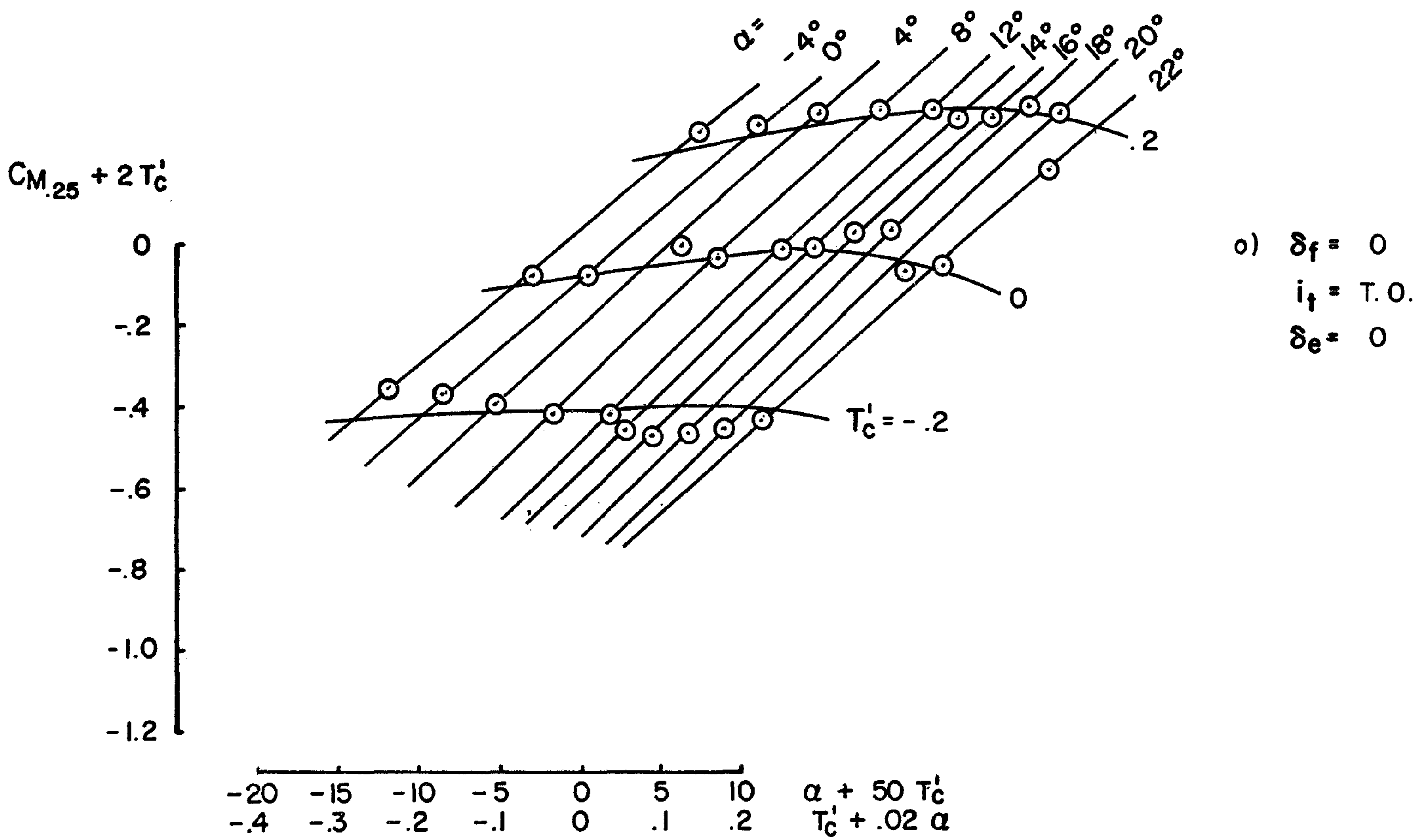

FIGURE 17 Continued

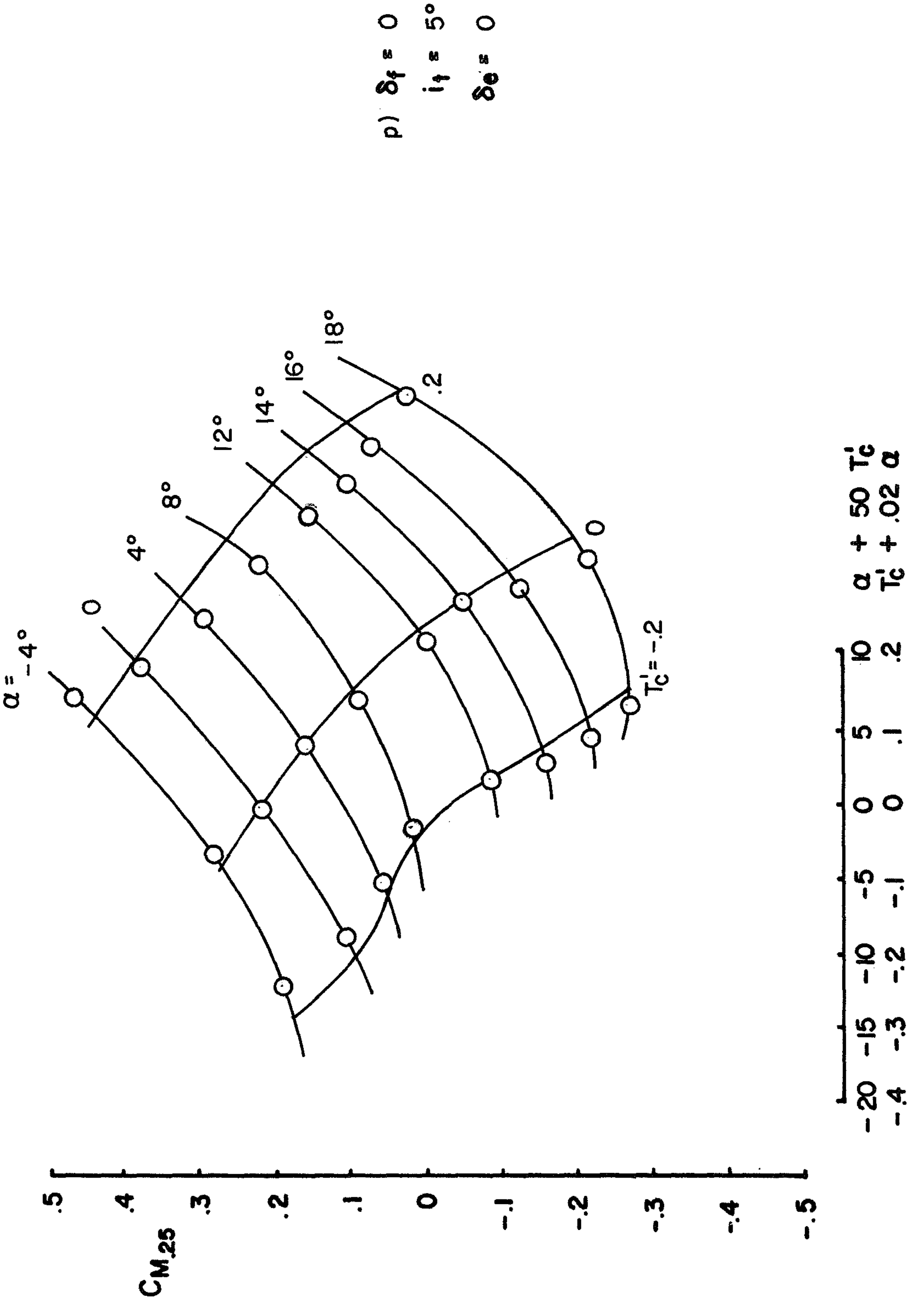

FIGURE 17 Continued

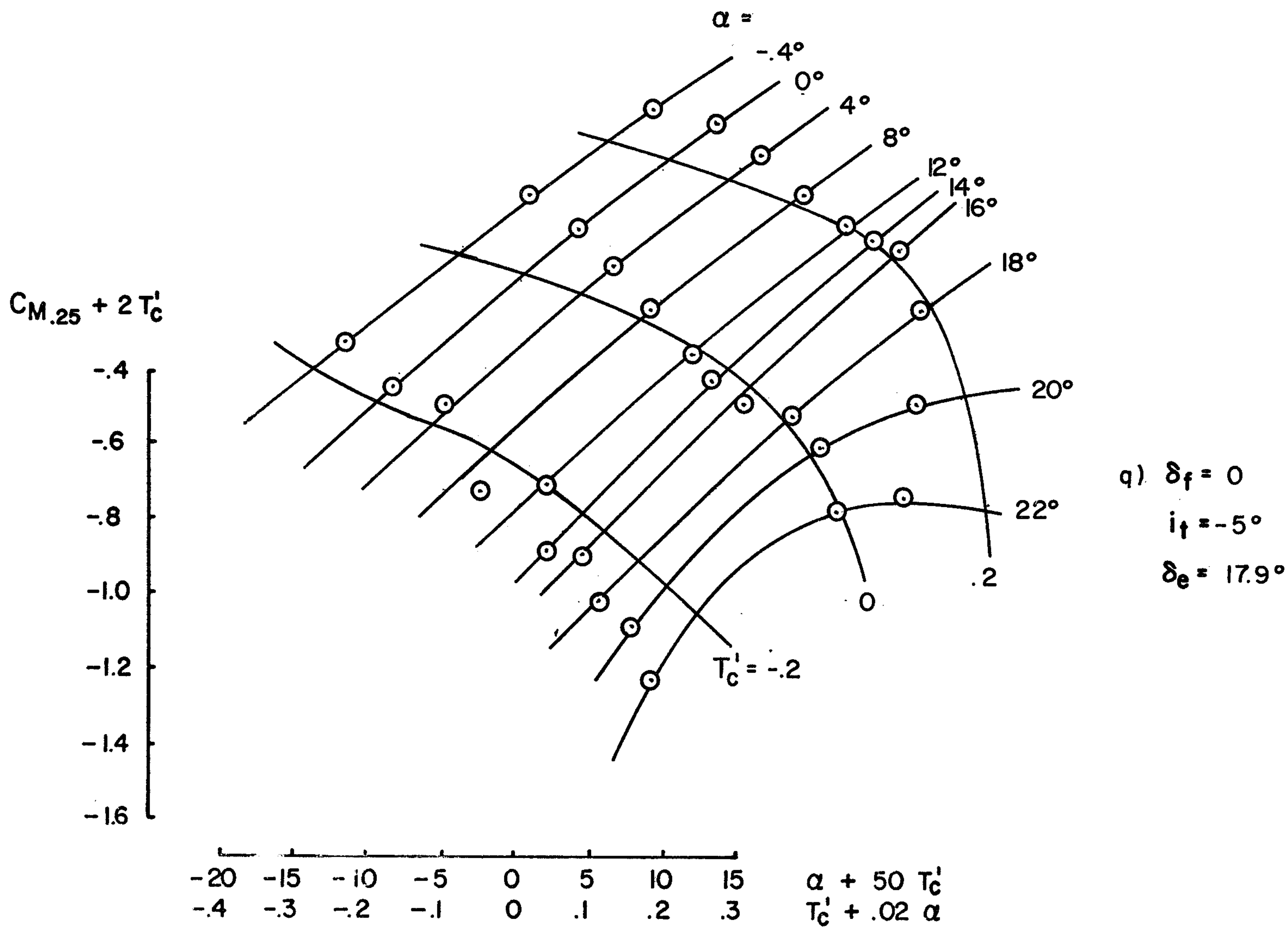

FIGURE 17 Continued

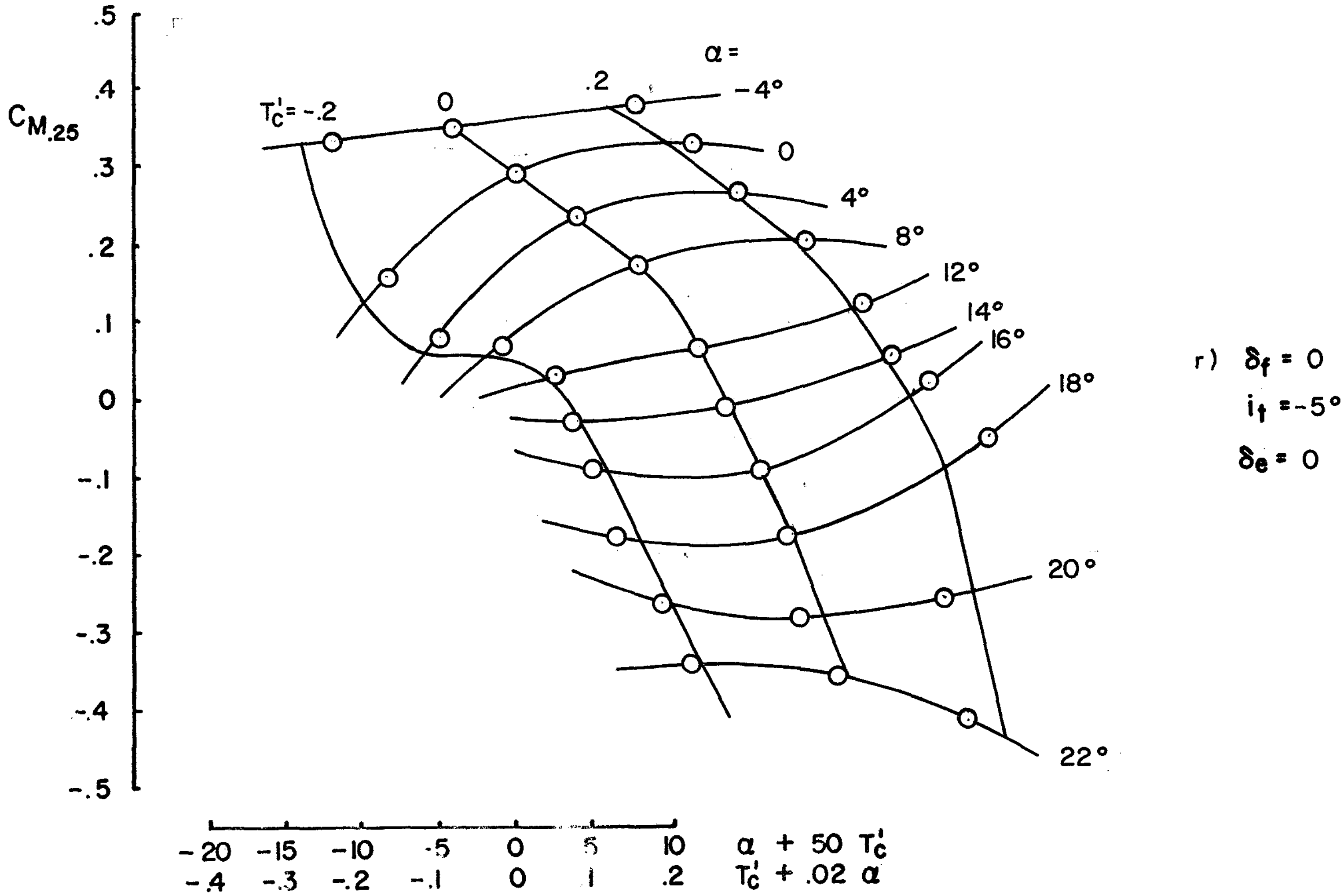

FIGURE 17 Continued

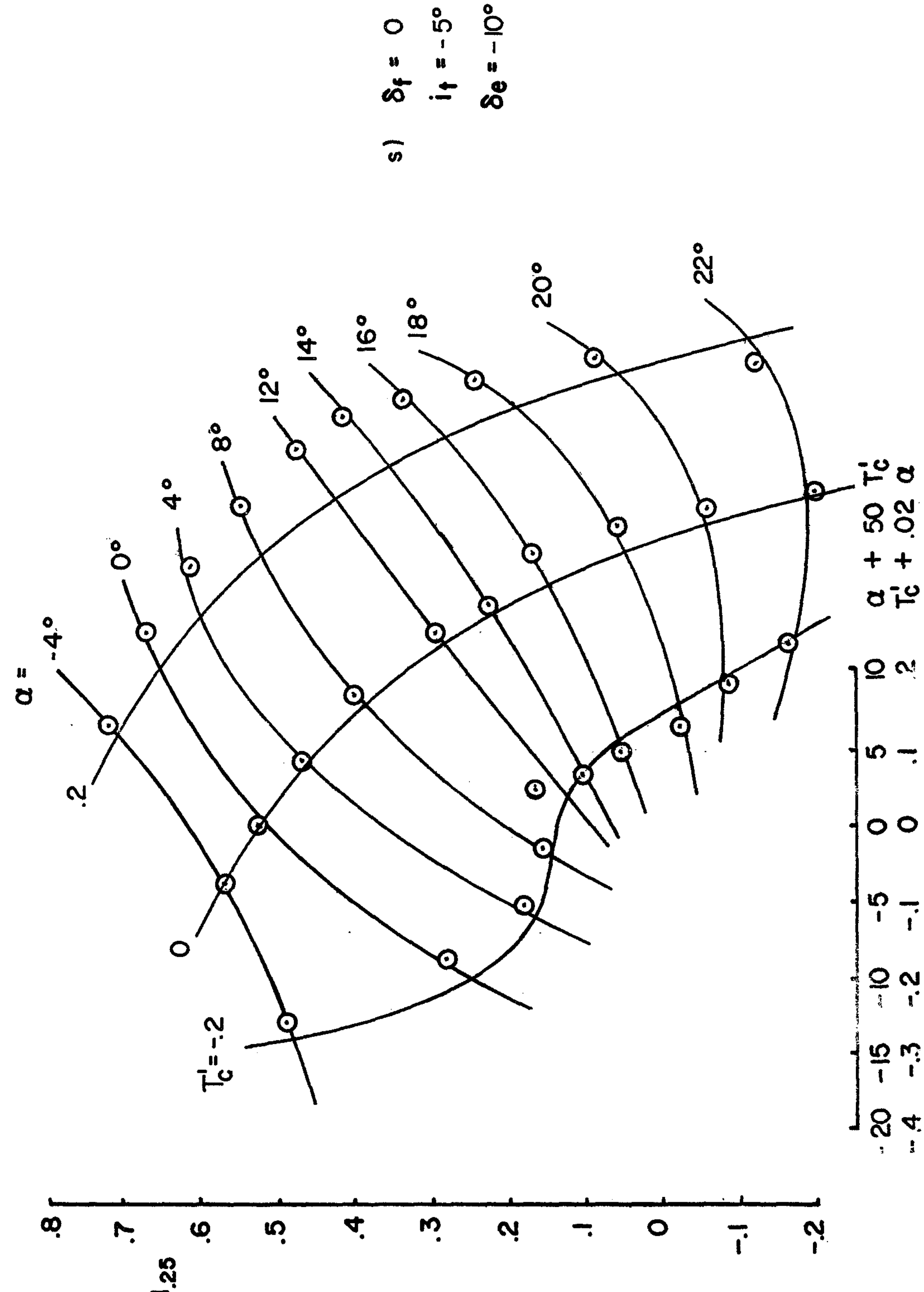

FIGURE 17 Continued

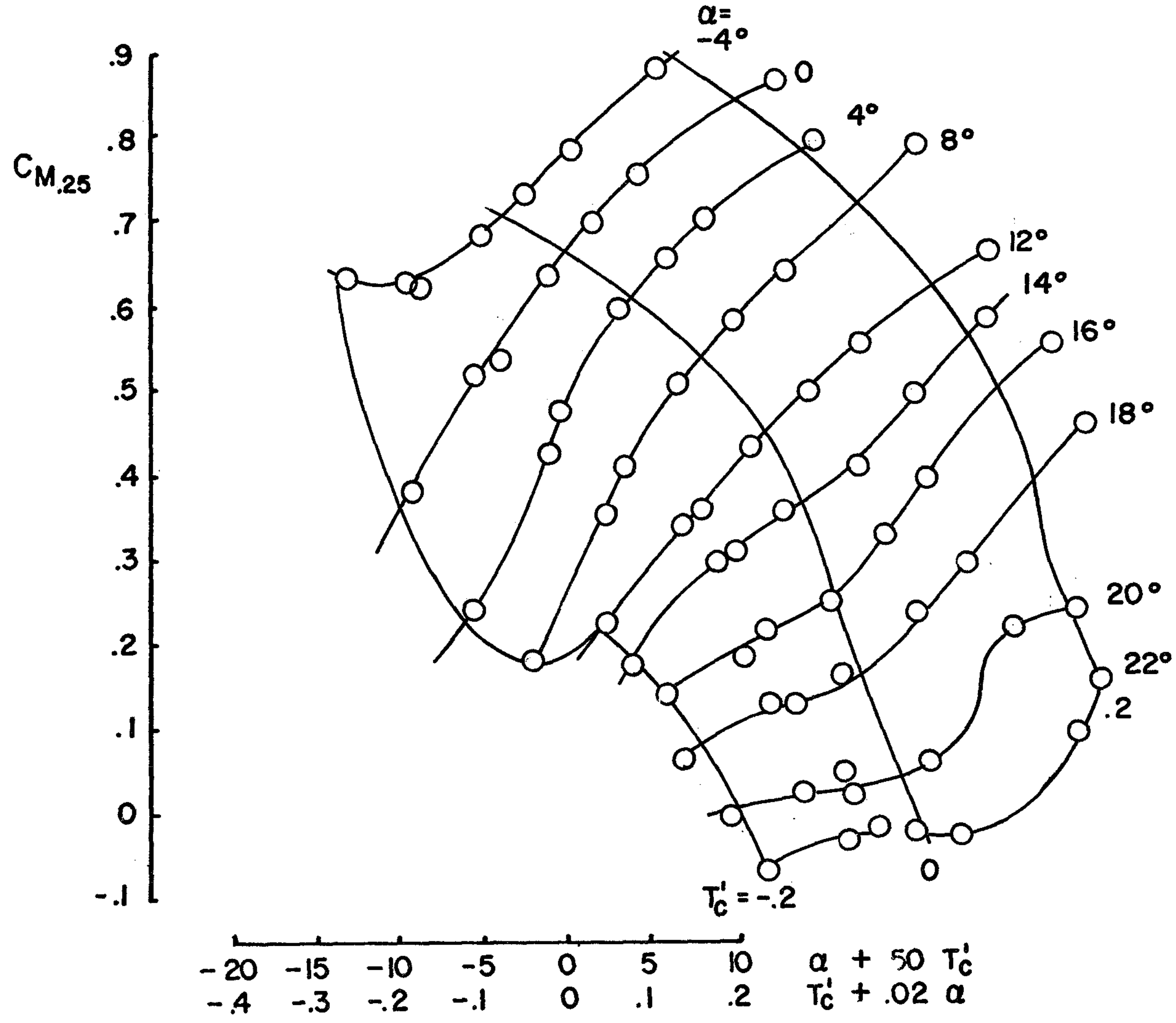

t) $\delta_f = 0$

$i_t = -5°$

$\delta_e = -17°$

FIGURE 17 Continued

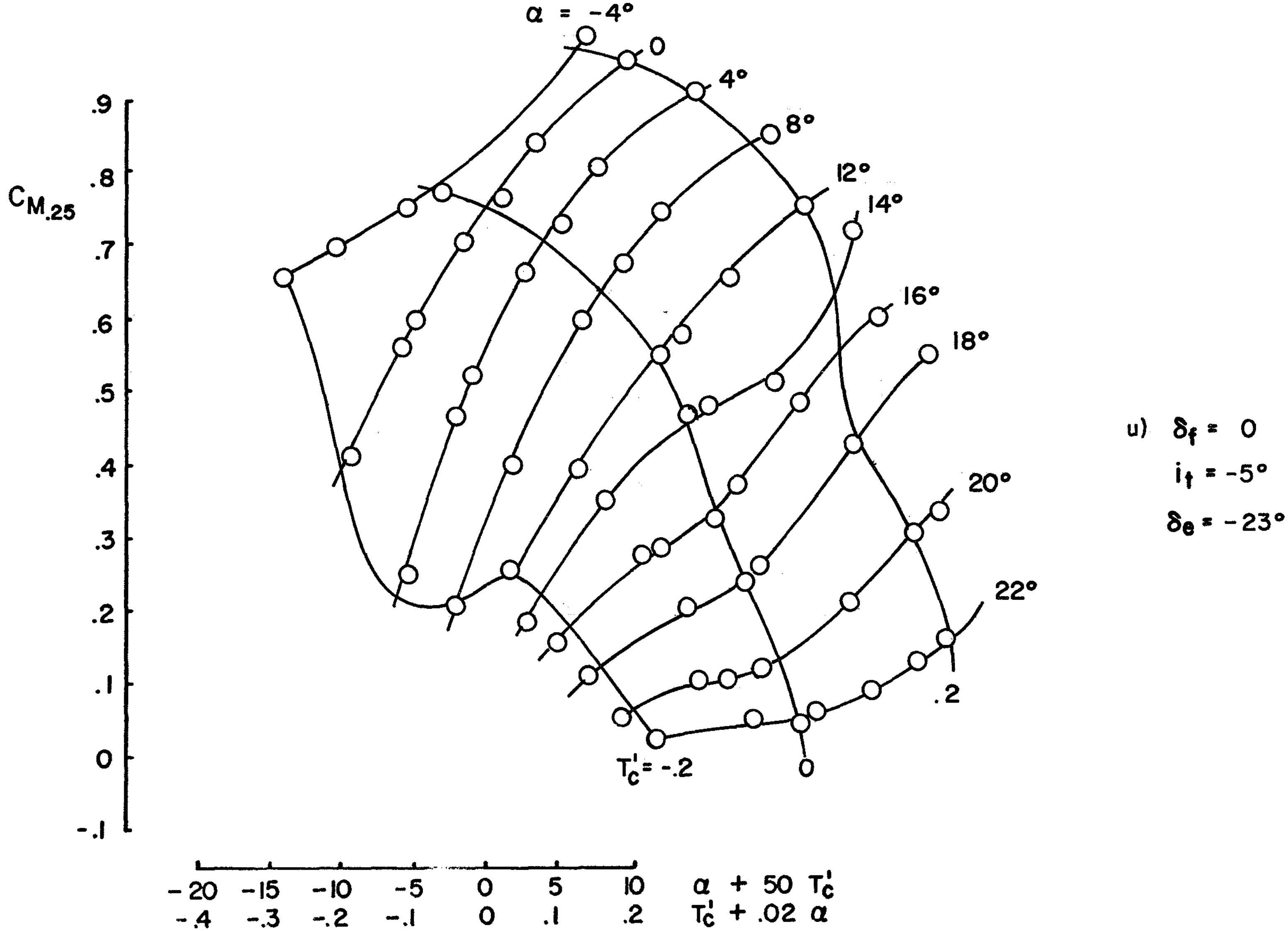

FIGURE 17 Continued

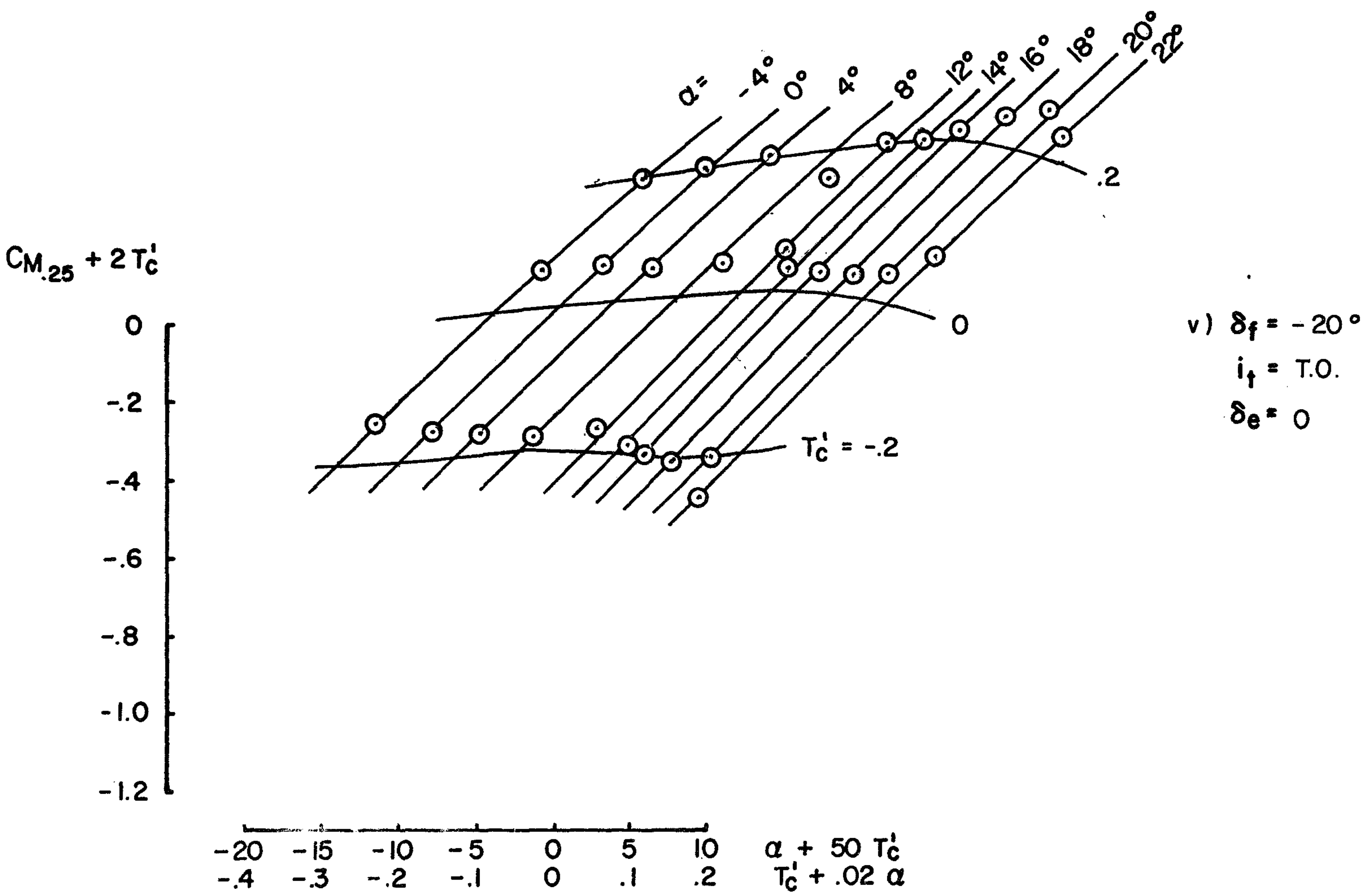

FIGURE 17 Continued

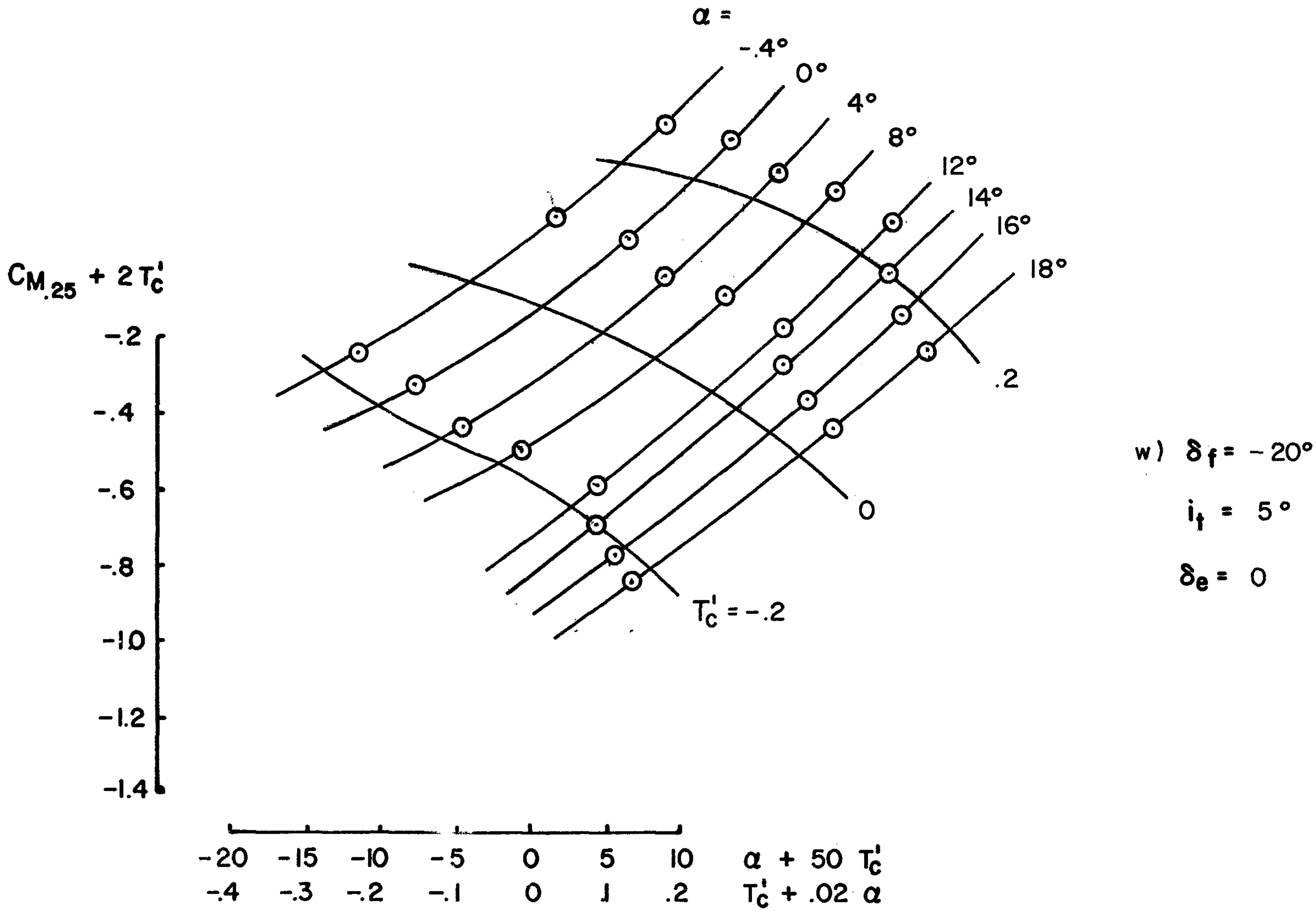

FIGURE 17 Continued

x) $\delta_f = -20°$

$i_t = -5°$

$\delta_e = 17.9°$

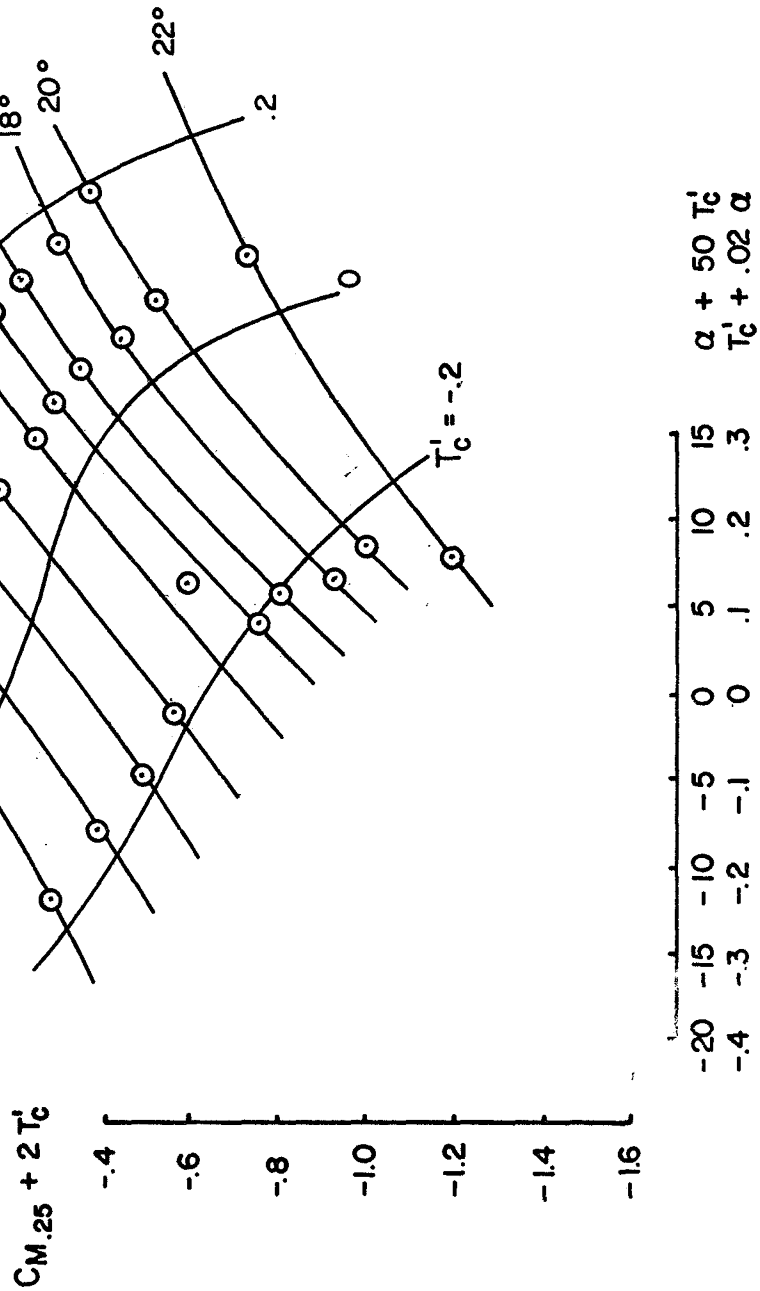

FIGURE 17 Continued

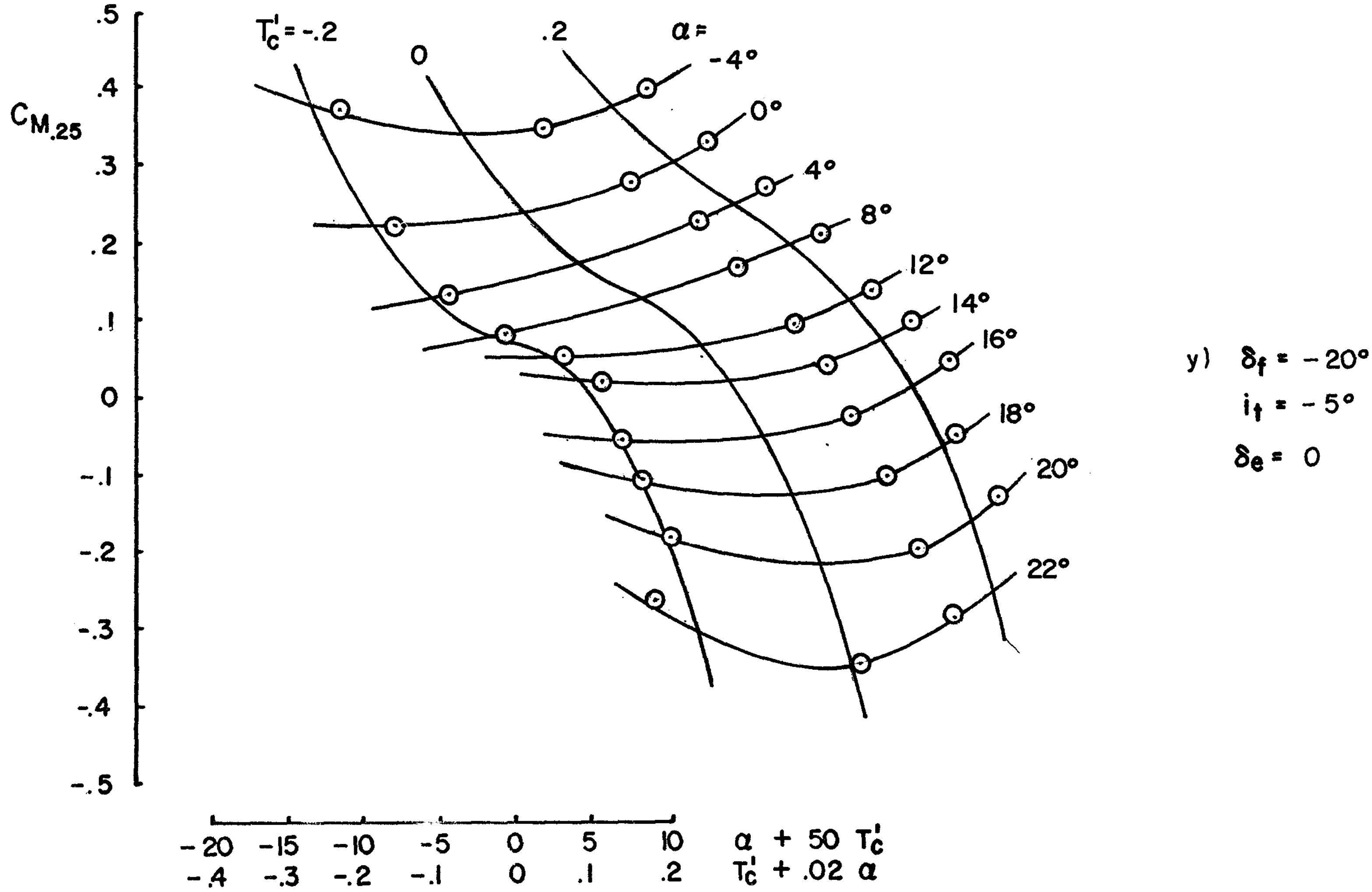

FIGURE 17 Continued

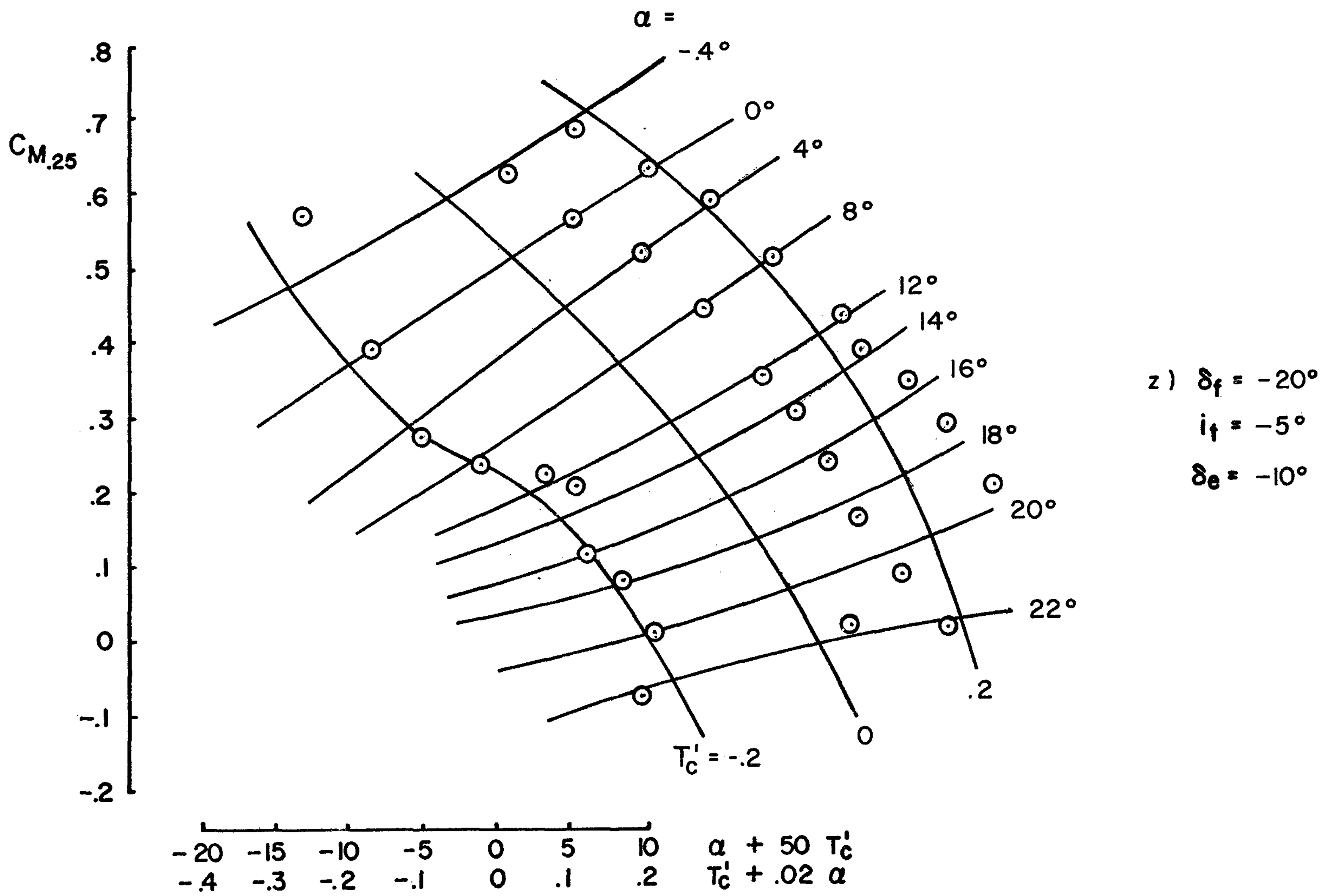

FIGURE 17 Continued

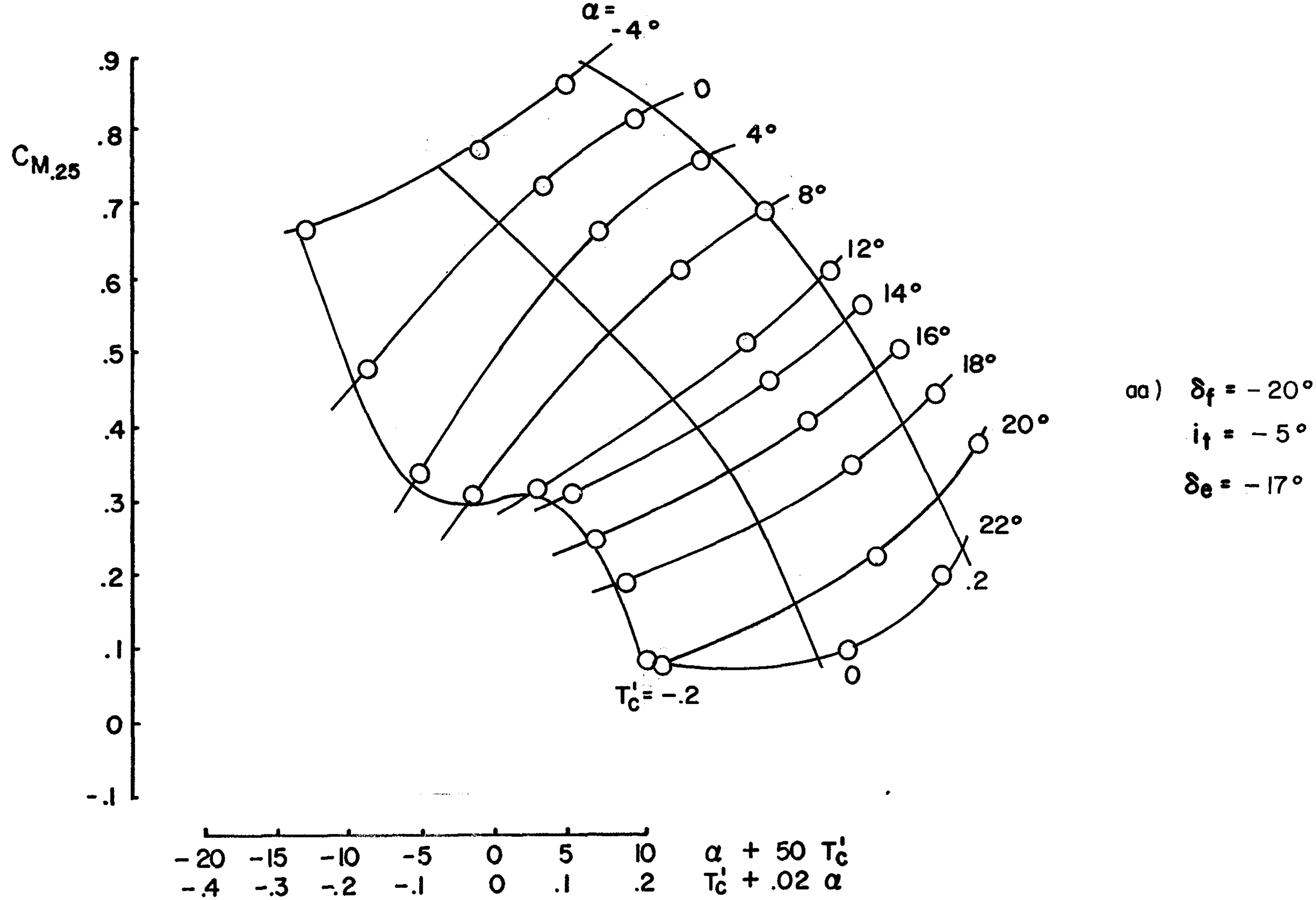

FIGURE 17 Continued

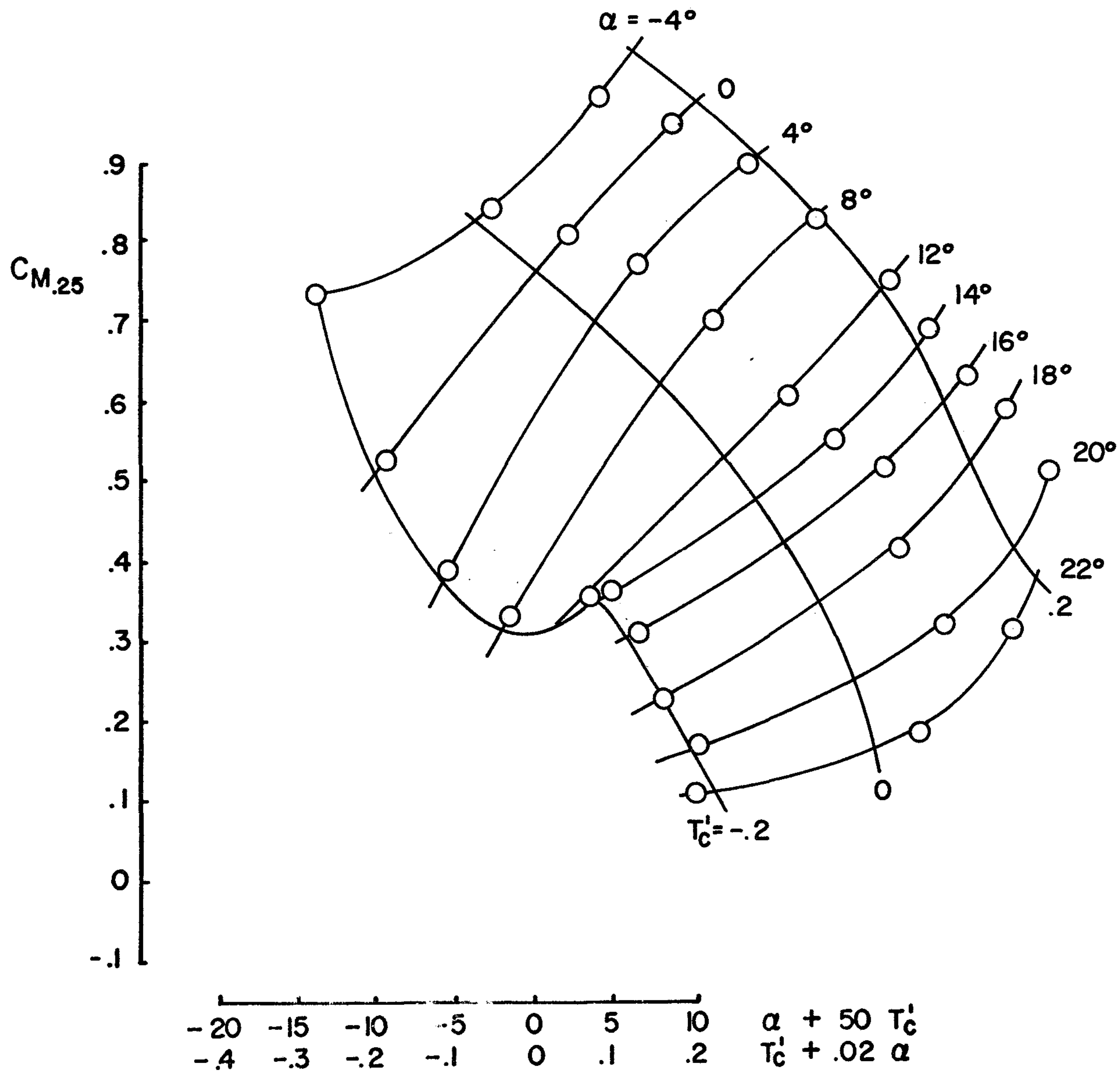

bb) $\delta_f = -20°$
$i_t = -5°$
$\delta_e = -23°$

FIGURE 17 Continued

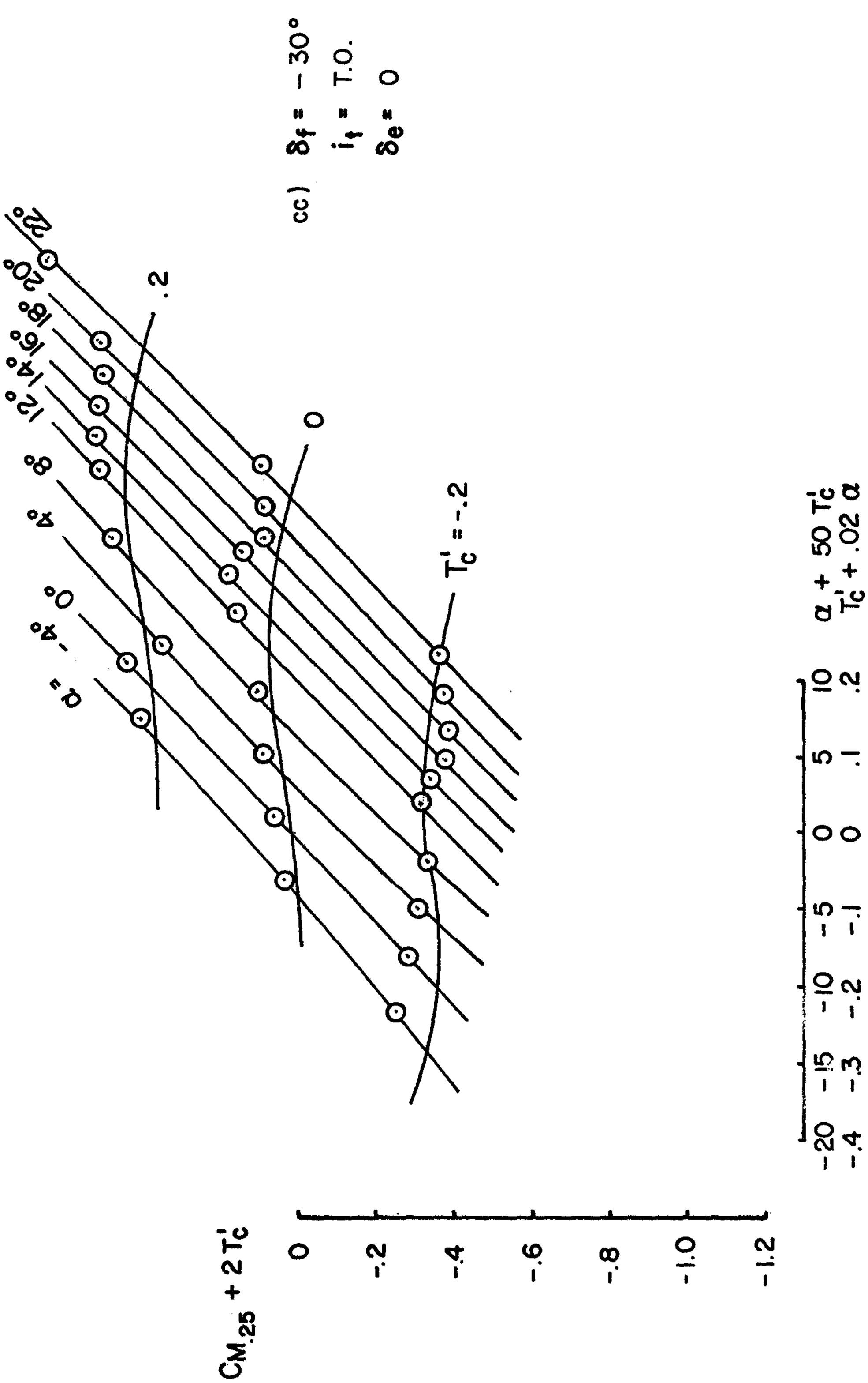

FIGURE 17 Continued

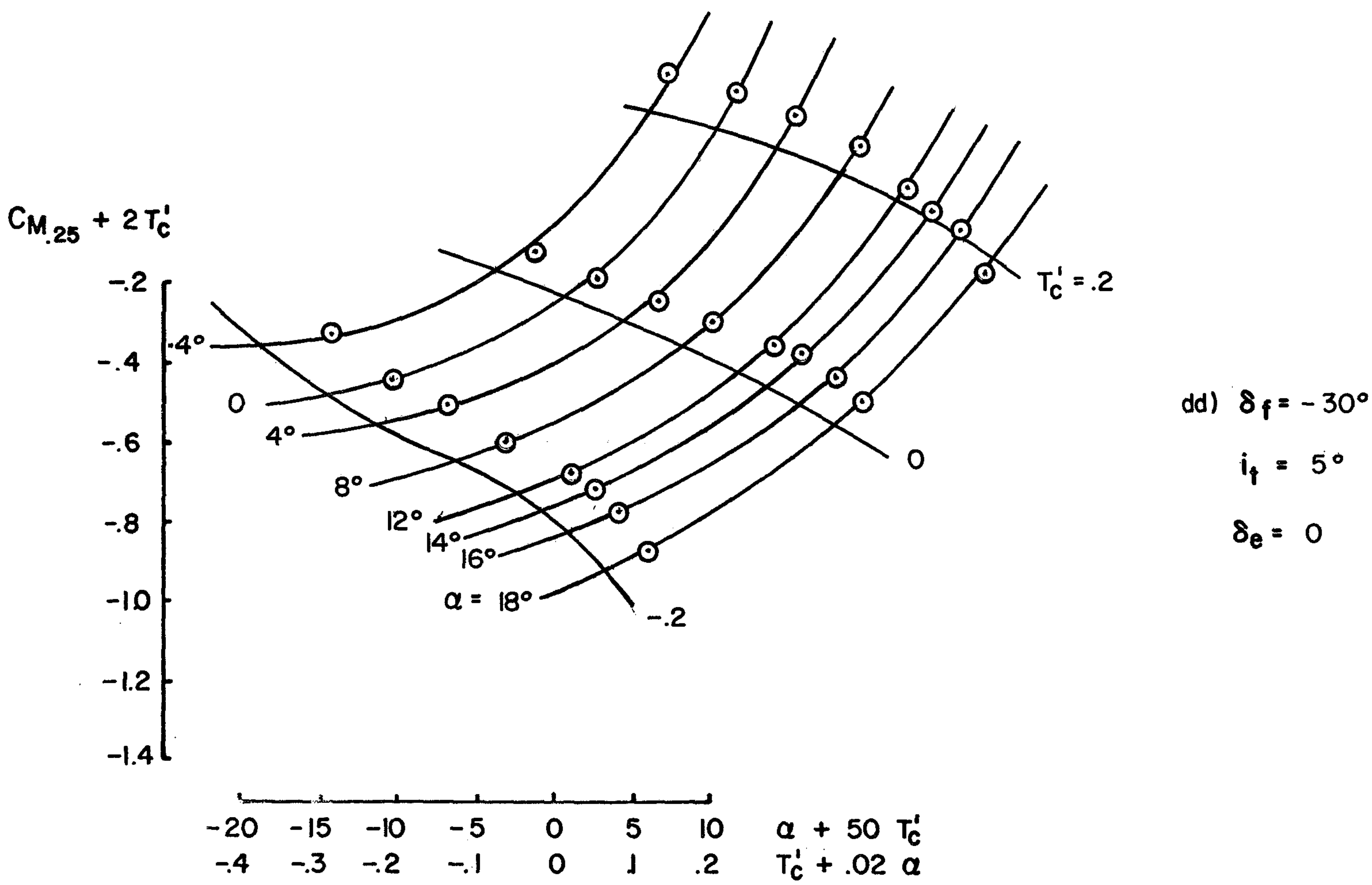

FIGURE 17 Continued

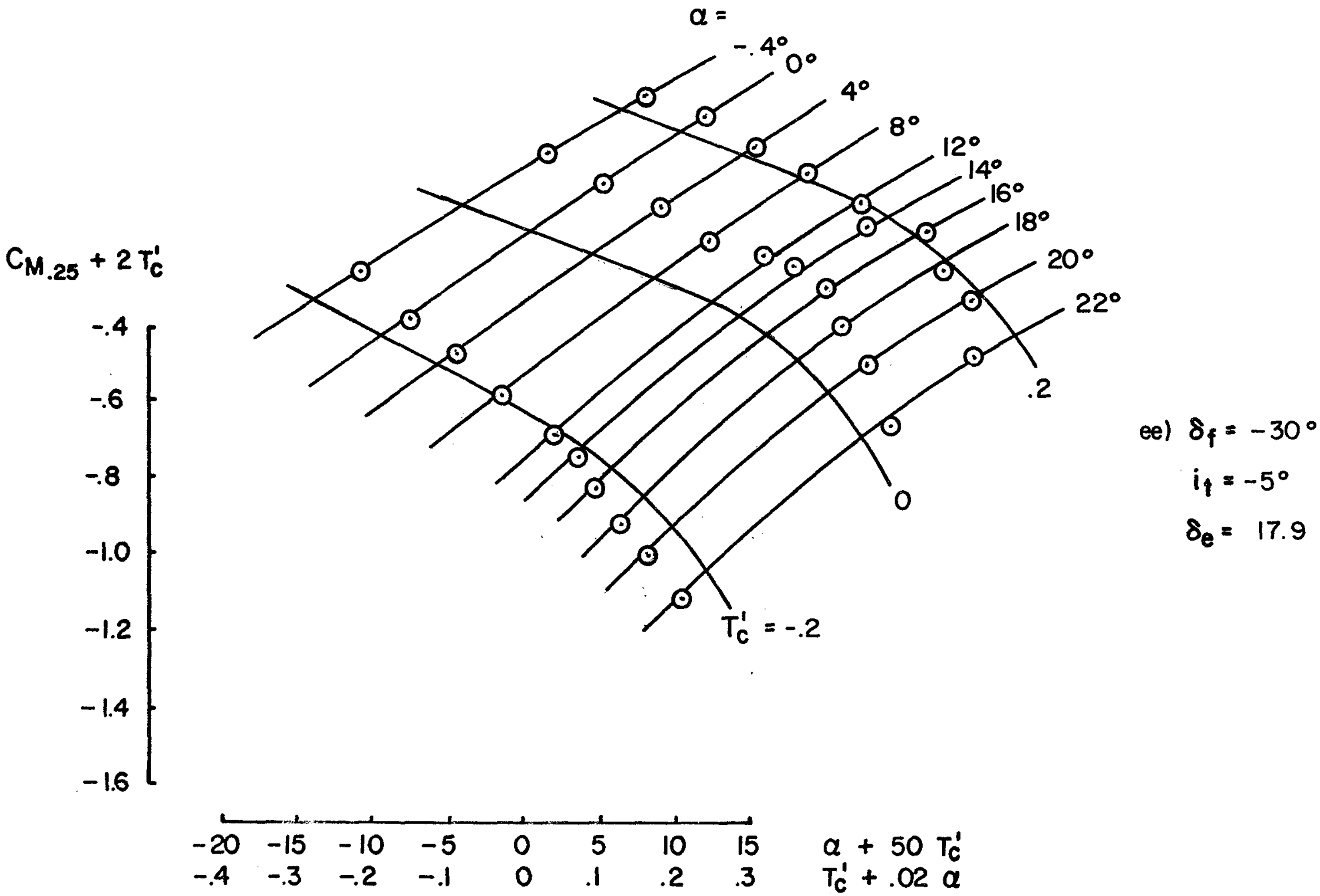

FIGURE 17 Continued

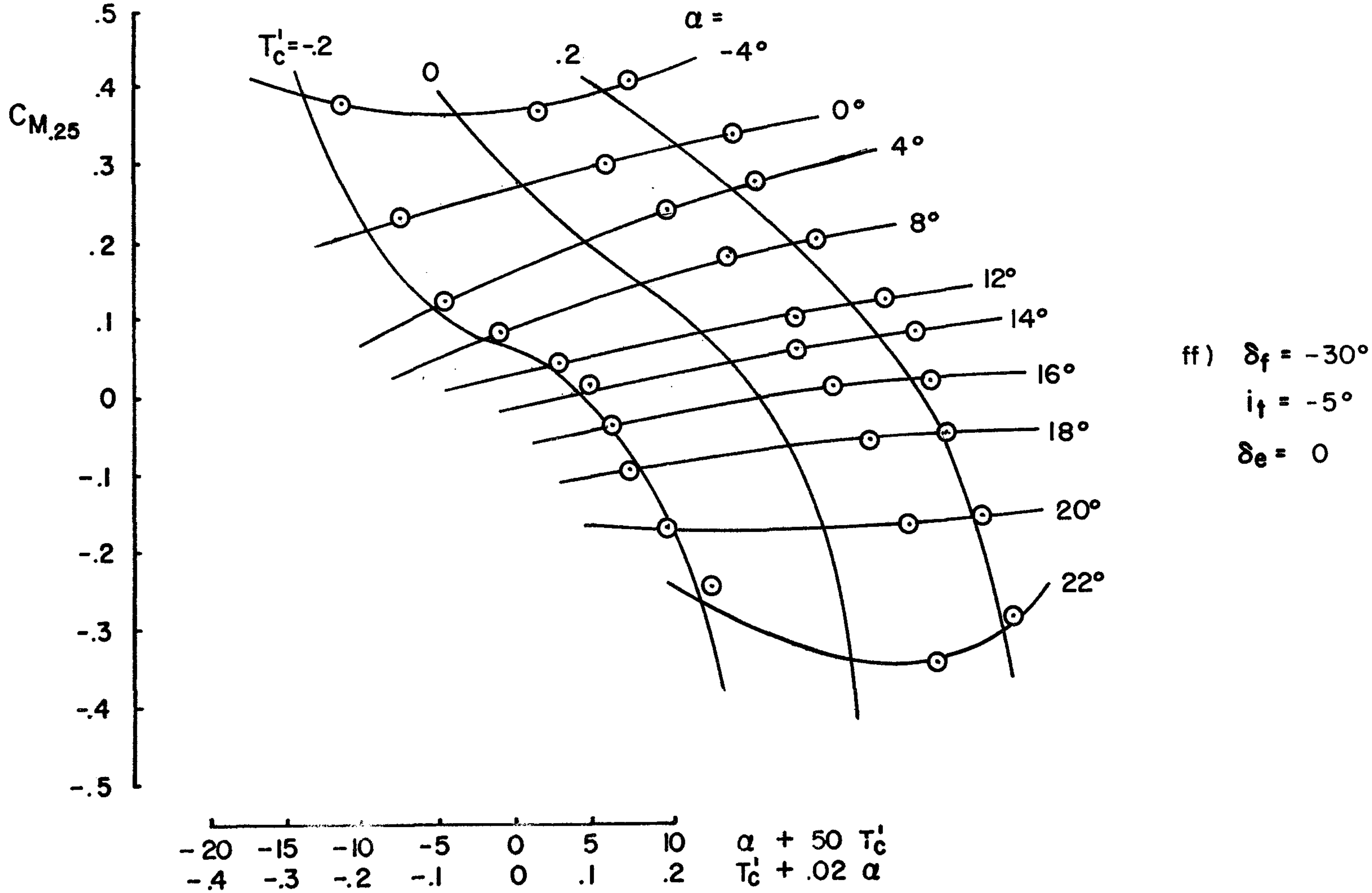

FIGURE 17 Continued

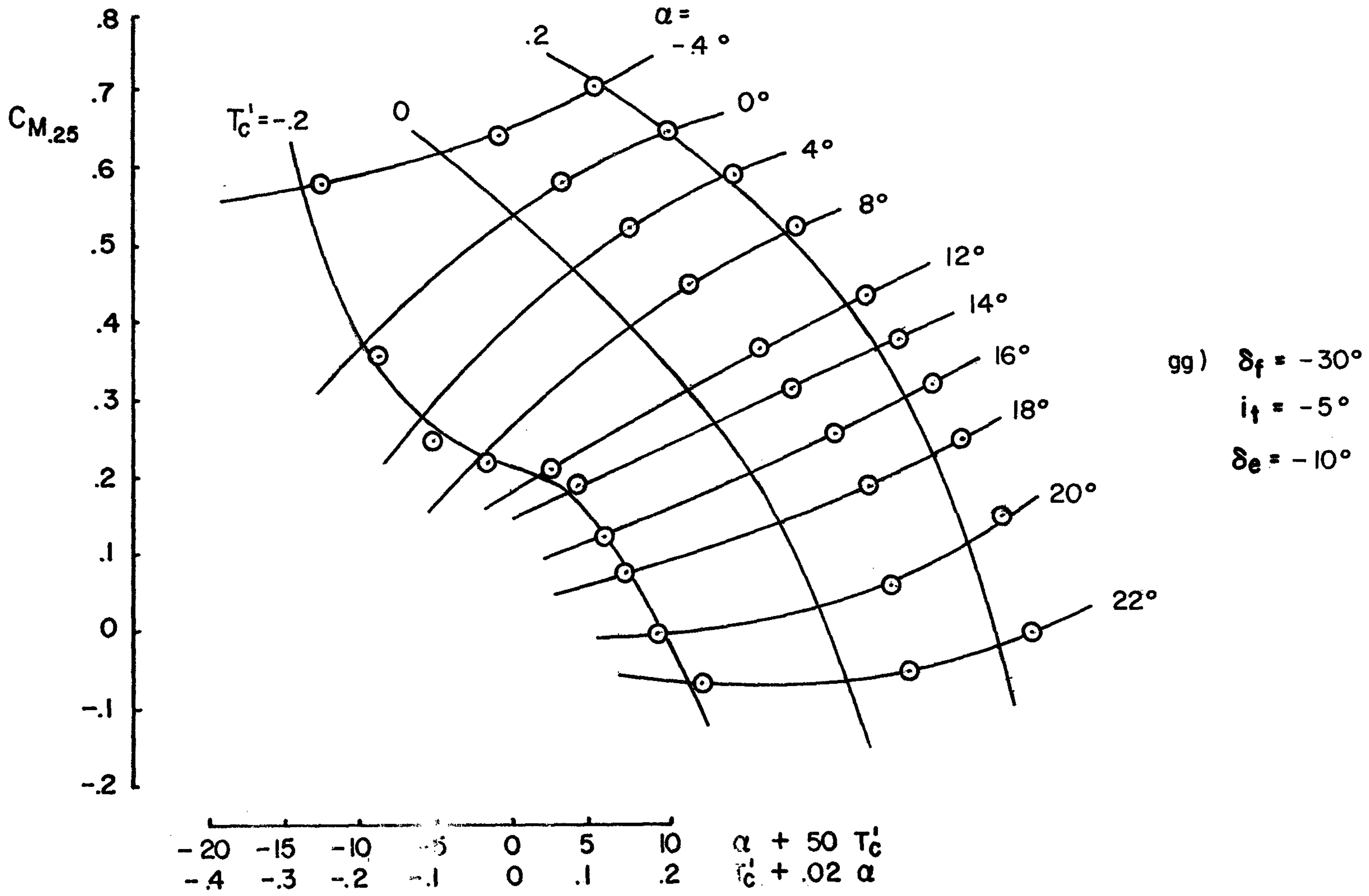

FIGURE 17 Continued

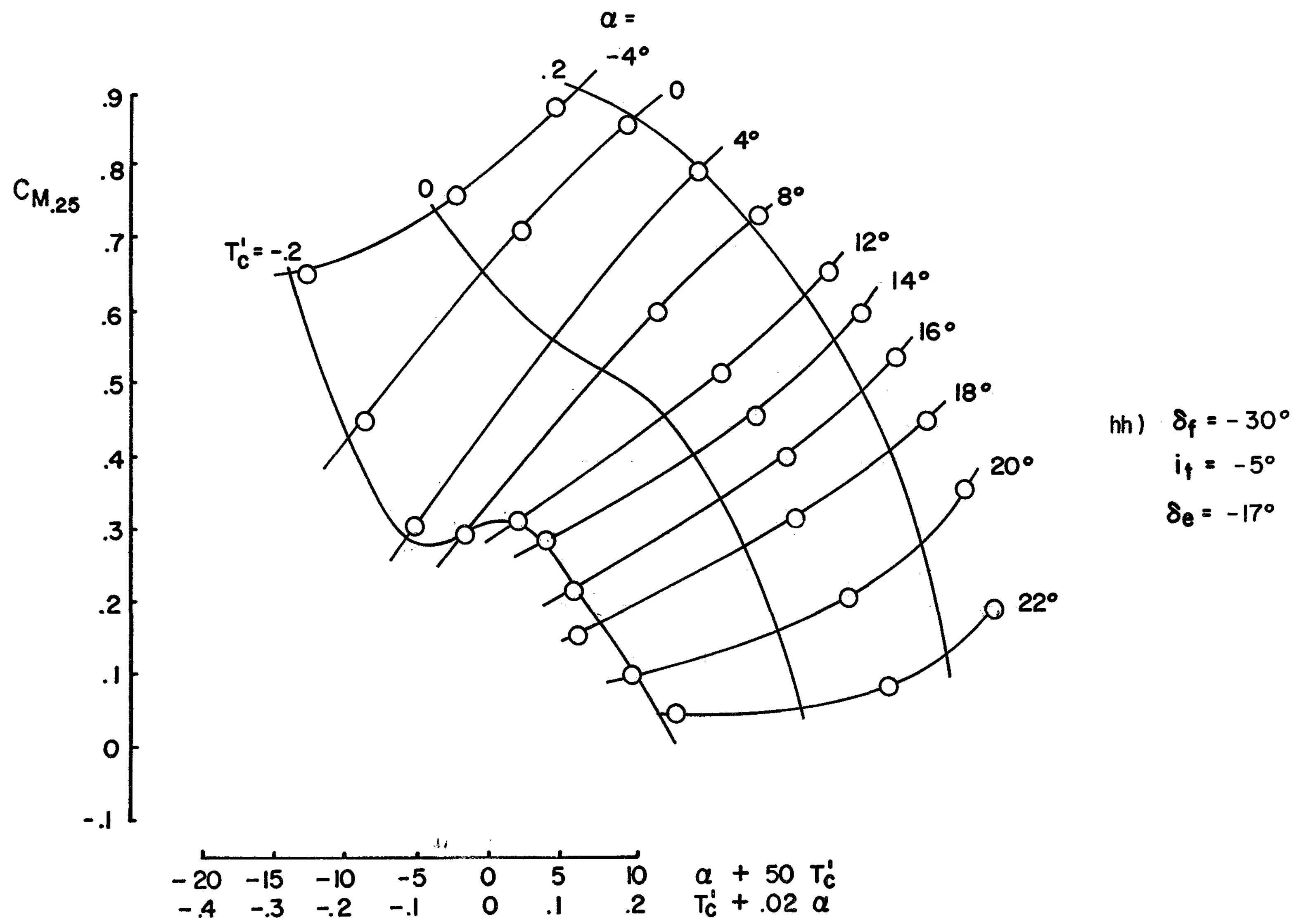

FIGURE 17 Continued

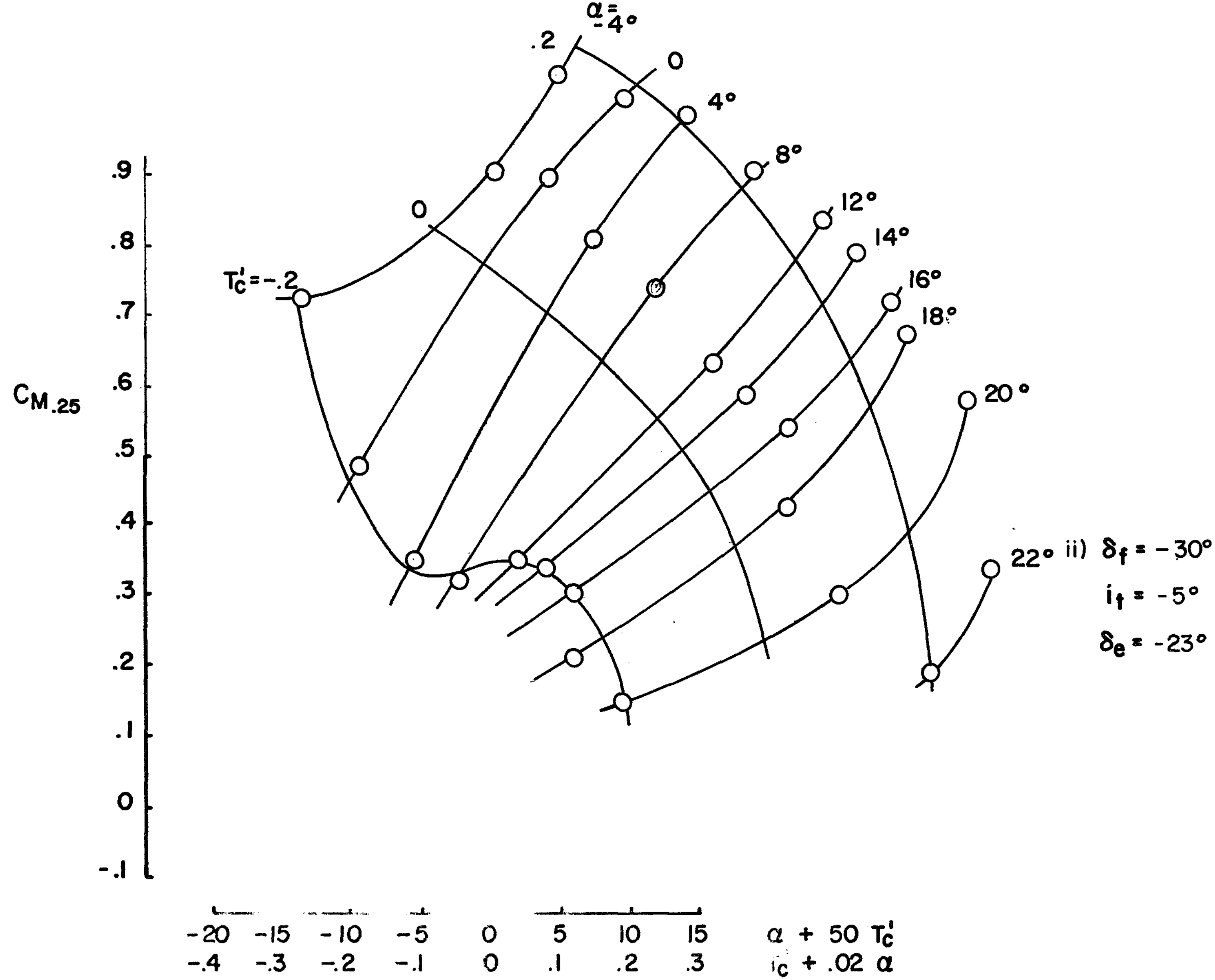

FIGURE 17 Concluded

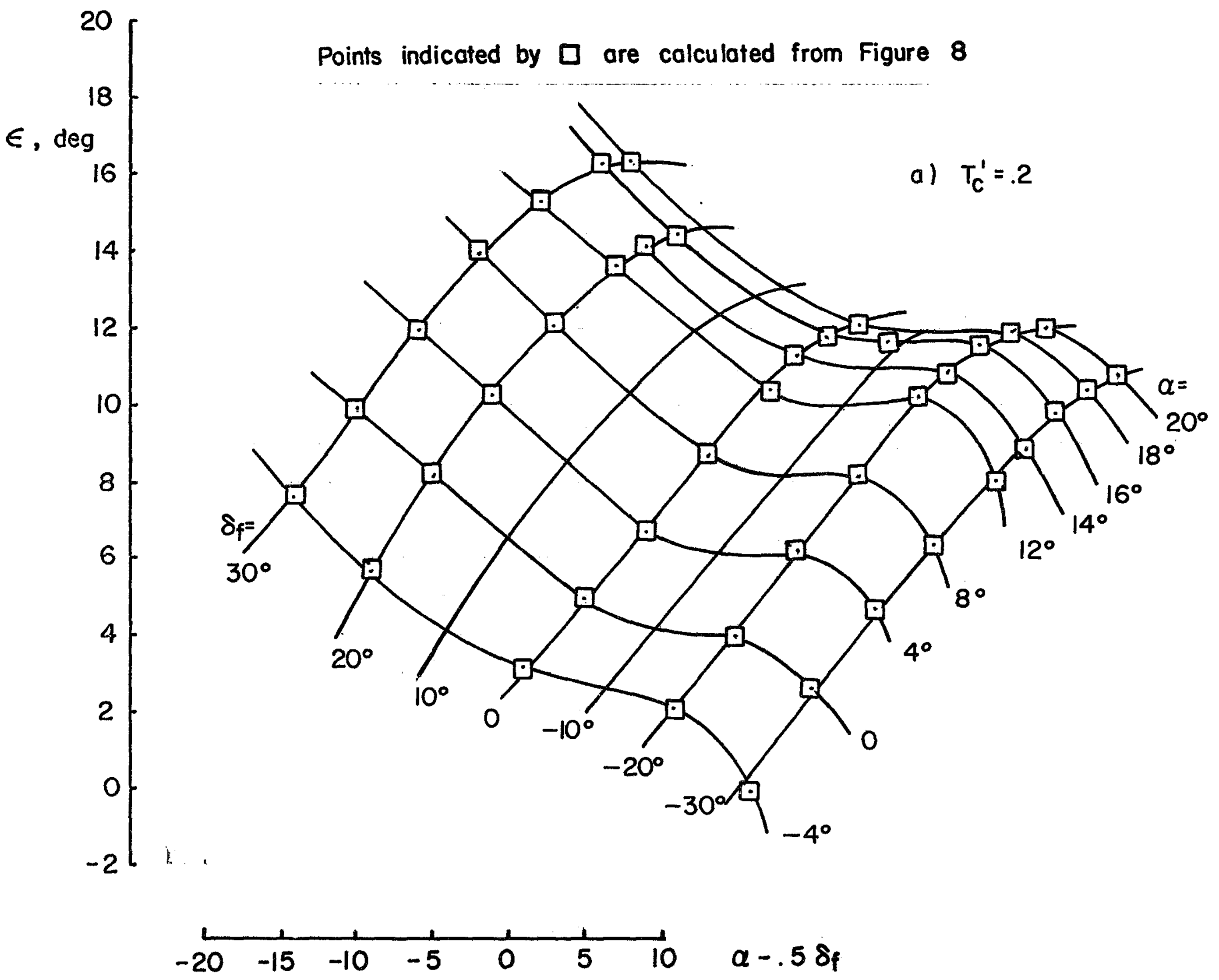

FIGURE 18 VARIATION OF DOWNWASH WITH ANGLE OF ATTACK AND FLAP ANGLE

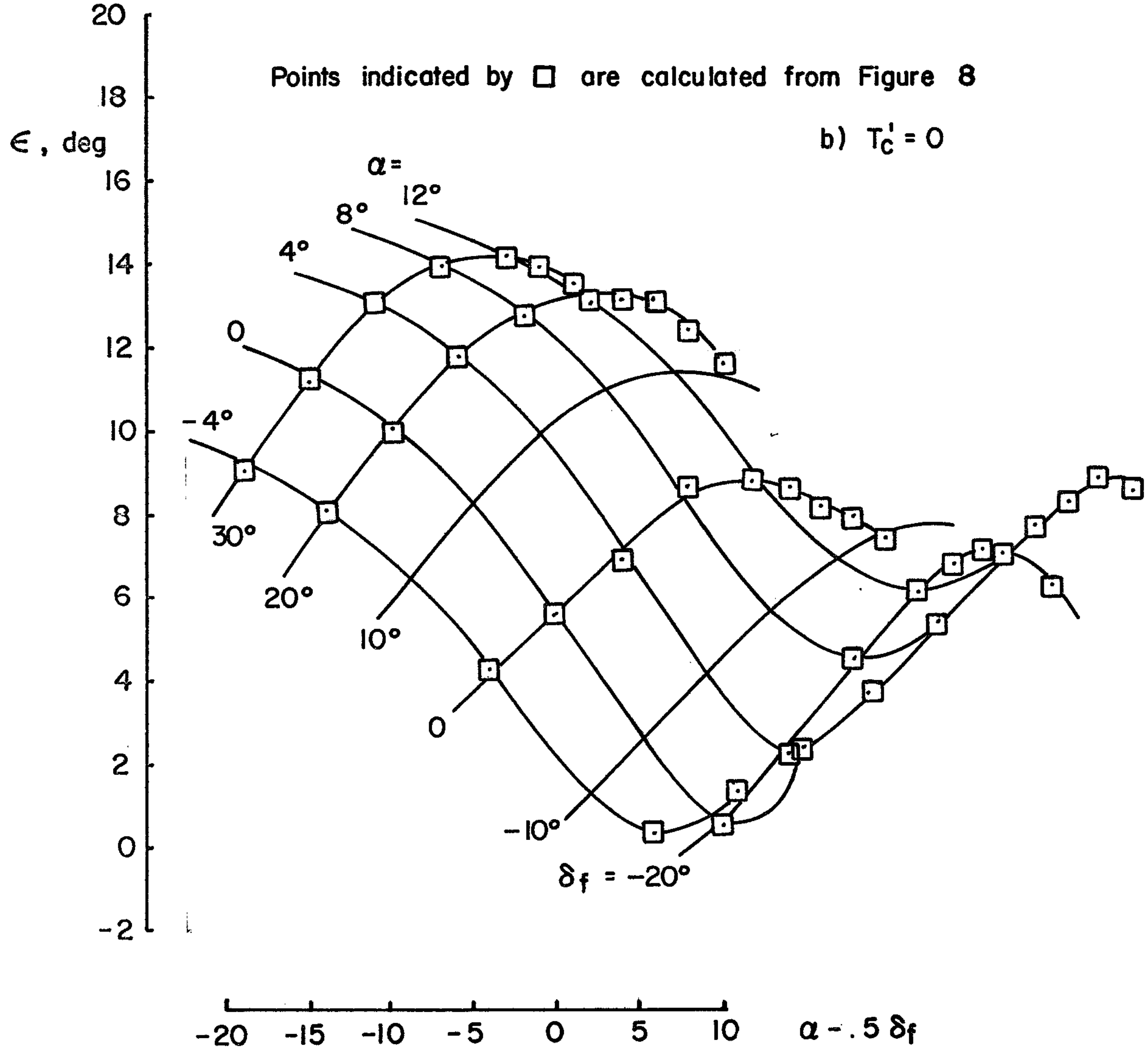

FIGURE 18 Continued

Points indicated by □ are calculated from Figure 8

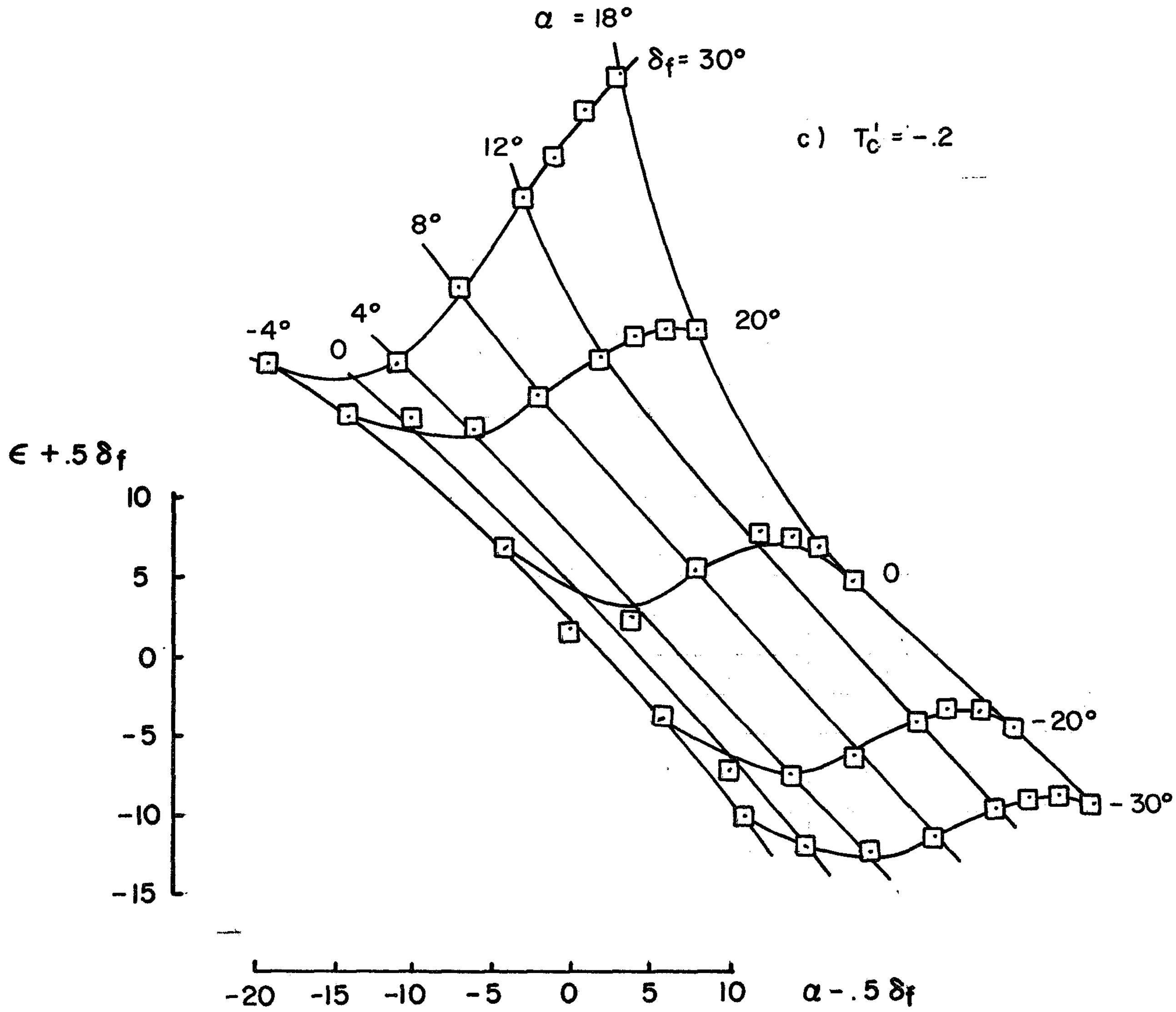

FIGURE 18 Concluded

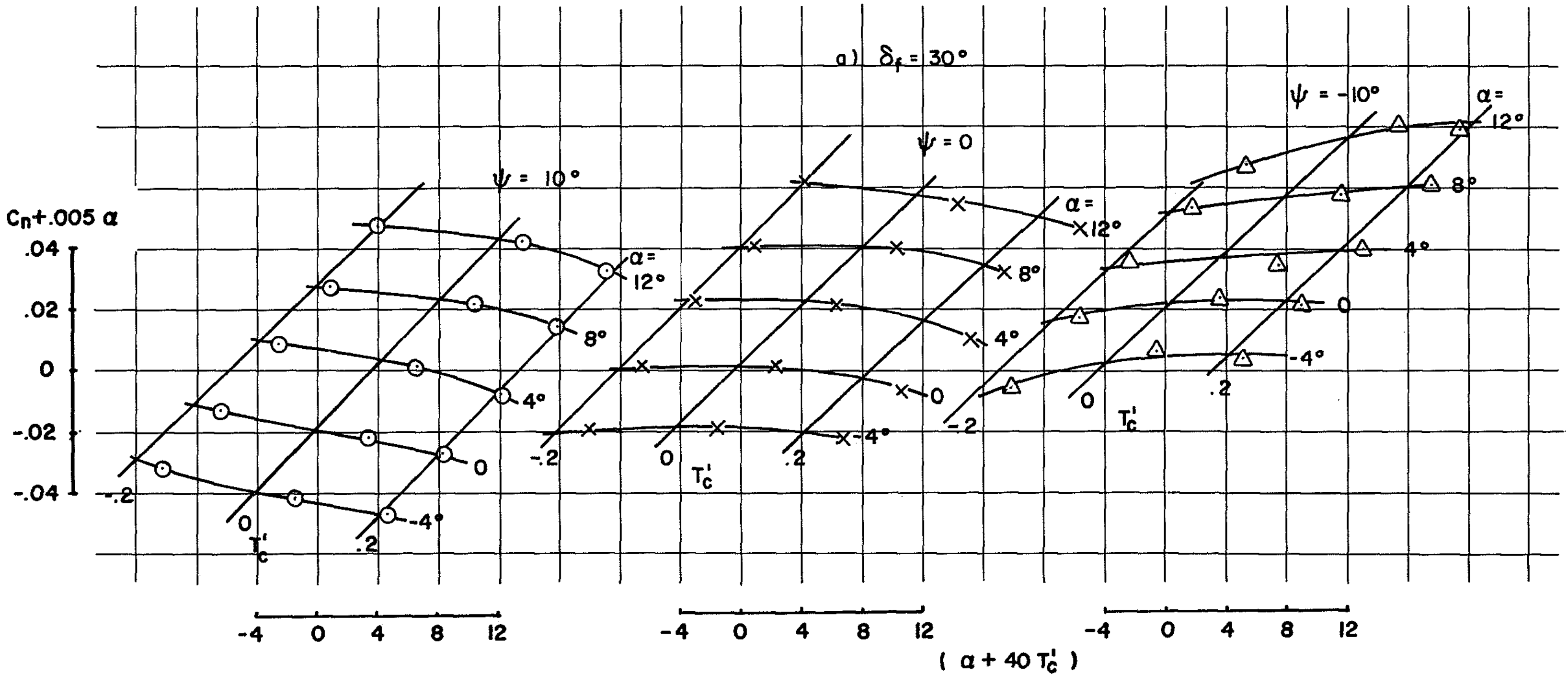

FIGURE 19 VARIATION OF YAWING MOMENT COEFFICIENT WITH ANGLE OF ATTACK AND THRUST COEFFICIENT

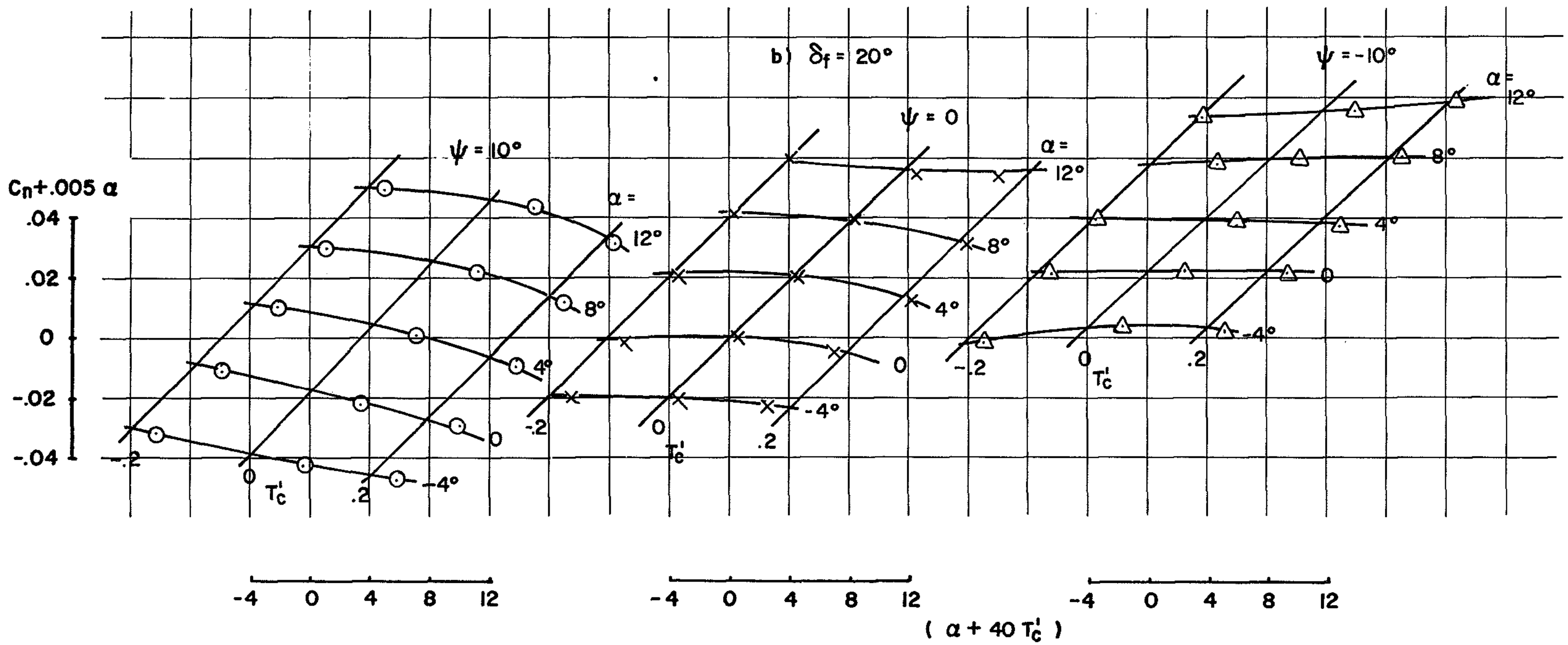

FIGURE 19 Continued

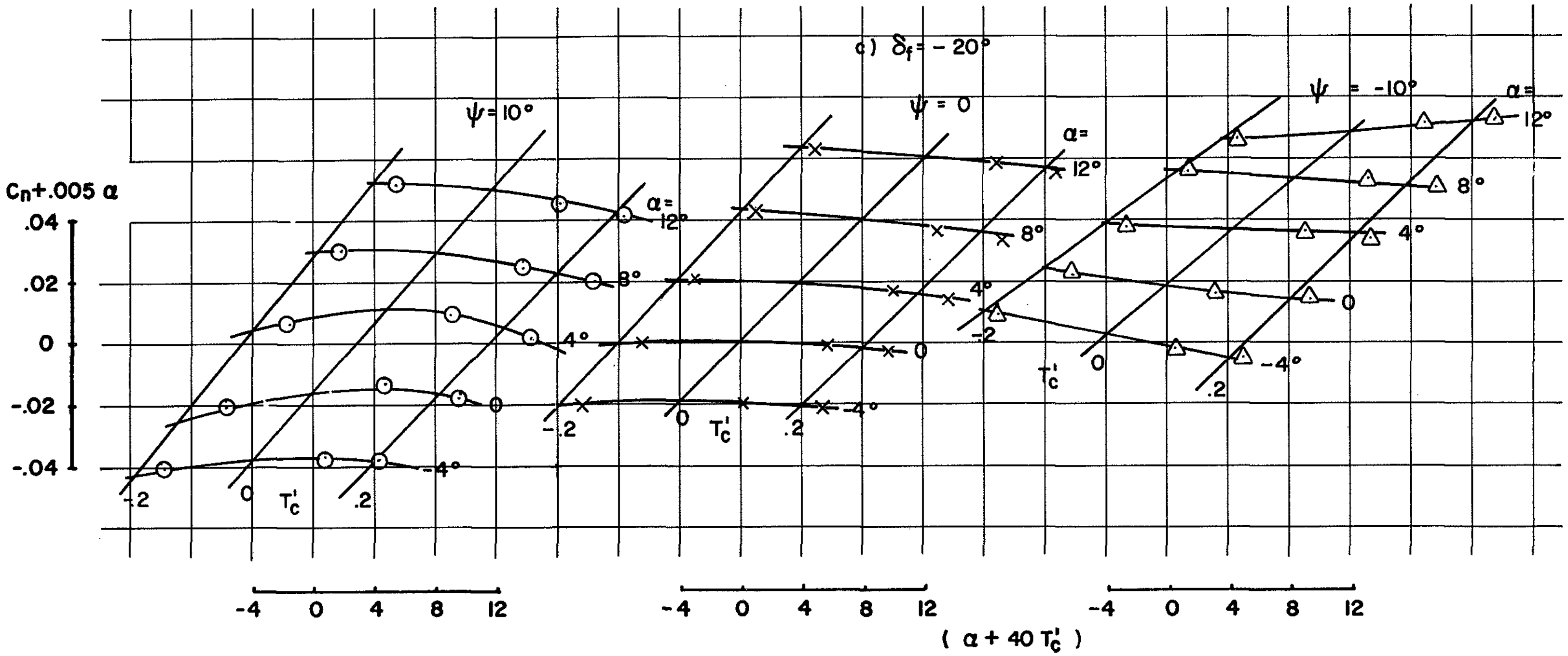

FIGURE 19 Continued

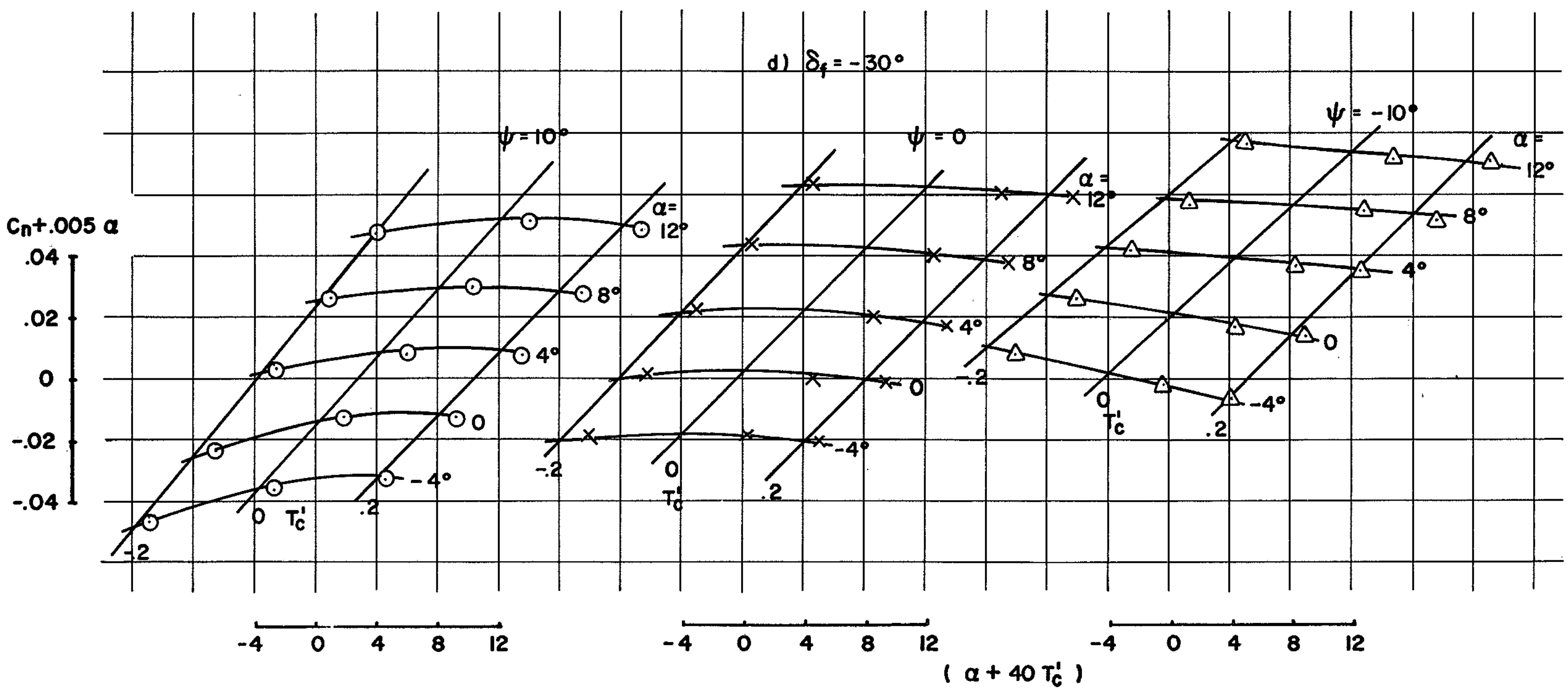

FIGURE 19 Concluded

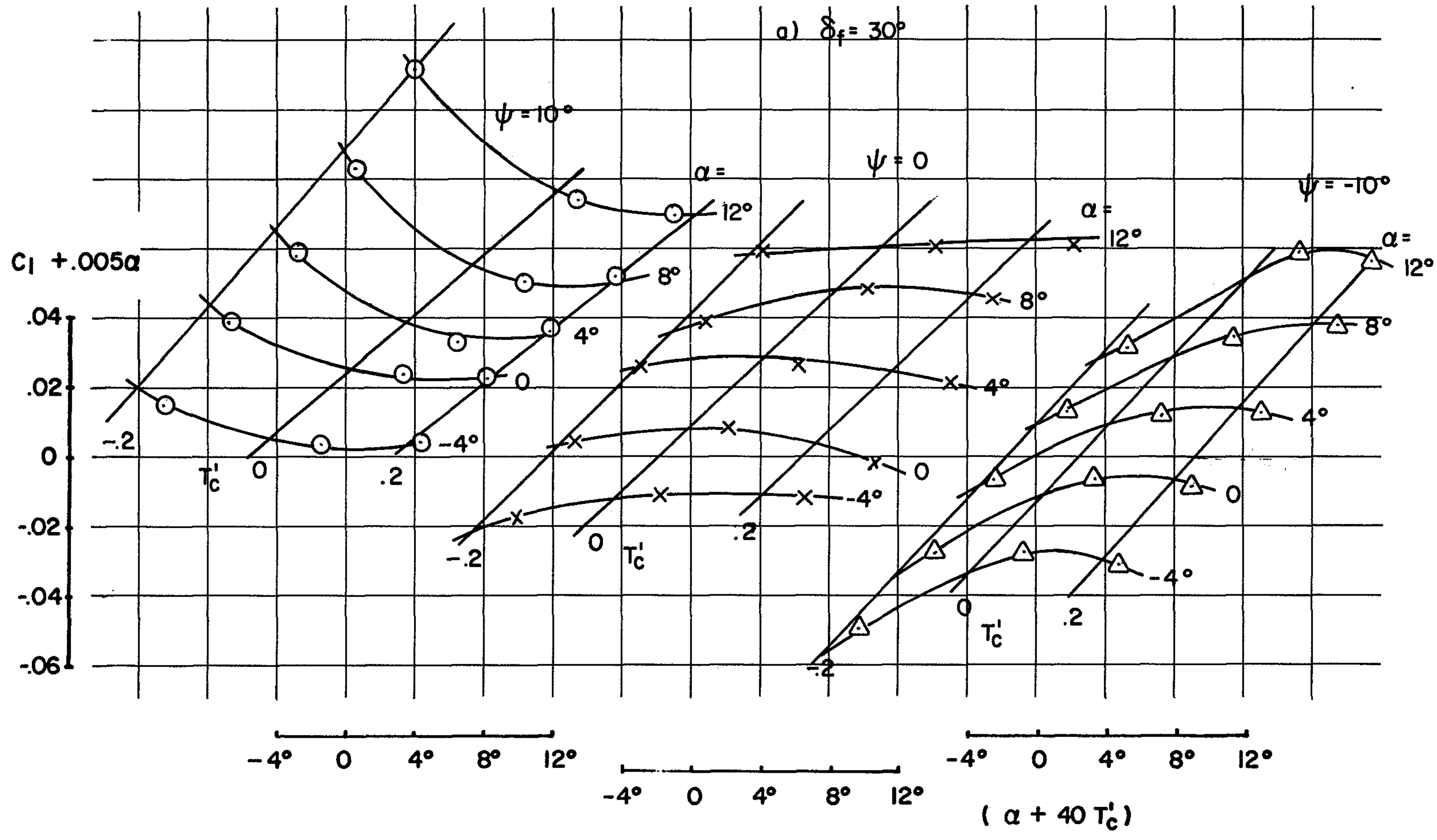

FIGURE 20 VARIATION OF ROLLING MOMENT COEFFICIENT WITH ANGLE OF ATTACK AND THRUST COEFFICIENT

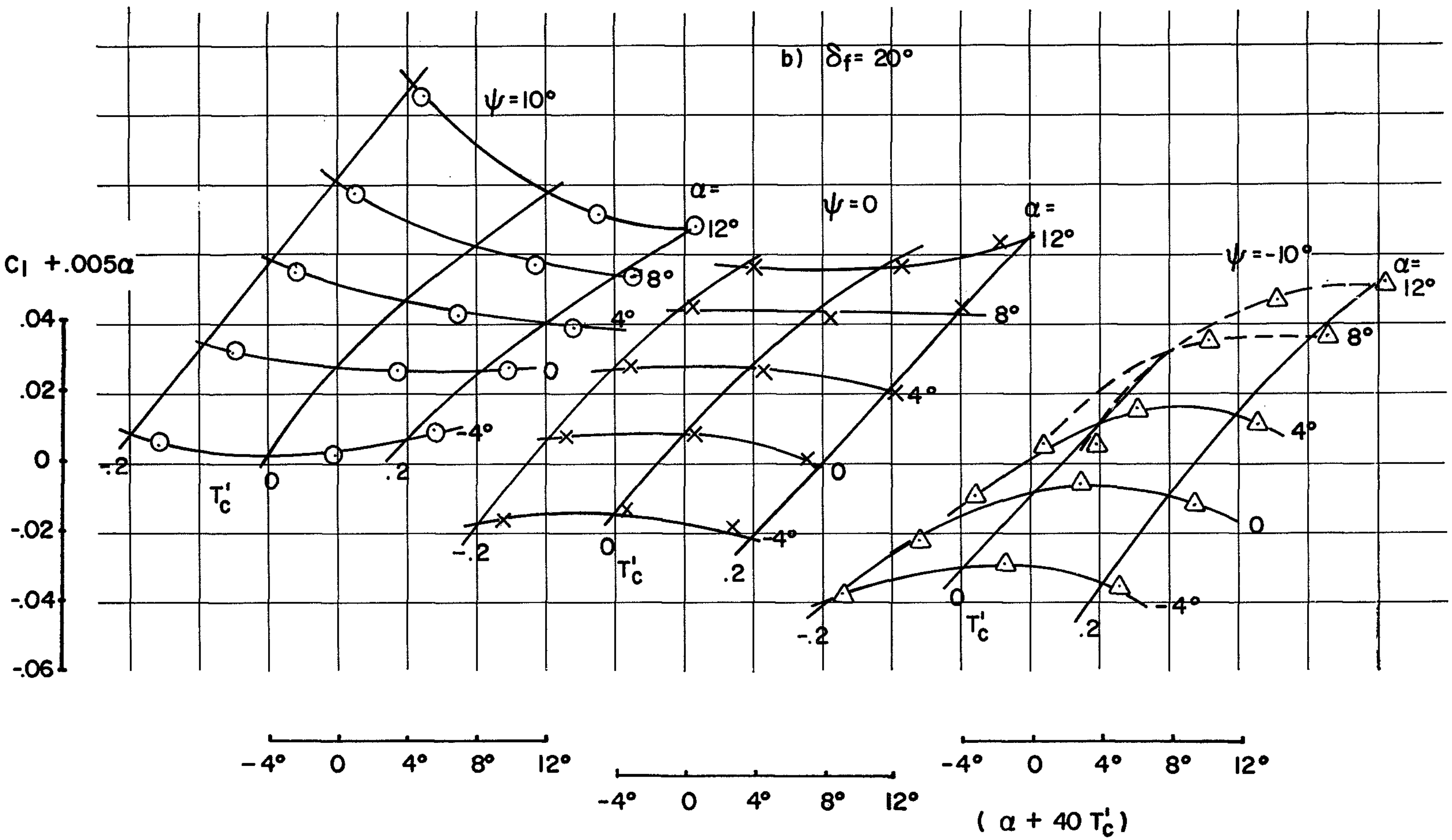

FIGURE 20 Continued

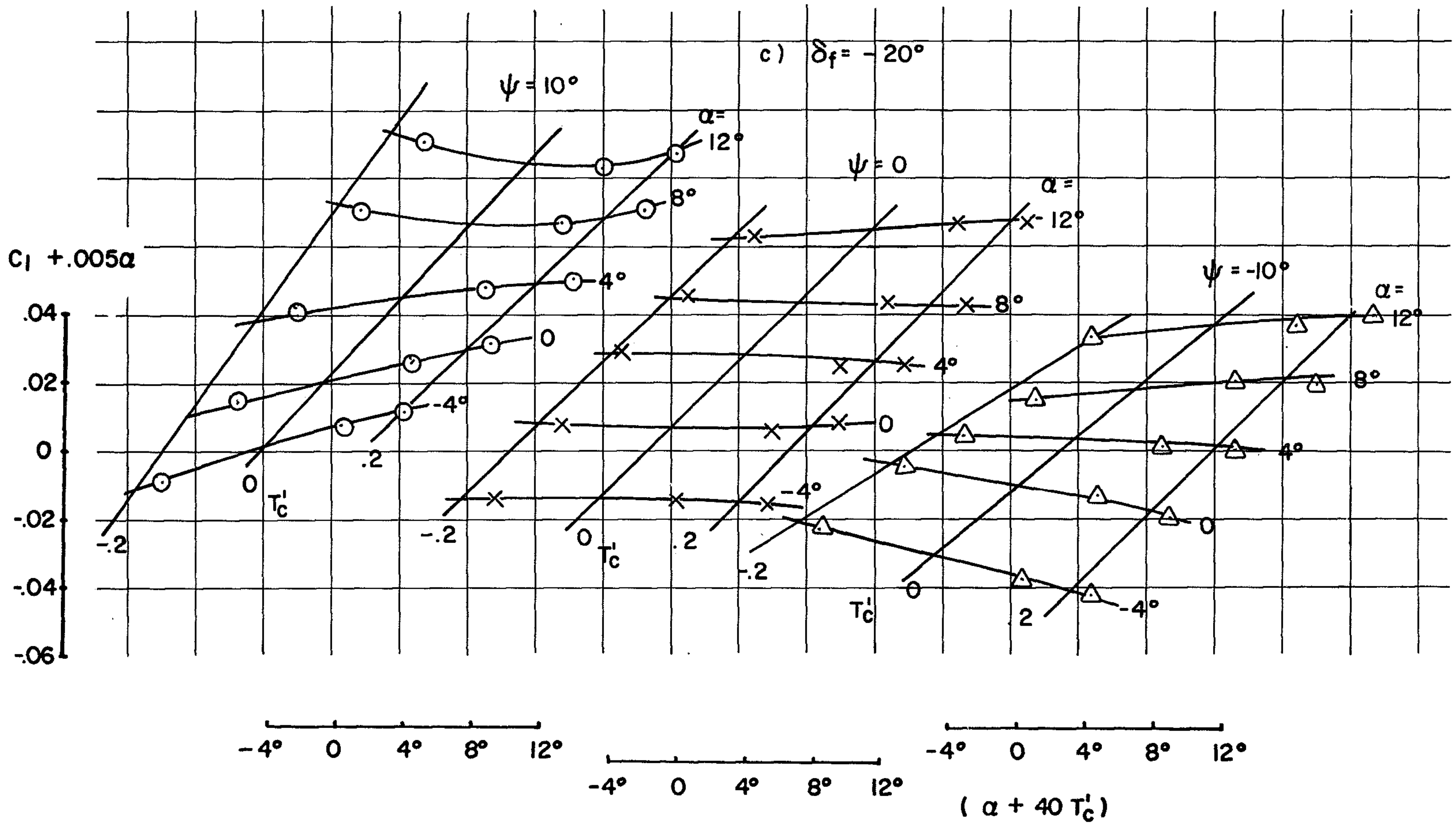

FIGURE 20 Continued

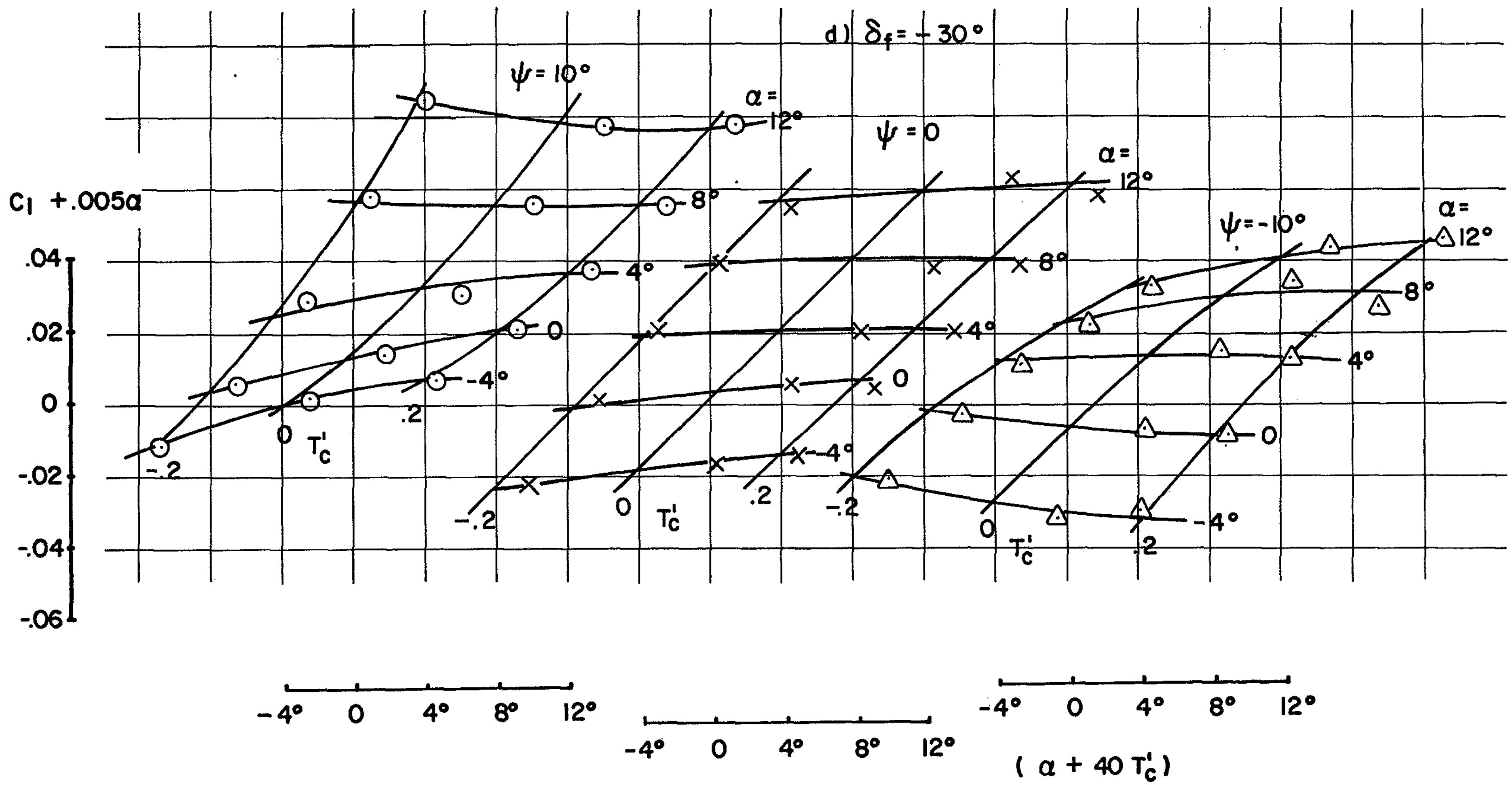

FIGURE 20 Concluded

NASA-Langley, 1971 —— 2

"The aeronautical and space activities of the United States shall be conducted so as to contribute . . . to the expansion of human knowledge of phenomena in the atmosphere and space. The Administration shall provide for the widest practicable and appropriate dissemination of information concerning its activities and the results thereof."

—NATIONAL AERONAUTICS AND SPACE ACT OF 1958

NASA SCIENTIFIC AND TECHNICAL PUBLICATIONS

TECHNICAL REPORTS: Scientific and technical information considered important, complete, and a lasting contribution to existing knowledge.

TECHNICAL NOTES: Information less broad in scope but nevertheless of importance as a contribution to existing knowledge.

TECHNICAL MEMORANDUMS: Information receiving limited distribution because of preliminary data, security classification, or other reasons.

CONTRACTOR REPORTS: Scientific and technical information generated under a NASA contract or grant and considered an important contribution to existing knowledge.

TECHNICAL TRANSLATIONS: Information published in a foreign language considered to merit NASA distribution in English.

SPECIAL PUBLICATIONS: Information derived from or of value to NASA activities. Publications include conference proceedings, monographs, data compilations, handbooks, sourcebooks, and special bibliographies.

TECHNOLOGY UTILIZATION PUBLICATIONS: Information on technology used by NASA that may be of particular interest in commercial and other non-aerospace applications. Publications include Tech Briefs, Technology Utilization Reports and Technology Surveys.

Details on the availability of these publications may be obtained from:

SCIENTIFIC AND TECHNICAL INFORMATION OFFICE

NATIONAL AERONAUTICS AND SPACE ADMINISTRATION

Washington, D.C. 20546